Daniel R. Bes

Quantum Mechanics

A Modern and Concise Introductory Course

Third Edition

Graduate Texts in Physics

Graduate Texts in Physics

Graduate Texts in Physics publishes core learning/teaching material for graduate- and advanced-level undergraduate courses on topics of current and emerging fields within physics, both pure and applied. These textbooks serve students at the MS- or PhD-level and their instructors as comprehensive sources of principles, definitions, derivations, experiments and applications (as relevant) for their mastery and teaching, respectively. International in scope and relevance, the textbooks correspond to course syllabi sufficiently to serve as required reading. Their didactic style, comprehensiveness and coverage of fundamental material also make them suitable as introductions or references for scientists entering, or requiring timely knowledge of, a research field.

Series Editors

Professor William T. Rhodes
Florida Atlantic University
Department of Computer and Electrical Engineering and Computer Science
Imaging Science and Technology Center
777 Glades Road SE, Room 456
Boca Raton, FL 33431, USA
E-mail: wrhodes@fau.edu

Professor H. Eugene Stanley
Boston University
Center for Polymer Studies
Department of Physics
590 Commonwealth Avenue, Room 204B
Boston, MA 02215, USA
E-mail: hes@bu.edu

Professor Richard Needs
Cavendish Laboratory
JJ Thomson Avenue
Cambridge CB3 0HE, UK
E-mail: rn11@cam.ac.uk

Please view available titles in *Graduate Texts in Physics* on series homepage
http://www.springer.com/series/8431/

Daniel R. Bes

Quantum Mechanics

A Modern and Concise Introductory Course

Third Edition

With 63 Figures

Springer

Daniel R. Bes
Comision Nacional de Energia Atomica
Av. General Paz 1499
1650 Prov. de Buenos Aires, Argentina
Universidad Favaloro
Solis 453
1078 C.A.B.A., Argentina

A primeval representation of the hydrogen atom

This beautiful mandala is displayed at the temple court of Paro Dzong, the monumental fortress of Western Bhutan [1]. It may be a primeval representation of the hydrogen atom: the outer red circle conveys a meaning of strength, which may correspond to the electron binding energy. The inner and spherical nucleus is surrounded by large, osculating circles that represent the motion of the electron: the circles not only occupy a finite region of space (as in Fig. 6.4) but are also associated with trajectories of different energies (colors) and/or with radiation transitions of different colors (wavelengths). At the center, within the nucleus, there are three quarks. Reality can display charming coincidences with religious/artistic creations. See also figure at the end of the chapters.

Foreword

Quantum mechanics is undergoing a revolution. Not that its substance is changing, but major developments are placing it in the focus of renewed attention, both within the physics community and among the scientifically interested public. First, wonderfully clever table-top experiments involving the manipulation of single photons, atomic particles and molecules are revealing in an ever-more convincing manner theoretically predicted facts about the counterintuitive and sometimes "spooky" behavior of quantum systems and have led to a renewed interest in the formulation of a strictly physics-based (non-philosophical) foundation of quantum mechanics. Second, the prospect of building quantum computers with enormously increased capacity of information-processing is developing great interest and high hopes in the engineering and computer science communities. Third, condensed matter physics and nanotechnology are narrowing down the gap between classical and quantum domains in the practical realm. These developments demand more and better training in quantum mechanics at the universities, with emphasis on a clear and solid understanding of the subject. Cookbook-style learning of quantum mechanics, in which equations and methods for their solution are memorized rather than understood, may help the students to solve some standard problems and pass multiple-choice tests, but it will not enable them to break new ground in real life as physicists. On the other hand, some "Mickey Mouse courses" on quantum mechanics for engineers, biologists and computer analysts may give an idea of what this discipline is about, but too often the student ends up with an incorrect picture or, at best, a bunch of uncritical, blind beliefs in linear algebra wizardry. The present book represents a fresh start toward helping achieve a deep *understanding* of the subject. It presents the material with utmost rigor and will require ironclad, old-fashioned discipline from the students in their study.

Too frequently, in today's universities, we hear the demand that the courses offered be "entertaining," in response to which some departmental brochures declare that "physics is fun"! Studying physics requires many hours of hard work, deep concentration, long discussions with buddies, periodic consultation with faculty, and tough self-discipline. But it can, and should, become a passion: the *passion* to achieve a deep understanding of how Nature works. This understanding usually

comes in discrete steps, and students will experience such a step-wise mode of progress as they work their way diligently through the present book. The satisfaction of having successfully mastered each step will then indeed feel very rewarding!

The "amount of information per unit surface" of text is very high in this book – its pages cover *all* the important aspects of present-day quantum mechanics, from the one-dimensional harmonic oscillator to teleportation. Starting from a few basic principles and concentrating on the fundamental behavior of quantum systems (particles) with only a few degrees of freedom (low-dimension Hilbert space) allows the author to plunge right into the core of quantum mechanics. It also makes it possible to introduce first the Heisenberg matrix approach – in my opinion, a pedagogically rewarding method that helps sharpen the mental and mathematical tools needed in this discipline right at the beginning. For instance, solving the quantization of the harmonic oscillator *without* the recourse of a differential equation is illuminating and teaches dexterity in handling the vector and matrix representation of states and operators, respectively.

Daniel Bes is a child of the Copenhagen school. Honed in one of the cradles of quantum mechanics by Åge Bohr, son of the great master, and by Ben Mottelson, he developed an unusually acute understanding of the subject, which after years of maturing he now has projected into a book – now in its third edition. The emphasis given throughout the text to the fundamental role and meaning of the measurement process will help the student overcome the initial reaction to the counterintuitive aspects of quantum mechanics and better comprehend the physical meaning and properties of Schrödinger's wave function. The human brain is an eminently classical system (albeit the most complex one in the Universe as we know it), whose phylo- and ontogenetic evolution are driven by *classical* interactions between organism and the environment, and which processes *pragmatic* information, definable only in the classical domain. It is therefore only natural that when this classical brain looks into the microscopic domain, using human-designed instruments which must translate quantum happenings into classical, microscopically observable effects, strange things with unfamiliar behavior may appear in our mental images! And it is only natural that, thus, the observer's way of thinking and instruments should not be left completely outside the fundamental framework of quantum physics! Bes' book helps to recognize, understand and accept quantum "paradoxes" not as such but as the facts of "Nature under human observation." Once this acceptance has settled in the mind, the student will have developed a true intuition or, as the author likes to call it, a "feeling" for quantum mechanics.

Chapter 2 contains the real foundation on which quantum mechanics is built; it thus deserves, in my opinion, repeated readings – not just at the beginning but after each subsequent chapter. With the exception of the discussion of two additional principles, the rest of the book describes the mathematical formulations of quantum mechanics (both the Heisenberg matrix mechanics, most suitable for the treatment of low-dimension state vectors, and Schrödinger's wave mechanics for continuous variables) as well as many up-to-date applications. The examples cover a wide variety of topics, from the simple harmonic oscillator mentioned above to subjects in condensed matter physics, nuclear physics, electrodynamics and

quantum computing. It is interesting to note, regarding the latter, that the concept of qubit appears in a most natural way in the middle of the book, almost in passing, well before the essence of quantum computing is discussed towards the end. Of particular help are the carefully thought-out problems at the end of each chapter, as well as the occasional listings of "common misconceptions." A most welcome touch is the inclusion of a final chapter on the history of theoretical quantum mechanics – indeed, it is regrettable that so little attention is given to it in university physics curricula: much additional understanding can be gained from learning how ideas have matured (or failed) during the historical development of a given discipline!

Let me conclude with a personal note. I have known Daniel Bes for almost 70 years. As a matter of fact, I had known of him even before we met in person: our fathers were "commuter–train acquaintances" in Buenos Aires, and both served on the PTA of the primary school that Daniel and I attended (in different grades). Daniel and I were physics students at the University of Buenos Aires (again, at different levels), then on the physics faculty, and years later, visiting staff members of Los Alamos National Laboratory. We always were friends, but we never worked together – Daniel was a theoretician almost from the beginning, whereas I started as a cosmic-ray and elementary-particle experimentalist (see Fig. 2.7). Interestingly, reading the first edition of this book has motivated me a few years ago to expand my current interest in foundations of information theory and work towards developing yet another interpretation of quantum mechanics (which I call "information-based")!

It gives me a particular pleasure that after so many decades and despite residing at opposite ends of the American continent, we have become professionally "entangled" through this wonderful textbook!

Fairbanks   *Juan G. Roederer*

Preface to the Third Edition

The preparation of another edition of a text on quantum mechanics is always a challenge. On the one hand, one may decide to cover some previously omitted topics, after gauging again their relevance. On the other hand, the fast evolution of the subject implies the need to incorporate not only new experimental facts and theoretical developments but also new concepts in the description of nature. Therefore, self-imposed constraints about the overall length of the book become strained. This is a good motivation for a revision. As a consequence, few items have been omitted and many more included, even some which are usually not discussed in introductory texts (like the breakdown of symmetries).

The book consists of two main parts. The first one displays the following organization:

- As in the previous editions, the basic principles of quantum mechanics are introduced within the framework of Hilbert spaces. Their empirical consequences (both thought and real experiments) and theoretical implications (uncertainty relations, no-cloning theorem) are discussed.
- The Heisenberg matrix realization of the basic principles allows us to solve the two-state system, the harmonic oscillator and a combination of the two, the Jaynes–Cummings model. The Schrödinger realization covers conventional subjects, including both bound and scattering examples. The contrast between these two realizations underscores the appearance of the most important quantum observable, the spin.
- The description of many-body systems requires the distinction between fermions and bosons and the indistinguishability among each of the two types of particles. As a consequence of these two features, there appears another formulation of quantum mechanics, the so-called second quantization.

  Most of the many-body examples that are presented – in fact, most of the many-body systems existing in nature – are treated within the framework of independent degrees of freedom. This is true both for fermion cases (atoms, nuclei, molecules, metals, band structures in crystals, etc.) and for boson systems

(Bose–Einstein condensates). One explicit exception is outlined (fractional Hall effect).

- Perturbation theory makes it possible to improve over-simplified approximations. Hartree–Fock procedures allow us to optimize these zero-order descriptions. The Born–Oppenheimer approximation is an essential tool in the treatment of molecules.
- *The time principle*. Time evolutions are calculated both exactly (spin systems) and perturbatively. The main motivation for the creation of quantum mechanics was to explain the stability of electron orbits in atomic hydrogen. Therefore, a brief introduction to Quantum Electrodynamics is presented so that this formalism can then be used to verify the extent to which this explanation has been accomplished by the formalism.
- Symmetry properties under transformations (translations, rotations, parity, exchange, etc.) are essential tools to obtain solutions to problems displaying such symmetries. However, the descriptions of many relevant systems involve the breaking of some symmetries, as exemplified by the BCS theory of superconductivity. The restoration of such symmetries is made through the introduction of collective variables.
- Our everyday life has been altered in an essential way through technologies based on quantum properties, the most conspicuous cases being the transistor and the laser. Quantum dots, scanning tunneling microscope, magnetic resonance imaging and Josephson junctions are also described in the corresponding chapters.
- Eigenstates of the position operators are normalized through the introduction of the Dirac delta function. They lead to the notion of propagators and to the path-integral formulation of quantum mechanics.

The second part of the text is based on the concept of entanglement, which is the superposition principle applied to two or more systems. The following items are included:

- Even more counterintuitive consequences of quantum mechanics appear in experiments involving the entanglement of two particles. Technological improvements have allowed the experimental verifications of such consequences.
- The EPR paper (1935) pointed at inconsistencies between experiments involving two entangled particles separated by superluminal distances, the locality principle and the predictions of quantum mechanics. These inconsistencies lead to the introduction of additional hidden mechanisms. In 1964, J. Bell proved that any local mechanism implied correlations that were violated by quantum mechanics. Experiments verified the quantum predictions. Nature is non-local.
- Quantum information theory concerns the possible use of quantum superpositions inherent to quantum bits (qubits), which carry much more information than classical bits. This program has succeeded in problems concerning cryptography and teleportation. However, it is presently stalling on problems of quantum computation, due to the inherent fragility of superposed states, which are destroyed through interactions with the environment (decoherence).

- Decoherence also allows us to explain the coexistence of microsystems described by quantum mechanics and macrosystems obeying Newton's laws. In fact, macrosystems emerge from the quantum substrate as a consequence of interactions with the environment. A new interpretation of quantum measurements appears within a consistent scheme.

Finally, a brief history of quantum mechanics is presented. Quantum mechanics emerges as an animated subject under permanent, albeit discontinuous, evolution.

Buenos Aires   *Daniel R. Bes*

Excerpts from the Preface to the First Edition

This text follows the tradition of starting an exposition of quantum mechanics with the presentation of the basic principles. This approach is logically pleasing and it is easy for students to comprehend. Paul Dirac, Richard Feynman and, more recently, Julian Schwinger have all written texts which are epitomes of this approach.

This approach also pays dividends through the natural appearance of the most quantum of all operators: the spin. In addition to its intrinsic conceptual value, spin allows us to simplify discussions on fundamental quantum phenomena like interference and entanglement, on time dependence (as in nuclear magnetic resonance) and on applications of quantum mechanics in the field of quantum information.

Any presentation of material from many different branches of physics requires the assistance of experts in the respective fields. I am most indebted to my colleagues and friends Ben Bayman, Horacio Ceva, Osvaldo Civitarese, Roberto Liotta, Juan Pablo Paz, Alberto Pignotti, Juan Roederer, Marcos Saraceno, Norberto Scoccola and Guillermo Zemba for corrections and/or suggestions. However, none of the remaining mistakes can be attributed to them.

My training as a physicist owes very much to Åge Bohr and Ben Mottelson of Niels Bohr Institutet and NORDITA (Copenhagen). During the 1950s Niels Bohr, in his long-standing tradition of receiving visitors from all over the world, used his institute as an open place where physicists from East and West could work together and understand each other. From 1956 to 1959, I was there as a young representative of the South. My wife and I met Margrethe and Niels Bohr at their home in Carlsberg. I remember gathering there with other visitors listening to Bohr's profound and humorous conversation. He was a kind of father figure, complete with a pipe that would go out innumerable times while he was talking. Years later I became a frequent visitor to the Danish institute, but after 1962 Bohr was no longer there.

My wife Gladys carried the greatest burden while I was writing this book. It must have been difficult to be married to a man who was mentally absent for the better part of almost 2 years. I owe her much more than a mere acknowledgment, because she never gave up in her attempts to change this situation (as she never did on many other occasions in our life together). My three sons, David, Martin and

Juan, have been a permanent source of strength and help. They were able to convey their encouragement even from distant places. This is also true of Leo, Flavia and Elena, and of our two granddaughters, Carla and Lara.

My dog Mateo helped me with his demands for a walk whenever I spent too many hours sitting in front of the monitor. He does not care about Schrödinger's cats.

Buenos Aires,   *Daniel R. Bes*
January 2004

To the list of friends and colleagues thanked in the previous excerpts – many of whom continued to help me for the second and third editions – I would like to add the names of Roberto De Luca, Alejandro Hnilo, Dario Mitnik and Augusto Roncaglia.

My new grandson Tomas was most welcomed in 2011.

Contents

Chapter 1
Introduction

The construction of classical physics started at the beginning of the seventeenth century. By the end of the nineteenth century, the building appeared to have been completed: the mechanics of Galileo Galilei and of Isaac Newton, the electromagnetism of Michael Faraday and James Maxwell, and the thermodynamics of Ludwig Boltzmann and Hermann Helmholtz were by then well established, from both the theoretical and the experimental points of view. The edifice was truly completed when Albert Einstein developed the special and the general theories of relativity, in the early twentieth century.

Classical physics deals with the trajectory of particles (falling bodies, motion of planets around the sun) or with the propagation of waves (light waves, sound waves). The construction of this edifice required intuition to be abandoned in favor of a formalism, i.e., a precise treatment that predicts the evolution of the world through mathematical equations. Classical physics has a deterministic character. The existence of a physical reality, independent of the observer, is an implicitly accepted dogma.

Cracks in this conception appeared around the beginning of the last century. Light waves not only appeared to be absorbed and emitted in lumps (black-body radiation) [2], but turned out to behave completely like particles (photoelectric and Compton effects [3, 4]). Experiments with electrons displayed diffraction patterns that had up to then been seen as characteristic of waves [5]. However, the most disturbing discovery was that an atom consists of a positively charged, small, heavy nucleus, surrounded by negatively charged light electrons [6]. According to classical physics, matter should collapse in a fraction of a second. Nor was it understood why atoms emitted light of certain wavelengths only, similar to an organ pipe that produces sounds at certain well-defined frequencies [7].

In 1913 Niels Bohr was able to explain both the stability of the hydrogen atom and the existence of discrete energy levels by means of a partial rejection of classical mechanics and electromagnetism [8]. However, this model was largely a patch. Bohr himself assumed the role of leader in the quest for an adequate formalism. In 1925 Werner Heisenberg alone [9] and, subsequently, in collaboration with Max Born and Pascual Jordan [10] developed a quantum mechanical formalism

in which the classical variables of position and momentum were represented by (non-commuting) matrices. Also in 1925, Dirac introduced the idea that physical quantities are represented by operators (of which Heisenberg's matrices are just one representation) and physical states by vectors in abstract Hilbert spaces [11]. In 1926 Erwin Schrödinger produced the differential formalism of quantum mechanics, an alternative approach based on the differential equations that bear his name [12].

Since the presentation of the Heisenberg and Schrödinger formulations[1] is at least twice as difficult as the introduction of a single one, a relatively large number of undergraduate quantum mechanics textbooks confine themselves to a discussion of the Schrödinger realization. The present author contends that such a presentation of quantum mechanics is conceptually misleading, since it leads to the impression that quantum mechanics is another branch of classical wave physics. It is not. Let me quote Schwinger's opinion [14].

> I have never thought that this simple wave approach [de Broglie waves and the Schrödinger equation] was acceptable as a general basis for the whole subject.

This approach of presenting both Heisenberg and Schrödinger formulations also pays dividends through the natural appearance of the most quantum of all operators: the spin. In addition to its intrinsic conceptual value, spin allows us to simplify discussions on fundamental quantum phenomena like interference and entanglement, on time dependence (as in nuclear magnetic resonance), and on applications of quantum mechanics in the field of quantum information.

The uncertainty of a presentation may be reduced by increasing the amount of detail, and vice versa. Bohr used to say that accuracy and clarity were complementary concepts (Sect. 15.5.1). Thus, a short and clear statement can never be precise. We may go further and state that the product of the indeterminacy inherent in any message ($\Delta\pi$) times the amount of details ($\Delta\sigma$) is always larger or equal than a constant k ($\Delta\pi \times \Delta\sigma > k$). The quality of textbooks should be measured by how close this product is to k, rather than by their (isolated) clarity or completeness. It is up to the reader to judge how closely we have been able to approach the value k. If we have achieved our aim, a more rigorous and sufficiently simple presentation of quantum mechanics will be available to undergraduate and first-year graduate students.

This book should be accessible to students who are reasonably proficient in linear algebra, calculus, classical mechanics and electromagnetism. Previous exposure to other mathematical and/or physics courses constitutes an advantage, but it is by no means a *sine qua non*.

---

[1]There also exist other formulations of quantum mechanics. All of them yield the same result for the same problem, but one of them may be easier to apply or may provide a better insight in a given situation. The list of quantum formalisms includes the path-integral (Feynman), phase space (Wigner), density matrix, second quantization, variational, pilot wave (Bohm) and the Hamilton–Jacobi formulations [13]. In the present text the second quantization formalism is presented in Sect. 7.8†, the density matrix in Sect. 14.4 and the path integral in Sect. 11.3†.

The reader will be confronted in Chap. 2 with a condensed presentation of Hilbert spaces and Hermitian and unitary operators. This early presentation implies the risk that the reader might receive the (erroneous) impression that the book is mathematically oriented, and/or that he or she will be taught mathematics instead of physics. However, Sects. 2.7* and 2.8* include practically all the mathematical tools that are used in the text (outside of elementary linear algebra and calculus, both being prerequisites). Consistent with this "physics" approach, the results are generally starkly presented, with few detailed derivations. It is the author's contention that these derivations do not significantly contribute to filling the gap between merely recognizing quantum mechanical expressions and learning how to "do" and "feel" quantum mechanics. This last process is greatly facilitated by solving the problems at the end of each chapter (with answers provided at the end of the book). The instructor should act as an "answerer" and "motivator" of students' questions and not merely as a "problem solver on the blackboard," to facilitate the filling of the aforementioned gap.

Sections labeled by a dagger display a somewhat more advanced degree of difficulty. The student may leave them for a second reading, unless he or she is specially interested on the subject. An asterisk indicates the mathematical background of material that has been previously presented.

Although the text has been conceived as a whole unit, it also allows for different shorter readings:

- If the aim is to operate with the formalism within some particular branch of microphysics (solid state, molecular, atomic, nuclear, etc.), one can progress straightforwardly from Chap. 2 to Chap. 9, probably leaving Chaps. 10 and 11 for a second reading.
- Readers more interested in recent advances on quantum theory and on applications to quantum information may skip Chaps. 7, 8, 10, and 11, to get to Chaps. 12–14 (concerning entanglement and its consequences).
- A reading with more emphasis on conceptual aspects of quantum mechanics should proceed through Chaps. 2–7, 9, 11, 12 and 14.

A brief history of quantum mechanics is presented to acquaint the newcomer with the development of one of the most spectacular adventures of the human mind to date (Chap. 15). It also intends to convey the feeling that, far from being finished, this enterprise is continuously being updated.

Chapter 2
The Principles of Quantum Mechanics

This introduction describes the mathematical tools used in the formulation of quantum mechanics and the connections between the physical world and mathematical formalism. Such links constitute the fundamental principles of quantum mechanics.[1] They are valid for every specific realization of these principles. Subsequently, their most immediate consequences are presented. Frequent shortcomings existing in many introductions can thus be avoided.[2]

2.1 Classical Physics
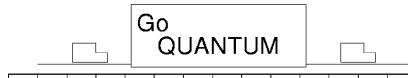
If our vision of a moving object is interrupted by a large billboard and is resumed after the reappearance of the object, we naturally assume that it has traveled all the way behind the billboard (Fig. 2.1). This is implied in the notion of physical reality, one of the postulates in the famous EPR paradox written by Einstein in collaboration with Boris Podolsky and Nathan Rosen [16]: "If, without in any way disturbing a system, we can predict with certainty the value of a physical quantity, then there is an element of physical reality corresponding to this physical quantity."

This classical framework relies on the acceptance of some preconceptions, most notably the existence of the continuous functions of time called trajectories $\mathbf{x}(t)$ [or $\mathbf{x}(t)$ and $\mathbf{p}(t)$, where $\mathbf{p}$ is the momentum of the particle]. A trajectory describes the

---

[1]Presentations of quantum mechanics resting upon few basic principles start with [15], which remains a cornerstone on the subject.

[2]In many presentations it is assumed that the solution of any wave equation for a free particle is the plane wave $\exp[i(kx - \omega t)]$. Subsequently, the operators corresponding to momentum and energy are manipulated to obtain an equation yielding the plane wave as the solution. This procedure is not very satisfactory because (a) plane waves display some difficulties as wave functions, not being square integrable; (b) quantum mechanics appears to be based on arguments that are only valid within a differential formulation; (c) it leads to the misconception that the position wave function is the only way to describe quantum states.

Fig. 2.1 The trajectory of the car behind the billboard as an element of physical reality

motion of a point particle, an abstract concept that does not exist in nature. The concept of trajectory provides an important link between the physical world and its mathematical description. For instance, it allows us to formulate Newton's second law,

$$\mathbf{F}(\mathbf{x}) = \frac{M\, d^2\, \mathbf{x}}{d\, t^2}\,. \tag{2.1}$$

This equation of motion predicts the evolution of the system in a continuous and deterministic way. Since this is a second order equation, the state of a system is specified if the position and the momentum of each particle are known at any one time.

Maxwell's theory of electromagnetism is also part of classical physics. It is characterized in terms of fields, which must be specified at every point in space and time. Unlike particles, fields can be made as small as desired. Electromagnetism is also a deterministic theory.

Essential assumptions in classical physics about both particles and fields are:

- The possibility of non-disturbing measurements
- There is no limit to the accuracy of the values assigned to physical properties

In fact, there is no distinction between physical properties and the numerical values they assume. Schwinger characterizes classical physics as "the idealization of non-disturbing measurements and the corresponding foundations of the mathematical representation, the consequent identification of physical properties with numbers, because nothing stands in the way of the continual assignment of numerical values to these physical properties" [14], p. 11.

Such "obvious" assumptions are no longer valid in quantum mechanics. Therefore, other links have to be created between the physical world and mathematical formalism.

2.2   Mathematical Framework of Quantum Mechanics

According to classical electromagnetism, an inhomogeneous magnetic field **B** directed along an axis (for instance, the z-axis) should bend the trajectory of particles perpendicular to this axis. The amount of bending of these tiny magnets will be proportional to the projection μ_z of their magnetic moment $\boldsymbol{\mu}$. Therefore, if the beam is unpolarized (all values $(-|\boldsymbol{\mu}| \le \mu_z \le |\boldsymbol{\mu}|)$ are present), particles are classically expected to impact over a continuous region of a screen. However, it was shown in 1921 by Otto Stern and Walther Gerlach that silver atoms distribute themselves over

each of two lines. Since the magnetic moment is proportional to an intrinsic angular momentum called spin ($\mu \propto \mathbf{S}$), it is apparent that only two projections of the spin are allowed by nature [17] (for more details see Sect. 5.2.1).

Note, however, that the fact that a physical quantity may have only two values does not require by itself to abandon classical physics. For instance, your PC is made up from bits, i.e. classical systems that may be in one of two states.[3] As befits classical systems, their state is not altered upon measurement (thus contributing to the stability of classical computers).

A different description is provided by vectors on a plane. While the sum of the two states of a bit does not make sense, the addition of two vectors on a plane is always another vector. Any vector Ψ may be written as a linear combination (Fig. 2.2, top)

$$\Psi = c_x \varphi_x + c_y \varphi_y , \tag{2.2}$$

where c_x, c_y are amplitudes and φ_x, φ_y are two perpendicular vectors of module one. This last property is expressed as $\langle \varphi_i | \varphi_j \rangle = \delta_{ij}$, which is a particular case of the scalar product

$$\langle \Psi | \Psi' \rangle = c_x^* c_x' + c_y^* c_y' . \tag{2.3}$$

In quantum mechanics we allow complex values of the amplitudes. Thus, the definition of normalized vectors becomes

$$\langle \Psi | \Psi \rangle = |c_x|^2 + |c_y|^2 = 1 . \tag{2.4}$$

Another crucial property of the chosen vector space is that the same vector Ψ may be expressed as a combination of other sets of perpendicular vectors χ_x, χ_y along rotated axes (Fig. 2.2, bottom)

$$\Psi = b_x \chi_x + b_y \chi_y ,$$
$$1 = |b_x|^2 + |b_y|^2 . \tag{2.5}$$
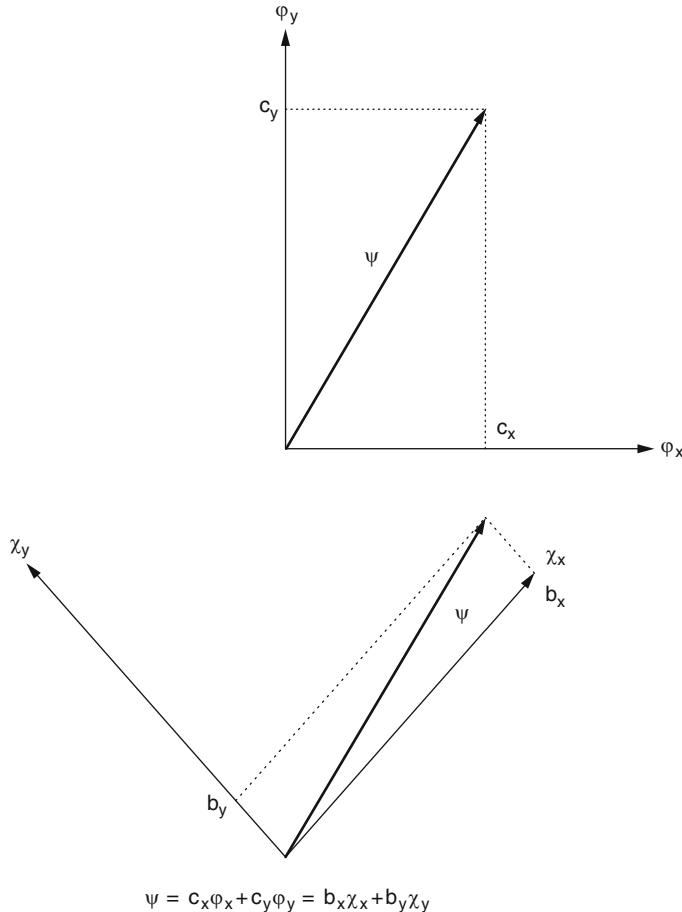
This two-dimensional space may be easily generalized to spaces with any number of dimensions, called Hilbert spaces. Here we outline some properties that are specially relevant from the point of view of quantum mechanics. This overview is expanded in Sect. 2.7*.

- As in (2.2), any vector Ψ may be expressed as a linear combination of orthonormal basis states φ_i:

$$\Psi = \sum_i c_i \varphi_i ; \quad c_i = \langle \varphi_i | \Psi \rangle \equiv \langle i | \Psi \rangle , \tag{2.6}$$

---

[3]Although the bits in your PC function on the basis of quantum processes (for instance, semiconductivity) they are not used in PCs as quantum systems.

$$\psi = c_x\varphi_x + c_y\varphi_y = b_x\chi_x + b_y\chi_y$$

Fig. 2.2 The same vector Ψ can be expressed as the sum of two different systems of basis vectors

$$\delta_{ij} = \langle\varphi_i|\varphi_j\rangle. \tag{2.7}$$

- Linear operators $\hat{Q}$ act on vectors belonging to a Hilbert space, transforming one vector into another: $\hat{Q}\,\Psi = \Phi$. These operators obey a non-commutative algebra, as shown in Sect. 2.7* for the case of rotations in three dimensions. We define the commutation operation through the symbol

$$[\hat{Q},\hat{R}] \equiv \hat{Q}\,\hat{R} - \hat{R}\,\hat{Q}, \tag{2.8}$$

where the order of application of the operators is from right to left ($\hat{Q}\,\hat{R}\,\Psi = \hat{Q}\,(\hat{R}\Psi)$).

- If the vector $\hat{Q}\varphi_i$ is proportional to φ_i, then φ_i is said to be an eigenvector of the operator $\hat{Q}$. The constant of proportionality q_i is called the eigenvalue

$$\hat{Q}\,\varphi_i = q_i\,\varphi_i. \tag{2.9}$$

- The scalar product between a vector $\hat{Q}\Psi_a$ and another vector Ψ_b is called the matrix element of the operator $\hat{Q}$ between the vectors Ψ_a and Ψ_b, and it is symbolically represented[4] as

$$\langle\Psi_b|\hat{Q}\Psi_a\rangle \equiv \langle\Psi_b|Q|\Psi_a\rangle \equiv \langle b|Q|a\rangle\,. \tag{2.10}$$

The matrix element is said to be diagonal if the same vector appears on both sides of the matrix element ($\langle\Psi|Q|\Psi\rangle$). The matrix elements of the unit operator are the scalar products $\langle\Psi_a|\Psi_b\rangle \equiv \langle a|b\rangle = \langle\Psi_b|\Psi_a\rangle^*$. The norm $\langle\Psi|\Psi\rangle^{1/2}$ is a real, positive number.
- The Hermitian conjugate $\hat{Q}^+$ of an operator $\hat{Q}$ is defined through the relation

$$\langle\varphi_b|Q^+|\varphi_a\rangle = \langle\varphi_a|Q|\varphi_b\rangle^*\,. \tag{2.11}$$

The operator is said to be Hermitian if

$$\hat{Q}^+ = \hat{Q}\,. \tag{2.12}$$

The eigenvalues q_i of a Hermitian operator are real numbers and the corresponding eigenvectors φ_i constitute a set of basis vectors.
- The matrix $\mathcal{U}$ with matrix elements $\mathcal{U}_{ab}$ is said to be unitary if the matrix elements of the inverse are given by

$$(\mathcal{U}^{-1})_{ab} = \mathcal{U}_{ba}^*\,. \tag{2.13}$$

Unitary transformations preserve the norm of the vectors and relate two sets of basis states (see Fig. 2.2)

$$\chi_a = \sum_i \mathcal{U}_{ai}\varphi_i\,. \tag{2.14}$$

These abstract mathematical tools (vectors, Hermitian operators and unitary transformations) may be represented through concrete, well-known mathematical objects, such as column vectors and matrices (Chap. 3), or by means of functions of the coordinate and differential operators (Chap. 4).

2.3   Basic Principles of Quantum Mechanics

In this section we present the quantum mechanical relation between the physical world and the mathematical tools that have been outlined in the previous section. It is formulated through the following quantum principles:

---

[4]The symbols $|a\rangle$ and $\langle a|$ have been called by Dirac ket and bra, respectively [15].

Principle 1. *The state of the system[5] is completely described by a vector* Ψ – *the state vector or state function – belonging to a Hilbert space.*

The state vector Ψ constitutes an unprecedented way of describing nature. It is an abstract entity that carries information about the results of possible measurements. It replaces the classical concepts of position and momentum in the description of physical systems.

The state vector may be multiplied by an arbitrary complex constant and still represent the same physical state. Even if we enforce the requirement of normalization, an arbitrary overall phase is left, which has no physical significance. This is not the case for the relative phase of the terms in the sum $c_a \Psi_a + c_b \Psi_b$, which encodes important physical information.

The fact that the sum of two state vectors is another state vector belonging to the same Hilbert space, i.e. describing another state of the system, is usually called the superposition principle. The sum $c_a \Psi_a + c_b \Psi_b$ must not be interpreted in the sense that we have a conglomerate of systems in which some of them are in the state Ψ_a and some in the state Ψ_b, but rather that the system is simultaneously in both component states. This statement is also valid when the system is reduced to a single particle.

The weirdness of quantum mechanics can be traced back to this superposition. It is fundamentally different from any property of classical particles, which are never found as a linear combination of states associated with different trajectories: a tossed coin may fall as a head or a tail, but not as a superposition of both.

By establishing that the state vector completely describes the state of the system, Principle 1 assumes that there is no way of obtaining information about the system, unless this information is already present in the state vector.

The state vector may only concern some degree(s) of freedom of the physical system, such as position and momentum of a particle and the spin.

The relation between the physical world and states Ψ is more subtle than the classical relation with position and momentum $\mathbf{x}$, $\mathbf{p}$. It relies on principles 2 and 3.

Principle 2. *To every physical quantity there corresponds a single linear operator. In particular, the operators* $\hat{x}$ *and* $\hat{p}$, *corresponding to the coordinate and momentum of a particle, fulfil the commutation relation*

$$[\hat{x}, \hat{p}] = i\hbar \,, \tag{2.15}$$

The commutator is defined in (2.8) and $\hbar$ is Planck's constant h divided by 2π (Table A.1).[6] The constant $\hbar$ provides an estimate of the domain in which quantum

---

[5]This notion of the state of a system is close to the one appearing in classical thermodynamics. It is applied there to many-body systems in which the path of the constituents cannot be traced in practice (for instance, molecules in a gas). However, in quantum mechanics the concept of state is applied even in the case of a single particle.

[6]This commutation relation is related to the classical Poisson bracket (Sect. 2.6.3). It has been derived from relativistic invariance [18], using the fact that spatial translations [generated by $\hat{p}$, see (4.10)] do not commute with Lorentz transformations even in the limit $c \to \infty$.

mechanics becomes relevant. It has the dimensions of classical action (energy × time). Classical physics should be applicable to systems in which the action is much larger than $\hbar$.

This is also fundamentally different from classical physics, for which physical properties are identified with (commuting) numbers (Sect. 2.1).

Since any classical physical quantity may be expressed as a function of coordinate and momentum ($Q = Q(x, p)$), the replacement $x \rightarrow \hat{x}$ and $p \rightarrow \hat{p}$ in the classical expression $Q(x, p)$ yields the operator $\hat{Q} = Q(\hat{x}, \hat{p})$. The requirement of hermiticity is usually sufficient to account for the non-commutativity of operators [for instance, $xp \leftrightarrow \frac{1}{2}(\hat{x}\hat{p} + \hat{p}\hat{x})$]. Thus, a one-to-one correspondence between physical quantities or observables Q and operators $\hat{Q}$ is established. However, there are also purely quantum operators, such as the spin operators, that cannot be obtained through such substitution.

The operator corresponding to the classical Hamilton function $H(p, x)$ is called the Hamiltonian. For a conservative system

$$\hat{H} = \frac{1}{2M}\hat{p}^2 + V(\hat{x}) \,, \tag{2.16}$$

where M is the mass of the particle and V is the potential.

Principle 3. *The eigenvalues q_i of an operator $\hat{Q}$ constitute the possible results of the measurements of the physical quantity Q. The probability[7] of obtaining the eigenvalue q_i is the modulus squared $|c_i|^2$ of the amplitude of the eigenvector φ_i in the state vector Ψ representing the state of the system.*

Since the results of measurements are real numbers, the operators representing physical observables are restricted to be Hermitian (2.12) and (2.53). In particular, the possible values of the energy E_i are obtained by solving the eigenvalue equation

$$\hat{H}\,\varphi_i = E_i\,\varphi_i \,. \tag{2.17}$$

As in the case of classical mechanics, quantum mechanics may be applied to very different systems, from single-particle and many-body systems to fields. Thus, quantum mechanics constitutes a framework in which to develop physical theories, rather than a physical theory by itself. A number of simple, typical, well-known problems of a particle moving in a one-dimensional space are discussed in Chaps. 3 and 4.

It is almost as useful to state what the principles do not mean, as to say what they do mean. In the following we list some common misconceptions regarding quantum states [19]:

- "The state vector is similar to other fields present in the physical world." It is fundamentally different from the electric or magnetic fields in electromagnetic

---

[7]Notions of probability theory are given in Sect. 2.8*.

waves, which carry momentum, energy, etc., and in which any externally caused change propagates at a finite, medium-dependent speed. The state vector does not interact with particles.

- "Energy eigenstates are the only allowed ones." This misconception probably arises from the generalized emphasis on the solution of the eigenvalue equation (2.17) and from its similarity to the correct statement "Energy eigenvalues are the only allowed energies."
- "A state vector describes an ensemble of classical systems." In the standard Copenhagen interpretation, the state vector describes a single system.[8] In none of the acceptable statistical interpretations is the ensemble classical.
- "A state vector describes a single system averaged over some amount of time." The state vector describes a single system at a single instant.

The above three principles are sufficient for the treatment of static situations involving a single particle. Two more principles, concerning many-body systems and the time-evolution of states, are presented in Chaps. 7 and 9, respectively.

2.4 Measurement Process

2.4.1 The Concept of Measurement

In this section we specify some basic concepts involved in the process of measurement.[9]

Two or more systems are in interaction if the presence of one leads to changes in the other, and vice versa. Different initial conditions generally lead to different changes, although this may not always be the case.

A measurement is a process in which a system is put in interaction with a piece of apparatus. The apparatus determines the physical quantity or observable to be measured (length, weight, etc.).
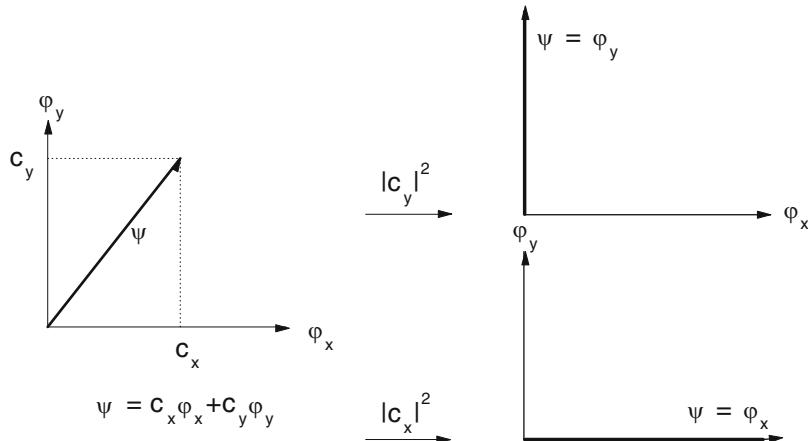
There are two important steps in a measurement. The first is the preparation of the system to be measured, i.e. the determination of the initial state. Bohr's definition of the word "phenomenon" refers to "an observation obtained under specified circumstances, including an account of the whole experimental arrangement" [21], p. 64. This should be contrasted with the EPR definition of physical reality (Sect. 2.1).

The second important step, also crucial in the case of quantum systems, is a (macroscopic) change in the apparatus that should be perceptible by a cognitive system. In many cases this change is produced by a detector at one end of the

---

[8]See Sect. 12.3.3.

[9]Many definitions included here are extracted from [20].

Fig. 2.3 The change in the state vector due to the measurement

apparatus. The magnitude of the physical quantity has a value if the change can be represented in numerical form.

For some systems the interaction with the apparatus does not produce a change in the system or produces a change which is completely determined. This is the case of classical systems (see Sect. 2.1). Our deeply ingrained notion of classical reality has emerged as a consequence of the fact that many independent observers may carry out measurements on the same system without disturbing it (and agree upon the results). On the contrary, this can only be exceptionally achieved in quantum measurements, where a change of the system is generally associated with a change of the apparatus (see Sect. 2.4.2).

2.4.2 Quantum Measurements

The most fundamental difference between a classical and a quantum system is that the latter cannot be measured without being irrevocably altered, no matter how refined the measuring instruments are. This is a consequence of the principles presented in Sect. 2.3.

Assume that the measurement of the physical quantity Q, performed on a system in the state Ψ expanded as in (2.6), yields the result q_j. If the same measurement is repeated immediately afterwards, the same value q_j should be obtained with certainty. Thus, the measurement has changed the previous value of the coefficients $c_i \rightarrow c_i = \delta_{ij}$. In other words, as a result of the measurement, the system "jumps" to an eigenstate of the physical quantity that is being measured (the reduction of the state vector). The only exceptions occur when the initial state is already represented by one of the eigenvectors.

Given an initial state vector Ψ, we do not know in general to which eigenstate the system will jump. Only the probabilities, represented by $|c_i|^2$, are determined (Fig. 2.3). This identification of the probabilities is consistent with the following facts:

- Their value is always positive.
- Their sum is 1 (if the state Ψ is normalized).
- The orthogonality requirement (2.7) ensures that the probability of obtaining any eigenvalue $q_j \neq q_i$ vanishes, if the system is initially represented by an eigenstate φ_i (see Table 2.1).

The fact that, given a state vector Ψ, we can only predict the probability $|c_i|^2$ of obtaining eigenvalues q_i constitutes an indeterminacy inherent to quantum mechanics. Our knowledge about the system cannot be improved, for instance, through a second measurement, since the state Ψ has been transformed into φ_i. The coefficients c_i are also called *probability amplitudes*. The concept of probability implies that we must consider a large number of measurements performed on identical systems, all of them prepared in the same initial state Ψ.

If in the expansion (2.6) there is a subset of basis states φ_k with the same eigenvalue $q_k = q$, the probability of obtaining this eigenvalue is $\sum_k |c_k|^2$. The system is projected after the measurement into the (normalized) state

$$\Psi' = \frac{1}{\sqrt{\sum_k |c_k|^2}} \sum_k c_k \varphi_k. \tag{2.18}$$

So far we have accepted the reduction interpretation of the measurement process without further discussion. This has been, historically, the path followed by most physicists. However, we present one more discussion of the measurement problem in Chap. 14.

The diagonal matrix element is also called the expectation value or mean value of the operator $\hat{Q}$. It is given by the sum of the eigenvalues weighted by the probability of obtaining them

$$\langle \Psi | Q | \Psi \rangle = \sum_i q_i \, |c_i|^2. \tag{2.19}$$

The mean value does not need to be the result q_i of any single measurement, but it is the average value of all the results obtained through the measurement of identical systems.

Measurements of expectation values of non-commuting operators yield the relative phases of the amplitudes (see Sect. 2.6.2).

The uncertainty or standard deviation ΔQ in a given measurement is defined as the square root of the average of the quadratic deviation

$$\Delta Q = \langle \Psi | \left(Q - \langle \Psi | Q | \Psi \rangle \right)^2 | \Psi \rangle^{\frac{1}{2}}$$
$$= \left(\langle \Psi | Q^2 | \Psi \rangle - \langle \Psi | Q | \Psi \rangle^2 \right)^{\frac{1}{2}}, \tag{2.20}$$

where

$$\langle \Psi | Q^2 | \Psi \rangle = \sum_i q_i^2 \, |c_i|^2. \tag{2.21}$$

We have postulated the existence of links between the physical world and mathematics that are different from those characterizing classical physics. In quantum mechanics, physical quantities are related to (non-commuting) operators; the state vectors are constructed through operations with these mathematical entities; the feedback to the physical world is made by measurements that yield, as possible results, the eigenvalues of the corresponding operators. An example of this two-way connection between formalism and the physical world is the following: assume that the system is constructed in a certain physical state, to which the state vector Ψ is assigned. This assignment is tested by means of various probes, i.e. measurements of observables Q, for which we may know the eigenvector φ_i and, therefore, the probability $|\langle i | \Psi \rangle|^2$ of obtaining the eigenvalues q_i.

This two-way relation between physical world and formalism is not an easy relation [22]:

"The most difficult part of learning quantum mechanics is to get a good feeling for how the abstract formalism can be applied to actual phenomena in the laboratory. Such applications almost invariably involve formulating oversimplified abstract models of the real phenomena, to which the quantum formalism can effectively be applied. The best physicists have an extraordinary intuition for what features of the actual phenomena are essential and must be represented in the abstract model, and what features are inessential and can be ignored. "

2.5   Some Experimental Consequences of the Basic Principles

2.5.1   Thought Experiments

This section displays some consequences of quantum principles in the form of thought experiments. Alternatively, one may obtain the quantum principles as a generalization of the results of such thought experiments (see [23]).

Let us consider a Hilbert space consisting of only two independent states $\varphi_{\pm}$. We also assume that these states are eigenstates of an operator $\hat{S}$ corresponding to the eigenvalues ± 1, respectively. Thus the eigenvalue equation $\hat{S}\varphi_{\pm} = \pm\varphi_{\pm}$ is satisfied. The scalar products $\langle \varphi_+ | \varphi_+ \rangle = \langle \varphi_- | \varphi_- \rangle = 1$ and $\langle \varphi_+ | \varphi_- \rangle = 0$ are verified. There are many examples of physical observables that may be represented by such operator. For instance, the z-component of the spin[10] is frequently used in these notes (Sects. 2.2, 3.2, 5.2, 9.2, etc.).

---

[10]Another example is given by the polarization states of the photon (see Sect. 9.8.2†). Most of the two-state experiments are realized by means of such optical devices.

We start by constructing a filter, i.e. an apparatus such that the exiting particles are in a definite eigenstate. In the first part of the apparatus, a beam of particles is split into the two separate $\varphi_\pm$ beams, as in the experiment of Stern and Gerlach (Sect. 5.2.1). In the second part, each beam is pushed towards the original direction. Each separate beam may be masked off at the half-way point. Such an apparatus is sketched in Fig. 2.4a with the φ_- beam masked off. It will be called a φ-filter. It is enclosed within a box drawn with continuous lines.

Any experiment requires first the preparation of the system in some definite initial state. Particles leave the oven in unknown linear combinations Ψ of $\varphi_\pm$ states

$$\Psi = \langle \varphi_+ | \Psi \rangle \, \varphi_+ \, + \, \langle \varphi_- | \Psi \rangle \, \varphi_- \, . \tag{2.22}$$

They are collimated and move along the y-axis. In the following cases, we prepare the particles in the filtered state φ_+, by preventing particles in the state φ_- from leaving the first filter (Fig. 2.4b). In the last stage of the experimental set-up we insert another filter as part of the detector, to measure the degree of filtration. The detector includes also a photographic plate which records the arriving particles and is observed by an experimentalist (Fig. 2.4c).
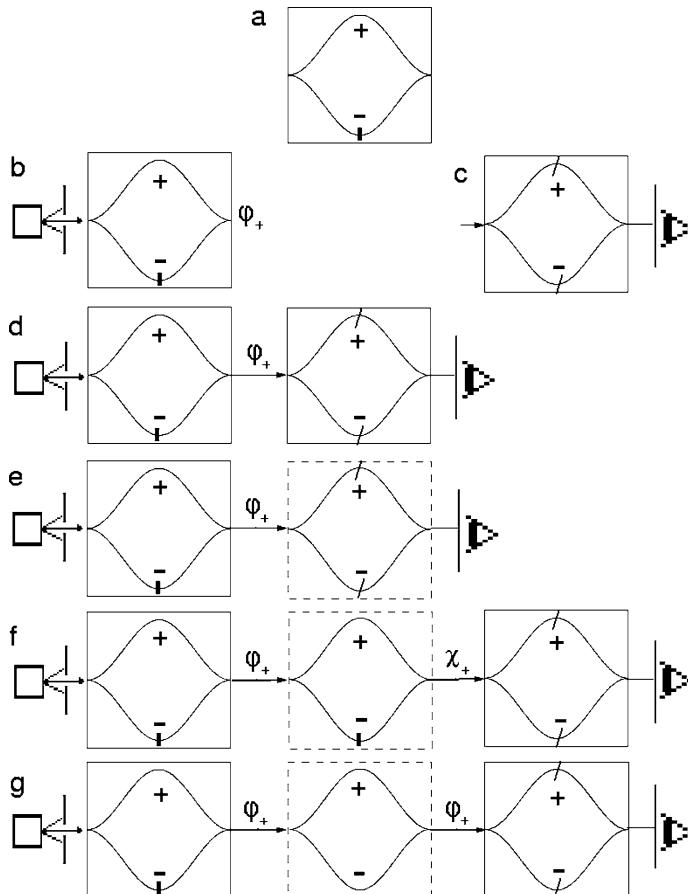
In the first experiment, we place the detector immediately after the first filter (Fig. 2.4d). If the φ_- channel is also blocked in the detector, every particle goes through; if the channel φ_+ is blocked, nothing passes. The amplitudes for these processes are $\langle \varphi_+ | \varphi_+ \rangle = 1$ and $\langle \varphi_- | \varphi_+ \rangle = 0$, respectively. The corresponding probabilities, $|\langle \varphi_+ | \varphi_+ \rangle|^2$ and $|\langle \varphi_- | \varphi_+ \rangle|^2$, also are 1 and 0.

We now consider another set of basis states $\chi_\pm$, also satisfying the orthonormality conditions $\langle \chi_+ | \chi_+ \rangle = \langle \chi_- | \chi_- \rangle = 1$, $\langle \chi_+ | \chi_- \rangle = 0$ (Fig. 2.2, bottom). It is easy to verify that an operator $\hat{R}$, satisfying the eigenvalue equation $\hat{R} \chi_\pm = \pm \chi_\pm$, does not commute with $\hat{S}$. Let us perform the necessary modifications of the detector filter so that it can block the particles in either of the states $\chi_\pm$. If $\hat{R}$ corresponds the spin component in the x-direction, the required modification of the detector amounts to a rotation of its filter by an angle $\pi/2$ around the y-axis. Dashed boxes represent filters such that particles exit in the $\chi_\pm$ states (χ-type filters) (Fig. 2.4e).

A particle exiting the first filter in the state φ_+ reorients itself, by chance, within the second filter. This process is expressed within the formalism by expanding the states $\varphi_\pm$ in terms of the new basis set

$$\varphi_\pm = \langle \chi_+ | \varphi_\pm \rangle \chi_+ \, + \, \langle \chi_- | \varphi_\pm \rangle \chi_- \, . \tag{2.23}$$

According to Principle 3, a particle emerging from the first filter in the state φ_+ will either emerge from the detector filter in the state χ_+ with probability $|\langle \chi_+ | \varphi_+ \rangle|^2$ or in the state χ_- with probability $|\langle \chi_- | \varphi_+ \rangle|^2$. If the χ_- channel of the second filter is blocked, the particle is either projected into the state χ_+ or is absorbed with probability $1 - |\langle \varphi_+ | \chi_+ \rangle|^2 = |\langle \varphi_+ | \chi_- \rangle|^2$. This result sounds classical: it is the quantum version of the classical Malus law. However, the projection process is probabilistic. Any information about the previous orientation φ_+ is lost.

Fig. 2.4 Quantum mechanical thought experiments illustrating the basic principles listed in Sect. 2.3. (**a**) Schematic representation of a filter; (**b**) preparation of the state of a particle; (**c**) detector (filter, photoplate, observer); (**d**)–(**g**) experiments (see text). The *vertical bars* denote fixed path blockings, while the *diagonal bars* indicate paths that can be either opened or closed. For each experiment we perform a measurement in which the upper channel of the detector is open and the down channel blocked, and another measurement with opposite features

We now perform two other experiments which yield results that are spectacularly different from classical expectations. Let us restore the detector filter to the φ-type and introduce a filter of the χ-type between the first filter and the detector (Fig. 2.4f). Thus, particles prepared in the φ_+ state exit the second filter in the χ_+ state. In the spin example, particles leave the first filter with the spin pointing in the direction of the positive z-axis, and the second filter pointing along the positive x-axis. The detector measures the number of particles exiting in one of the $\varphi_\pm$ states (spin

pointing up or down in the z-direction). We use now the inverse expansion[11] of (2.23), namely

$$\chi_\pm = \langle\varphi_+|\chi_\pm\rangle\varphi_+ + \langle\varphi_-|\chi_\pm\rangle\varphi_- \,. \tag{2.24}$$

Thus, the total amplitudes for particles emerging in one of the states $\varphi_\pm$ are[12]:

$$\langle\varphi_+|\chi_+\rangle\langle\chi_+|\varphi_+\rangle, \tag{2.25}$$

$$\langle\varphi_-|\chi_+\rangle\langle\chi_+|\varphi_+\rangle \,. \tag{2.26}$$

Both components $\varphi_\pm$ may emerge from the detector filter, in spite of the fact that the fraction of the beam in the φ_- state was annihilated inside the first filter. There is no way in classical physics to explain the reconstruction of the beam φ_-. This example illustrates the quantum rule concerning the impossibility of determining two observables associated with operators which do not commute: a precise determination of R destroys the previous information concerning S.

The result of this experiment is also consistent with Principle 1 in Sect. 2.3, since the state vector χ_+ contains all possible information about the system: its past history is not relevant for what happens to it next. The information is lost because of the blocking mask that has been put inside the second filter.

If we repeat the last experiment, but remove the mask from the second filter (Fig. 2.4g), the total amplitude is given by the sum of the amplitudes associated with the two possible intermediate states

$$\langle\varphi_+|\chi_+\rangle\langle\chi_+|\varphi_+\rangle + \langle\varphi_+|\chi_-\rangle\langle\chi_-|\varphi_+\rangle = \langle\varphi_+|\varphi_+\rangle = 1, \tag{2.27}$$

$$\langle\varphi_-|\chi_+\rangle\langle\chi_+|\varphi_+\rangle + \langle\varphi_-|\chi_-\rangle\langle\chi_-|\varphi_+\rangle = \langle\varphi_-|\varphi_+\rangle = 0 \,, \tag{2.28}$$

where the closure property has been applied (2.59). All the particles get through in the first case; none in the second case. In going from amplitude (2.26) to (2.28) we get fewer particles, despite the fact that more channels are opened.
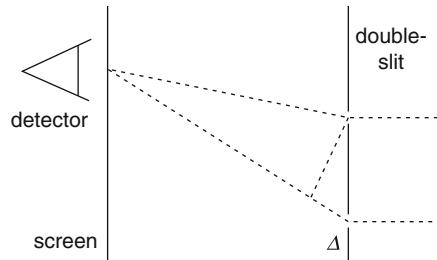
It is important that none of the intermediate beams suffers an additional disturbance (for example, the influence of an electric field), which may change the relative phases of the two channels.

The result of this last experiment is equivalent to an interference pattern. Classically, such patterns are associated with waves. However, unlike the case of waves, the particles are always detected as lumps of the same size on a screen placed in front of the exit side of the detector filter. No fractions of a lump are ever detected, as befits the behavior of indivisible particles. Therefore, these experiments display wave–particle duality, which is thus accounted for by Principles 1–3.

---

[11]The amplitudes in (2.23) and (2.24) are related by $\langle\varphi_+|\chi_\pm\rangle = \langle\chi_{\pm1}|\varphi_+\rangle^*$ and $\langle\varphi_-|\chi_\pm\rangle = \langle\chi_{\pm1}|\varphi_-\rangle^*$, according to Table 2.1.

[12]One reads from right to left.

Fig. 2.5 A double-slit experiment. No intensity is detected at points of the screen if the difference Δ between the two paths is an odd multiple of π/k

Feynman has commented this result as follows [23], pp. 1–1: "We choose to examine a phenomenon[13] which is impossible, *absolutely* impossible, to explain in any classical way, and which has in it the heart of quantum mechanics. In reality, it contains the only[14] mystery."

2.5.2   Real Two-Slit Experiments

Thought experiments played a crucial role in the clarification of controversial aspects of quantum mechanics. The discussions between Bohr and Einstein are paradigmatic in this respect (Sect. 15.5.2). However, since the end of the twentieth century, real experiments have replaced thought ones. Not only have earlier views been confirmed, but also more counterintuitive aspects of quantum mechanics have been brought into focus.

Since Thomas Young established the wave nature of light in 1801 (using candles as sources of light), two-slit interference experiments have become crucial to decide between wave and particle behavior (Fig. 2.5).

The usual experimental set-up consists of a source emitting particles and three screens placed on their path. The first screen displays a hole used to collimate the beam. The second one is pierced by two narrow slits placed within the aperture of the beam. The third screen is paved by detectors recording the impact of the particles.
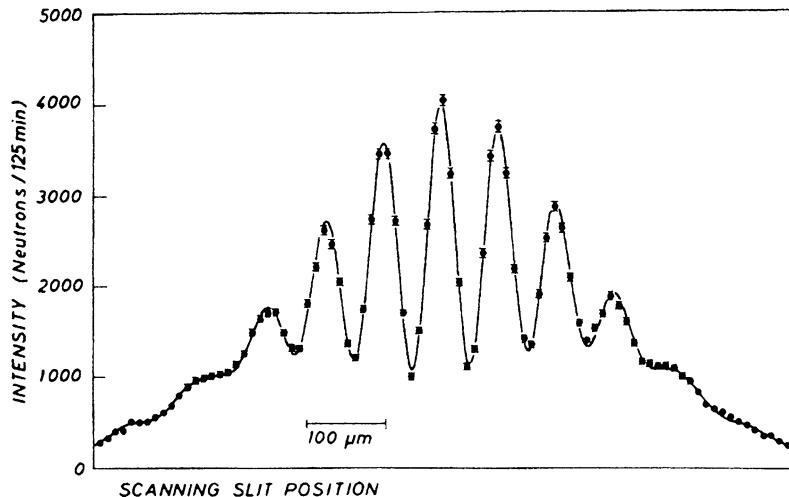
The slits in the intermediate screen define two distinct paths for the particles. Each particle crosses this screen in a linear superposition of two states

$$\Psi = \frac{1}{\sqrt{2}} \left(\varphi_a + \varphi_{a'} \right) . \tag{2.29}$$

The pattern on the detection screen builds up in a pointillist way by accumulation of discrete spots, each one produced by a single particle. It is not possible to predict the final spot for any one particle (only the fringes where no particle will impinge

---

[13]Matter wave phenomena were experimentally verified for the first time in [5].

[14]Other fundamental issue in quantum physics is entanglement (Chap. 12).

Fig. 2.6 A double-slit diffraction pattern measured with neutrons (Reprinted from [78]. Copyright by the American Physical Society and the Institut für Experimentalphysik, Universität Wien)

can be determined beforehand). After the detection of a large number of particles, a pattern of equidistant fringes with a high density of impacts can be seen at the detection screen.

In a relatively recent version (1988), neutrons of de Broglie wavelength 2 nm (4.34) impinge on two slits 22 μm and 23 μm wide, respectively, separated by a distance of 104 μm. The main results of this experiment are [24]:

- A diffraction pattern indicating the existence of a wave interference phenomenon (Fig. 2.6). The observation plane was located at a distance of 5 m from the slits to insure a resolution of ≈ 100 μm. The solid line represents first-principle predictions from quantum mechanics, including all features of the experimental apparatus.
- The state (2.29) describes a superposition of amplitudes rather than a sum of probabilities, leading to interference terms in the probability $|\Psi|^2$.
- The discreetness of the detection events exhibits the corpuscular nature of the neutrons.
- Neutrons were collected one by one at the observation plane, at a maximum rate of one neutron every 2 s. Therefore, while one neutron was being registered, the next one to arrive was usually still inside the uranium parent nucleus. The particle nature of neutrons is thus also confirmed. Moreover, constraints on the validity of quantum physics to statistical ensembles are ruled out.

Similar interference patterns have been obtained with atoms, molecules and clusters, including fullerenes, a composite molecule of 64 carbon atoms [25].

The superposition giving rise to interference phenomena requires that there is no way to know, even in principle, which path the particle took, a or a'. Interference is destroyed if this information exists, even if it is dispersed in the environment.

2.6 Other Consequences of the Basic Principles

It is shown in Sect. 2.6.1 that the commutation relation between two Hermitian operators $\hat{r}, \hat{s}$ determines the precision with which the values of the corresponding physical quantities may be simultaneously determined. Thus, Heisenberg uncertainty relations between momenta and coordinates become extended to any pair of observables and appear as a consequence of their commutation relations.

We also present the no-cloning theorem (Sect. 2.6.2) and point out the relation between quantum commutators and Poisson brackets (Sect. 2.6.3).

2.6.1 Commutation Relations and the Uncertainty Principle

One assumes two Hermitian operators, $\hat{R}, \hat{S}$, and defines a third (non-Hermitian) operator $\hat{Q}$, such that

$$\hat{Q} \equiv \hat{R} + i\lambda\hat{S}, \tag{2.30}$$

where λ is a real constant. The minimization with respect to λ of the positively defined norm [see (2.52)]

$$\begin{aligned}
0 &\leq \langle \hat{Q}\Psi | \hat{Q}\Psi \rangle = \langle \Psi | Q^+ Q | \Psi \rangle \\
&= \langle \Psi | R^2 | \Psi \rangle + i\lambda \langle \Psi | [R, S] | \Psi \rangle + \lambda^2 \langle \Psi | S^2 | \Psi \rangle
\end{aligned} \tag{2.31}$$

yields the value

$$\begin{aligned}
\lambda_{\min} &= -\frac{i}{2} \langle \Psi | [R, S] | \Psi \rangle / \langle \Psi | S^2 | \Psi \rangle \\
&= -\frac{i}{2} \langle \Psi | [R, S]^+ | \Psi \rangle^* / \langle \Psi | S^2 | \Psi \rangle \\
&= \frac{i}{2} \langle \Psi | [R, S] | \Psi \rangle^* / \langle \Psi | S^2 | \Psi \rangle.
\end{aligned} \tag{2.32}$$

In the second line we have used the definition (2.11) of the Hermitian conjugate. In the last line, the relation $[\hat{R}, \hat{S}]^+ = -[\hat{R}, \hat{S}]$ stems from the Hermitian character of the operators [see (2.51)]. Substitution of the value $\lambda_{\min}$ in (2.31) yields

$$0 \leq \left(\langle \Psi | R^2 | \Psi \rangle - \frac{1}{4} \frac{|\langle \Psi | [R, S] | \Psi \rangle|^2}{\langle \Psi | S^2 | \Psi \rangle} \right) \tag{2.33}$$

or

$$\langle\Psi|R^2|\Psi\rangle\,\langle\Psi|S^2|\Psi\rangle \ge \frac{1}{4}\,|\langle\Psi|[R,S]|\Psi\rangle|^2\,. \tag{2.34}$$

The following two operators $\hat{r}, \hat{s}$ have zero expectation value

$$\hat{r} \equiv \hat{R} - \langle\Psi|R|\Psi\rangle\,, \qquad \hat{s} \equiv \hat{S} - \langle\Psi|S|\Psi\rangle, \tag{2.35}$$

and the product of their uncertainties is constrained by [see (2.20)]

$$\Delta r\,\Delta s \ge \frac{1}{2}\,|\langle\Psi|[r,s]|\Psi\rangle|\,. \tag{2.36}$$

Operators corresponding to observables can always be written in the form (2.35). If we prepare a large number of quantum systems in the same state Ψ and then perform some measurements of the observable r in some of the systems, and of s in the others, then the standard deviation Δr of the r-results times the standard deviation Δs of the s-results should satisfy the inequality (2.36). These are intrinsic limitations to the accuracy with which the values of two observables can be determined.

In the case of coordinate and momentum operators, the relation (2.15) yields the Heisenberg uncertainty relation
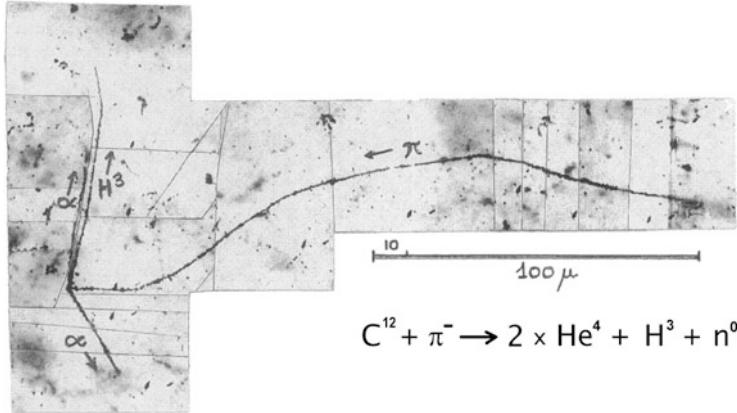
$$\Delta x\,\Delta p \ge \frac{\hbar}{2}. \tag{2.37}$$

We emphasize the fact that this relation stems directly from basic principles and, in particular, from the commutation relation (2.15). It constitutes an intrinsic limitation upon our knowledge. This limitation cannot be overcome, for instance, by any improvement of the experiment.

If the state of the system is an eigenstate of the operator $\hat{r}$, then a measurement of the observable r yields the corresponding eigenvalue. The value of the observable s associated with a non-commuting operator $\hat{s}$ is undetermined. This is the case of a plane wave describing a particle in free space (Sect. 4.3) for which the momentum may be determined with complete precision, while the particle is spread over all space.

Another consequence of the relation (2.36) is that the state vector Ψ may be simultaneously an eigenstate of $\hat{r}$ and $\hat{s}$ only if these two operators commute, since in this case the product of their uncertainties vanishes. Moreover, if the operators commute and the eigenvalues of $\hat{s}$ are all different within a subset of states, then the matrix elements of $\hat{r}$ are also diagonal within the same subset of states (see Sect. 2.7.1*).

Heisenberg conceived the uncertainty relations to solve the wave-particle paradox. Pure particle behavior requires localization of the particle, while clear wave behavior appears only when the particle has a definite momentum. Heisenberg's interpretation of this was that each of these extreme classical descriptions is satisfied only when the other is completely untenable. Neither picture is valid for

Fig. 2.7 Apparent classical trajectory of a pion. (Reproduced with permission from the authors)

intermediate situations. However, quantum mechanics has to be compatible with the description of the motion of elementary particles (not only with the description of the motion of macroscopic bodies) in terms of trajectories. Heisenberg's answer is that one may construct states Ψ that include a certain amount of localization $\mathbf{p}_0(t)$ and $\mathbf{x}_0(t)$ in both momentum and coordinate. Thus the motion of a particle has some resemblance to classical motion along trajectories. However, there should be a certain spread in the momentum and in the coordinate, such that the amplitudes $\langle \mathbf{p} | \Psi \rangle$ and $\langle \mathbf{x} | \Psi \rangle$, in momentum eigenstates and in position eigenstates, allow uncertainty relations to hold [26].

For an illuminating example, Fig. 2.7 displays the capture of a pion by a carbon nucleus [27]. One can determine the mass, energy and charge of the particles, by measuring the length, the grain density and the scattering direction of their tracks. Let us assume a pion kinetic energy of 10 MeV. Using the pion mass (139 MeV/c^2), one obtains a momentum of $p_\pi = 53$ MeV/c. The uncertainty in the direction perpendicular to the track may be estimated from the width of the track to be $\approx 1\,\mu$m, which yields $\Delta p_\perp \approx 10^{-7}$ MeV/c. The ratio $\Delta p_\perp / p_\pi \approx 10^{-9}$ is too small to produce a visible alteration of the apparent trajectory

2.6.2 No-Cloning Theorem

Let us assume that there are many systems prepared in the state

$$\Psi = a_+ \varphi_+ + a_- \varphi_- , \tag{2.38}$$

and that the two amplitudes $a_\pm$ are unknown to us. By measuring two (non-commuting) observables such as

$$\hat{Q} = |\varphi_+\rangle\langle\varphi_+| - |\varphi_-\rangle\langle\varphi_-| , \qquad \hat{R} = |\varphi_+\rangle\langle\varphi_-| + |\varphi_-\rangle\langle\varphi_+| , \tag{2.39}$$

we obtain the averages

$$\langle \Psi | Q | \Psi \rangle = |a_+|^2 - |a_-|^2 , \qquad \langle \Psi | R | \Psi \rangle = a_+^* a_- + a_-^* a_+ , \qquad (2.40)$$

from which we can deduce the value of the amplitudes $a_\pm$, including the relative phase.

The situation is different if there is a single copy, since the probability amplitudes are lost after the first measurement. A possible way out would be to produce many copies of the initially single system, but this is prevented by the no-cloning theorem, which also reflects the fragility of quantum states. The theorem says that the state of a particle cannot be copied onto another particle, while the original particle remains in the same state [28]. This is also completely different from what happens in classical mechanics, where we can specify as much as required the state of the system by performing additional measurements without disturbing it.

Suppose the state of two particles is given by

$$\varphi(1) \chi(2) \qquad (2.41)$$

and that some unitary evolution effects the copying process

$$\varphi(1) \varphi(2) = \mathcal{U} \varphi(1) \chi(2) . \qquad (2.42)$$

Suppose now that this copying procedure also works for another state

$$\phi(1) \phi(2) = \mathcal{U} \phi(1) \chi(2) . \qquad (2.43)$$

The scalar product between (2.42) and (2.43) yields

$$\langle \varphi | \phi \rangle^2 = \langle \chi \varphi | \mathcal{U}^+ \mathcal{U} | \phi \chi \rangle = \langle \varphi | \phi \rangle . \qquad (2.44)$$

Since this equation has two solutions, 0 and 1, either $\varphi = \phi$ or they are mutually orthogonal. Therefore, a general quantum cloning device is impossible.

Even if one allows non-unitary cloning devices, the cloning of non-orthogonal pure states remains impossible unless one is willing to tolerate a finite loss of fidelity in the cloned states.

On the positive side, the impossibility of determining the components of a vector state prevents non-relativistic quantum mechanics to clash with relativity theory (Sects. 12.1 and 13.3).

2.6.3   Commutation Relations and Poisson Brackets

From the commutation relation (2.15), one obtains

$$[\hat{x}^n, \hat{p}] = i\hbar \, n \, \hat{x}^{n-1} , \qquad [\hat{x}, \hat{p}^n] = i\hbar \, n \, \hat{p}^{n-1} , \qquad (2.45)$$

which shows that the commutation operation acts as a sort of differential operation. Arbitrary functions of the coordinate and the momenta, $\hat{u} = u(\hat{x}, \hat{p})$, satisfy the following relations:

$$[\hat{u}, \hat{v}] = -[\hat{v}, \hat{u}]$$

$$[\hat{u}, c] = 0$$

$$[(\hat{u} + \hat{v}), \hat{w}] = [\hat{u}, \hat{w}] + [\hat{v}, \hat{w}]$$

$$[\hat{u}\hat{v}, \hat{w}] = [\hat{u}, \hat{w}]\hat{v} + \hat{u}[\hat{v}, \hat{w}]$$

$$0 = [\hat{u}, [\hat{v}, \hat{w}]] + [\hat{v}, [\hat{w}, \hat{u}]] + [\hat{w}, [\hat{u}, \hat{v}]] , \qquad (2.46)$$

as may be verified through power series expansions. These properties are shared by the (classical) Poisson brackets

$$\{u, v\}_{PB} = \frac{\partial u}{\partial x} \frac{\partial v}{\partial p} - \frac{\partial u}{\partial p} \frac{\partial v}{\partial x} . \qquad (2.47)$$

Dirac has pointed out that "classical mechanics provides a valid description of dynamical systems under certain conditions. We should thus expect that important concepts in classical mechanics correspond to important concepts in quantum mechanics" [15]. In fact, the quantum mechanical commutator can be obtained from the classical Poisson bracket through the replacement of the coordinate and momentum by the corresponding quantum operators and multiplication by $i\hbar$

$$i\hbar\{u, v\}_{PB} \rightarrow [\hat{u}, \hat{v}] . \qquad (2.48)$$

The commutativity of the classical multiplication rule is obtained in the limiting case $\hbar \rightarrow 0$.

However, the Poisson brackets (2.47) can only be defined with reference to a definite set of coordinates and momenta (although they are invariant under a change of this set). The quantum commutation relation is not limited by this condition and, therefore, has a more fundamental character. A particularly relevant example is the case of the spin components, which do not have classical counterparts (see Sect. 5.2).

2.7*   Properties of Hilbert Spaces and Operators

In the following, we briefly review some properties of these mathematical tools.

A Hilbert space is a generalization of the Euclidean, three-dimensional space (see Table 2.1). As in ordinary space, the summation $c_a \Psi_a + c_b \Psi_b$ and the scalar

Table 2.1 Some relevant properties of vectors and operators in Euclidean and Hilbert spaces

	Euclidean space	Hilbert space
Vectors	$\mathbf{r}$	Ψ
Superposition	$\mathbf{r} = c_a \mathbf{r}_a + c_b \mathbf{r}_b$	$\Psi = c_a \Psi_a + c_b \Psi_b$
Scalar product	$\langle \mathbf{r}_a | \mathbf{r}_b \rangle = \mathbf{r}_a \cdot \mathbf{r}_b = c_{ab}$	$\langle \Psi_a | \Psi_b \rangle = \langle \Psi_b | \Psi_a \rangle^* = c_{ab}$
	$c_a, c_b, c_{ab} = $ real	$c_a, c_b, c_{ab} = $ complex
Basis set	$\langle \mathbf{v}_i | \mathbf{v}_j \rangle = \delta_{ij}$	$\langle \varphi_i | \varphi_j \rangle \equiv \langle i | j \rangle = \delta_{ij}$
Dimension ν	3	$2 \leq \nu \leq \infty$
Completeness	$\mathbf{r} = \sum_i x_i \mathbf{v}_i$	$\Psi = \sum_i c_i \varphi_i$
Projection	$x_i = \langle \mathbf{v}_i | \mathbf{r} \rangle$	$c_i = \langle \varphi_i | \Psi \rangle$
Scalar product	$\langle \mathbf{r}_a | \mathbf{r}_b \rangle = \sum_i x_i^{(a)} x_i^{(b)}$	$\langle \Psi_a | \Psi_b \rangle = \sum_i \left(c_i^{(a)} \right)^* c_i^{(b)}$
Norm	$\langle \mathbf{r} | \mathbf{r} \rangle^{1/2} = \left(\sum_i x_i^2 \right)^{1/2}$	$\langle \Psi | \Psi \rangle^{1/2} = \left(\sum_i |c_i|^2 \right)^{1/2}$
Operators	$\hat{R}_\eta(\theta) \, \mathbf{r}_a = \mathbf{r}_b$	$\hat{Q} \Psi_a = \Psi_b$
Commutators	$[\hat{R}_x(\frac{\pi}{2}), \hat{R}_y(\frac{\pi}{2})] \neq 0$	$[\hat{Q}, \hat{R}]$
Eigenvalues	$\hat{D}_i \mathbf{v}_i = \lambda_i \mathbf{v}_i$	$\hat{Q} \varphi_i = q_i \varphi_i$

product $\langle \Psi_b | \Psi_a \rangle = c_{ab}$ between two vectors are well-defined operations.[15] While the constants c_a, c_b, c_{ab} are real numbers in everyday space, it is essential to allow for complex values in quantum mechanics.

The norm of a vector is defined as the square root of the scalar product of a vector with itself. A vector is said to be normalized if its norm equals 1. Two vectors are orthogonal if their scalar product vanishes. A vector Ψ is linearly independent of a subset of vectors $\Psi_a, \Psi_b, \ldots, \Psi_d$ if it cannot be expressed as a linear combination of them[16] ($\Psi \neq c_a \Psi_a + c_b \Psi_b + \cdots + c_d \Psi_d$).

These last two concepts allow us to define sets of basis vectors φ_i satisfying the requirement of orthonormalization. Moreover, these sets may be complete, in the sense that any vector Ψ may be expressed as a linear combination of them[17] [see (2.6)]. The scalar product $\langle i | \Psi \rangle$ is the projection of Ψ onto φ_i. The scalar product between two vectors Ψ_a, Ψ_b and the square of the norm of the vector Ψ are also given in terms of the amplitudes c_i in Table 2.1.
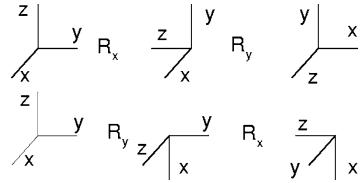
The number of states in a basis set is the dimension ν of the associated Hilbert space. It has the value 3 in normal space. In this book, we use Hilbert spaces with dimensions ranging from two to infinity.

---

[15]Definition of these fundamental operations is deferred to each realization of Hilbert spaces [(3.2), (3.4) and (4.1), (4.2)]. In the present chapter we use only the fact that they exist and that $\langle a | b \rangle = \langle b | a \rangle^*$.

[16]Although the term "linear combination" usually refers only to finite sums, we extend its meaning to also include an infinity of terms.

[17]The most familiar case of the expansion of a function in terms of an orthonormal basis set is the Fourier expansion in terms of the exponentials $\exp[ikx]$, which constitute the complete set of eigenfunctions corresponding to the free particle case (see Sect. 4.3).

Fig. 2.8 The final orientation of the axes depends on the order of the rotations. R_η here represents a rotation of $\pi/2$ around the η-axis

In ordinary space, vectors are defined by virtue of their transformation properties under rotation operations $\hat{R}_\eta(\theta)$ (η denoting the axis of rotation, and θ the angle). These operations are generally non-commutative, as the reader may easily verify by performing two successive rotations of $\theta = \pi/2$, first around the x-axis and then around the y-axis, and subsequently comparing the result with the one obtained by reversing the order of these rotations (Fig. 2.8). Mathematically, this is expressed through the non-vanishing of the operator (2.8).

In ordinary space, a dilation $\hat{D}$ is an operation yielding the same vector multiplied by a (real) constant. This operation has been generalized in terms of eigenvectors and eigenvalues in (2.9). In general, linear combinations of such eigenvectors do not satisfy the eigenvalue equation.

2.7.1* Some Properties of Hermitian Operators

The Hermitian conjugate operator $\hat{Q}^+$ is defined through the (2.11). Similarly, we may write

$$\langle \Psi_b | Q | \Psi_a \rangle = \langle \hat{Q} \Psi_a | \Psi_b \rangle^* = \langle \hat{Q}^+ \Psi_b | \Psi_a \rangle . \tag{2.49}$$

The following properties are easy to demonstrate

$$\left(\hat{Q} + c \hat{R} \right)^+ = \hat{Q}^+ + c^* \hat{R}^+, \tag{2.50}$$

$$\left(\hat{Q} \hat{R} \right)^+ = \hat{R}^+ \hat{Q}^+. \tag{2.51}$$

According to (2.11), the norm of the state $\hat{Q}\Psi$ is obtained by

$$\langle \hat{Q}\Psi | \hat{Q}\Psi \rangle^{1/2} = \langle \Psi | Q^+ Q | \Psi \rangle^{1/2} . \tag{2.52}$$

The norm is a real, positive number.

An operator is said to be Hermitian if it is equal to its own Hermitian conjugate operator

$$\hat{Q}^+ = \hat{Q}. \tag{2.53}$$

Assume now that the state φ_i is an eigenstate of the Hermitian operator $\hat{Q}$ corresponding to the eigenvalue q_i. In this case

$$\langle i|Q|i\rangle = q_i\,\langle i|i\rangle\,, \qquad \langle i|Q|i\rangle^* = q_i^*\,\langle i|i\rangle$$

$$\langle i|Q|i\rangle = \langle i|Q|i\rangle^* \;\rightarrow\; q_i = q_i^*. \tag{2.54}$$

Therefore, the eigenvalues of Hermitian operators are real numbers.

Consider now the non-diagonal terms

$$\langle j|Q|i\rangle = q_i\langle j|i\rangle\,, \qquad \langle i|Q|j\rangle^* = q_j^*\langle i|j\rangle^* = q_j^*\langle j|i\rangle\,, \tag{2.55}$$

then

$$0 = (q_i - q_j)\,\langle j|i\rangle, \tag{2.56}$$

i.e. two eigenstates, belonging to different eigenvalues, are orthogonal. They may also be orthonormal, upon multiplication by an appropriate normalization constant, which is determined up to a phase.

The eigenvectors of a Hermitian operator constitute a complete set of states for a given system. This means that any state function Ψ, describing any state of the same system, may be expressed as a linear combination of basis states φ_i [see (2.6)].

We define the projection operator (a theoretical filter) $|i\rangle\langle i|$ through the equation

$$|i\rangle\langle i\,|\,\varphi_j \equiv \langle i\,|\,j\rangle\varphi_i = \delta_{ij}\,\varphi_i\,, \tag{2.57}$$

which implies that

$$\sum_i |i\rangle\langle i|\,\Psi = \Psi \tag{2.58}$$

for any Ψ. Thus, unity may be expressed as the operator $\sum_i |i\rangle\langle i|$. From this property stems the closure property, according to which the matrix elements of the product of Hermitian operators may be calculated as the sum over all possible intermediate states of products of the matrix elements corresponding to each separate operator

$$\langle i|QR|j\rangle = \sum_k \langle i|Q|k\rangle\langle k|R|j\rangle. \tag{2.59}$$

2.7.2*   *Unitary Transformations*

The unitary matrix $(\mathcal{U}_{ai}) = (\langle i|a\rangle)$ in (2.14) transforms the basis set φ_i into the basis set χ_a. Such a matrix does not represent a physical observable and it is not therefore required to be Hermitian.

The inverse transformation to (2.14) is written as

$$\varphi_i = \sum_a \langle a|i \rangle \chi_a \,. \tag{2.60}$$

Therefore, the inverse transformation $\mathcal{U}^{-1}$ is the transposed conjugate:

$$\mathcal{U}^{-1} = (\langle a|i \rangle) = \mathcal{U}^+ \,, \quad \mathcal{U}^+\mathcal{U} = \mathcal{U}\mathcal{U}^+ = \mathcal{I}, \tag{2.61}$$

where $\mathcal{I}$ is the unit matrix. A matrix satisfying (2.61) is said to be unitary. Equation (2.61) implies that

$$\sum_i \langle a|i \rangle \langle i|b \rangle = \delta_{ab}$$

$$\sum_a \langle i|a \rangle \langle a|j \rangle = \langle i|j \rangle = \delta_{ij} \tag{2.62}$$

If states are transformed according to $\chi = \mathcal{U}\,\varphi$, then the state $\mathcal{U}\,\hat{Q}\,\varphi$ may be written as

$$\mathcal{U}\,\hat{Q}\,\varphi = \mathcal{U}\,\hat{Q}\,\mathcal{U}^+\mathcal{U}\,\varphi = \mathcal{R}\,\chi, \tag{2.63}$$

which yields the rule for the transformation of operators, namely

$$\hat{R} = \mathcal{U}\,\hat{Q}\,\mathcal{U}^+. \tag{2.64}$$

In addition to the norm, unitary transformations preserve the value of the determinant and the trace

$$\det(\langle a|R|b \rangle) = \det(\langle i|Q|j \rangle),$$

$$\mathrm{trace}(Q) \equiv \sum_i \langle i|Q|i \rangle = \mathrm{trace}(R) \equiv \sum_a \langle a|R|a \rangle. \tag{2.65}$$

2.8* Notions on Probability Theory

Probability theory studies the likelihood P_i that the outcome q_i of an event will take place. The limits of P_i are

$$0 \le P_i \le 1 \,. \tag{2.66}$$

If $P_i = 0$, the outcome q_i cannot occur; if $P_i = 1$, it will take place with certainty.

If two events (i, j) are statistically independent, the probability that both i and j take place is given by the product

$$P_{(i\,\mathrm{and}\,j)} = P_i\,P_j. \tag{2.67}$$

If two events are mutually exclusive, the probability that one or the other occur is
the sum

$$P_{(i \text{ or } j)} = P_i + P_j.$$ (2.68)

Probability may be defined as

$$P_i \equiv \lim_{N \to \infty} \frac{n_i}{N},$$ (2.69)

where n_i is the number of outcomes q_i of a total of $N \equiv \sum_i n_i$ outcomes. Since
the limit $N \to \infty$ is never attained, in practice N should be made large enough so
that the fluctuations become sufficiently small.

The collection of P_is is called the (discrete) probability distribution. The
concepts of average $\langle Q \rangle$, root mean square $\langle Q^2 \rangle^{1/2}$ and root mean square deviation
ΔQ, applied in Sect. 2.4, are given by

$$\langle Q \rangle = \sum_i q_i \, P_i,$$

$$\langle Q^2 \rangle^{1/2} = \left(\sum_i q_i^2 \, P_i \right)^{1/2},$$

$$\Delta Q = \langle (Q - \langle Q \rangle)^2 \rangle^{1/2} = \left(\langle Q^2 \rangle - \langle Q \rangle^2 \right)^{1/2}.$$ (2.70)

In the case of a continuous distribution, the sums $\sum_i$ are replaced by integrals
$\int dx$. Instead of probabilities P_i one defines probability densities $\rho(x)$ such that

$$1 = \int_{-\infty}^{\infty} \rho(x) \, dx,$$

$$\langle Q \rangle = \int_{-\infty}^{\infty} q(x) \, \rho(x) dx.$$ (2.71)

Problems

Problem 1. Assume that the state Ψ is given by the linear combination $\Psi = c_1 \Psi_1 + c_2 \Psi_2$, where the amplitudes c_1, c_2 are arbitrary complex numbers, and both
states Ψ_1, Ψ_2 are normalized.

1. Normalize the state Ψ, assuming that $\langle 1|2 \rangle = 0$.
2. Find the probability of the system being in the state Ψ_1.

Problem 2. Use the same assumptions as in Problem 2, but $\langle 1|2 \rangle = c \neq 0$

1. Find a linear combination $\Psi_3 = \lambda_1 \Psi_1 + \lambda_2 \Psi_2$, such that it is orthogonal to Ψ_1 and normalized.
2. Express the vector Ψ as a linear combination of Ψ_1 and Ψ_3.

Problem 3. Prove (2.50) and (2.51).
Hint: Apply successively the definition of Hermitian conjugate to the operators $\hat{Q}, \hat{R}$. For instance, start with $\langle \Psi_b | Q\, R | \Psi_a \rangle = \langle \hat{R}\Psi_a | Q^+ | \Psi_b \rangle^* = \cdots$.

Problem 4. Show that

$$[\hat{Q}, \hat{R}] = -[\hat{R}, \hat{Q}]$$
$$[\hat{Q}\,\hat{R}, \hat{S}] = [\hat{Q}, \hat{S}]\,\hat{R} + \hat{Q}\,[\hat{R}, \hat{S}].$$

Problem 5. Find the commutation relation between the coordinate operator $\hat{x}$ and the one-particle Hamiltonian (2.16). Discuss the result in terms of the simultaneous determination of energy and position of a particle.

Problem 6. Find the commutation relations

1. $[\hat{p}^n, \hat{x}]$, where n is an integer
2. $[f(\hat{p}), \hat{x}]$. Hint: Expand $f(\hat{p})$ in power series of $\hat{p}$ and apply the previous commutation relation.

Problem 7. Verify that the commutation relation (2.15) is consistent with the fact that the operators $\hat{x}$ and $\hat{p}$ are Hermitian.

Problem 8. Assume the basis set of states φ_i

1. Calculate the effect of the operator $\hat{R} \equiv \sum_i |i\rangle\langle i|$ on an arbitrary state Ψ.
2. Repeat for the operator $\hat{R} \equiv \Pi_i \left(\hat{Q} - q_i \right)$, assuming that the equation $\hat{Q}\varphi_i = q_i \varphi_i$ is satisfied.

Problem 9. Find the relation between the matrix elements of the operators $\hat{p}$ and $\hat{x}$ in the base of eigenvectors of the Hamiltonian (2.16).

Problem 10. Consider the eigenvalue equations

$$\hat{F}\varphi_1 = f_i \varphi_1, \quad \hat{F}\varphi_2 = f_2 \varphi_2, \quad \hat{G}\chi_1 = g_1\chi_1, \quad \hat{G}\chi_2 = g_2\chi_2, \qquad (2.72)$$

and the relations

$$\varphi_1 = \frac{1}{\sqrt{5}}(2\chi_1 + \chi_2), \qquad \varphi_2 = \frac{1}{\sqrt{5}}(\chi_1 - 2\chi_2). \qquad (2.73)$$

1. Is it possible to simultaneously measure the observables F and G?

2. Assume that a measurement of F has yielded the eigenvalue f_1. Subsequently G and F are measured (in this order). Which are the possible results and their probabilities?

Problem 11. Consider eigenstates φ_p of the momentum operator. Assume that the system is prepared in the state

$$\Psi = \frac{1}{\sqrt{6}}(\varphi_{2p} + \varphi_p) + \sqrt{\frac{2}{3}}\varphi_{-p}. \qquad (2.74)$$

1. What are the possible results of a measurement of the kinetic energy K, and what are their respective probabilities?
2. Calculate the expectation value and the standard deviation of the kinetic energy.
3. What is the vector state after a measurement of the kinetic energy that has yielded the value $k_p = p^2/2M$?

Problem 12. Evaluate, in m.k.s. units, possible values of the precision to which the velocity and the position of a car should be measured to verify the uncertainty relation (2.37).

Problem 13. A 10 MeV proton beam is collimated by means of diaphragms with a 5 mm aperture.

1. Show that the spread in energy ΔE_H, associated with the uncertainty principle, is negligible relative to the total spread, $\Delta E \approx 10^{-3}$ MeV.
2. Calculate the distance x that a proton has to travel to traverse 5 mm in a perpendicular direction, if the perpendicular momentum is due only to the uncertainty principle.

Problem 14. Verify (2.46).

Chapter 3
The Heisenberg Realization of Quantum Mechanics

In this chapter, we present the simplest realization of the basic principles of quantum mechanics. We employ column vectors as state vectors and square matrices as operators. This formulation is especially suitable for Hilbert spaces with finite dimensions. However, we also treat within this framework the problem of the harmonic oscillator and the Jaynes–Cummings model.

3.1   Matrix Formalism

3.1.1   A Realization of the Hilbert Space

The state vector Ψ may be expressed by means of the amplitudes c_i filling the successive rows of a column vector:

$$\Psi = (c_i) \equiv \begin{pmatrix} c_a \\ c_b \\ \vdots \\ c_v \end{pmatrix}. \tag{3.1}$$

The dimension of the Hilbert space is given by the number of rows. The sum of two column vectors is another column vector in which the amplitudes are added:

$$\alpha_B \Psi_B + \alpha_C \Psi_C = (\alpha_B b_i + \alpha_C c_i). \tag{3.2}$$

The scalar product requires the definition of the adjoint vector Ψ^+, i.e. a row vector obtained from Ψ with amplitudes

$$\Psi^+ = (c_a^*, c_b^*, \ldots, c_v^*). \tag{3.3}$$

The scalar product of two vectors Ψ_B and Ψ_C is defined as the product of the adjoint vector Ψ_B^+ and the vector Ψ_C, viz.,

$$\langle \Psi_B | \Psi_C \rangle = \sum_{i=a}^{i=v} b_i^* c_i,$$

$$\langle \Psi | \Psi \rangle = \sum_{i=a}^{i=v} |c_i|^2 = 1. \tag{3.4}$$

A useful set of (orthonormal) basis states is given by the vector columns φ_i with amplitudes $c_j = \delta_{ij}$. In such a basis, the arbitrary vector (3.1) may be expanded as

$$\Psi = c_a \begin{pmatrix} 1 \\ 0 \\ \vdots \\ 0 \end{pmatrix} + c_b \begin{pmatrix} 0 \\ 1 \\ \vdots \\ 0 \end{pmatrix} + \cdots + c_v \begin{pmatrix} 0 \\ 0 \\ \vdots \\ 1 \end{pmatrix}. \tag{3.5}$$

All the properties listed in Table 2.1 are reproduced within the framework of column vectors.

Operators are represented by square matrices

$$\hat{Q} = (\langle i|Q|j \rangle) \equiv \begin{pmatrix} \langle a|Q|a \rangle & \langle a|Q|b \rangle & \cdots & \langle a|Q|v \rangle \\ \langle b|Q|a \rangle & \langle b|Q|b \rangle & \cdots & \langle b|Q|v \rangle \\ \vdots & \vdots & \ddots & \vdots \\ \langle v|Q|a \rangle & \langle v|Q|b \rangle & \cdots & \langle v|Q|v \rangle \end{pmatrix}. \tag{3.6}$$

The matrices corresponding to physical observables are Hermitian [see (2.11)]. The initial state j labels the columns, while the final state i labels the rows. The order $a, b, \ldots, v$ is immaterial, provided it is the same in both columns and rows (i.e. the matrix elements $\langle i|Q|i \rangle$ should lie on the diagonal). The matrix elements $\langle i|Q|j \rangle$ are constructed as in (2.10). If φ_i belongs to the basic set

$$\hat{Q}\,\varphi_i = \sum_j c_j^{(i)} \varphi_j \quad \rightarrow \quad \langle j|Q|i \rangle = c_j^{(i)}. \tag{3.7}$$

A matrix multiplying a vector yields another vector, so that

$$\Psi_B = \hat{Q}\,\Psi_C \longleftrightarrow b_i = \sum_j \langle i|Q|j \rangle c_j. \tag{3.8}$$

The product of two matrices is another matrix:

$$\hat{S} = \hat{Q}\,\hat{R} \longleftrightarrow \langle i|S|j\rangle = \sum_k \langle i|Q|k\rangle\langle k|R|j\rangle, \tag{3.9}$$

which is consistent with the closure property (2.59). The multiplication of matrices is a non-commutative operation, as befits the representation of quantum operators.

3.1.2 Solution of the Eigenvalue Equation

In matrix form, the eigenvalue equation (2.9) reads

$$\begin{pmatrix} \langle a|Q|a\rangle & \langle a|Q|b\rangle & \cdots & \langle a|Q|v\rangle \\ \langle b|Q|a\rangle & \langle b|Q|b\rangle & \cdots & \langle b|Q|v\rangle \\ \vdots & \vdots & \ddots & \vdots \\ \langle v|Q|a\rangle & \langle v|Q|b\rangle & \cdots & \langle v|Q|v\rangle \end{pmatrix} \begin{pmatrix} c_a \\ c_b \\ \vdots \\ c_v \end{pmatrix} = q \begin{pmatrix} c_a \\ c_b \\ \vdots \\ c_v \end{pmatrix}, \tag{3.10}$$

which is equivalent to the v linear equations (one equation for each value of i)

$$\sum_{j=1}^{j=v} \langle i|Q|j\rangle\, c_j = q\, c_i. \tag{3.11}$$

The eigenvalues q and the amplitudes c_i are the unknowns to be determined.[1]

The solution to (3.11) is obtained by casting the original matrix $(\langle i|Q|j\rangle)$ into a diagonal form. In this case the diagonal matrix elements become the eigenvalues, $\langle i|Q|j\rangle = \delta_{ij} q_i$. The ith eigenvector is given by the amplitudes $c_j = \delta_{ij}$, as in (3.5). For instance,

$$\begin{pmatrix} q_1 & 0 & \cdots & 0 \\ 0 & q_2 & \cdots & 0 \\ \vdots & \vdots & \ddots & \vdots \\ 0 & 0 & \cdots & q_v \end{pmatrix} \begin{pmatrix} 0 \\ 1 \\ \vdots \\ 0 \end{pmatrix} = q_2 \begin{pmatrix} 0 \\ 1 \\ \vdots \\ 0 \end{pmatrix}. \tag{3.12}$$

The linear homogeneous equations (3.11) have the trivial solution $c_i = 0$, to be discarded. The existence of additional, non-trivial solutions requires the determinant to vanish:

$$\det\left(\langle i|Q|j\rangle - q\delta_{ij}\right) = 0. \tag{3.13}$$

---

[1]This equation may be obtained directly by using the expansion (2.6) on both sides of the general eigenvalue equation $\hat{Q}\Psi = q\Psi$. One obtains $\sum_j c_j \hat{Q}\varphi_j = q \sum_j c_j \varphi_j$. The scalar product with φ_i of both sides of this last equation yields (3.11).

This eigenvalue equation is equivalent to a polynomial equation for q. Its ν roots are the eigenvalues of the operator $\hat{Q}$.

The vanishing of the determinant (3.13) implies that one of the equations (3.11) may be expressed as a linear combination of the other $\nu - 1$ equations. Therefore, by disregarding one of these equations (for instance, the one corresponding to the last row) and dividing the remaining equations by c_a, one obtains a set of $\nu - 1$ non-homogeneous linear equations[2] yielding the value of the ratios $c_b/c_a, c_c/c_a, \ldots, c_\nu/c_a$, for each eigenvalue q. The normalization equation (3.4) determines the value of $|c_a|^2$, up to the usual overall arbitrary phase of the state vector. Note that the relative phases in the linear combination have physical significance, although the overall phase is unimportant.

Diagonalization yields a new set of eigenstates ϕ_a. Each of them may be expressed as a linear combination of the old basis states φ_i.

$$\phi_a = \sum_i \langle i | a \rangle \varphi_i. \tag{3.14}$$

The amplitudes $\langle i | a \rangle$ are the matrix elements of a unitary matrix $\mathcal{U} = (\langle i | a \rangle)$ (2.14). The modulus squared $|\langle a | i \rangle|^2$ is both the probability of measuring the eigenvalue q_i, associated with the eigenstate φ_i, if the system is in the state ϕ_a, and the probability of measuring the eigenvalue r_a, associated with the eigenstate ϕ_a, when the state of the system is φ_i.

3.2 Two-Dimensional Spaces

A general vector state is written as a superposition of the basis states (3.5):

$$\Psi = c_a \varphi_a + c_b \varphi_b$$
$$\varphi_a = \begin{pmatrix} 1 \\ 0 \end{pmatrix}, \quad \varphi_b = \begin{pmatrix} 0 \\ 1 \end{pmatrix}. \tag{3.15}$$

We define the Hermitian, traceless, Pauli matrices σ_i $(i = x, y, z)$

$$\sigma_x = \begin{pmatrix} 0 & 1 \\ 1 & 0 \end{pmatrix}, \qquad \sigma_y = \begin{pmatrix} 0 & -i \\ i & 0 \end{pmatrix}, \qquad \sigma_z = \begin{pmatrix} 1 & 0 \\ 0 & -1 \end{pmatrix}, \qquad \mathcal{I} = \begin{pmatrix} 1 & 0 \\ 0 & 1 \end{pmatrix}. \tag{3.16}$$

They all square to the unit matrix $\mathcal{I}$. The basis states (3.15) are eigenstates of σ_z with eigenvalues ± 1.

---

[2]If several roots have the same eigenvalue, more equations should be discarded to get a non-homogeneous set of equations.

The most general observable can be written as a linear combination of the matrices (3.16) with real parameters κ_0, κ_i

$$\hat{Q} = \kappa_0 \mathcal{I} + \sum_i \kappa_i \sigma_i. \tag{3.17}$$

The two-component states satisfy the eigenvalue equation

$$\begin{pmatrix} \langle a|Q|a\rangle & \langle a|Q|b\rangle \\ \langle b|Q|a\rangle & \langle b|Q|b\rangle \end{pmatrix} \begin{pmatrix} c_a \\ c_b \end{pmatrix} = q_{\pm} \begin{pmatrix} c_a \\ c_b \end{pmatrix}, \tag{3.18}$$

where $\langle a|Q|a\rangle = \kappa_0 + \kappa_z$, $\langle b|Q|b\rangle = \kappa_0 - \kappa_z$ and $\langle a|Q|b\rangle = \langle b|Q|a\rangle^* = \kappa_x - i\kappa_y$. The resulting eigenvalues are

$$q_{\pm} = \frac{1}{2}(\langle a|Q|a\rangle + \langle b|Q|b\rangle) \pm \frac{1}{2}\sqrt{(\langle a|Q|a\rangle - \langle b|Q|b\rangle)^2 + 4|\langle a|Q|b\rangle|^2}, \tag{3.19}$$
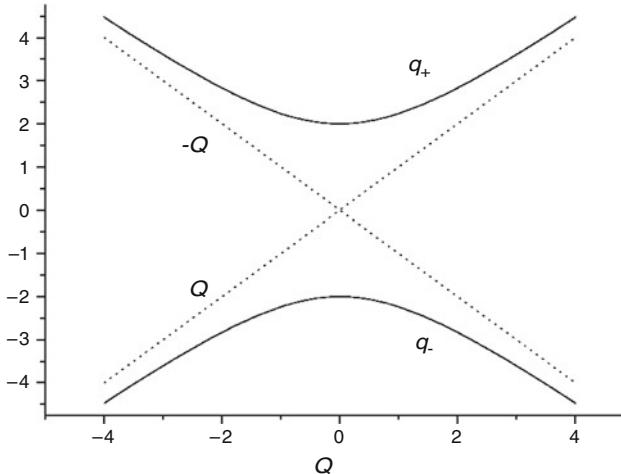
while the amplitudes of the eigenvectors are given by

$$\left.\frac{c_b}{c_a}\right|_{\pm} = \frac{q_{\pm} - \langle a|Q|a\rangle}{\langle a|Q|b\rangle}, \qquad (c_a)_{\pm} = \left(1 + \left|\frac{c_b}{c_a}\right|_{\pm}^2\right)^{-\frac{1}{2}}. \tag{3.20}$$

Figure 3.1 plots the eigenvalues $q_{\pm}$ and the initial expectation values as functions of $Q \equiv \langle a|Q|a\rangle$, assuming a traceless situation ($\langle a|Q|a\rangle = -\langle b|Q|b\rangle$) and $\langle a|Q|b\rangle = 2$. The eigenvalue q_+ is always higher than $|Q|$, while q_- is always below $-|Q|$: the two eigenvalues repel each other and never cross, if $\langle a|Q|b\rangle \neq 0$. The distance $\Delta = \sqrt{Q^2 + |\langle a|Q|b\rangle|^2} - Q$ measures the increase in the highest eigenvalue of Q, due to the superposition of the states φ_a, φ_b, and it is maximized at the crossing point $Q = 0$.

The physical world displays many systems with two states, the spin being the most conspicuous one. But in fact, any two states sufficiently isolated from the remaining ones may be approximated as a two-state system, for which the no-crossing rule holds. Another example is given by an electron and two protons. As a reasonable approximation, we may neglect the motion of the protons, since they are much heavier than the electron. The two states φ_a, φ_b represent the electron bound to each of the protons: a hydrogen atom and a separate proton in each case. In this case the Hamiltonian $\hat{H}$ plays the role of $\hat{Q}$ in (3.18) and (3.19). The extra binding Δ, arising from the superposition of states φ_a, φ_b, allows for the existence of a bound state: the stability of the ionized hydrogen molecule thus has a purely quantum mechanical origin. This problem is discussed in more detail in Sect. 8.4.1.

Let us consider the case $\hat{Q} = \sigma_x$. Equation (3.19) yields the eigenvalues $s_x = \pm 1$ and the eigenvectors

Fig. 3.1 Eigenvalues $q_\pm$ of a 2×2 system (*continuous curves*) as functions of Q, half of the energy distance between the diagonal matrix elements (*dotted lines*)

$$\phi_a^{(x)} = \frac{1}{\sqrt{2}} \begin{pmatrix} 1 \\ 1 \end{pmatrix} = \frac{1}{\sqrt{2}} \varphi_a + \frac{1}{\sqrt{2}} \varphi_b,$$

$$\phi_b^{(x)} = \frac{1}{\sqrt{2}} \begin{pmatrix} 1 \\ -1 \end{pmatrix} = \frac{1}{\sqrt{2}} \varphi_a - \frac{1}{\sqrt{2}} \varphi_b. \tag{3.21}$$

These equations express the eigenstates of σ_x as linear combinations of the eigenstates (3.15) of σ_z. The relevance of the relative sign is apparent, in spite of the fact that the probability of obtaining any component of σ_z is the same for both cases.

The unitary transformation

$$\mathcal{U} = \frac{1}{\sqrt{2}} \begin{pmatrix} 1 & 1 \\ 1 & -1 \end{pmatrix} \tag{3.22}$$

transforms the basis set of eigenvectors of the operator σ_z into the basis set of eigenvectors of σ_x, in accordance with (3.14)

$$\mathcal{U} \begin{pmatrix} 1 \\ 0 \end{pmatrix} = \frac{1}{\sqrt{2}} \begin{pmatrix} 1 \\ 1 \end{pmatrix}, \qquad \mathcal{U} \begin{pmatrix} 0 \\ 1 \end{pmatrix} = \frac{1}{\sqrt{2}} \begin{pmatrix} 1 \\ -1 \end{pmatrix}. \tag{3.23}$$

Similarly, the operator σ_z is transformed into the operator σ_x [see (2.14)]

$$\begin{pmatrix} 0 & 1 \\ 1 & 0 \end{pmatrix} = \mathcal{U} \begin{pmatrix} 1 & 0 \\ 0 & -1 \end{pmatrix} \mathcal{U}^+. \tag{3.24}$$

It happens that the operators representing the spin components are given by $\hat{S}_i = \frac{\hbar}{2}\sigma_i$. Thus, the fact that the eigenvalues of σ_z are the same as those of σ_x is to be expected for physical reasons: the eigenvalues do indeed have physical significance, while the orientation of the coordinate system in an isotropic space does not.

3.3 Harmonic Oscillator

Here we present a solution to the harmonic oscillator problem, a solution that stems directly from the basic principles listed in Sect. 2.3. The Hamiltonian corresponding to the one-dimensional harmonic oscillator is

$$\hat{H} = \frac{1}{2M}\hat{p}^2 + \frac{M\omega^2}{2}\hat{x}^2, \tag{3.25}$$

where ω is the classical frequency (Fig. 3.2).

The harmonic oscillator potential is probably the most widely used potential in physics, because of its ability to represent physical potentials in the vicinity of stable equilibrium [e.g. vibrational motion in molecules (8.28)].

It is always convenient to start by finding the order of magnitude of the quantities involved. To do so, we apply the Heisenberg uncertainty principle (2.37). If the substitutions $\hat{x} \to \Delta x$ and $\hat{p} \to \hbar/2\Delta x$ are made in the harmonic oscillator energy, so that

$$E \geq \frac{\hbar^2}{8M\,(\Delta x)^2} + \frac{M\omega^2\,(\Delta x)^2}{2}, \tag{3.26}$$

then minimization with respect to Δx gives the value at the minimum:

$$(\Delta x)_{\text{min}} = \sqrt{\frac{\hbar}{2M\omega}}, \tag{3.27}$$

which yields the characteristic orders of magnitude

$$x_{\text{c}} = \sqrt{\frac{\hbar}{M\omega}}, \qquad p_{\text{c}} = \sqrt{\hbar M\omega}, \qquad E_{\text{c}} = \hbar\omega. \tag{3.28}$$

3.3.1 Solution of the Eigenvalue Equation

We intend to solve (2.17). The unknowns are the eigenvalues E_i and the eigenfunctions φ_i. The fundamental tool entering the present solution is the commutation relation (2.15).

We first define the operators a^+, a

$$a^+ \equiv \sqrt{\frac{M\omega}{2\hbar}} \hat{x} - \frac{\mathrm{i}}{\sqrt{2M\hbar\omega}} \hat{p}, \qquad a \equiv \sqrt{\frac{M\omega}{2\hbar}} \hat{x} + \frac{\mathrm{i}}{\sqrt{2M\hbar\omega}} \hat{p}. \qquad (3.29)$$

The operators $\hat{x}$ and $\hat{p}$ are Hermitian, since they correspond to physical observables. Therefore, the operators a, a^+ are Hermitian conjugates of each other, according to (2.50). They satisfy the commutation relations

$$\left[\hat{H}, a^+\right] = \hbar\omega a^+, \qquad (3.30)$$

$$\left[a, a^+\right] = 1. \qquad (3.31)$$

We now construct the matrix elements (2.10) for both sides of (3.30), making use of two eigenstates φ_i, φ_j:

$$\langle i|[\hat{H}, a^+]|j\rangle = (E_i - E_j)\langle i|a^+|j\rangle = \hbar\omega\langle i|a^+|j\rangle. \qquad (3.32)$$

We conclude that the matrix element $\langle i|a^+|j\rangle$ vanishes, unless the difference $E_i - E_j$ between the energies of the two eigenstates is the constant $\hbar\omega$. This fact implies that we may sequentially order the eigenstates connected by a^+, the difference between two consecutive energies being $\hbar\omega$. Another consequence is that we may assign an integer number n to each eigenstate.

Since a, a^+ are Hermitian conjugate operators, we may also write

$$\langle n+1|a^+|n\rangle = \langle n|a|n+1\rangle^*. \qquad (3.33)$$

Finally, we expand the expectation value of (3.31):

$$\begin{aligned} 1 &= \langle n|[a, a^+]|n\rangle \\ &= \langle n|a|n+1\rangle\langle n+1|a^+|n\rangle - \langle n|a^+|n-1\rangle\langle n-1|a|n\rangle \\ &= |\langle n+1|a^+|n\rangle|^2 - |\langle n|a^+|n-1\rangle|^2. \end{aligned} \qquad (3.34)$$

This is a finite difference equation in $y_n = |\langle n+1|a^+|n\rangle|^2$, of the type $1 = y_n - y_{n-1}$. Its solutions are

$$|\langle n+1|a^+|n\rangle|^2 = n + c, \qquad \langle n+1|a^+|n\rangle = \sqrt{n+1}, \qquad (3.35)$$

where c is a constant. Since the left-hand side is positive definite, the quantum number n must have a lower limit, which we may choose to be $n = 0$. It corresponds to the ground state φ_0. In such a case, the matrix element $\langle 0|a^+|-1\rangle$ should disappear, which fixes the value of the constant $c = 1$. Therefore, according to (3.33), $\langle -1|a|0\rangle = 0$, which is equivalent to

$$a\,\varphi_0 = 0, \qquad (3.36)$$

i.e. the ground state is annihilated by the operator a, which is called the annihilation operator.

The whole set of orthogonal eigenstates may be constructed by repeatedly applying the operator a^+, the creation operator:

$$\varphi_n = \frac{1}{\sqrt{n!}} \left(a^+\right)^n \varphi_0, \qquad n = 0, 1, \ldots. \tag{3.37}$$

These states are labeled with the quantum number n. They are eigenstates of the operator $\hat{n} = a^+ a$, the number operator, with eigenvalues n:

$$\hat{n}\,\varphi_n = \frac{1}{\sqrt{n!}} a^+ [a, (a^+)^n]\varphi_0 = \frac{1}{\sqrt{n!}} a^+ n \left(a^+\right)^{n-1} \varphi_0 = n\varphi_n. \tag{3.38}$$

The factor $1/\sqrt{n!}$ ensures the normalization of the eigenstates.

To find the matrix elements of the operators $\hat{x}$ and $\hat{p}$, we invert the definition in (3.29):

$$\hat{x} = \sqrt{\frac{\hbar}{2M\omega}} \left(a^+ + a\right), \qquad \hat{p} = i\sqrt{\frac{M\hbar\omega}{2}} \left(a^+ - a\right), \tag{3.39}$$

and obtain the non-vanishing matrix elements

$$\langle n+1|x|n\rangle = \langle n|x|n+1\rangle = \sqrt{\frac{\hbar}{M\omega} \frac{n+1}{2}}, \tag{3.40}$$

$$\langle n+1|p|n\rangle = \langle n|p|n+1\rangle^* = i\sqrt{M\hbar\omega \frac{n+1}{2}}. \tag{3.41}$$

Substitution of (3.39) into the Hamiltonian yields
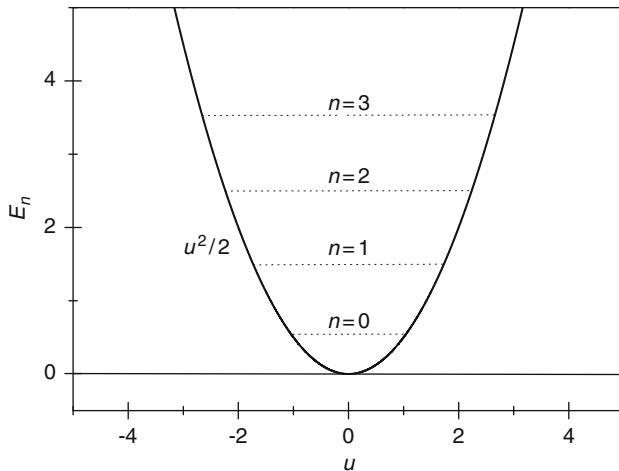
$$\hat{H} = \hbar\omega \left(\hat{n} + \frac{1}{2}\right), \tag{3.42}$$

where the operator $\hat{n}$ has the quantum number n ($= 0,1,2, \ldots$) as eigenvalues. Thus, the Hamiltonian matrix is diagonal, with eigenvalues E_n represented in Fig. 3.2

$$\langle n|H|n\rangle = E_n = \hbar\omega \left(n + \frac{1}{2}\right). \tag{3.43}$$

The creation and annihilation operators are often used in many-body quantum physics (Sects. 7.4.4[†] and 7.8[†]). They are also essential tools in quantum field theory, since they allow us to represent the creation and annihilation of phonons, photons, mesons, etc. (Sects. 9.8.2[†] and 9.8.3[†]).

Quantum mechanics has provided the present derivation based on the fundamental commutation relation (2.15), which yield the properties of the matrix elements

Fig. 3.2 Harmonic oscillator potential and its eigenvalues. All energies are given in units of $\hbar\omega$. The dimensionless variable $u = x/x_{\mathrm{c}}$ has been used

$\langle n|a^+|m\rangle$ in a straightforward way. The results are also valid for any problem involving two operators satisfying (2.15), with a Hamiltonian that is quadratic in these operators.

3.3.2 Some Properties of the Solution

In the following we use this exact, analytical solution of the harmonic oscillator problem to deduce some relevant features of quantum mechanics.[3] The discussion of the spatial dependence of the harmonic oscillator problem is deferred to Sect. 4.2.

- The classical equilibrium position $x = p = 0$ is not compatible with the uncertainty principle, because it implies a simultaneous determination of coordinate and momentum. The replacement of Δx in (3.26) with (3.27) yields the zero-point energy[4] (3.43)

$$E_0 = \frac{1}{2}\hbar\omega, \tag{3.44}$$

---

[3]However, the reader is warned against concluding that most quantum problems are analytically solvable, a conclusion that may be reinforced throughout these notes by the repeated utilization of exactly soluble examples. Most quantum problems require insight into physics to approximate the solution and/or sizeable computing facilities.

[4]The procedure is only expected to yield correct orders of magnitude. It is a peculiarity of the harmonic oscillator that the results are exact.

i.e. the minimum energy that the harmonic oscillator may have. This purely quantum effect was observed even before the invention of quantum mechanics. Roger Mulliken showed in 1924 that the inclusion of (3.44) leads to a better agreement with data obtained by comparing the vibrational spectra (see Sect. 8.4.2) of two molecules made up from different isotopes of the same element [29]. Applications of the zero-point energy concept range from the explanation of the intermolecular Van der Vaals force (Problem 11, Chap. 8) to speculations about massive effects of the electromagnetic vacuum represented by the ground state of infinite harmonic oscillators (Sect. 9.8.2†).

- By using the closure property (2.59) and the matrix elements (3.40) and (3.41), one obtains the matrix element of the commutator $[\hat{x}, \hat{p}]$:

$$
\begin{aligned}
\langle n|[x, p]|m\rangle &= \langle n|x|n+1\rangle\langle n+1|p|m\rangle + \langle n|x|n-1\rangle\langle n-1|p|m\rangle \\
&\quad - \langle n|p|n+1\rangle\langle n+1|x|m\rangle - \langle n|p|n-1\rangle\langle n-1|x|m\rangle \\
&= i\hbar\delta_{nm}.
\end{aligned}
\tag{3.45}
$$

The matrix elements of the operators $\hat{x}^2$ and $\hat{p}^2$ may be constructed in a similar way:

$$
\frac{M\omega}{\hbar}\langle n|x^2|n\rangle = \frac{1}{\hbar M\omega}\langle n|p^2|n\rangle = n + \frac{1}{2},
\tag{3.46}
$$

which implies the equality between the kinetic energy and potential expectation values (virial theorem).

Applying the definition of the root mean square deviation ΔQ given in (2.20), the product $\Delta x \Delta p$ yields

$$
(\Delta x)_n(\Delta p)_n = \frac{E_n}{\omega} = \hbar\left(n + \frac{1}{2}\right) \geq \frac{1}{2}\hbar.
\tag{3.47}
$$

This inequality expresses the uncertainty principle (Sect. 2.6.1). We have thus verified the intimate connection between the commutation relation of two operators and the uncertainties in the measurement of the corresponding physical quantities.

- The invariance with respect to the parity transformation $\hat{\Pi}$ ($x \to -x$) plays an important role in quantum mechanics. The fact that neither the kinetic energy nor the harmonic oscillator potential energy is altered by the parity transformation is expressed by the commutation relation

$$
[\hat{H}, \hat{\Pi}] = 0.
\tag{3.48}
$$

As a consequence of this relation, it is possible to know simultaneously the eigenvalues of the two operators $\hat{H}$, $\hat{\Pi}$ (see Sect. 2.6.1). In this case the eigenstates of the harmonic oscillator Hamiltonian are also eigenstates of the parity operator $\hat{\Pi}$. The eigenvalues of the operator $\hat{\Pi}$ are determined by the fact that the operator $\hat{\Pi}^2$

must have the single eigenvalue $\pi^2 = 1$, since the system is left unchanged after two applications of the parity transformation. There are thus two eigenvalues corresponding to the operator $\hat{\Pi}$, namely $\pi = \pm 1$. The eigenfunctions are either invariant under the parity transformation ($\pi = 1$, even functions) or change sign ($\pi = -1$, odd functions). This is verified in the case of the harmonic oscillator, since the operators a^+, a change sign under the parity transformation and the parity of the state labeled by the quantum number n is therefore

$$\hat{\Pi}\varphi_n = (-1)^n \varphi_n. \tag{3.49}$$

Symmetries constitute essential tools in the characterization and solution of quantum problems. Every symmetry gives rise to a new quantum number.

3.4 The Jaynes–Cummings Model

Consider a system consisting of a two-state atom coupled to a harmonic oscillator. The Hamiltonian of the uncoupled subsystems is

$$\hat{H}_0 = \frac{\hbar}{2} \left[\omega_a \sigma_z + \omega_{\text{ho}} (2\hat{n} + 1) \right]. \tag{3.50}$$

The eigenvalues of this Hamiltonian are organized as ladder doublets separated by the oscillator distance $\hbar \omega_{\text{ho}}$. The atom excitation energy is $\hbar \omega_a$. The eigenvectors of $\hat{H}_0$ are given by the product states $\varphi_a \chi_n$ and $\varphi_b \chi_n$ [see (3.15) and (3.37)].

Let us introduce a coupling Hamiltonian

$$H_{\text{coup}} = -i\frac{\hbar}{2}\Omega \left(a\sigma_+ - a^+\sigma_- \right), \quad \sigma_\pm = \frac{1}{2}(\sigma_x \pm i\sigma_y), \tag{3.51}$$

which feeds the population of the upper atomic state with a simultaneous de-exitation of the oscillator, and vice versa. Therefore, it only displays a non-vanishing matrix element between the states $\varphi_a \chi_n$ and $\varphi_b \chi_{n+1}$, which remain uncoupled from all other pairs. Aside from a common constant energy, the Hamiltonian of the pair is

$$\hat{H}_0 + \hat{H}_{\text{ho}} = \frac{\hbar}{2} \left(W\sigma_z + \Omega_n \sigma_y \right) = \frac{\hbar}{2} \begin{pmatrix} W & -i\Omega_n \\ i\Omega_n & -W \end{pmatrix}, \tag{3.52}$$

where $W = \omega_a - \omega_{\text{ho}}$ and $\Omega_n = \Omega \sqrt{n+1}$. Since this is a particular case of the Hamiltonian (3.18), the discussion following that equation applies. In particular, the resulting eigenstates are of the form

$$\Psi_\pm = c_{an}^{(\pm)} \varphi_a \chi_n + c_{b(n+1)}^{(\pm)} \varphi_b \chi_{n+1}. \tag{3.53}$$

This simple Jaynes–Cummings model [30] is applicable to recent tests of quantum mechanics based on the interaction between a single atom and the electromagnetic field (Sect. 12.3.3).

Problems

Problem 1. Consider the matrix

$$\begin{pmatrix} 0 & 1 & 0 \\ 1 & 0 & 1 \\ 0 & 1 & 0 \end{pmatrix}.$$

1. Find the eigenvalues and verify the conservation of the trace after diagonalization.
2. Find the eigenvector corresponding to each eigenvalue.
3. Check the orthogonality of states corresponding to different eigenvalues.
4. Construct the unitary transformation from the basic set of states used in (3.5) to the eigenstates of this matrix.

Problem 2. Consider the matrix

$$\begin{pmatrix} a & c \\ c & -a \end{pmatrix}.$$

1. Calculate the eigenvalues as functions of the real numbers a, c.
2. Show that the odd terms in c vanish in an expansion in powers of c ($|c| \ll |a|$).
3. Show that the linear term does not disappear if $|c| \gg |a|$.

Problem 3. Which of the following vector states are linearly independent?

$$\varphi_1 = \begin{pmatrix} i \\ 1 \end{pmatrix}, \qquad \varphi_2 = \begin{pmatrix} -i \\ 1 \end{pmatrix}, \qquad \varphi_3 = \begin{pmatrix} 1 \\ i \end{pmatrix}, \qquad \varphi_4 = \begin{pmatrix} 1 \\ -i \end{pmatrix}.$$

Problem 4. Consider the two operators

$$\hat{Q} = \begin{pmatrix} 0.5 & 0 & 0 \\ 0 & 0.5 & 0 \\ 0 & 0 & -1 \end{pmatrix} \quad \text{and} \quad \hat{R} = \begin{pmatrix} 0 & 0.5 & 0 \\ 0.5 & 0 & 0 \\ 0 & 0 & 1 \end{pmatrix}.$$

1. Calculate the eigenvalues.
2. Determine whether or not the operators commute.
3. If so, obtain the simultaneous eigenvectors of both operators.

Problem 5. Consider a unit vector with components $\cos \beta$ and $\sin \beta$ along the z- and x-axes, respectively. The matrix representing the spin operator in this direction is written as $\hat{S}_\beta = \hat{S}_z \cos \beta + \hat{S}_x \sin \beta$.

1. Find the eigenvalues of $\hat{S}_\beta$ using symmetry properties.
2. Diagonalize the matrix.
3. Find the amplitudes of the new eigenstates in a basis for which the operator $\hat{S}_z$ is diagonal.

Problem 6. If a and a^+ are the annihilation and creation operators defined in (3.29), show that $[a, (a^+)^n] = n(a^+)^{(n-1)}$.

Problem 7. 1. Calculate the energy of a particle subject to the potential $V(x) = V_0 + c\hat{x}^2/2$ if the particle is in the third excited state.
2. Calculate the energy eigenvalues for a particle moving in the potential $V(x) = c\hat{x}^2/2 + b\hat{x}$.

Problem 8. 1. Express the distance x_c as a function of the mass M and the restoring parameter c used in Problem 7.
2. If c is multiplied by 9, what is the separation between consecutive eigenvalues?
3. Show that x_c is the maximum displacement of a classical particle moving in a harmonic oscillator potential with an energy of $\hbar\omega/2$.

Problem 9. Evaluate the matrix elements $\langle n + \eta | x^2 | n \rangle$ and $\langle n + \eta | p^2 | n \rangle$ in the harmonic oscillator basis for $\eta = 1, 2, 3, 4$:

1. Using the closure property and the matrix elements (3.41)
2. Applying the operators $\hat{x}^2$ and $\hat{p}^2$, expressed in terms of the a^+, a, on the eigenstates (3.37)

Find the ratio $\langle n + \nu | K | n \rangle : \langle n + \nu | V | n \rangle$ ($\nu = 0, \pm 2$) in the harmonic oscillator basis, where $\hat{K}, \hat{V}$ are the operators corresponding to the kinetic and the potential energies, respectively. Justify the resulting sign difference between these three cases on quantum mechanical grounds.

Problem 10. Calculate the expectation value of the coordinate operator for a linear combination of harmonic oscillator states with the same parity.

Problem 11. 1. Construct the normalized, linear combination of harmonic oscillator states $\Psi = c_0\varphi_0 + c_1\varphi_1$ for which the expectation value $\langle \Psi | x | \Psi \rangle$ becomes maximized.
2. Evaluate in such a state the expectation values of the coordinate, the momentum and the parity operators.
   Note: In some chemical bonds, nature takes advantage of the fact that electrons protrude from the atom in a state similar to the linear combination Ψ. This situation is called hybridization.

Problem 12. Verify the normalization of the states (3.37).

Problem 13. Find the amplitudes $c_i^{(\pm)}$ in (3.53) for the resonant case $\omega_a = \omega_{ho}$.

Chapter 4
The Schrödinger Realization
of Quantum Mechanics

The realization of the basic principles of quantum mechanics by means of position wave functions is presented in Sect. 4.1. This is where the time-independent Schrödinger equation is obtained, and where the spatial dimension in quantum problems appears explicitly.

The harmonic oscillator problem is solved again in Sect. 4.2. The reader will thus be able to contrast two realizations of quantum mechanics by comparing the results obtained here with those presented in Sect. 3.3.

Solutions to the Schrödinger equation in the absence of forces are discussed in Sect. 4.3. Such solutions present normalization problems which are solved by taking into consideration the limiting case of particles moving either in a large, infinitely deep square well potential, or along a circumference with a large radius (Sect. 4.4.1). These solutions are applied to some situations that are interesting both conceptually and in practical applications: the step potential (Sect. 4.5.1) and the square barrier (Sect. 4.5.2), which are schematic versions of scattering experiments. The free-particle solutions are also applied to the bound-state problem of the finite square well (Sect. 4.4.2), to the periodic potential (Sect. 4.6[†]) and to a practical application, the tunneling microscope (Sect. 4.5.3).

4.1 Time-Independent Schrödinger Equation

In the formulation of quantum mechanics presented in this chapter, the state vector is a complex function of the coordinate, $\Psi = \Psi(x)$. This type of state vector is usually known as a wave function. The sum of two wave functions is another wave function

$$\Psi(x) = \alpha_B \Psi_B(x) + \alpha_C \Psi_C(x). \tag{4.1}$$

The scalar product is defined as

$$\langle \Psi_B | \Psi_C \rangle = \int_{-\infty}^{\infty} \Psi_B^* \Psi_C \, \mathrm{d}x. \tag{4.2}$$

As a consequence of this choice of $\Psi(x)$, the coordinate operator is simply the coordinate itself

$$\hat{x} = x. \tag{4.3}$$

A realization of the algebra (2.15) is given by the assignment[1]

$$\hat{p} = -\mathrm{i}\hbar \frac{\mathrm{d}}{\mathrm{d}x}, \tag{4.4}$$

since for an arbitrary function $f(x)$,

$$[x, \hat{p}] f = -\mathrm{i}\hbar x \frac{\mathrm{d}f}{\mathrm{d}x} + \mathrm{i}\hbar \frac{\mathrm{d}(xf)}{\mathrm{d}x} = \mathrm{i}\hbar f. \tag{4.5}$$

It is simple to verify that the operator x is Hermitian, according to the definition (2.53). This is also true for the momentum operator, since

$$\int_{-\infty}^{\infty} \Phi^* \hat{p} \Psi \mathrm{d}x = -\mathrm{i}\hbar \Phi^* \Psi |_{-\infty}^{\infty} + \mathrm{i}\hbar \int_{-\infty}^{\infty} \Psi \frac{\mathrm{d}}{\mathrm{d}x} \Phi^* = \left(\int_{-\infty}^{\infty} \Psi^* \hat{p} \Phi \mathrm{d}x \right)^*, \tag{4.6}$$

where we have assumed $\Psi(\pm\infty) = 0$, as is the case for bound systems. The eigenfunctions of the momentum operator are discussed in Sect. 4.3.

A translation of the state vector by the amount a can be performed by means of the unitary operator

$$\mathcal{U}(a) = \exp\left(\frac{\mathrm{i}}{\hbar} a \hat{p} \right), \tag{4.7}$$

since

$$\mathcal{U}(a)\Psi(x) = \sum_n \frac{a^n}{n!} \frac{\mathrm{d}^n \Psi}{\mathrm{d}x^n} = \Psi(x + a). \tag{4.8}$$

An observable is translated as

$$\mathcal{U} \hat{Q}(x) \mathcal{U}^+ = \hat{Q}(x + a). \tag{4.9}$$

A finite translation may be generated by a series of infinitesimal steps

$$\mathcal{U}(\delta a) = 1 + \frac{\mathrm{i}}{\hbar} \delta a \, \hat{p}, \tag{4.10}$$

and $\hat{p}$ is referred to as the generator of infinitesimal translations.

---

[1] Although any function of x may be added to (4.4) and still satisfy (2.15), such a term should be dropped because free space is homogeneous.

The replacement of the operators (4.3) and (4.4) in the classical expression of any physical observable $Q(x, p)$ yields the corresponding quantum mechanical operator $\hat{Q} = Q(x, \hat{p})$ in a differential form. Given any complete set of orthonormal wave functions $\varphi_i(x)$, the matrix elements associated with the operator $\hat{Q}$ are constructed as in (2.10). This construction provides the link between the Heisenberg and the Schrödinger realizations of quantum mechanics.

The conservation law associated with translational symmetry is expressed by the commutation $[\hat{H}, \hat{p}] = 0$. This is the second symmetry that we have come across in the present text.

The Hamiltonian (2.16) yields the eigenvalue equation

$$-\frac{\hbar^2}{2M}\frac{\mathrm{d}^2\varphi_i}{\mathrm{d}x^2} + V(x)\varphi_i = E_i\varphi_i, \tag{4.11}$$

which is called the time-independent Schrödinger equation.

4.1.1 Probabilistic Interpretation of Wave Functions

Information may be extracted from the wave function through the probability density (2.71) [31]

$$\rho(x) = |\Psi(x)|^2. \tag{4.12}$$

The probability of finding the particle in the interval $L_1 \le x \le L_2$ is given by the integral

$$\int_{L_1}^{L_2} |\Psi(x)|^2 \mathrm{d}x. \tag{4.13}$$

In particular, the probability of finding the particle anywhere must equal 1:

$$1 = \langle\Psi|\Psi\rangle, \tag{4.14}$$

which implies that the wave function should be normalized.

We now discuss how this probability changes with time t. We therefore allow for a time dependence of the wave function[2] $[\Psi = \Psi(x, t)]$:

$$\frac{\mathrm{d}}{\mathrm{d}t}\int_{L_1}^{L_2} |\Psi(x,t)|^2 \mathrm{d}x = \int_{L_1}^{L_2} \left(\dot{\Psi}^*\Psi + \Psi^*\dot{\Psi}\right)\mathrm{d}x$$

$$= \frac{\mathrm{i}}{\hbar}\int_{L_1}^{L_2}\left[\left(\mathrm{i}\hbar\dot{\Psi}\right)^*\Psi - \Psi^*\left(\mathrm{i}\hbar\dot{\Psi}\right)\right]\mathrm{d}x. \tag{4.15}$$

---

[2]The time dependence of the wave function is discussed in Chap. 9. We anticipate the result here because the notion of probability current is needed in the next few sections.

We may replace $i\hbar\dot{\Psi}$ with $\hat{H}\Psi$, according to the time-dependent Schrödinger equation (9.5). We are left with only the kinetic energy contribution, since the terms proportional to the potential cancel inside (4.15):

$$\frac{\mathrm{d}}{\mathrm{d}t}\int_{L_1}^{L_2}|\Psi(x,t)|^2\mathrm{d}x = -\frac{i\hbar}{2M}\int_{L_1}^{L_2}\left(\frac{\mathrm{d}^2\Psi^*}{\mathrm{d}x^2}\Psi - \Psi^*\frac{\mathrm{d}^2\Psi}{\mathrm{d}x^2}\right)\mathrm{d}x$$

$$= \frac{i\hbar}{2M}\int_{L_1}^{L_2}\frac{\mathrm{d}}{\mathrm{d}x}\left(-\frac{\mathrm{d}\Psi^*}{\mathrm{d}x}\Psi + \Psi^*\frac{\mathrm{d}\Psi}{\mathrm{d}x}\right). \qquad (4.16)$$

We obtain the equation

$$\frac{\partial\rho}{\partial t} + \frac{\partial j}{\partial x} = 0, \qquad (4.17)$$

where we have defined the probability current

$$j(x,t) \equiv -\frac{i\hbar}{2M}\left(-\frac{\partial\Psi^*}{\partial x}\Psi + \Psi^*\frac{\partial\Psi}{\partial x}\right). \qquad (4.18)$$

Equation (4.17) is a continuity equation, similar to the one used in hydrodynamics to express conservation of mass. Imagine a long prism along the x-axis, bound by two squares of area $\mathcal{A}$ at $x = L_1$ and $x = L_2$, respectively. The variation of the probability of finding the particle inside the prism, i.e.

$$-\frac{\partial}{\partial t}\int_{L_1}^{L_2}\rho\,\mathrm{d}x,$$

is equal to the difference between the fluxes leaving and entering the prism, viz. $\mathcal{A}[j(L_2) - j(L_1)]$ (see Fig. 4.1).

The probability density and the probability current give spatial dimensions to the Schrödinger realization of quantum mechanics. These spatial features are especially useful in chemistry, where bulges of electron distribution in atoms are associated with increases in the chemical affinities of elements (Fig. 5.2).

The expression for the probability current underscores the need to use complex state vectors in quantum mechanics, since the current vanishes for real wave functions.

j₁   **j₂**

dρ/dt

Fig. 4.1 Conservation of probability density. The rate of change within a certain interval is given by the flux differences at the boundaries of the interval

Here we may continue the list of misconceptions that prevail in quantum mechanics [19]:

- "The probability current $j(x)$ is related to the speed of that part of the particle which is located at the position x." This statement gives the false impression that, although the particle as a whole has neither a definite position nor a definite momentum, it is made up of parts that do. In fact, particles are not made up of parts.
- "For any energy eigenstate, the probability density must have the same symmetry as the Hamiltonian." This statement is correct in the case of inversion symmetry, for even states of a parity-invariant Hamiltonian (see Sect. 4.2). It is not correct for odd states. It is also generally false for a central potential, since only $l = 0$ states have probability densities with a spherical shape (Fig. 5.2).
- "A quantum state $\Psi(x)$ is completely specified by its associated probability density $|\Psi(x)|^2$." The probability densities, being real numbers, cannot give information about all the properties of the state, such as, for example, those related to momentum.
- "The wave function is dimensionless." It has the dimensions $[\text{length}]^{-dN/2}$, where N is the number of particles and d is the dimension of the space.
- "The wave function $\Psi(x)$ is a function of regular three-dimensional space." This is true only for one-particle systems. For two-particle systems, the wave function $\Psi(x_1, x_2)$ exists in six-dimensional, configuration space.
- "The wave function is similar to other waves appearing in classical physics." Unlike electromagnetic or sound waves, the wave function is an abstract entity. In particular, it does not interact with particles.

Both the probability density and the probability current are defined at each point in space. Other quantum predictions require integration over the whole space. For instance, the expectation value of an operator $\hat{Q}$ is

$$\langle \Psi | Q | \Psi \rangle \equiv \int_{-\infty}^{\infty} \Psi(x,t)^* \hat{Q} \Psi(x,t) \mathrm{d}x. \tag{4.19}$$

For an operator depending only on the coordinate x, this definition is a direct consequence of Born's probability density (4.12). However, for a differential operator such as $\hat{p}$, the alternative $\int \Psi(\hat{Q}\Psi)^* \mathrm{d}x$ is also possible. Nevertheless, the two definitions are identical for physical (Hermitian) operators.

4.2 The Harmonic Oscillator Revisited

The Schrödinger equation (4.11) corresponding to the harmonic oscillator Hamiltonian (3.25) reads

$$-\frac{\hbar^2}{2M}\frac{d^2\varphi_n(x)}{dx^2} + \frac{M\omega^2}{2}x^2\varphi_n(x) = E_n\varphi_n(x). \tag{4.20}$$

4.2.1 Solution of the Schrödinger Equation

It is always useful to rewrite any equation in terms of dimensionless coordinates. Not only does one get rid of unnecessarily cumbersome constants, but the solution may apply just as well to cases other than the one being considered. Therefore, in the present problem, the coordinate x and the energy E are divided by the value of the characteristic length and energy (3.28), namely

$$u = x/x_c, \qquad e = E/\hbar\omega. \tag{4.21}$$

The Schrödinger equation thus simplified reads

$$-\frac{1}{2}\frac{d^2\varphi_n(u)}{du^2} + \frac{1}{2}u^2\varphi_n(u) = e_n\varphi_n(u). \tag{4.22}$$

This equation must be supplemented with the boundary conditions

$$\varphi_n(\pm\infty) = 0. \tag{4.23}$$

The eigenfunctions and eigenvalues are of the form

$$\varphi_n(x) = N_n \exp\left(-\frac{1}{2}u^2\right) H_n(u), \qquad e_n = n + \frac{1}{2}. \tag{4.24}$$

The H_n are Hermite polynomials[3] of degree $n = 0, 1, 2, \ldots$. The eigenfunctions and eigenvalues are also labeled by the quantum number n. Up to a phase, the constants N_n are obtained from the normalization condition (4.14)

$$N_n = 2^{n/2}\left(\pi^{\frac{1}{2}}n!x_c\right)^{-1/2}. \tag{4.25}$$

Since the Hamiltonian is a Hermitian operator, the eigenfunctions are orthogonal to each other and constitute a complete set of states:

---

[3]The reader is encouraged to verify that the few cases listed in Table 4.1 are correct solutions. Use can be made of the integrals

$$\int_{-\infty}^{\infty} \exp(-u^2)u^{2n}du = \frac{(2n-1)!!}{2^n}\pi^{\frac{1}{2}}, \qquad \int_{-\infty}^{\infty} \exp(-u^2)u^{2n+1}du = 0.$$

Table 4.1 Solutions to the harmonic oscillator problem for small values of n. P_n is defined in (4.30)

n	e_n	H_n	$N_n \pi^{1/4} x_c^{1/2}$	$P_n(\%)$
0	1/2	1	1	15.7
1	3/2	u	$\sqrt{2}$	11.2
2	5/2	$u^2 - 1/2$	$\sqrt{2}$	9.5
5	11/2	$u^5 - 5u^3 + 15u/4$	$2/\sqrt{15}$	5.7
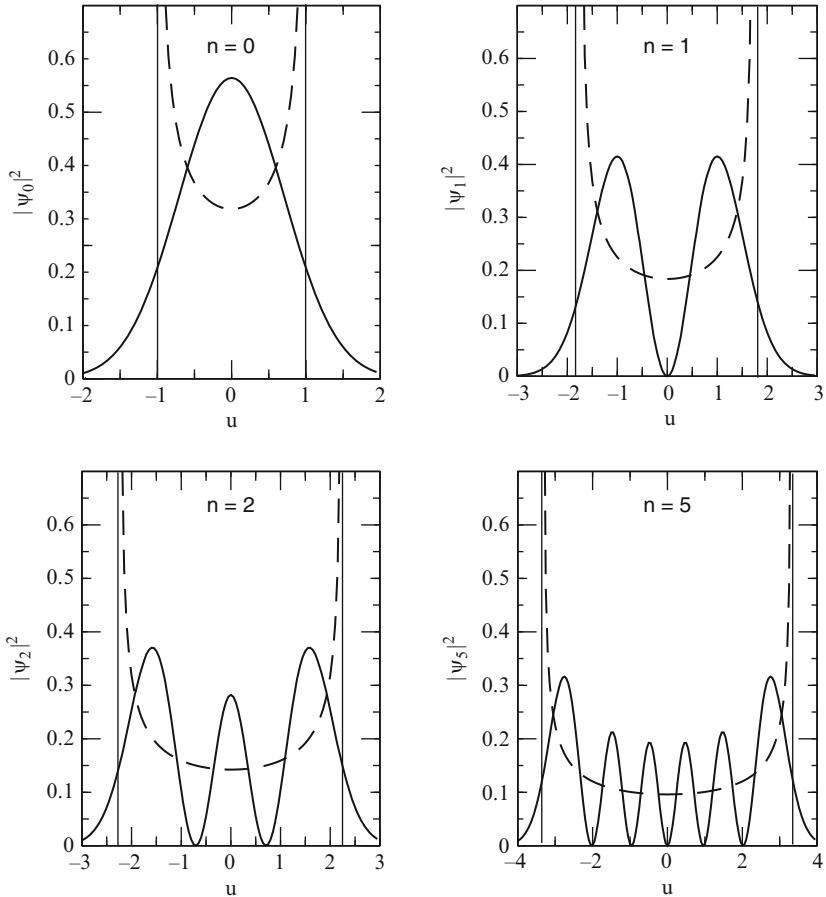
$$\langle n|m \rangle = \int_{-\infty}^{\infty} \varphi_n^* \varphi_m dx = \delta_{nm}, \qquad \Psi(x) = \sum_n c_n \varphi_n. \qquad (4.26)$$

The solutions corresponding to the lower quantum numbers are displayed in Table 4.1 and Fig. 4.2.

4.2.2 Spatial Features of the Solutions

The following features arise from the spatial dimension associated with the Schrödinger formulation:

- *Probability density.* There are nodes in the probability density (except for the $n = 0$ state). The existence of such nodes is incompatible with the classical notion of a trajectory $x(t)$, according to which the particle bounces from one side of the potential to the other, while going through every intermediate point. The fact is that the particle can never be found at the nodes. The quantum picture reminds us of the stationary wave patterns obtained, for instance, inside an organ pipe. The role that is played in the case of sound by the ends of the pipe is played in the case of the quantum harmonic oscillator by the boundary conditions.
- *Comparison between the classical and quantum mechanical probability densities.* The classical probability for finding a particle is inversely proportional to its speed [$v = \left(2E/M - \omega^2 x^2\right)^{1/2}$ for the harmonic oscillator]. Therefore, we may define a classical probability density $P_{\text{clas}} = \omega/\pi v$. The probability of finding the particle in any place, within the classically allowed interval $-x_n \leq x \leq x_n$, is 1. Here, $x_n = x_c(2n + 1)^{1/2}$ for a particle with energy $\hbar\omega(n + 1/2)$. The classical probability density displays a minimum around the origin and diverges as the particle approaches the end points of the allowed interval. The quantum mechanical density distribution for the ground state has exactly the opposite features. However, as n increases, the quantum mechanical density distribution tends towards the classical limit (Fig. 4.2). In fact, the quantum probability $P_n(x_0, \Delta x)$ satisfies the limiting relation

Fig. 4.2 Quantum mechanical probability densities and the classical probability densities of a harmonic oscillator potential as a function of the dimensionless distance u, for the quantum numbers $n = 0, 1, 2$ and 5. *Vertical lines* represent the limits of the classically allowed interval

$$\lim_{n \to \infty} P_n(x_0, \Delta x) = P_{\text{clas}}(x_0, \Delta x)$$

$$P_n(x_0, \Delta x) = \int_{x_0 - \Delta x/2}^{x_0 + \Delta x/2} |\varphi_n|^2 \mathrm{d}x, \tag{4.27}$$

as required by Bohr's correspondence principle.

- *Tunnel effect.* Outside the allowed interval $-x_c \le x \le x_c$, the classical particle would have a negative kinetic energy and thus an imaginary momentum. However, this argument does not hold in the quantum case, because it would imply some simultaneous determination of the particle location and the momentum, contradicting the uncertainty principle. Let us suppose that a particle in its ground

state has been detected within the interval $x_c \leq x \leq \sqrt{2}x_c$, i.e. within the region following the classically allowed one. In this interval, the probability density decreases from N_0^2/e at $x = x_c$ to N_0^2/e^3 (i.e. by a factor e^{-2}). If we measure the particle within this interval, and we take it to be a reasonable measure of the uncertainty in the position of the particle, then

$$\Delta x \approx 0.41 x_c. \tag{4.28}$$

According to the Heisenberg principle, the minimum uncertainty in the determination of the momentum is

$$\Delta p \geq 1.22 \sqrt{\hbar \omega M}, \tag{4.29}$$

which is consistent with an uncertainty in the kinetic energy larger than $(\Delta p)^2/2M \geq \frac{3}{4}\hbar\omega$. Since the potential energy in the same interval increases from $\hbar\omega/2$ to $\hbar\omega$, we cannot make any statement about a possible imaginary value for the momentum, which would rule out the possibility that the particle penetrates into the classically forbidden region.

The probability of finding the particle in the classically forbidden region is

$$P_n = \frac{2^{n+1}}{\pi^{1/2}n!} \int_{\sqrt{2n+1}}^{\infty} e^{-u^2} |H_n|^2 du. \tag{4.30}$$

This probability is a finite number, as large as 16% for the ground state. It decreases as the quantum number n increases, consistent with the tendency to approach the classical behavior for higher values of the energy (see Table 4.1).

4.3 Free Particle

If there are no forces acting on the particle, the potential is constant: $V(x) = V_0$. Let us assume in the first place that the energy $E \geq V_0$. In such a case the Schrödinger equation reads
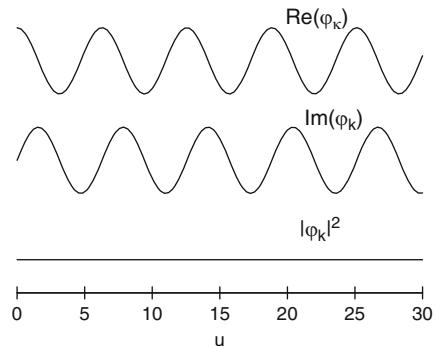
$$-\frac{\hbar^2}{2M} \frac{d^2\varphi_k(x)}{dx^2} = (E - V_0)\varphi_k(x). \tag{4.31}$$

There are two independent solutions to this equation, namely

$$\varphi_{\pm k}(x) = A\exp(\pm ikx), \qquad k = \frac{\sqrt{2M(E - V_0)}}{\hbar}. \tag{4.32}$$

The parameter k labeling the eigenfunction is called the wave number and has dimensions of a reciprocal length. The eigenvalues of the energy and the momentum are

$$E = \hbar^2 k^2 / 2M + V_0, \qquad p = \pm\hbar k. \tag{4.33}$$

Unlike the case of the harmonic oscillator (a typical bound case), the eigenvalues of both the momentum and the energy belong to a continuous set. The free-particle solutions satisfy the de Broglie relation [32]

$$p = \hbar k = h/\lambda, \tag{4.34}$$

where λ is the particle wave length. The probability density is constant over the whole space (Fig. 4.3)

$$\rho_{\pm k}(x) = \varphi^*_{\pm k}(x)\varphi_{\pm k}(x) = |A|^2, \tag{4.35}$$

while the probability current reads

$$j_{\pm k}(x) = -\mathrm{i}\frac{\hbar}{2M}\left[\varphi^*_{\pm k}\frac{\mathrm{d}\varphi_{\pm k}(x)}{\mathrm{d}x} - \varphi_{\pm k}(x)\frac{\mathrm{d}\varphi^*_{\pm k}(x)}{\mathrm{d}x}\right] = \pm\frac{|A|^2\hbar k}{M}. \tag{4.36}$$

These results pose normalization problems, which may be

- Solved by applying more advanced mathematical tools, as in Sect. 11.1[†]
- Taken care of through the use of tricks, as in Sect. 4.4.1
- Circumvented, by looking only at the ratios of the probabilities of finding the particle in different regions of space (Sects. 4.5.1 and 4.5.2)

Since there are two degenerate solutions,[4] the most general solution for a given energy E is a linear combination

$$\Psi(x) = A_+ \exp(\mathrm{i}kx) + A_- \exp(-\mathrm{i}kx). \tag{4.37}$$

---

[4]Two or more solutions are called degenerate if they are linearly independent and have the same energy.

Let us consider now the case $E \leq V_0$, which makes no sense from the classical point of view. However, the solution of the harmonic oscillator problem (third item in Sect. 4.2.2) has warned us not to reject this situation out of hand in the quantum case. In fact, the general solution is the linear combination[5]

$$\Psi(x) = B_+ \exp(\kappa x) + B_- \exp(-\kappa x), \qquad \kappa = -ik = \frac{\sqrt{2M(V_0 - E)}}{\hbar}. \quad (4.38)$$

This general solution diverges at infinity: $|\Psi| \to \infty$ as $x \to \pm\infty$. Rather than a total rejection, this feature implies that the solution (4.38) can only be used if at least one of the extremes cannot be reached. For instance, if $V_0 > E$ for $x > a$, one imposes $B_+ = 0$.

4.4 One-Dimensional Bound Problems

4.4.1 Infinite Square Well Potential. Electron Gas

The potential in this case is $V(x) = 0$ if $|x| \leq a/2$ and $V(x) = \infty$ for $|x| \geq a/2$ (Fig. 4.4).

The two infinite discontinuities should be canceled in the Schrödinger equation by similar discontinuities in the second derivative at the same points. This is accomplished by requiring the wave function to be a continuous function and requiring the first derivative to have a finite discontinuity at the boundaries of the potential. Since the wave function vanishes outside the classically allowed interval, the continuity of the wave function requires $\Psi(\pm a/2) = 0$.

According to (3.48), we may demand that the eigenfunctions of the Hamiltonian carry a definite parity. This is accomplished by using the solutions (4.37) with $A_+ = A_-$ for the even parity states, and $A_+ = -A_-$ for the odd ones. The eigenfunctions are written as

$$\varphi_n^{\text{even}}(x) = \sqrt{\frac{2}{a}} \cos(k_n x), \qquad \varphi_n^{\text{odd}}(x) = \sqrt{\frac{2}{a}} \sin(k_n x) \quad (4.39)$$
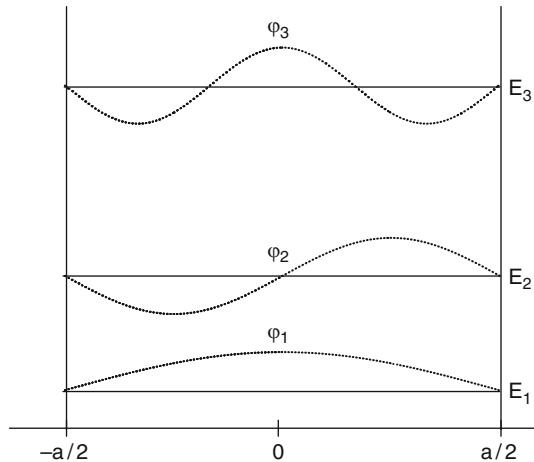
inside the well, and vanish outside the well. As a consequence of the boundary conditions,

$$\frac{k_n a}{2\pi} = n', \qquad n' = \frac{1}{2}, 1, \frac{3}{2}, 2, \ldots, \quad (4.40)$$

where the half-integer values correspond to the even solutions and the integer values to the odd ones. The eigenvalues of the energy are

---

[5]The only difference between the two solutions (4.37) and (4.38) is whether k is real or imaginary.

Fig. 4.4 Infinite square well potential. The energies E_n (*continuous lines*) and wave functions $\varphi_n(x)$ (*dotted curves*) are represented for the quantum numbers $n = 1, 2$ and 3

$$E_n = \frac{\hbar^2 k_n^2}{2M} = \frac{\hbar^2 \pi^2}{2Ma^2} n^2, \tag{4.41}$$

with $n = 2n' = 1, 2, \ldots$.

The reader is recommended to check that the quantum features associated with the solution of the harmonic oscillator problem (Sect. 4.2.2) are reproduced in the case of the infinite square well. The exception is the one related to the tunnel effect, which is prevented here by the infinite discontinuity in the potential.

By increasing the size of the box, the infinite potential well may be used to model the potential binding the electrons in a metal. In the electron gas model in one dimension, the (non-interacting) electrons are confined to a (large) segment a, which is much larger than the size of a given experimental set-up.

However, the standing waves (4.39) are not convenient for discussing charge and energy transport by electrons. In fact, the probability current associated with them vanishes. In the theory of metals, it is more convenient to use running waves $\exp(\pm ikx)$ (4.32). We may use an alternative boundary condition by imagining that the end point at $x = a/2$ is joined to the opposite point at $x = -a/2$. In this way the segment transforms into a circumference with the same length a. An electron arriving at the end of the well is not reflected back in, but leaves the metal and simultaneously re-enters at the opposite end. The representation of a free particle becomes more adequate as the radius $a/2\pi$ gets larger. This procedure results in the boundary condition $\Psi(x) = \Psi(x + a)$, or

$$\frac{k_n a}{2\pi} = n, \qquad n = 0, \pm 1, \pm 2, \ldots. \tag{4.42}$$

The total number of states is the same as for the standing waves (4.40), since the presence of half-integer and integer numbers in that case is compensated for here by the existence of two degenerate states $\pm n$. The eigenfunctions and energy eigenvalues are

$$\varphi_n(x) = \frac{1}{\sqrt{a}} \exp(ik_n x), \qquad E_n = \frac{\hbar^2 k_n^2}{2M}. \tag{4.43}$$

As mentioned in Sect. 4.3, these functions are also eigenfunctions of the momentum operator $\hat{p}$ with eigenvalues $\hbar k_n$. Although the momenta (and the energies) are discretized, the gap

$$\Delta k = 2\pi/a \tag{4.44}$$

between two consecutive eigenvalues becomes smaller than any prescribed interval, if the radius of the circumference is taken to be sufficiently large.

In quantum mechanics, sums over intermediate states often appear. In the case of wave functions of the type (4.43), this procedure may be simplified by transforming the sums into integrals, using the length element in the integrals $(a/2\pi)\mathrm{d}k$, according to (4.44):

$$\sum_k f_k \rightarrow \frac{a}{2\pi} \int f_k \, \mathrm{d}k. \tag{4.45}$$

The extension of the model to include a periodic crystal structure is performed in Sect. 4.6[†]. Calculations with the electron gas model for the three-dimensional case are carried out in Sect. 7.4.1.
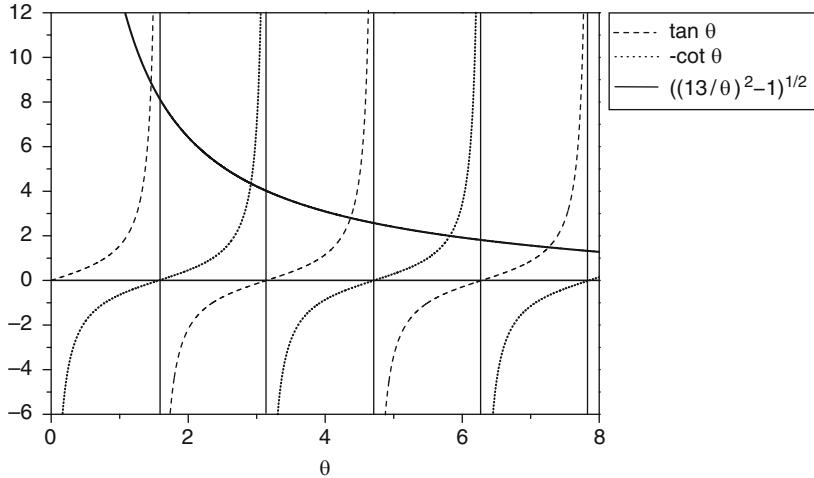
4.4.2 Finite Square Well Potential

The potential reads $V(x) = -V_0 < 0$ if $|x| < a/2$ and $V(x) = 0$ for other values of x. Here we consider only bound states, with a negative energy ($0 \geq -E \geq -V_0$).

As in the harmonic oscillator case, the potential is invariant under the parity transformation $x \rightarrow -x$. Thus we expect the eigenfunctions to be either even or odd with respect to this transformation. Therefore, the solution (4.37) applies in the region $|x| \leq a/2$, with

$$A_+ = \pm A_- \quad \text{and} \quad k = \frac{1}{\hbar}\big[2M(V_0 - E)\big]^{1/2}.$$

Moreover, invariance under the parity transformation allows one to confine calculation of the boundary conditions to the position $x = a/2$. The wave function to the right of this point is given by (4.38) with $B_+ = 0$ and $\kappa = (1/\hbar)(2ME)^{1/2}$.

Fig. 4.5 Graphical determination of the energy eigenvalues of a finite square well potential. The intersections of the *continuous curve* $\sqrt{(13/\theta)^2 - 1}$ with the *dashed curves* correspond to even-parity solutions, while those with the *dotted curves* correspond to the odd ones. The value $M V_0 a^2 / \hbar^2 = 338$ is assumed

The ratio between the continuity conditions corresponding to the first derivative and to the function itself yields the eigenvalue equation

$$\frac{\kappa}{k} = \tan \frac{ka}{2}. \tag{4.46}$$

This is as far as we can go analytically in this case. Equation (4.46) must either be solved numerically or using the following graphical method: the equation determining the value of k is equivalent to the equation $E = V_0 - \hbar^2 k^2 / 2M$. Therefore, we obtain the ratio

$$\frac{\kappa}{k} = \sqrt{\frac{2M V_0}{\hbar^2 k^2} - 1}, \tag{4.47}$$

and (4.46) becomes

$$\sqrt{\frac{M V_0 a^2}{2\hbar^2 \theta^2} - 1} = \tan \theta, \tag{4.48}$$

where $\theta \equiv ka/2$. The function $\tan \theta$ increases from zero to infinity in the interval $0 \leq \theta \leq \pi/2$, while the left-hand side decreases from infinity to a finite value as θ increases in the same interval. Therefore, there is a value of θ at which the two curves intersect, corresponding to the lowest eigenvalue. An analogous argument is made for the successive roots of (4.48). The nth root is found in the interval $(n-1)\pi \leq \theta \leq (n-1/2)\pi$. (Fig. 4.5).

Unlike the harmonic oscillator case, the number of roots is limited, since (4.48) requires $\theta \leq \theta_{\max}$, where

$$\theta_{\max} = \sqrt{\frac{M V_0 a^2}{2\hbar^2}}. \tag{4.49}$$

There is a set of odd solutions that satisfy an equation similar to (4.46), namely

$$-\cot \frac{ka}{2} = \frac{\kappa}{k}. \tag{4.50}$$

Unlike the classical case, the probability density is not constant in the interval $|x| \leq a/2$. Moreover, there is a finite probability of finding the particle outside the classically allowed region. However, the solutions tend towards the classical behavior as n increases.

The spectrum of normalizable (bound) states is always discrete. Conversely, states that have a finite amplitude at infinity must be part of a continuous spectrum. This is the case for positive values of the energy (see Sect. 4.5.2).

4.5 One-Dimensional Unbound Problems

In this section we study problems related to the scattering of a particle by means of a potential. We assume that the particle impinges from the left and may be reflected and/or transmitted. There is no incoming wave from the right. Therefore the state vector must satisfy the following boundary conditions:
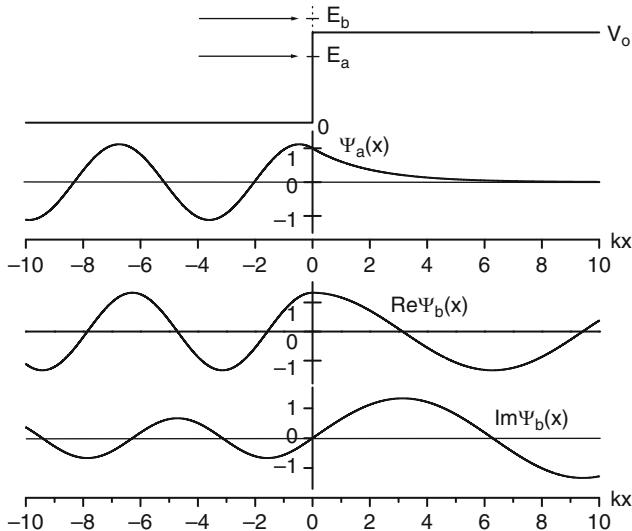
- It includes the term $A_+ \exp(ikx)$ for $x \to -\infty$;
- It does not include the term $A_- \exp(-ikx)$ for $x \to \infty$.

4.5.1 One-Step Potential

The one-step potential is written as $V(x) = 0$ for $x < 0$ and $V(x) = V_0 > 0$ for $x > 0$ (Fig. 4.6). It represents an electron moving along a conducting wire that is interrupted by a short gap. The electron feels a change in the potential as it crosses the gap.

$E_a < V_0$

Classically, the particle rebounds at $x = 0$ and cannot penetrate the region $x \geq 0$. Quantum mechanically this is no longer the case. For $x \leq 0$ the solution is given as the superposition of an incoming and a reflected wave (4.37), with $V_0 = 0$. Equation

Fig. 4.6 One-step potential. Subscripts a and b label wave functions corresponding to energies $E_a = 3V_0/4$ and $E_b = 5V_0/4$, respectively

(4.38) holds for $x \geq 0$. This last solution cannot be rejected, since it does not diverge on the right half-axis if we impose the boundary condition $B_+ = 0$.

To have a Schrödinger equation valid at every point of space, the wave function and its first derivative should be continuous everywhere, including the point at which there is a finite discontinuity in the potential. These two requirements imply that

$$A_+ + A_- = B_- , \qquad A_+ - A_- = i\frac{\kappa}{k}B_-. \tag{4.51}$$

Therefore

$$A_+ = \frac{1}{2}B_- \left(1 + i\frac{\kappa}{k}\right), \qquad A_- = \frac{1}{2}B_- \left(1 - i\frac{\kappa}{k}\right). \tag{4.52}$$

The total wave function is given by

$$\Psi_a(x) = \frac{1}{2}B_- \left[\left(1 + i\frac{\kappa}{k}\right)\exp(ikx) + \left(1 - i\frac{\kappa}{k}\right)\exp(-ikx)\right]$$

$$= B_- \left[\cos(kx) - \frac{\kappa}{k}\sin(kx)\right] \qquad (x \leq 0),$$

$$\Psi_a(x) = B_- \exp(-\kappa x) \qquad (x \geq 0). \tag{4.53}$$

The solution for $x \leq 0$ represents the superposition of an incident and a reflected wave. Since both amplitudes have equal module, they generate a standing wave with the corresponding nodes at positions such that $\tan(kx) = k/\kappa$, for $x \leq 0$ (see the first item in Sect. 4.2.2). The probability currents associated with the incident and

reflected waves are

$$j_I = -j_R = \frac{\hbar k}{M} \frac{|B_-|^2}{4} \left(1 + \frac{\kappa^2}{k^2}\right). \tag{4.54}$$

The reflection coefficient is defined as the absolute value of the ratio between reflected and incident currents. In the present case,

$$R \equiv \left|\frac{j_R}{j_I}\right| = 1. \tag{4.55}$$

The mutual cancelation between the two probability currents is correlated with the real character of the wave function (4.53).

There is a tunneling effect for $x \geq 0$, since the particle can penetrate into the forbidden region over a distance of the order of $\Delta x = 1/\kappa$. This length is accompanied by an uncertainty in the momentum and in the kinetic energy, so that

$$\Delta p \approx \frac{\hbar}{\Delta x} \approx \sqrt{2M(V_0 - E_a)}, \qquad \Delta E \approx \frac{(\Delta p)^2}{2M} \approx V_0 - E_a, \tag{4.56}$$

respectively. The consequences of these uncertainties parallel those discussed in Sect. 4.2.2.

$E_b > V_0$

The classical solution describes an incident particle which is totally transmitted, but with a smaller velocity. From the quantum mechanical point of view, the solution for $x \leq 0$ is again given by (4.37) with $V_0 = 0$, representing an incident plus a reflected wave. For $x \geq 0$ this same solution is valid, but with the wave number $k_b = \sqrt{2M(E_b - V_0)}/\hbar$. There is no incident wave from the right, since there is nothing that may bounce the particle back. Let C denote the amplitude of the transmitted wave $\exp(ik_b x)$. The continuity of the wave function and its first derivative at $x = 0$ requires that

$$A_+ + A_- = C , \qquad A_+ - A_- = \frac{k_b}{k}C. \tag{4.57}$$

Using these equations, we may express the amplitudes of the reflected and transmitted waves as proportional to the amplitude of the incident wave, so that

$$\Psi_b(x) = \begin{cases} A_+ \left[\exp(ikx) + \dfrac{k - k_b}{k + k_b} \exp(-ikx)\right] & (x \leq 0) , \\ A_+ \dfrac{2k}{k + k_b} \exp(ik_b x) & (x \geq 0). \end{cases} \tag{4.58}$$

The probability currents associated with the incident, reflected and transmitted waves are

$$j_I = \frac{\hbar k}{M} |A_+|^2,$$

$$j_R = -\frac{\hbar k}{M} \left(\frac{k - k_b}{k + k_b} \right)^2 |A_+|^2, \tag{4.59}$$

$$j_T = \frac{\hbar k_b}{M} \left(\frac{2k}{k + k_b} \right)^2 |A_+|^2,$$

respectively. In this case we also define a transmission coefficient $T \equiv j_T / j_I$

$$R = \left(\frac{k - k_b}{k + k_b} \right)^2, \qquad T = \frac{4 k k_b}{(k + k_b)^2}, \tag{4.60}$$

and we find that $R + T = 1$ as expected, since the current should be conserved in the present case.
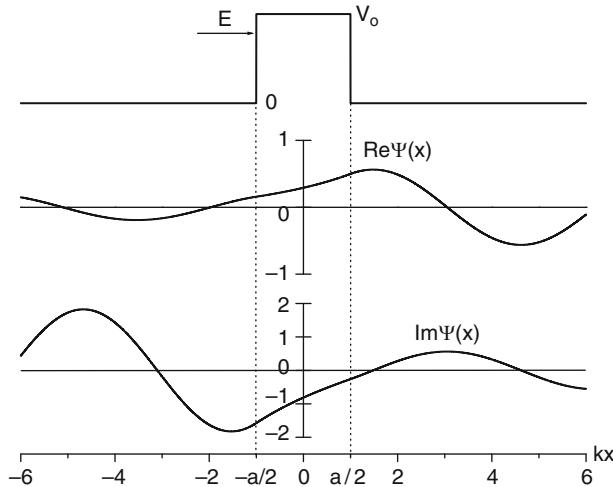
What makes the particle bounce? The quantum mechanical situation is similar to a beam of light crossing the boundary between two media with different indices of refraction. At least a partial reflection of the beam takes place.

Note that the wave functions (4.53) and (4.58) may be obtained from each other through the substitution $k_b(E) = i\kappa(E)$.

4.5.2 Square Barrier

The potential is given by $V(x) = 0$ ($|x| > a/2$) and $V(x) = V_0$ ($|x| < a/2$) (Fig. 4.7). We only consider explicitly the case $E \leq V_0$. Classically, the particle can only be reflected at $x = -a/2$.

For $x \leq -a/2$ and for $x \geq a/2$, the solution to the Schrödinger equation again takes the form (4.37), with the same value of k for both regions ($V_0 = 0$). However, there is only a transmitted wave, $C \exp(ikx)$, for $x \geq a/2$. Within the intermediate region $-a/2 \leq x \leq a/2$, the solution is as in (4.38). We cannot now reject either of the two components on account of their bad behavior at infinity. We thus have five amplitudes. The continuity conditions at the two boundaries provide us with four equations: the four remaining amplitudes may be expressed in terms of the amplitude of the incident wave A_+. We may also obtain here the currents associated with the incident beam j_I, the reflected beam j_R, the transmitted beam j_T and the beam within the barrier j_B, and the reflection and transmission coefficients R, T:
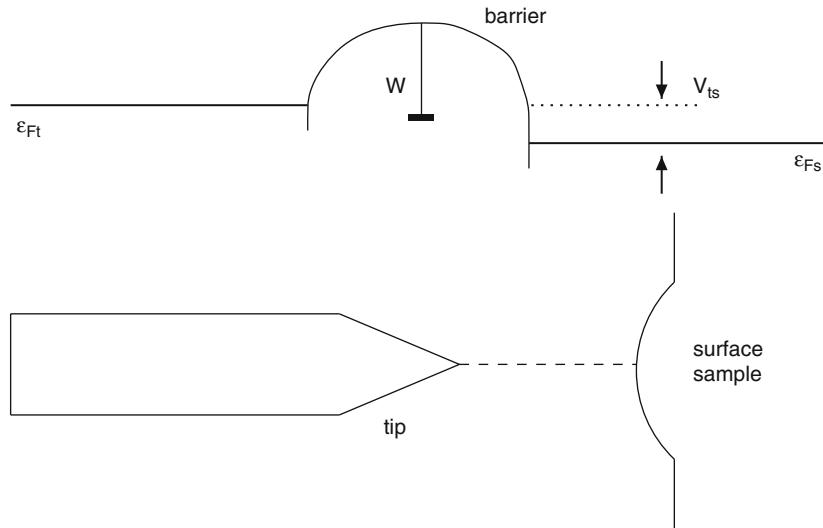
Fig. 4.7 Square barrier and associated wave function. Here $E = 3V_0/4$

$$j_I = \frac{\hbar k}{M}|A_+|^2, \qquad j_R = -\frac{\hbar k}{M}|A_-|^2,$$

$$j_T = \frac{\hbar k}{M}|C|^2, \qquad j_B = \frac{2\hbar\kappa}{M}\Big[\text{Re}\,(B_+)\text{Im}\,(B_-) - \text{Re}\,(B_-)\text{Im}\,(B_+)\Big],$$

$$R = \left|\frac{j_R}{j_I}\right| = \frac{\sinh^2(\kappa a)}{\dfrac{4E}{V_0}\left(1 - \dfrac{E}{V_0}\right) + \sinh^2(\kappa a)},$$

$$T = \left|\frac{j_T}{j_I}\right| = \left|\frac{j_B}{j_I}\right| = \frac{\dfrac{4E}{V_0}\left(1 - \dfrac{E}{V_0}\right)}{\dfrac{4E}{V_0}\left(1 - \dfrac{E}{V_0}\right) + \sinh^2(\kappa a)}. \tag{4.61}$$

For values of $\kappa a > 1$ the transmission coefficient displays an exponential decay

$$T \approx \frac{16E}{V_0}\left(1 - \frac{E}{V_0}\right)\exp(-2\kappa a). \tag{4.62}$$

Transmission through a potential barrier is another manifestation of the tunnel effect, which has been discussed both in connection with the harmonic oscillator (Sect. 4.2.2) and with the one-step potential (Sect. 4.5.1). The tunnel effect manifests itself in the α-decay of nuclei, the tunneling microscope, etc.

Fig. 4.8 Scanning tunneling microscope
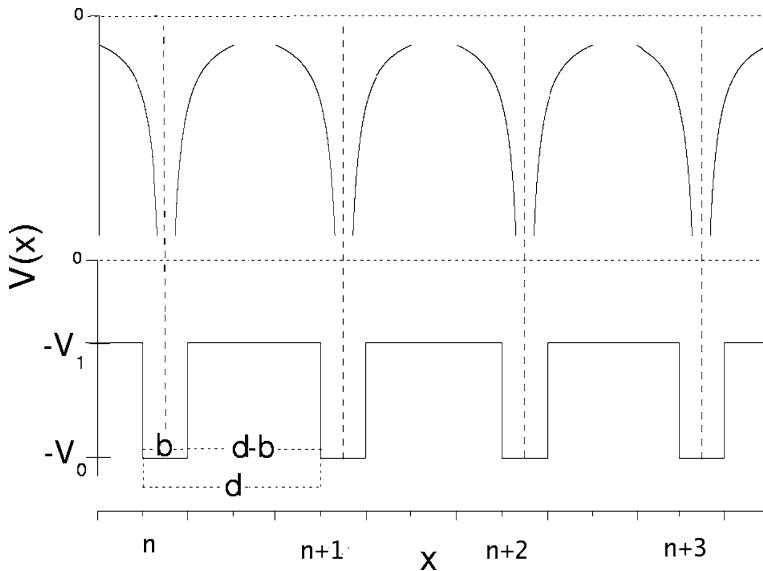
The corresponding analysis for the case of a potential well parallels the one made for the square barrier. A solution of type (4.37), instead of (4.38), should also be used for the region inside the well. There will also be incident, reflected and transmitted waves, and coefficients of reflection and transmission that sum to a value of unity.

4.5.3 Scanning Tunneling Microscope

The scanning tunneling microscope (STM) was developed in the 1980s by Gerd Binnig and Heinrich Rohrer [33]. A conducting probe ending in a very sharp tip is held close to a metal sample. In a metal, electrons move freely according to the electron gas model [Sects. (4.4.1) and (7.4.1)], filling all levels up to the Fermi energy ϵ_F. The potential rises at the surface of the metal forming a barrier, and electrons tunnel through the barrier between tip and surface sample (Fig. 4.8). The tunneling current[6] is proportional to the transmission coefficient T (4.62). Thus, it exponentially increases as the distance tip–surface decreases. The tip is mounted on a piezoelectric tube, which allows very small movements by applying voltage at its electrodes. The tip slowly scans the surface.

---

[6]A small voltage difference V_{ts} between tip and sample must be introduced, to ensure the existence of empty electron states in the sample, that should be occupied by tunneled electrons.

Fig. 4.9 Periodic potential. The upper part of the figure represents a realistic potential. The lower one mocks this potential as successive square wells

An effective value of κ can be estimated by replacing the difference $V_0 - E$ in (4.38) by an average of sample and tip work functions W (the smallest energy needed to remove an electron from a metal, about $4\,\mathrm{eV}$). Thus $\kappa \approx 2\,\text{Å}^{-1}$ and, consequently, the device is sensitive to changes in distance at the subangstrom scale (Problem 12).

The tip is moved over the surface of the sample, which requires high precision movement coupled to electrical control. This is achieved by means of piezoelectric elements.

The STM is used in both industrial and basic research to obtain atomic-scale images of metal surfaces and of other materials, from the atomic to the micron scale. It is also possible to achieve tiny tunnel currents if, for instance, biological materials are spread as thin films over conductive substrates.

Large electric fields applied to the tip can lift atoms one by one and deposit them at chosen locations. The contents of all books from the British Library could thus fit on top of one stamp. One can also make small "quantum corrals," a few angstrom wide.[7]

-----

[7]However, it is still difficult to find quantum features in these small systems because of decoherence (see Sect. 14.2[†]).

4.6[†]   Band Structure of Crystals

A crystal consists of an array of N positive ions displaying a periodic structure in space and electrons moving in the electric field generated by the ions. Figure 4.9 sketches the potential $V(x+d) = V(x)$ that an electron feels in the one-dimensional case. In this section we study the main features of the single-particle eigenstates in such a potential.

Classically, an electron moving in the potential of Fig. 4.9 may be bound to a single ion so that it is unable to transfer to another ion. Quantum mechanically, this may be ensured only if the distance d between the ions is very large. In such a case, the N states in which the electron is bound to one atom of the array constitute an orthogonal set of states which is N times degenerate. However, as the distance d is reduced to realistic values, we expect the degeneracy to be broken and the energy eigenvalues to be distributed within a band. In the following, we show how this picture is represented mathematically.

The Bloch theorem states that the wave function of a particle moving in a periodic potential has the form

$$\varphi_k(x) = \exp(ikx)u_k(x), \tag{4.63}$$

where k is real and $u_k(x + d) = u_k(x)$ is a periodic function [34].

Since the most relevant property of the potential is its periodicity and not its detailed shape, we replace the realistic potential with a periodic array of square well potentials (Fig. 4.9). We have learned by now how to solve square well problems. Here $V(x) = -V_0$ ($0 \le x \le b$) and $V(x) = -V_1$ ($b \le x \le d$). Moreover, $V(x + d) = V(x)$. We denote the energy by $-E$, with $E > 0$. We assume that the electron is bound to the crystal for negative energy values.

Region I: $-V_0 \le -E \le -V_1$

According to Sect. 4.3, the wave functions in the interval $nd \le x \le (n + 1)d$ are

$$\Psi(x) = \begin{cases} A_+ \exp(ik_b x) + A_- \exp(-ik_b x), & nd \le x \le nd + b, \\ B_+ \exp(\kappa_b x) + B_- \exp(-\kappa_b x), & nd + b \le x \le (n + 1)d, \end{cases} \tag{4.64}$$

where

$$k_b = \frac{1}{\hbar}\sqrt{2M(V_0 - E)}, \qquad \kappa_b = \frac{1}{\hbar}\sqrt{2M(E - V_1)}. \tag{4.65}$$

Thus the periodic function $u_k(x)$ is of the form

$$u_k(x) = \begin{cases} A_+ \exp[i(k_b - k)x] + A_- \exp[-i(k_b + k)x], & nd \le x \le nd + b, \\ B_+ \exp[(\kappa_b - ik)x] + B_- \exp[-(\kappa_b + ik)x], \\ \qquad\qquad\qquad\qquad\qquad\qquad nd + b \le x \le (n + 1)d. \end{cases} \tag{4.66}$$

The periodicity of u_k requires

$$u_k(x) = A_+ \exp[i(k_b - k)(x - d)] + A_- \exp[-i(k_b + k)(x - d)], \quad (4.67)$$

for

$$(n + 1)d \le x \le (n + 1)d + b.$$

The continuity conditions for the wave function, or equivalently for u_k, yield four linear equations for the amplitudes $A_\pm, B_\pm$ (two at $x = b$ and two at $x = d$). Therefore the determinant of the coefficients of the amplitudes should vanish. This condition leads to the equation

$$f(E) = \cos(kd), \quad (4.68)$$

where
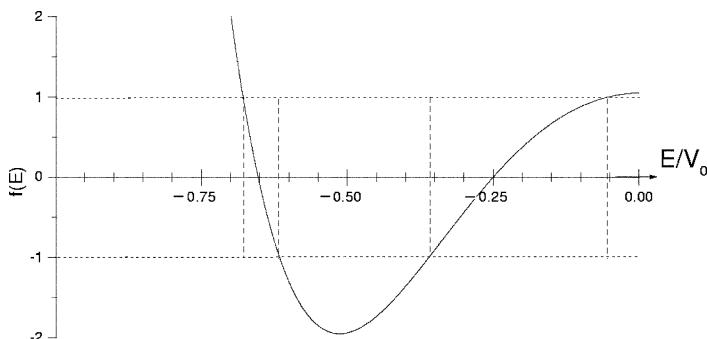
$$f(E) = \frac{\kappa_b^2 - k_b^2}{2k_b \kappa_b} \sinh\left[\kappa_b(d - b)\right] \sin(k_b b) + \cosh\left[\kappa_b(d - b)\right] \cos(k_b b). \quad (4.69)$$

Region II: $-V_1 \le -E \le 0$

The procedure is completely parallel to the previous case except for the fact that the wave function is also of the form (4.37) in the interatomic space $b \le x \le d$, with $k_c = (1/\hbar)\sqrt{2M(E - V_1)}$. Equation (4.68) still holds, with

$$f(E) = -\frac{k_c^2 + k_b^2}{2k_b k_c} \sin\left[k_c(b - d)\right] \sin(k_b b) + \cos\left[k_c(d - b)\right] \cos(k_b b). \quad (4.70)$$

The allowed values of E fall into bands satisfying the condition $|f(E)| \le 1$. Figure 4.10 represents the function $f(E)$, encompassing the two regions I and II, for the parameters $V_1 = V_0/2$ and $b = \hbar\sqrt{2/M V_0}$.

Fig. 4.10 Available intervals of energy (bands), obtained with the periodic square potential of Fig. 4.9

Equation (4.68) remains unchanged if k is increased by a multiple of $2\pi/d$. We therefore confine k to the interval

$$-\frac{\pi}{d} \le k \le \frac{\pi}{d}.\tag{4.71}$$

We now apply the periodic boundary conditions discussed in Sect. 4.4.1. The length of the circumference is $a = Nd$. Therefore,

$$\exp(ik_n Nd) = 1, \qquad k_n = \pm\frac{2\pi n}{Nd}, \qquad n = 0, \pm 1, \pm 2, \pm\frac{1}{2}N, \tag{4.72}$$

where the limits (4.71) have been taken into account. There are as many possible values of k as there are ions in the array. This result is consistent with the fact that binding the electron to each ion also constitutes a possible solution to the problem, as mentioned at the beginning of this section.

Problems

Problem 1. Using Table 4.1, verify that

1. The operator a (3.29) annihilates the ground state wave function φ_0
2. The operator a^+, applied to $\varphi_1(x)$ yields $\sqrt{2}\varphi_2(x)$

Hint: express the operators a, a^+ as differential operators.

Problem 2. Assume an infinite square well such that $V(x) = 0$ in the interval $0 < x < a$ and $V(x) = \infty$ for the remaining values of x.

1. Calculate the energies and wave functions.
2. Compare these results with those obtained in the text centering the well at the origin and explain the agreement on physical grounds.
3. Do the wave functions obtained in the first part have a definite parity?

Problem 3. Relate the minimum energy for a particle moving in a square well to the Heisenberg uncertainty principle.

Problem 4. Find the eigenvalue equations for a particle moving in a potential well such that $V(x) = \infty$ for $|x| \ge a/2$, $V(x) = V_0 \ge 0$ for $-a/2 \le x \le 0$ and $V(x) = 0$ for $0 < x < a/2$. Assume $0 \le E \le V_0$.

Problem 5. Estimate the error if we use (4.45) in the calculation of $\sum_k E_k$. Hint: recall that

$$\sum_{n=0}^{n=\nu} n^2 = \frac{\nu}{6}(\nu + 1)(2\nu + 1).$$

Problem 6. Assume a free electron gas confined to a one-dimensional well of width a

1. Obtain the density of states $\rho(E)$ as a function of energy.
2. Calculate ρ for $E = 1\,\text{eV}$ and $a = 1\,\text{cm}$.

Problem 7. Consider a square well such that $V(x) = \infty$ for $x < 0$, $V(x) = 0$ for $0 < x < a/2$ and $V(x) = V_0$ for $x > a/2$.

1. Write down the equation for the eigenvalues.
2. Compare this equation with the one obtained for the finite square well in Sect. 4.4.2.
3. For $V_0 \rightarrow \infty$, show that the wave function for the finite well satisfies the condition that it vanishes at $x = a/2$ and does not penetrate the classically forbidden region.

Problem 8. Calculate the number of even-parity states (EPS) and odd parity states (OPS) for a finite square well potential of depth V_0 centered at the origin, if the parameter

$$\theta = \frac{a}{\hbar}\sqrt{\frac{M V_0}{2}}$$

lies in the intervals $(0, \pi/2)$, $(0, \pi)$, $(0, 3\pi/2)$ and $(0, 2\pi)$.

Problem 9. Calculate the transmission and reflection coefficients for an electron with a kinetic energy of $E = 2\,\text{eV}$ coming from the right. The potential is $V(x) = 0$ for $x \le 0$ and $V(x) = V_0 = 1\,\text{eV}$ for $x \ge 0$.

Problem 10. The highest energy of an electron inside a block of metal is $5\,\text{eV}$ (Fermi energy). The additional energy that is necessary to remove the electron from the metal is $3\,\text{eV}$ (work function).

1. Estimate the distance through which the electron penetrates the barrier, assuming that the width of the (square) barrier is much greater than the penetration distance.
2. Estimate the transmission coefficient if the width of the barrier is $20\,\text{Å}$.

Problem 11. Obtain the transmission coefficients of a potential barrier in the limits $\kappa a \ll 1$ and $\kappa a \gg 1$.

Problem 12. Estimate the sensitivity to the distance tip-sample in an STM, assuming that a relative variation of 1% in the current can be detected and $\kappa = 2\,\text{Å}^{-1}$.

Problem 13. 1. Show that the eigenfunction of the Hamiltonian of a periodic potential is not an eigenfunction of the momentum operator.
2. Why is it not a momentum eigenstate?
3. Give an expression for the expectation value of the momentum.

Problem 14. In the presence of interactions, it is sometimes useful to mock the spectrum by one of a free particle (4.33) with an effective mass. Obtain the value of M_{eff} at the extremes of the intervals allowed by (4.68).
Hint: Expand both sides of (4.68) and add the resulting expression $\Delta E(k^2)$ to the kinetic energy (4.33).

Problem 15. A linear combination $\Psi(x)$ of momentum eigenstates (4.43) representing a localized particle is called a wave packet. Choose as amplitudes $c_p = \eta \exp[-p^2/\alpha^2]$.

1. Obtain the value of η such that the normalization condition $\sum_p |c_p|^2 = 1$ is satisfied.
2. Calculate the probability density $|\Psi(x)|^2$.
3. Obtain the matrix elements $\langle \Psi|x|\Psi \rangle$ and $\langle \Psi|x^2|\Psi \rangle$.
4. Obtain the matrix elements $\langle \Psi|p|\Psi \rangle$ and $\langle \Psi|p^2|\Psi \rangle$.
5. Verify Heisenberg uncertainty relation (2.37).

Hint: replace sums by integrals as in (4.45).
$\int_{-\infty}^{\infty} \exp[-(x + i\beta)^2/\alpha^2]dx = \alpha \sqrt{\pi/2}; \qquad \int_{-\infty}^{\infty} f(k)\exp[ikx]dx = 2\pi f(0).$

Chapter 5
Motion in Angular Subspace

This chapter deals with the angular degrees of freedom and, therefore, the crucial role is played by the spherical symmetry. The quantum angular momenta are treated from both matrix and differential equation points of view. The difference in the corresponding results reveals the existence of the most important quantum observable: the spin. Addition of angular momenta, quantum rotations and the Wigner–Eckart theorem are also discussed.

The commutation relation (2.15) is straightforwardly generalized to the three-dimensional case

$$[\hat{x}_i, \hat{p}_j] = i\hbar \delta_{ij}. \tag{5.1}$$

In classical physics, angular momentum is a physical, observable vector $\boldsymbol{L}$ that plays an important role, since it is a conserved quantity in the absence of external torques $\boldsymbol{\tau}$:

$$\boldsymbol{L} = \boldsymbol{r} \times \boldsymbol{p}, \qquad \frac{d\boldsymbol{L}}{dt} = \boldsymbol{\tau}. \tag{5.2}$$

As in the case of the Schrödinger equation, we quantize the problem by substituting

$$\hat{p}_i \rightarrow -i\hbar \frac{\partial}{\partial x_i} \tag{5.3}$$

into the classical expression (5.2). One obtains the commutation relations

$$[\hat{L}_x, \hat{L}_y] = i\hbar \hat{L}_z, \qquad [\hat{L}_y, \hat{L}_z] = i\hbar \hat{L}_x, \qquad [\hat{L}_z, \hat{L}_x] = i\hbar \hat{L}_y, \tag{5.4}$$

$$[\hat{L}^2, \hat{L}_x] = [\hat{L}^2, \hat{L}_y] = [\hat{L}^2, \hat{L}_z] = 0. \tag{5.5}$$

5.1   Eigenvalues and Eigenstates

5.1.1   Matrix Treatment

In the following, we take the commutation relations (5.4) as the definition of quantum angular momentum. Therefore, this definition also takes care of the quantum version of orbital angular momentum (5.2). However, as we shall see, definition (5.4) also includes other types of angular momenta of a purely quantum mechanical origin. From here on we let $\hat{J}_i$ denote operator components that satisfy the relations

$$[\hat{J}_i, \hat{J}_j] = i\hbar\epsilon_{ijk}\hat{J}_k, \tag{5.6}$$

where ϵ_{ijk} is the Levi–Civita tensor,[1] whatever their origin may be. We use the notation $\hat{L}_i$ for angular momentum operators associated with orbital motion (5.2).

The commutation relations ensure that one can precisely determine the modulus squared simultaneously with one projection of the angular momentum, but not two projections at the same time. Consequently, one may construct eigenfunctions that are common to the operators $\hat{J}^2$ and $\hat{J}_z$. The choice of the z-component is arbitrary, since the space is isotropic and, consequently, there are no preferred directions.

The procedure for solving this problem closely follows the matrix treatment of the harmonic oscillator (Sect. 3.3.1). It is given in detail in Sect. 5.4*. The following results are obtained:

- The two-dimensional angular subspace displays two more symmetries and thus provides two additional quantum numbers. The eigenvalue equations for the operators $\hat{\boldsymbol{J}}^2$ and $\hat{J}_z$ can be written as

$$\hat{\boldsymbol{J}}^2\varphi_{jm} = \hbar^2 j(j+1)\varphi_{jm}, \qquad \hat{J}_z\varphi_{jm} = \hbar m\varphi_{jm}, \tag{5.7}$$

  where the possible values of the quantum numbers j, m are
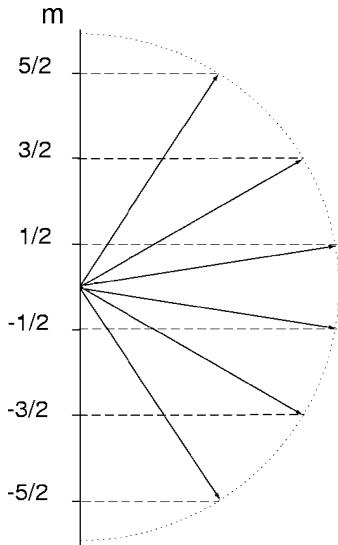
$$-j \le m \le j, \qquad j = 0, \frac{1}{2}, 1, \frac{3}{2}, \ldots, \tag{5.8}$$

  with m increasing in units of 1.
- Since the maximum value of m is j, and $j^2 < j(j+1)$, the maximum projection of the angular momentum is always smaller than the modulus (except for $j = 0$). Thus, the angular momentum vector can never be completely aligned with the z-axis. This fact is consistent with the lack of commutativity in (5.6): a complete alignment would imply the vanishing of the components $\hat{J}_x, \hat{J}_y$ and thus the simultaneous determination of the corresponding physical quantities and of J_z (see Problem 3).

---

[1] $\epsilon_{ijk} = 1$ if i, j, k are cyclical (as for $i = z, j = x, k = y$); otherwise $\epsilon_{ijk} = -1$ (as for $i = z, j = y, k = x$).

Fig. 5.1 Possible orientations of a $j = 5/2$ angular momentum vector

Figure 5.1 represents the possible orientations of the angular momentum vector for the case $j = 5/2$. It looks as if the angular momentum precesses around the z-axis. However, this picture is incorrect, since it implies that the end point of the angular momentum vector goes through a circular trajectory, something that does not make sense from the point of view of quantum uncertainty relations.

- The operators $\hat{J}_x$ and $\hat{J}_y$ display non-diagonal matrix elements within the basis (5.7), namely

$$\langle j'm'|J_x|jm\rangle = \delta_{j'j}\delta_{m'(m\pm1)}\frac{\hbar}{2}\sqrt{(j\mp m)(j\pm m+1)},$$

$$\langle j'm'|J_y|jm\rangle = \mp\delta_{j'j}\delta_{m'(m\pm1)}\frac{i\hbar}{2}\sqrt{(j\mp m)(j\pm m+1)}. \qquad (5.9)$$

- None of the operators $\hat{J}_x$, $\hat{J}_y$, $\hat{J}_z$, $\hat{J}^2$ connects states with different values of the quantum number j.
- Properties of the unitary operator associated with rotations are discussed in Sect. 5.3.2[†].

5.1.2 Treatment Using Position Wave Functions

The concept of orbital angular momentum is especially useful in problems with spherical symmetry (like those involving atoms, nuclei, etc.), for which it is convenient to use the spherical coordinates

$$x = r \sin \theta \cos \phi, \qquad y = r \sin \theta \sin \phi, \qquad z = r \cos \theta,$$

$$\mathrm{d}x \, \mathrm{d}y \, \mathrm{d}z = r^2 \sin \theta \, \mathrm{d}r \, \mathrm{d}\theta \, \mathrm{d}\phi, \tag{5.10}$$

$$0 \le \theta \le \pi, \qquad 0 \le \phi \le 2\pi, \qquad 0 \le r \le \infty.$$

In these coordinates, the orbital angular momentum operators read

$$\hat{L}_x = i\hbar \left(\sin \phi \frac{\partial}{\partial \theta} + \cot \theta \cos \phi \frac{\partial}{\partial \phi} \right),$$

$$\hat{L}_y = i\hbar \left(-\cos \phi \frac{\partial}{\partial \theta} + \cot \theta \sin \phi \frac{\partial}{\partial \phi} \right),$$

$$\hat{L}_z = -i\hbar \frac{\partial}{\partial \phi},$$

$$\hat{L}^2 = -\hbar^2 \left(\frac{\partial^2}{\partial \theta^2} + \cot \theta \frac{\partial}{\partial \theta} + \frac{1}{\sin^2 \theta} \frac{\partial^2}{\partial \phi^2} \right). \tag{5.11}$$

The detailed treatment of the orbital angular momentum operator is given in Sect. 5.5*. The results of such an approach are as follows:

- The simultaneous eigenfunctions of the operators $\hat{L}^2, \hat{L}_z$ are called spherical harmonics and denoted by $Y_{lm_l}(\theta, \phi)$. They satisfy the eigenvalue equations

$$\hat{L}_z Y_{lm_l} = \hbar m_l Y_{lm_l},$$

$$\hat{L}^2 Y_{lm_l} = \hbar^2 l(l+1) Y_{lm_l}, \tag{5.12}$$

$$\hat{\Pi} Y_{lm_l} = (-1)^l Y_{lm_l},$$

  where

$$-l \le m_l \le l, \qquad l = 0, 1, 2, \ldots. \tag{5.13}$$
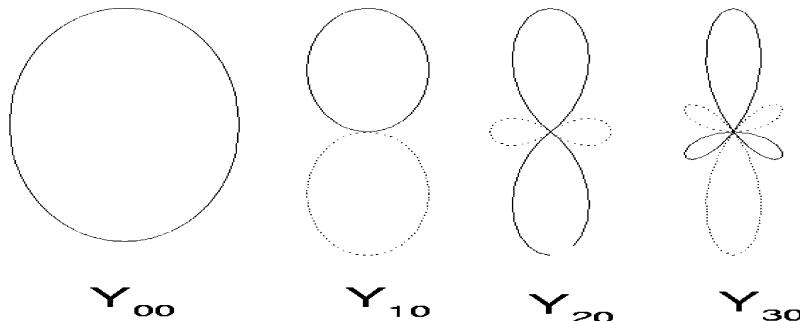
  and $\hat{\Pi}$ is the parity operator[2] (3.49).
- Using the expressions (5.11), one may construct the matrix elements of the operators $\hat{L}_x, \hat{L}_y$. One obtains the same form as the matrix elements in (5.9), with the replacement $j \to l, m \to m_l$.
- The spherical harmonics constitute a complete set of single-valued basis states on the surface of a sphere of unit radius:

$$\Psi(\theta, \phi) = \sum_{lm_l} c_{lm_l} Y_{lm_l}. \tag{5.14}$$

---

[2]For the three-dimensional case, the parity operation is written as $r \to -r$ or equivalently, $r \to r$, $\theta \to \pi - \theta, \phi \to \pi + \phi$.

Fig. 5.2 Projection of the spherical harmonics Y_{l0} on the (x, z) plane, for the values $l = 0$–3. While all the Y_{l0} are axially symmetric wave functions, $l = 0$ implies full spherical symmetry. The distance from the *center* to the *top* of the figures is $\sqrt{(2l + 1)/4\pi}$. *Solid lines* denote positive lobules; *dotted lines*, negative ones

They can be visualized as vibrational modes of a soap bubble.

- Figure 5.2 displays the projection of some spherical harmonics on the (x, z) plane. The protruding shapes have important consequences in the construction of chemical bonds.
- The rotational Hamiltonian of a molecule is proportional to the operator $\hat{L}^2$. The corresponding energy eigenvalues therefore follow the rule $l(l + 1)$ (see Sect. 8.4.2).

By taking the commutation relations as the definition of the angular momentum operators, we have obtained operators that are not derived from the classical orbital angular momentum (see Sects. 5.1.1 and 5.1.2). This statement is supported by the fact that the quantum numbers j, m associated with these quantum mechanical angular momenta may take either integer or half-integer values, in contrast with those labeling the orbital angular momentum, which can only take integer values. Otherwise we obtain the same matrix elements for the projections $\hat{J}_i$ (5.9) as for the orbital angular momentum projections $\hat{L}_i$. On the other hand, the probability densities associated with the orbital angular momentum display interesting and useful features that are lacking in the more general derivation (Fig. 5.2).

5.2 Spin

5.2.1 Stern–Gerlach Experiment

A particle with a magnetic moment μ and subject to a magnetic field B experiences a torque τ. When the particle is rotated through an angle $d\theta$ about the direction of τ, the potential energy U increases:

$$\tau = \mu \times B, \qquad dU = \mu B \sin\theta d\theta, \qquad U(\theta) = -\mu B \cos\theta = -\mu \cdot B. \quad (5.15)$$

According to classical electromagnetism, an electric current i produces a magnetic moment proportional to the area subtended by the current. If this current is due to a particle with charge e and velocity v moving along a circumference of radius r, then

$$\mu_l = i\,\mathcal{A} = \frac{ev}{2\pi r}\pi r^2 = \frac{e}{2M}L = \frac{e}{|e|}\frac{g_l\mu_\mathrm{B}}{\hbar}L. \tag{5.16}$$

Thus, the magnetic moment due to the orbital motion is proportional to the orbital angular momentum. In vector and operator notation,

$$\hat{\boldsymbol{\mu}}_l = \frac{e}{|e|}\frac{g_l\mu_\mathrm{B}}{\hbar}\hat{\boldsymbol{L}}, \tag{5.17}$$

where $\mu_\mathrm{B} \equiv |e|\hbar/2M$ is called the Bohr magneton (Table A.1) and $g_l = 1$ is the orbital gyromagnetic ratio.

Therefore, the presence of a magnetic field displaces the energy of a particle by an amount proportional to the component of the angular momentum along the magnetic field (Zeeman effect). Classically, this change is a continuous function of the orientation of the angular momentum but, according to quantum mechanics, the projections of the angular momentum are discretized (5.12):
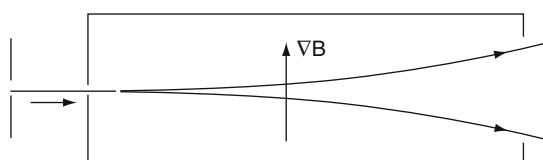
$$\Delta E_{m_l} = g_l\mu_\mathrm{B}Bm_l. \tag{5.18}$$

Therefore, an orbital angular momentum should give rise to an odd number $(2l+1)$ of energy eigenstates.

For a uniform magnetic field, there is no net force acting on the magnetic dipole. However, if the field has a gradient in the z-direction, the net force is

$$F_z = \frac{\partial}{\partial z}(\boldsymbol{\mu}\cdot\boldsymbol{B}) = \mu_z\frac{\partial B}{\partial z}. \tag{5.19}$$

Figure 5.3 is a sketch of the experimental set-up used by Stern and Gerlach [17]. Silver atoms are heated in an oven and escape through a hole. The beam is collimated and subsequently deflected by a nonuniform magnetic field perpendicular to its direction. Finally, a visible deposit is allowed to build up on a glass plate located far from the region of deflection.

Fig. 5.3 Sketch of the Stern–Gerlach experimental arrangement

Fig. 5.4 Two figures contained in a letter to Bohr from Stern, communicating his experimental results. Stern explains that the magnetic field was too weak at the extremes of the beam. The figure to the left was obtained, for comparison, in the absence of magnetic field. (Reproduced with permission from Niels Bohr Archive, Copenhagen)

We may ignore the nuclear contributions to the magnetic moment on the grounds that the nuclear magneton is about 2,000 times smaller than the Bohr magneton. (It includes the proton mass in the denominator, instead of the electron mass.) Moreover, 46 of the 47 electrons form a spherically symmetric electron cloud with no net angular momentum (see Sect. 7.3). Therefore, the total spin of the Ag atom may be ascribed to the last electron.

The Stern–Gerlach result is reproduced in Fig. 5.4. Neither the classical continuous pattern nor the orbital quantum mechanical results displaying the separation into an odd number of terms were obtained: the beam was split into only two other beams, as would befit an angular momentum with $j = s = 1/2$.

Spin has become the most important quantum observable, both due to its conceptual importance and because quantum information is based on two-state systems (Chap. 13). Consistently with this relevance, modern techniques for spin detection and manipulation have greatly improved since Stern and Gerlach's times. It is now possible to deal with individual spins, rising the hopes for spintronics – exploiting the spin degree of freedom in electronic circuits, playing a similar role as the charge degree of freedom (Sect. 7.4.5[†]).

5.2.2 Spin Formalism

Three years after the publication of the Stern–Gerlach experiment, George Uhlenbeck and Samuel Goudsmit proposed another quantum number to specify the state of electrons (and of many other fundamental particles) [35]. It labels the

two projections of the spin, by then a new physical entity representing an intrinsic angular momentum.

Since the spin is a pure quantum observable, only the matrix treatment formalism is possible. If $s = 1/2$, then the basis set of states is given by the two-component vectors (3.15) [36]

$$\varphi_\uparrow^{(z)} \equiv \varphi_{\frac{1}{2}\frac{1}{2}} = \begin{pmatrix} 1 \\ 0 \end{pmatrix}, \qquad \varphi_\downarrow^{(z)} \equiv \varphi_{\frac{1}{2}(-\frac{1}{2})} = \begin{pmatrix} 0 \\ 1 \end{pmatrix}. \tag{5.20}$$

The following representation of the spin operators reproduces (5.7) and (5.9) for $j = 1/2$

$$\hat{S}_i = \frac{\hbar}{2}\sigma_i, \qquad (\hat{S}_i)^2 = \frac{\hbar^2}{4}\mathcal{I}, \qquad i = x, y, z, \tag{5.21}$$

where the σ_i are the Pauli matrices (3.16). Therefore the algebra suited for the spin case has been developed in Sect. 3.2.

The spin has its own associated magnetic moment

$$\hat{\mu}_s = \frac{g_s\mu_v}{\hbar}\hat{S}, \tag{5.22}$$

with a gyromagnetic ratio of $g_s = 2.00$ for electrons,[3] $g_s = 5.58$ for protons and $g_s = -3.82$ for neutrons. The constant μ_v stands for minus the Bohr magneton μ_B in the case of electrons, or for the nuclear magneton $\mu_p = e_p\hbar/2M_p$ in the case of protons and neutrons (Table A.1), where e_p and M_p are the proton charge and mass, respectively. The total magnetic moment operator is given by

$$\hat{\mu} = \hat{\mu}_s + \hat{\mu}_l = \frac{\mu_v}{\hbar}\left(g_s\hat{S} + g_l\hat{L}\right). \tag{5.23}$$

Obviously, $g_l = 0$ for neutrons. The quantal magnetic moment is not always proportional to the angular momentum.

The eigenstates of the operator $\hat{S}_x$ have been obtained by means of a unitary transformation of the eigenvectors of $\hat{S}_z$ (3.21). This is a particular case of the more general transformation aligning the spin $s = 1/2$ operator with a direction of space labeled by the angles β, ϕ. The operator $\hat{S}_{\beta\phi}$ may be written as the scalar product of the spin vector $\hat{S}$ times a unit vector along the chosen direction (see Problem 5 in Chap. 3):

$$\hat{S}_{\beta\phi} = \sin\beta\cos\phi\hat{S}_x + \sin\beta\sin\phi\hat{S}_y + \cos\beta\hat{S}_z$$
$$= \frac{\hbar}{2}\begin{pmatrix} \cos\beta & \sin\beta\exp(-i\phi) \\ \sin\beta\exp(i\phi) & -\cos\beta \end{pmatrix}. \tag{5.24}$$

---

[3]The spectroscopy of single trapped electrons has yielded the value of $g_s = 2 \times 1.00159652188$. The theoretical QED calculation agrees within a few parts per billion [37], p. 5.

The same two eigenvalues $\pm\hbar/2$ are obtained upon diagonalization. As explained in Sect. 3.2, this is a consequence of space isotropy. The diagonalization also yields the state vectors

$$\varphi_\uparrow^{(\beta\phi)} = \begin{pmatrix} \cos\dfrac{\beta}{2} \\ \sin\dfrac{\beta}{2}\exp(i\phi) \end{pmatrix}_z, \qquad \varphi_\downarrow^{(\beta\phi)} = \begin{pmatrix} \sin\dfrac{\beta}{2}\exp(-i\phi) \\ -\cos\dfrac{\beta}{2} \end{pmatrix}_z, \qquad (5.25)$$

while the rotational unitary transformation acting on states (5.20) is

$$\mathcal{U}_{\beta\phi} = \begin{pmatrix} \cos\frac{\beta}{2} & \sin\frac{\beta}{2}\exp(-i\phi) \\ \sin\frac{\beta}{2}\exp(i\phi) & -\cos\frac{\beta}{2} \end{pmatrix}. \qquad (5.26)$$

The factor $1/2$ multiplying the angle β is characteristic of the effect of rotations on $j = 1/2$ objects. It may be verified through the value of the amplitudes (3.21) in the case of transformation from the z to the x eigenstates. In that case, $\beta = \pi/2, \phi = 0$.

An arbitrary linear combination of spin up and spin down states such as in (5.25) is called a qubit. The word "qubit" is short for "quantum bit," a concept used in quantum computation (Sect. 13.4[†]).

5.3 Other Features of the Motion in Angular Subspace

The contents of this section are extracted from [38], Appendix 1A.
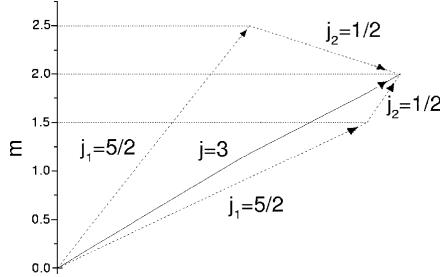
5.3.1 Addition of Angular Momenta

Consider two angular momentum vector operators, $\hat{\boldsymbol{J}}_1$ and $\hat{\boldsymbol{J}}_2$. They are independent vectors, i.e. $[\hat{\boldsymbol{J}}_1, \hat{\boldsymbol{J}}_2] = 0$. Therefore, the product states are simultaneous eigenstates of the operators $\hat{J}_1^2$, $\hat{J}_{z1}$, $\hat{J}_2^2$ and $\hat{J}_{z2}$:

$$\varphi_{j_1 m_1 j_2 m_2} = \varphi_{j_1 m_1}\varphi_{j_2 m_2}. \qquad (5.27)$$

These $(2j_1 + 1)(2j_2 + 1)$ eigenstates constitute a complete basis for states carrying the quantum numbers j_1, m_1, j_2, m_2. However, it may not be the most useful one. We may prefer a basis labeled by the quantum numbers associated with the total angular momentum $\hat{\boldsymbol{J}}$ (see Fig. 5.5):

$$\hat{\boldsymbol{J}} = \hat{\boldsymbol{J}}_1 + \hat{\boldsymbol{J}}_2. \qquad (5.28)$$

Fig. 5.5 Coupling of two vectors with $j_1 = 5/2$ and $j_2 = 1/2$ (*dotted lines*) may yield a vector with $j = 3$, $m = 2$ (*continuous line*). The superposition (5.31) has two components, with $m_1 = \frac{3}{2}$, $m_2 = \frac{1}{2}$ and $m_1 = \frac{5}{2}$, $m_2 = -\frac{1}{2}$, respectively

Since the components $\hat{J}_x$, $\hat{J}_y$, $\hat{J}_z$ also satisfy the commutation relations (5.4) and (5.6), there must exist another basis set made up from eigenstates of the operators $\hat{J}^2$ and $\hat{J}_z$. Since the commutation relations

$$[\hat{J}^2, \hat{J}_1^2] = [\hat{J}^2, \hat{J}_2^2] = [\hat{J}^2, \hat{J}_z] = [\hat{J}_1^2, \hat{J}_z] = [\hat{J}_2^2, \hat{J}_z] = 0 \qquad (5.29)$$

vanish, the new set of basis states may be labeled by the quantum numbers j_1, j_2, j, m

$$\varphi_{j_1 j_2 j m} \equiv \left[\varphi_{j_1} \varphi_{j_2}\right]_m^j. \qquad (5.30)$$

The two basis sets (5.27) and (5.30) are equally legitimate. According to Sect. 2.7.2*, there is a unitary transformation connecting the two bases

$$\varphi_{j_1 j_2 j m} = \sum_{m_1 m_2} c(j_1 m_1; j_2 m_2; j m)\, \varphi_{j_1 m_1 j_2 m_2}. \qquad (5.31)$$

The quantum numbers j_1, j_2 are valid for both sets and they are not therefore summed up in (5.31). The sum over m_1, m_2 is restricted by the addition of projections

$$m = m_1 + m_2 \qquad (5.32)$$

For classical vectors, the modulus of the sum of two vectors lies between the sum of their moduli and the absolute value of their difference. Something similar takes place in quantum mechanics:

$$j_1 + j_2 \geq j \geq |j_1 - j_2|. \qquad (5.33)$$

The quantum number j is an integer if both j_1, j_2 are integers or half-integers; j is a half-integer if only one of the constituents is an integer. The amplitudes $c(j_1 m_1; j_2 m_2; j m)$ are called Wigner or Clebsch–Gordan coefficients. They are real numbers satisfying the symmetry relations

$$
\begin{aligned}
c(j_1m_1; j_2m_2; jm) &= (-1)^{j_1+j_2-j} c\big(j_1(-m_1); j_2(-m_2); j(-m)\big) \\
&= (-1)^{j_1+j_2-j} c\big(j_2m_2; j_1m_1; jm\big) \\
&= (-1)^{j_1-m_1} \sqrt{\frac{2j+1}{2j_2+1}} c\big(j_1m_1; j(-m); j_2(-m_2)\big) \\
&= (-1)^{j_2+m_2} \sqrt{\frac{2j+1}{2j_1+1}} c\big(j(-m); j_2m_2; j_1(-m_1)\big).
\end{aligned}
$$

$$(5.34)$$

The inverse transformation is

$$
\varphi_{j_1m_1} \varphi_{j_2m_2} = \sum_{j=|j_1-j_2|}^{j=j_1+j_2} c(j_1m_1; j_2m_2; jm) \big[\varphi_{j_1}\varphi_{j_2}\big]^j_{m=m_1+m_2}. \tag{5.35}
$$

Replacement of (5.35) into the r.h.s. of (5.31) (and vice versa) yield the orthogonality relations

$$
\sum_{m_1m_2} c(j_1m_1; j_2m_2; jm) \, c(j_1m_1; j_2m_2; j'm') = \delta_{j'j}\delta_{m'm},
$$

$$
\sum_{jm} c(j_1m_1; j_2m_2; jm) \, c(j_1m_1'; j_2m_2'; jm) = \delta_{m_1'm_1}\delta_{m_2'm_2}. \tag{5.36}
$$

The example of the summation of an angular momentum j_1 with the spin $j_2 = s_2 = 1/2$ is given in Sect. 5.6* (See also Fig. 5.5).

5.3.2[†]   *Rotations*

In analogy with (4.7), the unitary operator associated with rotations is

$$
\mathcal{U}(\boldsymbol{\alpha}) = \exp\left(\frac{i}{\hbar}\boldsymbol{\alpha}\cdot\hat{\boldsymbol{J}}\right). \tag{5.37}
$$

The rotation is specified by the axis of rotation (direction of the vector $\boldsymbol{\alpha}$) and the magnitude of the rotation angle α. The operator $\hat{J}_i$ is referred to as the generator of rotations around the i-axis. The following properties stem from the commutators (5.4):

- The rotated state may be expressed as linear combinations of states carrying the same value of J.

$$
\varphi_{JM} = \sum_K D^J_{MK}(\boldsymbol{\alpha}) \, \varphi_{JK}. \tag{5.38}
$$

- The operator (5.37) cannot be straightforwardly written as a product of three successive rotations along orthogonal coordinate axes. Instead, the transformation may be decomposed into the following three rotations, using the Euler parametrization ($\alpha \rightarrow (\phi, \theta, \omega)$)

$$\mathcal{U}(\phi, \theta, \omega) = \exp\left(\frac{i}{\hbar} \hat{J}_z \phi\right) \exp\left(\frac{i}{\hbar} \hat{J}_y \theta\right) \exp\left(\frac{i}{\hbar} \hat{J}_z \omega\right)$$

$$D^J_{MK}(\phi, \theta, \omega) = \langle JM | \mathcal{U}(\phi, \theta, \omega) | JK \rangle$$

$$= \exp(iM\phi) \, d^J_{MK}(\theta) \, \exp(iK\omega), \tag{5.39}$$

where

$$0 \leq \phi \leq 2\pi, \quad 0 \leq \theta \leq \pi, \quad 0 \leq \omega \leq 2\pi. \tag{5.40}$$

The unitary character of the rotational transformation is expressed by the relations

$$\sum_M D^{J*}_{MK_1} D^J_{MK_2} = \delta_{K_1 K_2}, \quad \sum_K D^{J*}_{M_1 K} D^J_{M_2 K} = \delta_{M_1 M_2}. \tag{5.41}$$

For the inverse rotation $(\phi, \theta, \omega)^{-1} = (\pi - \omega, \theta, -\pi - \phi)$

$$D^J_{MK}((\phi, \theta, \omega)^{-1}) = D^{J*}_{KM}(\phi, \theta, \omega). \tag{5.42}$$

The D functions constitute a complete orthogonal set of basis functions in the ϕ, θ, ω space.[4] Their normalization is obtained from the integral

$$\int_0^\pi \sin\theta d\theta \int_0^{2\pi} d\phi \int_0^{2\pi} d\omega \, D^{J*}_{MK} D^{J'}_{M'K'} = \frac{8\pi^2}{2J+1} \delta_{J'J} \delta_{M'M} \delta_{K'K}. \tag{5.43}$$

They represent generalizations of spherical harmonics, which are the complete orthogonal set in θ, ϕ space (Sect. 5.5*)

$$D^J_{M0}(\phi, \theta, \omega) = \left(\frac{4\pi}{2J+1}\right)^{1/2} Y_{JM}(\theta, \phi). \tag{5.44}$$

5.3.3[†]   *The Wigner–Eckart Theorem*

One may also characterize operators $\hat{Q}_{\lambda\mu}$ by their transformation properties under rotations

---

[4]In fact, they are the eigenstates of the axially symmetric top, K being the projection over the symmetry axis.

$$\hat{Q}_{\lambda\mu} = \sum_{\nu} D^{\lambda}_{\mu\nu} \, \hat{Q}_{\lambda\nu}. \tag{5.45}$$

An operator carrying $\lambda = 0$ is a scalar. A vector corresponds to a tensor of rank $\lambda=1$. Any operator can be expanded in a series of spherical tensors.

Since the expansions (5.31) and (5.35) have a pure geometrical origin, they are valid even if one or both of the state vectors are replaced by operators carrying angular momentum quantum numbers:

$$\varphi_{J_2 M_2} = \sum_{\mu M_1} c(J_1 M_1; \lambda\mu; J_2 M_2) \, \hat{Q}_{\lambda\mu} \, \varphi_{J_1 M_1}. \tag{5.46}$$

The scalar product of both sides with a state carrying the quantum numbers J_2', M_2' is given by

$$\sum_{\mu M_1} c(J_1 M_1; \lambda\mu | J_2 M_2) \langle J_2' M_2' | Q_{\lambda\mu} | J_1 M_1 \rangle = \mathcal{N} \, \delta_{J_2' J_2} \delta_{M_2' M_2}, \tag{5.47}$$

where $\mathcal{N}$ is independent of the magnetic quantum numbers. The Wigner–Eckart theorem is obtained multiplying both sides by the coefficient $c(J_1 M_1'; \lambda\mu'; J_2 M_2)$ and applying the orthogonality properties (5.36) (i.e. summing over J_2, M_2)

$$\langle J_2 M_2 | Q_{\lambda\mu} | J_1 M_1 \rangle = \mathcal{N} \, c(J_1 M_1; \lambda\mu; J_2 M_2). \tag{5.48}$$

All the dependence of the matrix element on the magnetic quantum numbers is expressed by means of a Clebsch–Gordan coefficient. Let us remark that this result holds whatever the nature of the initial and final states. The constant $\mathcal{N}$ is usually expressed through the reduced matrix element,[5] which is defined as

$$\langle J_2 || Q_{\lambda} || J_1 \rangle = \mathcal{N} (2J_2 + 1). \tag{5.49}$$

As a consequence of (5.48), we obtain selection rules analogous to (5.32) and (5.33) for the matrix elements $\langle J_2 M_2 | Q_{\lambda\mu} | J_1 M_1 \rangle$. For instance, matrix elements of a spherically symmetric operator vanish unless initial and final states are characterized by the same angular momentum quantum numbers. This is frequently the case of the Hamiltonian. In addition, the product of parities should be $\pi_f \, \pi_Q \, \pi_i = +1$. See also Problem 5.

5.4*   Details of the Matrix Treatment

We define the operators

---

[5]The concept of reduced matrix element is applied in Sect. 9.8.5[†].

$$\hat{J}_{\pm} = \hat{J}_x \pm i\hat{J}_y. \tag{5.50}$$

They play a role similar to the creation and destruction operators a^+, a in the harmonic oscillator case (Sect. 3.3.1). Since the operator $\hat{J}_-$ is Hermitian conjugate to $\hat{J}_+$ (Sect. 2.7.1*),

$$\langle jm|J_+|jm'\rangle = \langle jm'|J_-|jm\rangle^*. \tag{5.51}$$

Applying the commutation relations (5.6), we obtain the relations

$$[\hat{J}_z, \hat{J}_+] = \hbar\hat{J}_+, \tag{5.52}$$

$$[\hat{J}_+, \hat{J}_-] = 2\hbar\hat{J}_z. \tag{5.53}$$

The matrix elements of (5.52) read

$$\langle jm'|[J_z, J_+]|jm\rangle = \hbar(m' - m)\langle jm'|J_+|jm\rangle = \hbar\langle jm'|J_+|jm\rangle, \tag{5.54}$$

which implies that $\langle jm'|J_+|jm\rangle$ is only different from zero if $m' = m + 1$. Therefore the operator $\hat{J}_+$ raises the projection of the angular momentum by one unit of $\hbar$ (and $\hat{J}_-$ does the opposite).

The expectation value of (5.53) yields

$$\begin{aligned}
\langle jm|[J_+, J_-]|jm\rangle &= \langle jm|J_+|j(m-1)\rangle\langle j(m-1)|J_-|jm\rangle \\
&\quad - \langle jm|J_-|j(m+1)\rangle\langle j(m+1)|J_+|jm\rangle \\
&= |\langle jm|J_+|j(m-1)\rangle|^2 - |\langle j(m+1)|J_+|jm\rangle|^2 \\
&= 2\hbar^2 m, \tag{5.55}
\end{aligned}$$

where (5.51) has been used. The solution to this first-order difference equation in $|\langle j(m+1)|J_+|jm\rangle\rangle|^2$ is

$$|\langle j(m+1)|J_+|jm\rangle\rangle|^2 = \hbar^2\big[c - m(m+1)\big]. \tag{5.56}$$

Since the left-hand side is positive, only the values of m that make the right-hand side positive are allowed and the matrix element between the last allowed eigenstate $\varphi_{jm_{max}}$ and the first rejected eigenstate $\varphi_{j(m_{max}+1)}$ should therefore vanish. Here m_{max} is the positive root of the equation $c = m(m+1)$. The assignment of quantum number $j = m_{max}$ determines the value of the constant $c = j(j+1)$. Therefore,

$$\langle j(m+1)|J_+|jm\rangle\rangle = \hbar\sqrt{(j-m)(j+m+1)}, \tag{5.57}$$

where the positive value for the square root is chosen by convention. The relative phases of states with different values of m are also fixed by this convention.

We verify the vanishing of the matrix elements connecting admitted and rejected states:

$$\langle j(j+1)|J_+|jj\rangle = \langle j(-j)|J_+|j(-j-1)\rangle = 0. \tag{5.58}$$

Since m increases in steps of one unit between $-j$ and j [see (5.54)], the possible values of the quantum numbers j, m are those given in (5.8).

The matrix elements (5.9) corresponding to the operators $\hat{J}_x$ and $\hat{J}_y$ can be obtained from (5.51) and from (5.57). Addition of the squares of these matrices yields the (diagonal) matrix elements of $\hat{J}^2$ (5.7).

5.5*   Details of the Treatment of Orbital Angular Momentum

Eigenvalue Equation for the Operator $\hat{L}_z$

The eigenvalue equation for the operator $\hat{L}_z$ is

$$-i\hbar \frac{d\Psi(\phi)}{d\phi} = l_z \Psi(\phi). \tag{5.59}$$

The solution is proportional to $\exp(il_z\phi/\hbar)$. We may require $\Psi(\phi + 2\pi) = \Psi(\phi)$, which implies the existence of discrete values for the eigenvalue $l_z = \hbar m_l$ ($m_l = 0, \pm 1, \pm 2, \ldots$). Thus the orthonormal set of eigenfunctions[6] of the operator $\hat{L}_z$ is given by

$$\varphi_{m_l}(\phi) = \frac{1}{\sqrt{2\pi}} \exp(im_l\phi). \tag{5.60}$$

Eigenvalue Equation for the Operators $\hat{L}^2, \hat{L}_z$

We try a function of the form $\Psi(\theta, \phi) = P_{lm_l}(\theta) \exp(im_l\phi)$. It follows that, in the eigenvalue equation for the operator $\hat{L}^2$:

- We can make the replacement $d^2/d\phi^2 \rightarrow -m_l^2$
- We may drop the exponential $\exp(im_l\phi)$ from both sides of the equation

We obtain a differential equation depending on the single variable θ :

$$-\hbar^2 \left(\frac{d^2}{d\theta^2} + \cot\theta \frac{d}{d\theta} - \frac{m_l^2}{\sin^2\theta} \right) P_{lm_l}(\theta) = \zeta P_{lm_l}(\theta). \tag{5.61}$$

---

[6]This is also the complete set in the angular subspace of a two-dimensional space.

The solutions to this equation for $m_l = 0$ may be expressed as polynomials $P_l(\cos\theta)$ of order l in $\cos\theta$, called Legendre polynomials ($l = 0, 1, 2, \ldots$). Each P_l gives rise to the $2l + 1$ associated Legendre functions $P_{lm_l}(\theta)$ with $|m_l| \leq l$. All of them are eigenfunctions of the operator $\hat{L}^2$ with eigenvalue $\zeta = l(l+1)\hbar^2$.

The simultaneous eigenfunctions of the operators $\hat{L}^2$ and $\hat{L}_z$ are called spherical harmonics:

$$Y_{lm_l}(\theta, \phi) = N_{lm_l} P_{lm_l}(\theta) \exp(im_l\phi), \tag{5.62}$$

where N_{lm_l} are constants chosen to satisfy the orthonormalization equation

$$\langle l'm_l'|lm_l\rangle = \int_0^\pi \sin\theta d\theta \int_0^{2\pi} d\phi\, Y_{l'm_l'}^* Y_{lm_l} = \delta_{ll'}\delta_{m_lm_l'}. \tag{5.63}$$

Here

$$Y_{lm_l}^* = (-1)^{m_l} Y_{l(-m_l)}. \tag{5.64}$$

The spherical harmonics corresponding to the lower values of l are given in Table 5.1.

In particular, the vector **r** can be written in terms of the spherical harmonics $Y_{1\mu}$:

$$x = \sqrt{\frac{2\pi}{3}}\, r\, (-Y_{11} + Y_{1(-1)}), \quad y = i\sqrt{\frac{2\pi}{3}}\, r\, (Y_{11} + Y_{1(-1)}), \quad z = \sqrt{\frac{4\pi}{3}}\, r\, Y_{10}. \tag{5.65}$$

The l values (5.13) are traditionally replaced by symbolic letters in the literature (Table 5.2). This correspondence has only historical support.

The coupling to angular momentum zero of two spherical harmonics depending on different orientations in space depends on the angle α_{12} subtended by the two orientations through the equation

Table 5.1 Spherical harmonics corresponding to the lowest values of l

$Y_{00} = \dfrac{1}{\sqrt{4\pi}}$	$Y_{1(\pm 1)} = \mp\sqrt{\dfrac{3}{8\pi}} \sin\theta \exp(\pm i\phi)$
$Y_{10} = \sqrt{\dfrac{3}{4\pi}} \cos\theta$	$Y_{2(\pm 1)} = \mp\sqrt{\dfrac{15}{32\pi}} \sin(2\theta) \exp(\pm i\phi)$
$Y_{20} = \sqrt{\dfrac{5}{16\pi}}(3\cos^2\theta - 1)$	$Y_{2(\pm 2)} = \sqrt{\dfrac{15}{32\pi}} \sin^2\theta \exp(\pm i2\phi)$

Table 5.2 Equivalence between quantum number l and symbolic letters

l	Symbol
0	s
1	p
2	d
3	f
4	g

$$\left[Y_l(\theta_1,\phi_1)Y_l(\theta_2\phi_2)\right]_0^0 = \frac{1}{\sqrt{2l+1}} \sum_{m_l=-l}^{m_l=l} (-1)^{l-m_l} Y_{lm_l}(\theta_1,\phi_1)Y_{l(-m_l)}(\theta_2,\phi_2)$$

$$= (-1)^l \frac{\sqrt{2l+1}}{4\pi} P_l(\cos\alpha_{12}). \tag{5.66}$$

5.6* Coupling with Spin $s = 1/2$

The use of (5.31) is exemplified in the case where the second angular momentum is the spin $j_2 = s = 1/2$ (Fig. 5.5). Here the summation consists of two terms, corresponding to the two values of the spin projection $m_s = \pm 1/2$. According to (5.33), there are also two values for the total angular momentum $j = j_1 \pm 1/2$. However, if $j_1 = 0$, only the value $j = 1/2$ is allowed:

$$\varphi_{(j_1=j+\frac{1}{2})sjm} = -\sqrt{\frac{j-m+1}{2j+2}}\,\varphi_{j_1(m-\frac{1}{2})_1}\begin{pmatrix}1\\0\end{pmatrix}_2$$

$$+\sqrt{\frac{j+m+1}{2j+2}}\,\varphi_{j_1(m+\frac{1}{2})_1}\begin{pmatrix}0\\1\end{pmatrix}_2, \tag{5.67}$$

$$\varphi_{(j_1=j-\frac{1}{2})sjm} = \sqrt{\frac{j+m}{2j}}\,\varphi_{j_1(m-\frac{1}{2})_1}\begin{pmatrix}1\\0\end{pmatrix}_2 + \sqrt{\frac{j-m}{2j}}\,\varphi_{j_1(m+\frac{1}{2})_1}\begin{pmatrix}0\\1\end{pmatrix}_2.$$

A particular application of this example is the coupling of orbital motion with the spin of an electron (Sect. 6.2). In this case, the eigenstates $\varphi_{j_1m_1}$ are the spherical harmonics $Y_{l_1m_{l_1}}$ (5.62). However, (5.67) is valid whatever the nature of the angular momentum j_1 may be.

If $j = j_1 + \frac{1}{2}$ and $|m| = j$, there is a single term in (5.67). For the particular case $j_1 = 0$, this is a physical consequence of the fact that a spherical object should be uncoupled from the total angular momentum (Fig. 5.2).

Problems

Problem 1. A plastic disk rotates with angular velocity 100 rad/s. Estimate, in units of $\hbar$, the order of magnitude of the angular momentum.

Problem 2. 1. Construct the matrix for the operator $\hat{L}_x$ (5.11) in the basis of spherical harmonics Y_{1m_l} (Table 5.1).
2. Diagonalize the matrix and compare its eigenvalues with those of the operator $\hat{L}_z$.

Problem 3. Verify that the product of the uncertainties $\Delta_{J_x}\Delta_{J_y}$ satisfies the inequality (2.36).

Problem 4. Calculate $\hat{\boldsymbol{J}}\times\hat{\boldsymbol{J}}$.

Problem 5. Consider the following matrix elements between spherical harmonic states:

$$\langle 00|Y_{20}|00\rangle, \quad \langle 10|Y_{20}|10\rangle, \quad \langle 11|Y_{21}|21\rangle, \quad \langle 00|Y_{11}|11\rangle, \quad \langle 00|Y_{11}|1(-1)\rangle,$$

$$\langle 00|\Pi|00\rangle, \quad \langle 11|\Pi|11\rangle, \quad \langle 00|\Pi|10\rangle.$$

1. Find out which of the above matrix elements vanishes due to conservation of orbital angular momentum and/or parity.
2. Calculate those that remain.

Problem 6. Calculate $[\hat{S}_x^2, \hat{S}_z]$ for spin $s = 1/2$ particles.

Problem 7. 1. Construct the eigenstates of $\hat{S}_x$ and $\hat{S}_y$ using the eigenstates of $\hat{S}_z$ as basis states.
2. If the spin S_x is measured when the particle is in an eigenstate of the operator $\hat{S}_y$, what are the possible results and their probabilities?
3. Construct the matrix corresponding to $\hat{S}_x$ using the eigenstates of $\hat{S}_y$ obtained in the first part as basis states.
4. Express the eigenstates $\varphi^{(s_x)}$ using the eigenstates $\varphi^{(s_y)}$ as basis states.

Problem 8. A particle is in the spin state $\begin{pmatrix} a \\ b \end{pmatrix}$, with a, b real. Calculate the probability of obtaining the eigenvalue $\hbar/2$ if:

1. S_x is measured
2. S_y is measured
3. S_z is measured

Problem 9. A particle is in the spin state $\Psi = \begin{pmatrix} \cos(\theta/2) \\ \sin(\theta/2) \end{pmatrix}$.

1. What are the values of S_z that would appear as a result of a measurement of this observable? What are the associated probabilities?
2. What is the mean value of S_z in this state?

Problem 10. 1. Construct the possible states with $m = 1/2$ that are obtained by coupling an orbital angular momentum $l = 2$ with a spin $s = 1/2$.
2. Verify the orthonormality of the coupled states.
3. Construct the wave vector corresponding to the state with $j = m = l + 1/2$. What is the probability that the spin points up?

Problem 11. Write the two-spin state vectors with $s = \frac{1}{2}$ that have a definite total angular momentum.

Problem 12. Apply the closure property as in (2.59) to the transformations (5.31) and (5.35).

Problem 13. Relate the coupling between an orbital angular momentum l and a spin $s = \frac{1}{2}$ to the coupling of the spin to the same orbital angular momentum.

Chapter 6
Three-Dimensional Hamiltonian Problems

In the present chapter, we broaden the quantum mechanical treatment of the problem of a single particle moving in three-dimensional space to incorporate the Hamiltonian. We only treat central potentials $V(\boldsymbol{r}) = V(r)$. In particular, we study the Coulomb and the three-dimensional harmonic oscillator potentials, including Rydberg atoms. We also present the spin–orbit interaction and elements of scattering theory.

6.1 Central Potentials

The solution to a given problem can be simplified by exploiting the associated symmetries. We have already shown that this is the case by applying invariance under the inversion operation (see the bound problems of Sects. 4.2 and 4.4). Since problems involving a central potential $V(r)$ are spherically symmetric, we shall make use of this symmetry. For this purpose, we write the kinetic energy Laplacian in spherical coordinates (5.10). The total Hamiltonian reads

$$
\begin{aligned}
\hat{H} &= \frac{1}{2M}\left(\hat{p}_x^2 + \hat{p}_y^2 + \hat{p}_z^2\right) + V(r) \\
&= \frac{\hbar^2}{2M}\left(-\frac{\partial^2}{\partial r^2} - \frac{2}{r}\frac{\partial}{\partial r}\right) + \frac{\hat{L}^2}{2Mr^2} + V(r),
\end{aligned} \tag{6.1}
$$

where the operator $\hat{L}^2$ is the square of the orbital angular momentum (5.11). Since the Hamiltonian (6.1) commutes with operators $\hat{L}^2$ and $\hat{L}_z$, there is a basis set of eigenfunctions for the three operators. The eigenvalue equation (4.11) is solved by factorizing the wave function into radial and angular terms, the latter being represented by the spherical harmonics (5.62):

$$
\Psi(r, \theta, \phi) = R_{n_r l}(r) Y_{l m_l}(\theta, \phi). \tag{6.2}
$$

In such a case, the operator $\hat{L}^2$ in the kinetic energy can be replaced by its eigenvalue $\hbar^2 l(l + 1)$, and moreover, the spherical harmonics cancel on both sides of the Schrödinger equation.[1] One is left with a differential equation depending on a single variable: the radius. Thus,

$$\left\{ \frac{\hbar^2}{2M} \left[-\frac{d^2}{dr^2} - \frac{2}{r}\frac{d}{dr} + \frac{l(l+1)}{r^2} \right] + V(r) \right\} R_{n_r l}(r) = E_{n_r l} R_{n_r l}(r), \quad (6.3)$$

where the new quantum number n_r distinguishes between states with the same value of l. Since the magnetic quantum number m_l does not appear in this equation, the eigenvalues $E_{n_r l}$ are also independent of it. In consequence, the eigenenergies of a central potential are necessarily degenerate, with degeneracy equal to $2l + 1$ (5.13). This result is to be expected since the quantum number m_l depends on the orientation of the coordinate axis. That is to say, the central potential has spherical symmetry and the resulting energies (which are physical quantities) should not depend on the orientation of the coordinate axis (which is an artifact of the calculation).

Systems for which the number of quantum numbers equals the number of degrees of freedom are called *integrable*. Do not get a wrong impression out of the present chapter: they are the exceptions.

6.1.1   Coulomb and Harmonic Oscillator Potentials

In this section, we discuss the solutions to the eigenvalue equation for two central potentials: the Coulomb potential $-Ze^2/4\pi\epsilon_0 r$ and the three-dimensional harmonic oscillator potential $M\omega^2 r^2/2$.

It is always useful to begin by estimating the orders of magnitude of the quantities involved. For the linear harmonic oscillator, this has already been done in (3.28). These orders of magnitude remain valid for the three-dimensional case, since the harmonic Hamiltonian is separable into three Cartesian coordinates, and the estimate (3.28) holds for each coordinate. For the Coulomb potential, we may again use the Heisenberg uncertainty relations

$$\boldsymbol{p}^2 \approx 3\,(\Delta p_x)^2 \geq \frac{3\hbar^2}{4}\frac{1}{(\Delta x)^2} \approx \frac{9\hbar^2}{4}\frac{1}{r^2}. \quad (6.4)$$

Therefore, the radius r_{m} is obtained by minimizing the lower bound energy

$$E \geq \frac{9\hbar^2}{8Mr^2} - \frac{Ze^2}{4\pi\epsilon_0 r}, \quad (6.5)$$

---

[1]This is another application of the separation of variables method for solving partial differential equations.

Table 6.1 Solutions to the Coulomb and harmonic oscillator potentials

Problem	Coulomb	Harmonic oscillator
Characteristic length	$a_0 = 4\pi\epsilon_0\hbar^2/Me^2$	$x_c = \sqrt{\hbar/M\omega}$
Wave function	$R_{n_r l}(u)Y_{lm_l}(\theta,\phi)$	$R_{n_r l}(u)Y_{lm_l}(\theta,\phi)$
	$u = Zr/a_0$	$u = r/x_c$
Radial quantum numbers	$n_r = 0, 1, \ldots$	$n_r = 0, 1, \ldots$
Principal quantum numbers	$n = n_r + l + 1 = 1, 2, \ldots$	$N = 2n_r + l = 0, 1, \ldots$
Energies	$Z^2 E_H/n^2$	$\hbar\omega(N + 3/2)$
	$E_H = -e^2/8\pi\epsilon_0 a_0$	
Degeneracy	n^2	$(N+1)(N+2)/2$

which yields

$$r_m = \frac{9}{4Z}a_0, \qquad E \geq \frac{16Z^2}{9}E_H, \tag{6.6}$$
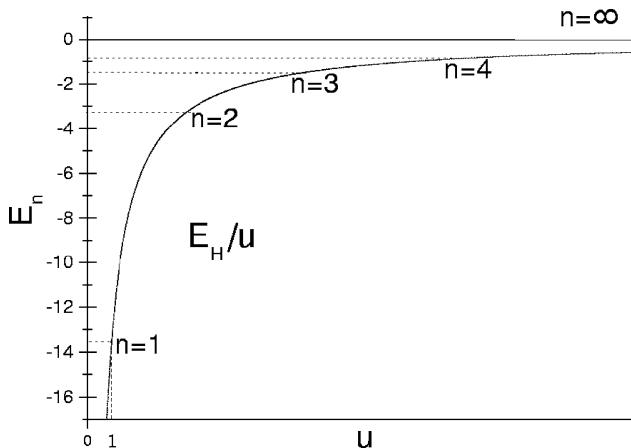
where the Bohr radius a_0 and the ground state energy of the hydrogen atom E_H are given in Tables 6.1 and A.1.

The solutions of the Schrödinger equation for the Coulomb[2] and the harmonic oscillator potentials are shown in Table 6.1. The corresponding details are outlined in Sect. 6.4*. The following comments stem from the comparison between the solutions for these two potentials:

- In both cases, the radial factor $R_{n_r l}(r)$ may be expressed as a product of an exponential decay, a power of u, u^l, and a polynomial of degree n_r (Coulomb) or $2n_r$ (harmonic oscillator).
- The radial factor u^l decreases the radial density $|R_{n_r l}|^2 r^2$ for small values of u and increases it for large values. It is a manifestation of centrifugal effects due to rotation of the particle.
- Both potentials display a higher degree of degeneracy than is required by spherical invariance.
- All degenerate states in the harmonic oscillator potential have the same value of $(-1)^l = (-1)^N$, where N is the principal quantum number (Table 6.1) and thus have the same parity. This is not true for the Coulomb potential, where states with even and odd values of l may be degenerate [see the last equation of (5.12)].
- The energies of the Coulomb potential are represented in Fig. 6.1, while those of the harmonic potential have the same pattern as in Fig. 3.2. The eigenvalues of the former display an accumulation point at $E_\infty = 0$. They are equidistant in the harmonic oscillator case.

---

[2]Solutions for the Coulomb potential applying matrix algebra can be found in [39].

Fig. 6.1 Coulomb potential and its eigenvalues. The dimensionless variable $u = r/a_0$ has been used

We have verified the commonly made statement that the Schrödinger equation is exactly soluble for the two central potentials treated in this section. In fact the two Schrödinger equations are related by a simple change of independent variable $r \rightarrow r^2$, if the energy and the strength of the potential are swapped and the orbital angular momentum is rescaled (Problem 8) [40]. Thus, the Schrödinger equations corresponding to the Coulomb and three-dimensional harmonic oscillator potential constitute only one soluble quantum mechanical central problem, not two.

The harmonic oscillator potential is also separable in Cartesian coordinates. As an exercise, derive the degeneracies using the Cartesian solution and check the results against those appearing in the last column of Table 6.1.

While the Coulomb potential is an essential tool for the systematic description of atomic spectra, the three-dimensional harmonic oscillator plays a similar role for the nuclear spectra. This similitude is remarkable in view of the very different constituents and interactions that are present in both systems (Sect. 7.3).

6.1.2 Rydberg Atoms

The set of degenerate single particle levels constitutes a shell (Sect. 7.3). Since all the magnetic substates are filled up in a closed shell, this system displays spherical symmetry. Alkali atoms have one electron outside closed shells. Their spectrum shows to a large extent the characteristic features of single-particle motion, the effect of the closed shell electrons being almost totally limited to screen the nuclear charge. Rydberg atoms are alkali atoms excited to states with large quantum number $n = \mathcal{O}(50)$, carrying an orbital angular momentum $l = n - 1$ with projection $m_l = l$.

Assuming that the outside electron feels a Coulomb potential with charge 1, the energies and wave functions [(6.2) and (6.27)] are given by

$$E_n = -R_H \hbar c / n^2,$$

$$\varphi_{n,n-1,n-1} = \frac{1}{\sqrt{\pi a_0^3}} \frac{1}{n^n n!} \left[-\frac{r}{a_0} \sin\theta \exp(i\phi) \right]^{n-1} \exp(-r/na_0), \quad (6.7)$$

where R_H is approximately the Rydberg constant and a_0 is the Bohr radius (Table A.1).

The mean value of the radius is

$$r_n \equiv \langle n, n-1, n-1 | r | n, n-1, n-1 \rangle = a_0 n(2n+1)/2 \approx a_0 n^2, \quad (6.8)$$

which tell us that the radius of the orbit n is much larger than the radius of the core, and that the approximation gets better the higher the value of n. Moreover, the relative dispersion is

$$\frac{\Delta r_n}{r_n} = 1/\sqrt{2n+1}, \quad (6.9)$$

with a similar expression for the θ degree of freedom. Thus the density distribution resembles a tire. In fact, it is the closest that one can get to the circular orbits of the old Bohr atomic model (see Problem 14). The azimuthal angle ϕ is completely unspecified, as required by Heisenberg's uncertainty principle. See also Problem 14 and Problem 14 in Chap. 9.

The coupling with other degenerate states (such as $\varphi_{n,n-2,n-2}$) can become sufficiently small by making use of an electric field along the direction of the angular momentum (Stark effect), which destroys this degeneracy (see Problem 12, Chap. 8).

Rydberg atoms with $40 < n < 60$ are presently used to verify quantum mechanical properties that were discussed by means of thought experiments during most of the last century (Sect. 12.3.3). They are also candidates to play the role of qubits in future quantum computers (Sect. 13.4[†]).

6.2 Spin–Orbit Interaction

One may incorporate the spin degree of freedom into the present treatment. The degeneracies displayed in Table 6.1 are thus doubled.

According to the results of Sect. 5.3.1, there are two complete sets of wave functions that may take care of the spin $s = 1/2$:

$$\varphi_{nlm_l sm_s} = R_{n_r l} Y_{lm_l} \varphi_{sm_s}, \quad (6.10)$$

$$\varphi_{nlsjm} = R_{n_r l} \sum_{m_l + m_s = m} c(l m_l; s m_s; j m) Y_{l m_l} \varphi_{s m_s}, \tag{6.11}$$

where the Clebsch–Gordan or Wigner coefficients are given in Sect. 5.6*. As mentioned in Sect. 5.3.1, the first set is labeled with the quantum numbers $l m_l s m_s$ specifying the modulus and the z-projection of the orbital angular momentum and the spin. In the second set, the moduli of the orbital angular momentum and the spin remain as good quantum numbers, to be accompanied by jm, associated with the modulus and z-projection of the total angular momentum $\hat{\boldsymbol{J}} = \hat{\boldsymbol{L}} + \hat{\boldsymbol{S}}$.

The Coulomb interaction is the strongest force acting inside an atom, and yields adequate results for many purposes. However, the experimental spectrum displays small shifts in energy associated with values of j. Another (weaker) force that is present in the atom is provided by the interaction between the magnetic moment of the spin and the magnetic field produced by the orbital motion of the electron[3]:

$$\hat{V}_{\text{so}} = v_{\text{so}} \hat{\boldsymbol{S}} \cdot \hat{\boldsymbol{L}}, \tag{6.12}$$

where we have approximated the radial factor by a constant v_{so}.

Suppose we sit on the electron. We see the charged nucleus orbiting around us. The current associated with this moving charged nucleus produces a magnetic field at the location of the electron. The $\hat{\boldsymbol{S}} \cdot \hat{\boldsymbol{L}}$ term can be interpreted as the interaction between the spin magnetic moment of the electron and this magnetic field.

There are additional terms, the hyperfine interactions, arising from the interaction between the nuclear and the electron spins. Although they are even smaller, they produce a splitting of the ground state of the hydrogen atom with astrophysical importance [which the interaction (6.12) does not].

The radial term $R_{n_r l}$ has been dropped in the present section, since the spin–orbit interaction (6.12) does not affect the radial part of the wave function.

The spin–orbit interaction satisfies the commutation relations

$$[\hat{V}_{\text{so}}, \hat{L}^2] = [\hat{V}_{\text{so}}, \hat{S}^2] = [\hat{V}_{\text{so}}, \hat{J}^2] = [\hat{V}_{\text{so}}, \hat{J}_z] = 0, \tag{6.13}$$

while $[\hat{V}_{\text{so}}, \hat{L}_z] \neq 0$, $[\hat{V}_{\text{so}}, \hat{S}_z] \neq 0$. Bearing in mind this property, different procedures – already developed in these notes – may be applied to incorporate the interaction (6.12).

1. The interaction is not diagonal within the set of eigenstates of the projections of the angular momenta (6.10). Since $\hat{V}_{\text{so}}$ commutes with $\hat{J}_z$, the spin–orbit interaction conserves the total projection $m = m_l + m_s$ and thus gives rise to matrices of order 2 which may be diagonalized according to Sect. 3.2.

---

[3]Criteria which are frequently used to construct interactions involving pure quantum variables are (1) simplicity and (2) invariance under transformations, such as rotations, parity and time-reversal operations. The interaction (6.12) satisfies all these criteria. Moreover, it may also be obtained in the non-relativistic limit of the Dirac equation.

2. The spin–orbit interaction is diagonal within the set of eigenstates (6.11). This constitutes a significant advantage. The diagonal matrix elements are the eigenvalues, which may be obtained through calculation.
3. Observing that

$$\hat{\boldsymbol{L}} \cdot \hat{\boldsymbol{S}} = \frac{1}{2} \left(\hat{J}^2 - \hat{L}^2 - \hat{S}^2 \right), \tag{6.14}$$

we obtain

$$\langle lsjm | \boldsymbol{S} \cdot \boldsymbol{L} | lsjm \rangle = \frac{\hbar^2}{2} \left[j(j+1) - l(l+1) - \frac{3}{4} \right]. \tag{6.15}$$

Due to the spin–orbit interaction, the two states with $j_\pm = l \pm 1/2$ become displaced by an amount proportional to the values appearing on the right-hand side of (6.15).
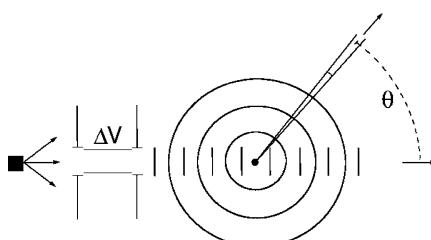
6.3   Some Elements of Scattering Theory

6.3.1   Boundary Conditions

We consider an incident particle scattered by a central, finite-sized potential. The asymptotic boundary condition for this problem requires the asymptotic wave function to be expressed as a superposition of an incident plane wave along the z-axis and an outgoing spherical wave (Fig. 6.2):

$$\lim_{r \to \infty} \Psi(r, \theta) = A \left[\exp(ikz) + \frac{\exp(ikr)}{r} f_k(\theta) \right], \tag{6.16}$$

where $k = \sqrt{2ME}/\hbar$ is the wave number (4.32) and $f_k(\theta)$ is the amplitude of the scattered wave in the polar direction θ. The spherical wave carries a factor $1/r$, since


Fig. 6.2 Schematic representation of a scattering experiment. After being produced in a source, the projectile is collimated, accelerated and collimated again. It collides with the target in the form of a plane wave. It is subsequently scattered as a spherical wave, within a solid angle that makes an angle θ with the direction of incidence

$|\Psi(r)|^2$ must be proportional to $1/r^2$ to conserve probability (see Problem 11). The azimuth angle ϕ does not appear, because the problem displays axial symmetry. Expression (6.16) constitutes a generalization of the boundary conditions discussed at the beginning of Sect. 4.5 to the three-dimensional case.

6.3.2 Expansion in Partial Waves

As in the case of a three-dimensional harmonic oscillator, the free particle problem admits solutions in both Cartesian and polar coordinates. The solutions to the Hamiltonian (6.1) with $V(r) = 0$ are, in spherical coordinates,

$$\varphi_{lm_l}^{(1)}(r, \theta, \phi) = j_l(kr)Y_{lm_l}(\theta, \phi), \qquad \varphi_{lm_l}^{(2)}(r, \theta, \phi) = n_l(kr)Y_{lm_l}(\theta, \phi), \quad (6.17)$$

where j_l and n_l are Bessel and Neumann functions, respectively (see Sect. 6.5*). The eigenstates (6.17) constitute a complete set. Our immediate task is to construct the most general linear combination which asymptotically yields (6.16). We first note that the function $\exp(ikz)$ may be expanded as

$$\exp(ikz) = \sqrt{4\pi} \sum_{l=0}^{l=\infty} i^l (2l + 1)^{1/2} j_l Y_{l0}. \qquad (6.18)$$

Secondly, the second term on the right-hand side of (6.16) can be written in terms of the Hankel function of the first kind, which behaves asymptotically as an outgoing spherical wave (6.37). Therefore, the most general and acceptable linear combination is

$$\Psi(r, \theta) = A \sum_{l=0}^{l=\infty} \left[\sqrt{4\pi} i^l (2l + 1)^{1/2} j_l + c_l h_l^{(+)}(kr) \right] Y_{l0}$$

$$= A\sqrt{\pi} \sum_{l=0}^{l=\infty} i^l (2l + 1)^{1/2} a_l \left(j_l \cos \delta_l - n_l \sin \delta_l \right) Y_{l0}. \qquad (6.19)$$

Here c_l, a_l are complex amplitudes, which may be expressed in terms of δ_l, the (real) phase shift of the l-partial wave:

$$c_l = \sqrt{\pi} i^l (2l + 1)^{1/2} (a_l^2 - 1), \qquad a_l = \exp(i\delta_l). \qquad (6.20)$$

We notice that $f_k(\theta)$ is provided by the second term in the first line of (6.19). Replacing the Hankel function by its asymptotic representation one gets

$$f_k(\theta) = -i \frac{\sqrt{\pi}}{k} \sum_{l=0}^{l=\infty} (2l + 1)^{1/2} \left[\exp(i2\delta_l) - 1 \right] Y_{l0}. \qquad (6.21)$$

6.3.3   Cross Sections

According to (6.16), the ratio between the scattered flux in the direction θ and the incident flux along the polar axis is given by $|f(\theta)|^2/r^2$. The differential cross section is defined as the number of particles that emerge per unit incident flux, per unit solid angle and per unit time:

$$\sigma(\theta) = |f(\theta)|^2 = \frac{\pi}{k^2} \left| \sum_{l=0}^{l=\infty} (2l+1)^{1/2} \big[\exp(i2\delta_l) - 1 \big] Y_{l0} \right|^2 . \tag{6.22}$$

The total cross section is the integral over the whole solid angle

$$\sigma = 2\pi \int_0^\pi \sigma(\theta) \sin\theta \, d\theta = \frac{4\pi}{k^2} \sum_{l=0}^{l=\infty} (2l+1) \sin^2 \delta_l . \tag{6.23}$$

The values of δ_l are determined by applying continuity equations at the border $r = a$ of the central potential. In the case of scattering by a rigid sphere of radius a, the phase shifts are given by (6.19) and (6.35):

$$\tan\delta_l = \frac{j_l(ka)}{n_l(ka)}, \qquad \lim_{ka\to 0} \tan\delta_l = \frac{(ka)^{2l+1}}{(2l+1)\big[(2l-1)!!\big]^2} . \tag{6.24}$$

If $ka = 0$, all the partial wave contributions vanish except for $l = 0$, due to the k^2 appearing in the denominator of the cross sections (6.22) and (6.23). We obtain

$$\sigma(\theta) = a^2, \qquad \sigma = 4\pi a^2 . \tag{6.25}$$

The scattering is spherically symmetric and the total cross section is four times the area seen by classical particles in a head-on collision. This quantum result also appears in optics and is characteristic of long-wavelength scattering. The fact that σ is the total surface area of the sphere is interpreted by saying that the waves "feel" all this area.

Some features of scattering theory deserve to be stressed:

- The classical distance of closest approach to the z-axis of a particle with orbital angular momentum $\hbar l$ and energy E is l/k. Therefore, a classical particle is not scattered if $l > ka$. A similar feature appears in quantum mechanics, since the first and largest maximum of $j_l(kr)$ lies approximately at $r = l/k$. Thus, for $l > ka$, the maximum occurs where the potential vanishes: the largest value of l to be included is of order ka.
- The calculation of the probability current (4.18) with wave function (6.16) should yield interference terms in the whole space. They would be nonphysical consequences of assuming an infinite plane wave for the incident beam.

In practice, the beam is collimated and, as a consequence, the incident plane wave and the scattered wave are well separated, except in the forward direction (Fig. 6.2). On the other hand, in most experimental arrangements, the opening of the collimator is sufficiently large to ensure that there are no measurable effects of the uncertainty principle due to collimation (see Problem 12 of Chap. 2).

- Interference in the forward direction between the incident plane wave and the scattered wave gives rise to the important relation

$$\sigma = \frac{4\pi}{k} \text{Im} \left[f_k(0) \right], \tag{6.26}$$

by comparing (6.21) and (6.23). The attenuation of the transmitted beam measured by $\text{Im}\left[f_k(0) \right]$ is proportional to the total cross section σ. The validity of (6.26) (optical theorem) is very general and is not restricted to scattering theory.

- The previous description of a scattering experiment is made in the center of mass coordinate system. We must therefore use the projectile–target reduced mass and the energy for the relative motion to determine the value of k. Moreover, there is a geometrical transformation between the scattering angles θ and θ_{lab} because the two systems of reference move relative to each other with the velocity of the center of mass.

6.4*   Solutions to the Coulomb and Oscillator Potentials

The hydrogen atom constitutes a two-body problem which can be transformed to a one-body form by changing to the center of mass frame. As a consequence, the reduced mass for relative motion should be used [as will be done in (8.22)]. However, for the sake of simplicity, we ignore the motion of the nucleus here, since it is much heavier than the electron.
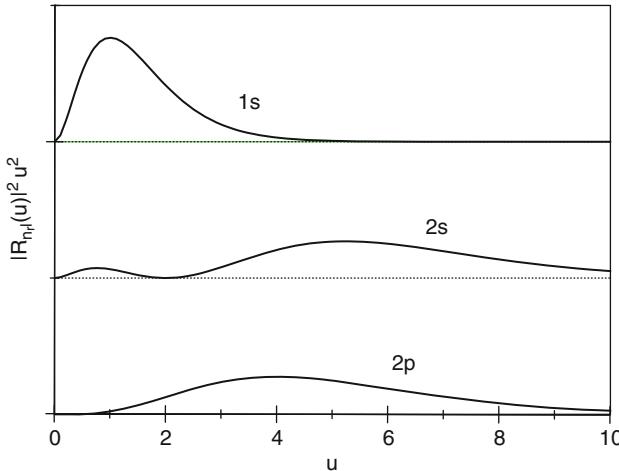
It is always helpful to work with dimensionless variables, as in (4.22). In the case of the hydrogen atom, the natural length is the Bohr radius (Table A.1). Thus, one may use $u = Zr/a_0$. The solution to the radial equation (6.3) takes the form

$$R_{n_r l}(r) = N_{nl}(Z/na_0)^{3/2} \exp(-u/n) u^l L_{n_r}(u), \tag{6.27}$$

where $L_{n_r}(u)$ are polynomials of degree $n_r = 0, 1, 2, \ldots$ called Laguerre polynomials. The N_{nl} are normalization constants such that

$$\int_0^\infty r^2 R_{n_r l} R_{n'_r l} \mathrm{d}r = \delta_{n_r n'_r}. \tag{6.28}$$

The energy $Z^2 |E_\text{H}|/n^2$ is the ionization or binding energy, i.e. the amount of energy that must be given to the Z atom to separate an electron in the n state. Figure 6.3 represents the probability density as a function of the radial coordinate for the

Fig. 6.3 Radial probability densities of the Coulomb potential

$n = 1, 2$ states (Table 6.2). The expression for the probability density includes a factor r^2 associated with the volume element (5.10).

Figure 6.4 combines the angular distribution associated with the spherical harmonics of Fig. 5.2 with the radial densities appearing in Fig. 6.3.

The Bohr radius a_0 may be compared with the expectation value of the coordinate r in the ground state of the hydrogen atom. According to Table 6.2, one gets

$$\langle 100|r|100 \rangle = \int_0^\infty \int_0^\pi \int_0^{2\pi} r^3 \, |\varphi_{100}|^2 \, dr \sin\theta d\theta d\phi$$

$$= \frac{4}{a_0^3} \int_0^\infty r^3 \exp(-2r/a_0) dr = \frac{3}{2} a_0. \qquad (6.29)$$

There are also positive energy, unbound solutions to the Coulomb problem. They are used in the analysis of scattering experiments between charged particles.

In the harmonic oscillator, the dimensionless length is given by the ratio $u = r/x_c$, as in (4.21). The radial eigenfunctions are

$$R_{n_r l} = N_{Nl} \frac{1}{\pi^{1/4} x_c^{3/2}} \exp(-u^2/2) u^l F\left(-n_r, l + \frac{3}{2}, u^2\right). \qquad (6.30)$$
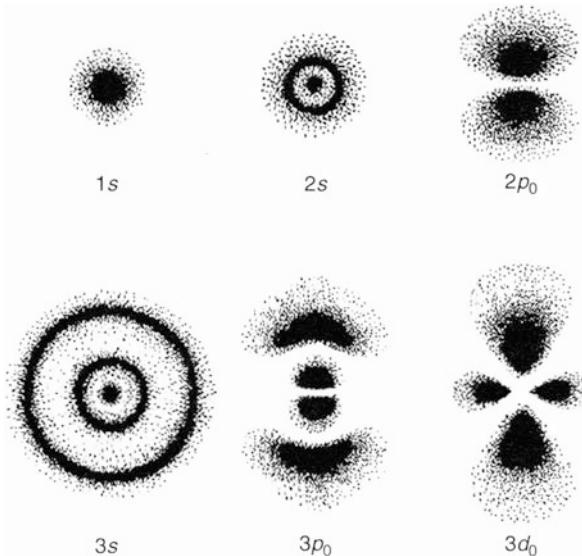
The confluent hypergeometric function $F(-n_r, l + 3/2, u^2)$ is a polynomial of the order n_r in u^2 ($n_r = 0, 1, 2, \ldots$). Some radial probability densities are displayed in Fig. 6.5. The N_{Nl} are normalization constants such that (6.28) also holds true in this case. The energy eigenvalues are given by
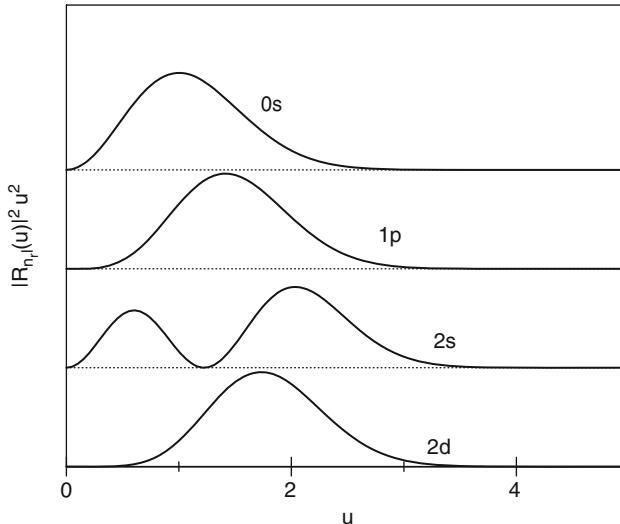
Table 6.2 Radial dependence of the lowest solutions for the Coulomb potential and the three-dimensional harmonic oscillator

Coulomb potential

n	n_r	l	N_{nl}	$L_{n_r}(u)$
1	0	0	2	1
2	1	0	2	$1 - \dfrac{1}{2}u$
2	0	1	$1/\sqrt{3}$	1
3	2	0	2	$1 - \dfrac{2}{3}u + \dfrac{2}{27}u^2$
3	1	1	$4\sqrt{2}/9$	$1 - \dfrac{1}{6}u$
3	0	2	$4/27\sqrt{10}$	1

Three-dimensional harmonic oscillator

N	n_r	l	N_{Nl}	$F\left(-n_r, l + \dfrac{3}{2}, u^2\right)$
0	0	0	2	1
1	0	1	$2\sqrt{2/3}$	1
2	1	0	$\sqrt{6}$	$1 - \dfrac{2}{3}u^2$
2	0	2	$4/\sqrt{15}$	1
3	1	1	$2\sqrt{5/3}$	$1 - \dfrac{2}{5}u^2$
3	0	3	$4\sqrt{2/105}$	1

Fig. 6.4 Probability density plots of some hydrogen atomic orbitals. The density of the dots represents the probability of finding the electron in that region [41]. (Reproduced with permission from University Science Books)

Fig. 6.5 Radial probability densities of the harmonic oscillator potential

$$E = \hbar\omega\left(N + \frac{3}{2}\right).\tag{6.31}$$

Using procedures similar to those applied for the linear harmonic oscillator, we may calculate the expectation values of the square of the radius and of the momentum. We thus verify the virial theorem (3.46) once again:

$$\langle Nlm_l|r^2|Nlm_l\rangle/x_c^2 = \langle Nlm_l|p^2|Nlm_l\rangle x_c^2/\hbar^2 = N + \frac{3}{2}.\tag{6.32}$$

The lowest energy solutions are given on the right-hand side of Table 6.2.

Useful definite integrals are

$$\int_0^\infty u^n \exp(-au)\mathrm{d}u = \frac{n!}{a^{n+1}}, \qquad \int_0^\infty u^{2n} \exp(-u^2)\mathrm{d}u = \frac{(2n-1)!!\sqrt{\pi}}{2^{n+1}},$$

$$\int_0^\infty u^{2n+1} \exp(-u^2)\mathrm{d}u = \frac{n!}{2}.$$

6.5* Some Properties of Spherical Bessel Functions

The spherical Bessel functions $j_l(kr)$ [and the Neumann $n_l(kr)$] satisfy the differential equation

Table 6.3 Lowest spherical Bessel functions

l	j_l	n_l
0	$\dfrac{1}{\rho}\sin\rho$	$-\dfrac{1}{\rho}\cos\rho$
1	$\dfrac{1}{\rho^2}\sin\rho - \dfrac{1}{\rho}\cos\rho$	$-\dfrac{1}{\rho^2}\cos\rho - \dfrac{1}{\rho}\sin\rho$
2	$\left(\dfrac{3}{\rho^3} - \dfrac{1}{\rho}\right)\sin\rho - \dfrac{3}{\rho^2}\cos\rho$	$-\left(\dfrac{3}{\rho^3} - \dfrac{1}{\rho}\right)\cos\rho - \dfrac{3}{\rho^2}\sin\rho$

$$-\frac{\hbar^2}{2M}\left[\frac{d^2}{dr^2} + \frac{2}{r}\frac{d}{dr} - \frac{l(l+1)}{r^2}\right] j_l(kr) = \frac{\hbar^2 k^2}{2M} j_l(kr). \qquad (6.33)$$

Their asymptotic properties for large arguments are

$$\lim_{\rho\to\infty} j_l(\rho) = \frac{1}{\rho}\sin\left(\rho - \frac{1}{2}l\pi\right), \qquad \lim_{\rho\to\infty} n_l(\rho) = -\frac{1}{\rho}\cos\left(\rho - \frac{1}{2}l\pi\right), \quad (6.34)$$

while for small arguments they are

$$\lim_{\rho\to 0} j_l(\rho) = \frac{\rho^l}{(2l+1)!!}, \qquad \lim_{\rho\to 0} n_l(\rho) = -\frac{(2l-1)!!}{\rho^{l+1}}. \qquad (6.35)$$

The spherical Hankel functions are defined by

$$h_l^{(+)}(\rho) = j_l(\rho) + in_l(\rho), \qquad h_l^{(-)}(\rho) = j_l(\rho) - in_l(\rho). \qquad (6.36)$$

Due to (6.34), these have the asymptotic expressions

$$\lim_{\rho\to\infty} h_l^{(+)}(\rho) = \frac{(-i)^{l+1}}{\rho}\exp(i\rho), \qquad \lim_{\rho\to\infty} h_l^{(-)}(\rho) = \frac{(i)^{l+1}}{\rho}\exp(-i\rho). \quad (6.37)$$

The first three j_ls and n_ls are given in Table 6.3.

Problems

Problem 1. Calculate the difference in the excitation energy of $n = 2$ states between hydrogen and deuterium atoms. Hint: use the reduced mass instead of the electron mass.

Problem 2. 1. Assign the quantum numbers nlj to the eigenstates of the Coulomb problem with $n \leq 3$.
2. Do the same for the three-dimensional harmonic oscillator with $N \leq 3$.

Problem 3. 1. Obtain the degeneracy of a harmonic oscillator shell N, including the spin.

2. Obtain the average value $\langle|L^2|\rangle_N$ of the operator $\hat{L}^2$ in an N shell.
3. Calculate the eigenvalues of a harmonic oscillator potential plus the interaction [see (7.16)]

$$-\frac{\omega}{16}\left(\frac{1}{\hbar}\hat{L}^2 - \hbar N(N+3)\right) - \frac{\omega}{4\hbar}\hat{L}\cdot\hat{S},$$

for $N = 0, 1, 2, 3$.
4. Give the quantum numbers of the states with minimum energy for a given shell N.

Problem 4. 1. Find the energy and the wave function for a particle moving in an infinite spherical well of radius a with $l = 0$. Hint: replace $\Psi(r) \rightarrow f(r)/r$.

2. Solve the same problem using the Bessel functions given in Sect. 6.5**.

Problem 5. 1. Find the values of r at which the probability density is at a maximum, assuming the $n = 2$ states of a hydrogen atom.

2. Calculate the mean value of the radius for the same states.

Problem 6. Solve the harmonic oscillator problem in Cartesian coordinates. Calculate the degeneracies and compare them with those listed in Table 6.1.

Problem 7. 1. Find the ratio between the nuclear radius and the average electron radius in the $n = 1$ state, for H and for Pb. Use $R_{\text{nucleus}} \approx 1.2A^{1/3}$ F, $A(\text{H}) = Z(\text{H}) = 1$, $A(\text{Pb}) = 208$ and $Z(\text{Pb}) = 82$.

2. Do the same for a muon ($M_\mu = 207M_e$).
3. Is the picture of a pointlike nucleus reasonable in all these cases?

Problem 8. Replace $r^2 \rightarrow s$ in the radial equation of a harmonic oscillator potential. Find the changes in the constants $l(l + 1)$, $M\omega^2$ and E that yield the Coulomb radial equation. Hint: make the replacement $R(r) \rightarrow s^{1/4}\Phi(s)$ and construct the radial equation using $s \equiv r^2$ as variable.

Problem 9. The positronium is a bound system of an electron and a positron (the same particle as an electron but with a positive charge). Their spin–spin interaction energy may be written as $\hat{H} = a\hat{S}_e\cdot\hat{S}_p$, where e and p denote the electron and positron, respectively.

1. Obtain the energies of the resultant eigenstates (see Problem 11 of Chap. 5).
2. Generalize (6.15) to the product of two arbitrary angular momentum $\hat{J}_1\cdot\hat{J}_2$

Problem 10. Calculate the splitting between the $2p$ states with $m = 1/2$ of a hydrogen atom in the presence of spin–orbit coupling and a magnetic field B in the z-direction:

1. At the limit $v_{\text{so}} = 0$
2. At the limit $B_z = 0$
3. As a function of the ratio $q = 2\mu_B B_z/\hbar^2 v_{\text{so}}$

Problem 11. Calculate the current associated with the spherical wave $A \exp(ikr)/r$ and show that the flux within a solid angle $d\Omega$ is constant.

Problem 12. A beam of particles is being scattered from a constant potential well of radius a and depth V_0. Calculate the differential and the total cross section in the limit of low energies.
Hint: Consider only the $l = 0$ partial waves.

1. Obtain the interior logarithmic derivative (times a) for $r = a$ (see Problem 4).
2. Obtain the exterior logarithmic derivative (times a) for $r = a$ in the low energy limit.
3. Calculate $\tan \delta_0$.
4. Calculate $\sigma(\theta)$.
5. Calculate σ.

Problem 13. Consider a planar motion.

1. What is the analogue of spherical symmetry in a two-dimensional space? Find the corresponding coordinates.
2. Write down the operator for the kinetic energy in these coordinates and find the degeneracy inherent in potentials with cylindrical symmetry.
3. Find the energies and degeneracies of the two-dimensional harmonic oscillator problem.
4. Verify that the function

$$\varphi_n = \frac{1}{x_c \sqrt{\pi n!}} \exp(-u^2/2) u^n \exp(\pm in\phi)$$

   is an eigenstate of the Hamiltonian $(u = \rho/x_c)$.

Problem 14. Consider the outer electron of a Rydberg atom

1. Calculate the quantum frequency ω_{ph} of the photon emitted in the transition $\varphi_{n,n-1,n-1} \rightarrow \varphi_{n-1,n-2,n-2}$ and the classical frequency ω_{cl} of the rotational motion of the electron.
2. Which principle relates these two frequencies?

Chapter 7
Many-Body Problems

So far, we have discussed only one-particle problems. We now turn our attention to cases in which more than one particle is present.

In the first place, we stress the fact that if $\hat{H} = \hat{H}(1) + \hat{H}(2)$, where $\hat{H}(1)$ and $\hat{H}(2)$ refer to different degrees of freedom (in particular, to different particles), and if $\hat{H}(1)\varphi_a(1) = E_a\varphi_a(1)$ and $\hat{H}(2)\varphi_b(2) = E_b\varphi_b(2)$, then

$$\varphi_{ab}(1,2) = \varphi_a(1)\,\varphi_b(2),$$
$$\hat{H}\,\varphi_{ab}(1,2) = (E_a + E_b)\,\varphi_{ab}(1,2). \tag{7.1}$$

In the second place, we note that the distinction between identical particles is prevented in quantum physics by Heisenberg indeterminacy (unless they are wide apart). The quantum treatment of identical particles requires a new principle – the Pauli Principle – which is presented in Sect. 7.1. Particles can be either fermions or bosons.

In this chapter, we deal with many-body problems that are amenable to an independent-particle description. Central potentials in atomic and nuclear physics, electron gas and periodic potentials in solid state physics are fermion problems to be treated with methods developed in Chap. 6 and Sects. 4.4 and 4.6[†]. Problems involving phonons in lattices and condensation of bosons are dealt with by means of generalizations of the harmonic oscillator solution (Sect. 3.3.1). An exception is represented by the fractional Hall effect. Rather than presenting an overview of these many-body fields, we restrict ourselves to illustrate the quantum formalism with relevant applications. However, even this restricted framework allows us to introduce some of the most spectacular discoveries of the recent decades, which are based on quantum mechanics and are (or may become) cornerstones of present and future technologies: transistors, quantum dots, Bose–Einstein condensation and quantum Hall effects.

The concept of creation and annihilation operators is extended to many-body boson and fermion systems in Sect. 7.8[†].

7.1 The Pauli Principle

Let us now consider the case of two identical particles, 1 and 2. Two particles are identical if their interchange, in any physical operator, leaves the operator invariant:

$$[\hat{P}_{12}, \hat{Q}(1,2)] = 0, \tag{7.2}$$

where $\hat{P}_{12}$ is the operator corresponding to the interchange process $1 \leftrightarrow 2$. As a consequence, the eigenstates of $\hat{Q}$ may be simultaneous eigenstates of $\hat{P}_{12}$ (Sect. 2.6.1). The operator $\hat{P}_{12}^2$ must have the single eigenvalue 1, since the system is left invariant by interchanging the particles twice. Thus the two eigenvalues of the operator $\hat{P}_{12}$ are ± 1. The eigenstates are said to be symmetric $(+1)$ or antisymmetric (-1) under the interchange of particles $1 \leftrightarrow 2$.

Consider two orthogonal single-particle states φ_p, φ_q which may be, in particular, eigenstates of a Hamiltonian. We construct the four two-body states by distributing the two particles in the two single-particle states. The symmetric combinations are

$$\Psi_{pp}^{(+)} = \varphi_p(1)\varphi_p(2), \tag{7.3}$$

$$\Psi_{qq}^{(+)} = \varphi_q(1)\varphi_q(2), \tag{7.4}$$

$$\Psi_{pq}^{(+)} = \frac{1}{\sqrt{2}}\Big[\varphi_p(1)\varphi_q(2) + \varphi_q(1)\varphi_p(2)\Big], \tag{7.5}$$

while the antisymmetric state is

$$\Psi_{pq}^{(-)} = \frac{1}{\sqrt{2}}\Big[\varphi_p(1)\varphi_q(2) - \varphi_q(1)\varphi_p(2)\Big]. \tag{7.6}$$

The states (7.5) and (7.6) are called entangled states, meaning that they are not simply written as a component of the tensor product of the state vectors of particle 1 and particle 2 (see Chap. 12).

The average distance between two entangled identical particles is

$$\langle pq|(\boldsymbol{r}_1-\boldsymbol{r}_2)^2|pq\rangle_{(\pm)}^{1/2} = \Big(\langle p|r^2|p\rangle + \langle q|r^2|q\rangle - 2\langle p|\boldsymbol{r}|p\rangle\langle q|\boldsymbol{r}|q\rangle \mp 2\,|\langle p|\boldsymbol{r}|q\rangle|^2\Big)^{1/2}, \tag{7.7}$$

where the subscripts $(\pm)$ denote symmetric and antisymmetric states. The first three terms correspond to the average "classical" distance which is obtained if state functions of the type $\varphi_p(1)\varphi_q(2)$ are used. According to (7.7), this classical distance may be decreased for entangled particles in symmetric states and increased if they are in antisymmetric states. Therefore, the symmetry induces correlations between identical particles, even in the absence of residual interacting forces.

We now generalize the construction of symmetric and antisymmetric states to ν identical particles. Let $\hat{P}_b$ denote the operator that performs one of the $\nu!$ possible

permutations. It can be shown that this operator may be written as a product of two-body permutations $\hat{P}_{ij}$. Although this decomposition is not unique, the parity of the number η_b of such permutations is. We construct the operators

$$\hat{\mathcal{S}} \equiv \frac{1}{\sqrt{\nu!}} \sum_b \hat{P}_b, \qquad \hat{\mathcal{A}} \equiv \frac{1}{\sqrt{\nu!}} \sum_b (-1)^{\eta_b} \hat{P}_b. \tag{7.8}$$

Acting with the operator $\hat{\mathcal{S}}$ on a state of ν identical particles produces a symmetric state, while acting with $\hat{\mathcal{A}}$ produces an antisymmetric state.

A new quantum principle has to be added to those listed in Chap. 2:

Principle 4. *There are only two kinds of particles in nature[1]: bosons described by symmetric state vectors and fermions described by antisymmetric state vectors.*

As long as the Hamiltonian is totally symmetric in the particle variables, its eigenstates may be labeled with their properties under the interchange of two particles (symmetry or antisymmetry). According to Principle 4, many otherwise possible states are eliminated. For instance, the only two-body fermion state that can be found in nature is (7.6).

All known particles with half-integer values of spin are fermions (electrons, muons, protons, neutrons, neutrinos, etc.). All known particles with integer spin are bosons[2] (photons, mesons, etc.).

Moreover, every composite object has a total angular momentum, which can be viewed as the composite particle spin, and which is obtained according to the addition rules of Sect. 5.3.1. If this spin has a half-integer value, the object behaves like a fermion, whereas a composite system with an integer value of the spin acts as a boson. For instance, He^3 is a fermion (two protons and one neutron), while He^4 is a boson (an α-particle, with two protons and two neutrons), in spite of the fact that both isotopes have the same chemical properties.

Let us distribute ν identical bosons into a set of single-particle states φ_p and denote by n_p the number of times that the single-particle state p is repeated. The n_p are called occupation numbers. To construct the symmetrized ν-body state vector, we start from the product

$$\Psi_{pq\cdots r}(1, 2, \ldots, \nu)$$
$$= \varphi_p(1)\varphi_p(2)\cdots\varphi_p(n_p)\varphi_q(n_p + 1)\varphi_q(n_p + 2)\cdots\varphi_q(n_p + n_q)\cdots\varphi_r(\nu)$$
$$= \varphi_p^{(n_p)}\varphi_q^{(n_q)}\cdots\varphi_r^{(n_r)}, \tag{7.9}$$

---

[1]For the last 20 years it has been understood that, although this postulate holds true in our three-dimensional world, there is a whole range of intermediate possibilities – anyons – between bosons and fermions, in two dimensions. In some cases there are surface layers a few atoms thick in which the concept of anyons is realized, as in the fractional quantum Hall effect (Sect. 7.6.2†).

[2]Pauli produced a demonstration of this relation between spin and statistics which involved many complications of quantum field theory. Feynman's challenge that an elementary proof of the spin-statistics theorem be provided has not yet been answered.

with $\sum_i n_i = \nu$. Subsequently, the state vector is symmetrized by applying the operator $\hat{\mathcal{S}}$. The final state is

$$\Psi_{n_p, n_q, \ldots, n_r}(1, 2, \ldots, \nu) = \mathcal{N}\hat{\mathcal{S}}\Psi_{pq\cdots r}(1, 2, \ldots, \nu), \tag{7.10}$$

where $\mathcal{N}$ is a normalization constant. The occupation numbers label the states. There are no restrictions on the number of bosons in a given single-boson state. For instance, in the two-particle case, the possible symmetric state vectors are (7.3), (7.4) and (7.5).

We may also characterize the state by using the occupation numbers in the case of fermions. The procedure for constructing the antisymmetric state is the same, but for the application of the operator $\hat{\mathcal{A}}$ instead of $\hat{\mathcal{S}}$. However, the results are different, in the sense that occupation numbers must be 0 or 1. Otherwise the state vector would not change its sign under the exchange of two particles occupying the same state. The antisymmetrization principle requires that fermions should obey Pauli's exclusion principle [42]: "If there is an electron in the atom for which these [four] quantum numbers have definite values, then the state is occupied, full, and no more electrons are allowed in."

The antisymmetric state function for ν fermions may be written as a Slater determinant:

$$\Psi_{pq\cdots r}(1, 2, \ldots, \nu) = \frac{1}{\sqrt{\nu!}} \begin{vmatrix} \varphi_p(1) & \varphi_p(2) & \cdots & \varphi_p(\nu) \\ \varphi_q(1) & \varphi_q(2) & \cdots & \varphi_q(\nu) \\ \vdots & \vdots & \ddots & \vdots \\ \varphi_r(1) & \varphi_r(2) & \cdots & \varphi_r(\nu) \end{vmatrix}. \tag{7.11}$$

The permutation of two particles is performed by interchanging two columns, which produces a change of sign. All the single-particle states must be different. Otherwise, the two rows are equal and the determinant vanishes.

A widely used representation of the states (7.9) and (7.11), in terms of creation and annihilation operators, is given in Sect. 7.8[†].

The possibility of placing many bosons in a single (symmetric) state gives rise to phase transitions, with important theoretical and conceptual implications that are illustrated for the case of the Bose–Einstein condensation (Sect. 7.5[†]). Even more spectacular consequences appear in the fermion case.[3] Some of them will be treated later in this chapter.

---

[3]To reconcile the successes of the (fermion) quark model with the requirement that the total wave function be antisymmetric, it is necessary to hypothesize that each quark comes into three different species, which are labeled by the colors red, green and blue. Baryon wave functions may thus be antisymmetrized in color subspace.

7.2   Two-Electron Problems

Let us consider the case of the He atom. For the moment, we disregard the interaction between the two electrons. The lowest available single-particle states for the two electrons are the $\varphi_{100\frac{1}{2}m_s}$, $\varphi_{200\frac{1}{2}m_s}$ and $\varphi_{21m_l\frac{1}{2}m_s}$ states, where we use the same representation as in (6.10).

This problem involves four angular momenta: the two orbital and the two spin angular momenta. The two orbital angular momenta and the two spins may be coupled first[4] ($\hat{\boldsymbol{L}} = \hat{\boldsymbol{L}}_1 + \hat{\boldsymbol{L}}_2$ and $\hat{\boldsymbol{S}} = \hat{\boldsymbol{S}}_1 + \hat{\boldsymbol{S}}_2$). Subsequently, the addition of the total orbital and total spin angular momenta yields the total angular momentum $\hat{\boldsymbol{J}} = \hat{\boldsymbol{L}} + \hat{\boldsymbol{S}}$.

The spin part of the state vector may carry spin 1 or 0. We obtain the corresponding states $\chi^s_{m_s}$ by using the coupling given in (5.67), with $j_1 = j_2 = 1/2$. The (three) two-spin states with spin 1 are symmetric, while the state with spin 0 is antisymmetric. Thus,

$$\chi^1_1(1,2) = \varphi_\uparrow(1)\varphi_\uparrow(2), \qquad \chi^1_0(1,2) = \frac{1}{\sqrt{2}}\Big[\varphi_\uparrow(1)\varphi_\downarrow(2) + \varphi_\uparrow(2)\varphi_\downarrow(1)\Big],$$

$$\chi^1_{-1}(1,2) = \varphi_\downarrow(1)\varphi_\downarrow(2), \qquad \chi^0_0(1,2) = \frac{1}{\sqrt{2}}\Big[\varphi_\uparrow(1)\varphi_\downarrow(2) - \varphi_\uparrow(2)\varphi_\downarrow(1)\Big].$$

$$(7.12)$$

We now consider different occupation numbers for the two electrons:

1. The two electrons occupy the lowest orbit $\varphi_{100\frac{1}{2}m_s}$. In this case, the spatial part is the same for both electrons and, thus, the state vector is necessarily spatially symmetric. Therefore the symmetric spin state with spin 1 is excluded by the exclusion principle. Only the (entangled) state with zero spin can exist.
2. One electron occupies the lowest level $\varphi_{100\frac{1}{2}m_s}$ and the other, the next level $\varphi_{200\frac{1}{2}m_s}$. In this case, the difference in the radial wave functions allows us to construct both a symmetric and an antisymmetric state for the spatial part of the wave function [(7.5) and (7.6), respectively]. Both spatial states carry $l = 0$. Two total states are now allowed by the Pauli principle: the combination of the symmetric spatial part with the antisymmetric spin state and vice versa. The (so far neglected) interaction between the electrons breaks the degeneracy between these two allowed total states: according to (7.7), two electrons in a spatially antisymmetric state are further apart than in a symmetric state. They thus feel less

---

[4]There is an alternative coupling scheme in which the orbital and spin angular momenta are first coupled to yield the angular momentum of each particle: $\hat{\boldsymbol{J}}_i = \hat{\boldsymbol{L}}_i + \hat{\boldsymbol{S}}_i$ ($i = 1, 2$), as in (6.11). Subsequently, the two angular momenta are coupled together: $\hat{\boldsymbol{J}} = \hat{\boldsymbol{J}}_1 + \hat{\boldsymbol{J}}_2$. The two coupling schemes give rise to two different sets of basis states.

Coulomb repulsion. Their energy decreases relative to the energy of the spatially symmetric state.
3. One electron occupies the lowest level $\varphi_{100\frac{1}{2}m_s}$ and the other, the level $\varphi_{21m_l\frac{1}{2}m_s}$. It is left for the reader to treat this case as an exercise. He or she may follow the same procedure as in the previous example, bearing in mind that the orbital angular momentum no longer vanishes.

7.3   Periodic Tables

7.3.1   The Atomic Case

The attraction exerted by the nuclear center, proportional to Ze^2, allows us to implement a central-field description for atomic systems displaying more than one electron. However, the Hamiltonian also includes the Coulomb repulsion between electrons. This interaction is weaker (since it is only proportional to e^2), but an electron experiences $Z-1$ such repulsions. We can nonetheless take them into account to a good approximation by modifying the central field because:

- Electrons from occupied levels cannot be scattered to other occupied levels (Pauli principle) and when scattered to empty levels have to overcome the gap between the energy of the occupied level and the energy of the last filled state, thus reducing the effectiveness of the residual interaction.
- The electric fields created by electrons lying outside a radius r' tend to cancel for radius $r < r'$, due to the well-known compensation between the field intensity ($\propto 1/r^2$) and the solid angle ($\propto r^2$).

Although the optimum choice of the single-particle central potential constitutes a more difficult problem (see Sect. 8.6.1[†] on the Hartree–Fock approximation), it is simple to obtain the behavior at the limits

$$\lim_{r\to 0} V(r) = -\frac{Ze^2}{4\pi\epsilon_0 r}, \qquad \lim_{r\to\infty} V(r) = -\frac{e^2}{4\pi\epsilon_0 r}. \tag{7.13}$$
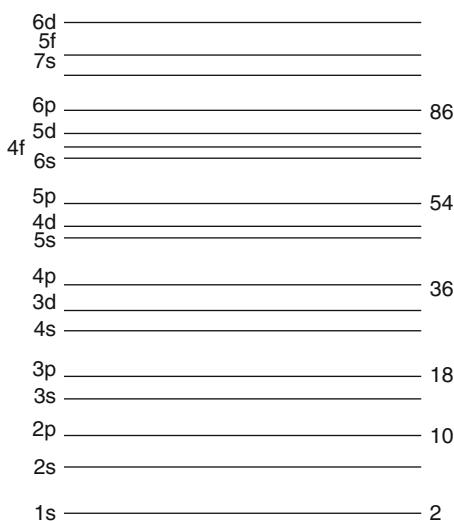
Close to the nucleus, the electron feels all the nuclear electric field. Far away, this field is screened by the remaining $Z-1$ electrons. The potential at intermediate points may be obtained qualitatively by interpolation.

The energy eigenvalues of this effective potential are also qualitatively reproduced by adding the term

$$\hat{H}_l = c\hat{L}^2 \tag{7.14}$$

to the Coulomb potential, since the centrifugal term $\hbar^2 l(l+1)/2Mr^2$ prevents the electrons occupying levels with large values of l from approaching the center and, thus, feeling the greater attraction of the potential at small radii.

Fig. 7.1 Electron shell
structure. The figure gives a
rough representation of the
order of single-electron
levels. Numbers to the *right*
indicate the number of
electrons in closed shell
atoms

The energies E_{nl} are also labeled by the orbital quantum number, since the
potential is no longer simply proportional to $1/r$ (Sect. 6.1.1). They are qualitatively
presented in Fig. 7.1, where the nomenclature of Table 5.2 is used. The set of energy
levels which are close to each other is called a shell. In a closed shell, all magnetic
substates are occupied.

The ground state of a given atom is determined by successively filling the
different single-particle states until the Z electrons are exhausted. A closed shell
carries zero orbital and zero spin angular momenta (see Problem 7). A closed shell
displays neither loose electrons nor holes, and thus constitutes a quite stable system.
This fact explains the properties of noble gases in the Mendeleev chart, for which
$Z = 2, 10, 18, 36, 54$ and 86 (Fig. 7.1). The angular momenta (including the
magnetic momenta), the degree of stability, the nature of chemical bonds and, in
fact, all the chemical properties are determined by the outer electrons lying in the
last, unfilled shell, a spectacular consequence of the Pauli principle.

The electron configuration of an atom with many electrons is specified by the
occupation of the single-particle states of the unfilled shell. For instance, the lowest
configuration in the Mg atom, with $Z = 12$, is[5] $(3s)^2$. Configurations $(3s)(3p)$ and
$(3p)^2$ lie close in energy.

In the atomic case the total single-particle angular momentum j is not usually
specified (as it was not in Sect. 7.2), because the strength of the spin–orbit coupling
is small relative to the electron repulsions. However, for heavier elements and inner
shells, the quantum numbers (l, j) become relevant once again.

---

[5]The first number is the Coulomb principal quantum number; the orbital angular momentum
follows the notation of Table 5.2; the exponent (2) denotes the number of particles with the previous
two quantum numbers.

7.3.2   The Nuclear Case

Let us now consider the nuclear table. A nucleus has A nucleons, of which N are neutrons and Z are protons. Nuclei with the same A are called isobars; with the same N, isotones and with the same Z, isotopes. In spite of the fact that there is no *ab initio* attraction from a nuclear center and the internuclear force is as complicated as it can be, the Pauli principle is still effective: the starting point for the description of most nuclear properties is a shell model. For systems with short-range interactions, a realistic central potential follows the probability density, which in the nuclear case has a Woods–Saxon shape, $w(r)$ (Fig. 7.3). A strong spin–orbit interaction must be included on the surface, with an opposite sign to the atomic case. A central Coulomb potential also appears for protons

$$\hat{V} = -v_0 w(r) - v_{\text{so}} \frac{r_0^2}{r} \frac{\mathrm{d}w(r)}{\mathrm{d}r} \hat{\boldsymbol{L}} \cdot \hat{\boldsymbol{S}} + V_{\text{coul}}$$

$$w(r) \equiv \left(1 + \exp \frac{r - R}{a} \right)^{-1}. \tag{7.15}$$

The empirical values of the parameters appearing in (7.15) are [38]

$$v_0 = \left(-51 + 33 \frac{N - Z}{A} \right) \text{ MeV} \quad \text{and} \quad v_{\text{so}} = 0.44 v_0.$$
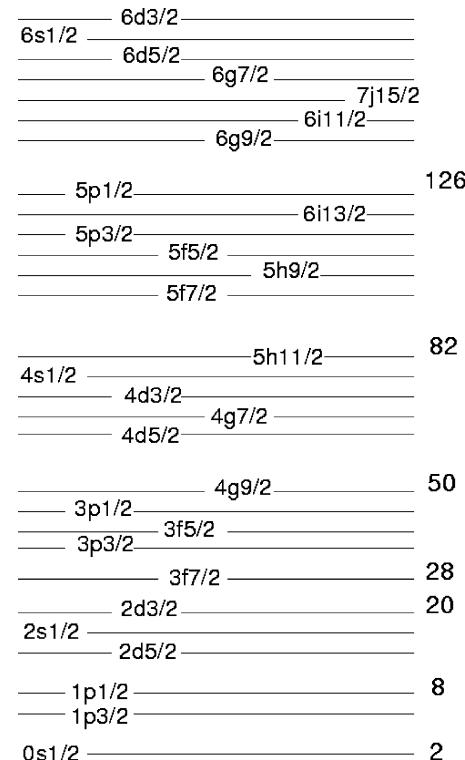
Here $a = 0.67$ F represents the skin thickness and $R = r_0 A^{1/3}$ is the nuclear radius, with $r_0 = 1.20$ F. The resulting shell structure is shown in Fig. 7.2.

Nucleons moving in a Woods–Saxon potential see a potential similar to the harmonic oscillator potential (Fig. 7.3). An attractive term of the form (7.14) should also be included, since the nuclear single-particle states in which nucleons lie close to the surface are more energetically favored by the Woods–Saxon potential than by the harmonic oscillator potential (Fig. 7.3). Therefore, the simpler effective potential
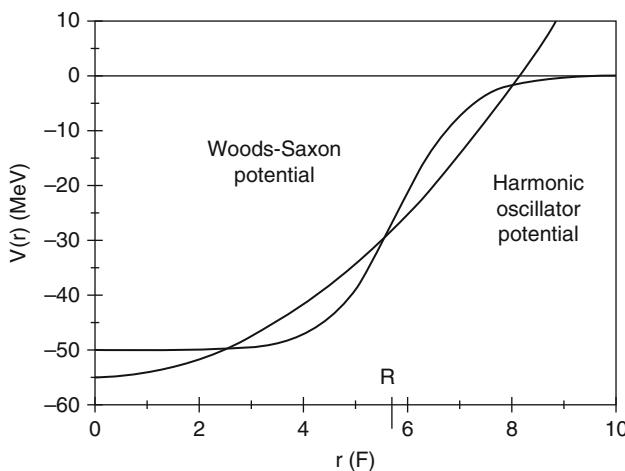
$$\hat{V} = \frac{M_{\text{p}} \omega^2}{2} r^2 - c \hat{\boldsymbol{L}} \cdot \hat{\boldsymbol{S}} - d \left(\hat{L}^2 - \langle L^2 \rangle_N \right) \tag{7.16}$$

may be used instead of (7.15), at least for bound nucleons, where $\hbar \omega = 41$ MeV $A^{-1/3}$, $c = 0.13 \omega / \hbar$, and $d = 0.038 \omega / \hbar$ for protons and $d = 0.024 \omega / \hbar$ for neutrons ([38], Chap. 2). The symbol $\langle L^2 \rangle_N$ denotes the average value of L^2 in an N-oscillator shell (Problem 3 of Chap. 6). The eigenstates are labeled with the quantum numbers $Nljm\tau$, where the new quantum number τ equals $1/2$ for neutrons and $-1/2$ for protons.

The lowest shell $N = 0$ is filled up with four nucleons, two protons and two neutrons, giving rise to the very stable α-particle. As in the electron case, closed shells do not contribute to the properties of low-lying excited states. Note that both nucleons should fill closed shells to obtain the analogy of noble gases. This occurs

Fig. 7.2 Nuclear shell structure. This figure is an approximation of the order of single-nucleon levels. They are labeled with the quantum numbers Nlj. The number of nucleons for closed shell systems is indicated on the *right*


Fig. 7.3 Comparison of the Woods–Saxon and harmonic oscillator potentials [38]

Table 7.1 Levels of Sn^{133} populated by transferring a neutron from the deuteron target to the closed shell Sn^{132}. Energies in keV

Level	Energy	S
5f7/2	g.s.	0.86 ± 0.16
5p3/2	854	0.92 ± 0.18
5p1/2	1,363	1.1 ± 0.3
5f5/2	2,005	1.1 ± 0.2

in the nuclear systems $Z = N = 2$; $Z = N = 8$; $Z = N = 20$; $Z = 20, N = 28$; $Z = N = 28$; $Z = N = 50$; $Z = 50, N = 82$ and $Z = 82, N = 126$.

It should be stressed that, unlike the hydrogen case, the description of heavier atoms/nuclei in terms of a central field is, at best, a semi-quantitative approximation: one-body terms can never completely replace two-body interactions. The approximation is more reliable for systems that have one more particle (or hole) than a closed shell. In fact, the single-particle spectrum can be determined by transferring one nucleon to the double closed shells, as in (d,p) reactions. For instance, the spectroscopic factor (the ratio between experimental and predicted cross sections) should be $S = 1$ if the single-particle states are pure, without admixtures of core excitations.

Recently, single-particle levels above the double closed shell nucleus $Z = 50$, $N = 82$ (mean lifetime of 40 s) have been measured [43]. Since it is not possible to make a target with such a short-lived nucleus, a beam of Sn^{132} has been runned upon a deuterium target. The Sn^{133} levels are disentangled through properties of the scattered protons (intensities, energies, angular distributions). The results are given in Table 7.1 and agree, within expectations, with predictions from Fig. 7.2.

7.4 Motion of Electrons in Solids

7.4.1 Electron Gas

In the simplest possible model of a metal, electrons move independently of each other. The electrostatic attraction of the crystalline lattice prevents them from escaping when they approach the surface. The electron gas results of Sect. 4.4.1 may be easily generalized to the three-dimensional case. The wave states are given as the product of three one-dimensional solutions (4.43)

$$\varphi_{n_x n_y n_z} = \frac{1}{\sqrt{V}} \exp\left[i(k_{n_x} x + k_{n_y} y + k_{n_z} z)\right]. \tag{7.17}$$

The volume is $V = a^3$. The allowed $\boldsymbol{k}$ values constitute a cubic lattice in which two consecutive points are separated by the distance $2\pi/a$ (4.42)

$$k_{n_i} = \frac{2\pi}{a} n_i, \qquad n_i = 0, \pm 1, \pm 2, \ldots, \quad i = x, y, z. \tag{7.18}$$

The energy of each level is

$$\epsilon_k = \frac{\hbar^2 |\mathbf{k}|^2}{2M}. \tag{7.19}$$

To build the ν-electron ground state, we start by putting two electrons on the level $k_x = k_y = k_z = 0$. We successively fill the unoccupied levels as their energy increases. When there is a large number of electrons, the occupied region will be indistinguishable from a sphere in k-space. The radius of this sphere is called k_F, the Fermi momentum, and its energy $\epsilon_F \equiv \hbar^2 k_F^2 / 2M$, the Fermi energy. At zero energy, the levels with $|\mathbf{k}| \leq k_F$ are occupied pairwise and those above are empty. Since we are interested in the large-volume limit, the levels are very close together and we may replace summations with integrals that have a volume element similar to (4.45). Thus,

$$\sum_k f_k \approx \frac{V}{8\pi^3} \int f_k \, \mathrm{d}^3 k. \tag{7.20}$$

An electron gas is characterized by the Fermi temperature $T_F \equiv \epsilon_F / k_B$, where k_B is the Boltzmann constant (Table A.1). If the temperature $T \ll T_F$, the electron gas has properties that are very similar to the $T = 0$ gas. The number of levels per unit volume with energy less than ϵ and the density of states per unit interval of energy per unit volume are

$$n(\epsilon) = \frac{2}{V} \sum_{n_x n_y n_z} \approx \frac{1}{4\pi^3} \int_{k \leq k_\epsilon} \mathrm{d}^3 k = \frac{k_\epsilon^3}{3\pi^2} = \frac{1}{3\pi^2} \left(\frac{2M\epsilon}{\hbar^2} \right)^{3/2},$$

$$\rho(\epsilon) = \frac{\partial n}{\partial \epsilon} = \frac{1}{\pi^2 \hbar^3} \left(2M^3 \epsilon \right)^{1/2}, \tag{7.21}$$

respectively. At the Fermi energy, the values of these quantities are

$$n_F = \frac{1}{3\pi^2} k_F^3, \qquad \rho_F = \frac{3n_F}{2\epsilon_F}. \tag{7.22}$$

For the Na typical case: $n_F \approx 2.65 \times 10^{22}$ electrons/cm³, $k_F \approx 0.92 \times 10^8$ cm⁻¹, $\epsilon_F \approx 3.23$ eV and $T_F \approx 3.75 \times 10^4$ K.

We now explore some thermal properties of an electron gas. If the electrons would obey classical mechanics, each of them should gain an energy of the order of $k_B T$ in going from absolute zero to the temperature T. The total thermal energy per unit volume of electron gas would be of the order of

$$u_{\text{cl}} = n_{\text{F}} k_{\text{B}} T, \tag{7.23}$$

and the specific heat at a constant temperature would thus be independent of the temperature:

$$(C_V)_{\text{cl}} = \frac{\partial u_{\text{cl}}}{\partial T} = n_{\text{F}} k_{\text{B}}. \tag{7.24}$$

However, the Pauli principle prevents most of the electrons from gaining energy. Only those with an initial energy ϵ_k such that $\epsilon_{\text{F}} - \epsilon_k < k_{\text{B}} T$ can be expected to gain energy. The number of such electrons is given roughly by

$$\rho_{\text{F}} k_{\text{B}} T = \frac{3 n_{\text{F}}}{2} \frac{T}{T_{\text{F}}}. \tag{7.25}$$

The total thermal energy and specific heat per unit volume are

$$u = \rho_{\text{F}} (k_{\text{B}} T)^2, \tag{7.26}$$

$$C_V = 3 n_{\text{F}} k_{\text{B}} \frac{T}{T_{\text{F}}}. \tag{7.27}$$

The specific heat is proportional to the temperature and is reduced by a factor $\approx 1/100$ at room temperature.

The probability of an electron being in a state of energy ϵ is given by the Fermi–Dirac distribution $\eta(\epsilon)$ (7.55). Using this distribution, the expression for the total energy per unit volume is

$$u = \frac{1}{2\pi^2} \int_0^\infty \epsilon \, \rho(\epsilon) \, \eta(\epsilon) \, k^2 \, \mathrm{d}k, \tag{7.28}$$

which is a better approximation than (7.26). Upon integration, one obtains results similar to (7.27).

7.4.2[†] *Band Structure of Crystals*

Although the electron gas model explains many properties of solids, it fails to account for electrical conductivity, which can vary by a factor of 10^{30} between good insulators and good conductors.

A qualitative understanding of conductors and insulators may be obtained from a simple generalization of the band model described in Sect. 4.6[†]. As a consequence of the motion of single electrons in a periodic array of ions, the possible individual energies are grouped into allowed bands. Each band contains $2N$ levels, where N is the number of ions, and the factor 2 is due to spin.

According to the Pauli principle, we obtain the ground state by successively filling the individual single-particle states of the allowed bands. The last filled band is called the valence band. If we place the solid within an electric field, the electrons belonging to a valence band cannot be accelerated by a small electric field, since they would tend to occupy other states of the same band, which are already occupied. Much like the case of closed shells in atoms and nuclei, electrons in a valence band constitute an inert system which do not contribute to thermal or electrical properties. A solid consisting only of filled bands is an insulator. The insulation gets better as the distance ΔE between the upper valence band and the next (empty) band increases.

By contrast, electrons in partially filled bands can easily absorb energy from an applied electric field. Such a band is called a conduction band.

The previous considerations are valid for $T = 0$. In solids which are insulators at $T = 0$, the thermal motion increases the energy of the electrons by an amount $k_{\mathrm{B}}T$. As the temperature increases, some electrons belonging to the valence band may jump to the conduction band. This system is a semiconductor. The conductivity varies as $\exp(-\Delta E/k_{\mathrm{B}}T)$.
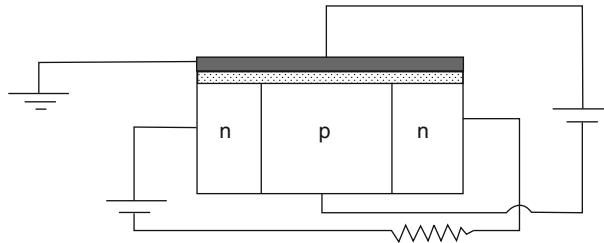
The existence of conductors, semiconductors and insulators is a consequence of the Pauli principle. Another consequence arises from the fact that the electrons which jump to the conduction band leave empty states called holes in the valence band. Other electrons of the same valence band may occupy these holes, leaving other holes behind them. Thus there is a current, due to the electrons of the valence band, which is produced by the holes. The holes carry a positive charge, because they represent the absence of an electron.

7.4.3[†] *Transistors*

Semiconductors have become key parts of electronic circuits and optical applications in modern electronic industry, due to the fact that their electrical conductivity can be greatly altered by means of external stimuli (voltage, photon flux, etc.) and by the introduction of selected impurities (doping).

There are different kinds of transistors, each one having different applications. Here we outline one of them, the metal-oxide semiconductor field effect transistor (MOSFET).

We denote by n a semiconductor with electrons at the conduction band and by p, one with holes at the valence band (Sect. 7.4.2[†]). As most transistors, the MOSFET consists of a sandwich made up by three semiconductors, the middle one being of different type than the other two (Fig. 7.4). On top there is an insulator followed by a metallic layer. If the control voltage applied between the metal and the bottom of the transistor vanishes, there is no electron output current flowing from left to right. However, if the bottom is at a negative potential, the positive free charges (holes) get attracted to it, and the output current flows on top, below the insulator layer. The output power can be much greater than at the control circuit.

Fig. 7.4 Diagram of a MOSFET transistor

Weak voltage signals, arising from an antenna, can replace the control voltage and get amplified by a transistor. This is the role of transistors at your TV set. The MOSFET can also be used as a classical bit of your PC, the control voltage allowing (or not) the current to flow. They also play the role of switches.

Because of their flexibility, reliability and low cost, transistors are the building blocks of modern electronic circuits. They are used either as isolated units or as parts of integrated circuits (chips). Transistors were invented by John Bardeen, Walter Brattain and William Shockley at the Bell Labs in 1947.

7.4.4[†]   *Phonons in Lattice Structures*

Up to now we have treated the ions as fixed in space at positions $\mathbf{R}_i$, giving rise to the crystal lattice structure. This is a consequence of the much larger ion mass M_I relative to the electron mass M. Subsequently we allow for a small fluctuation $\mathbf{u_i}$ in the coordinate $\mathbf{r}_i = \mathbf{R}_i + \mathbf{u}_i$ of the i ion (Born–Oppenheimer approximation). For the sake of simplicity, we make the following approximations:

- A linear, spinless chain of N ions separated by the distance d.
- Only terms up to quadratic order in u_i are kept in the ion–ion potential. Linear terms in the fluctuations vanish due to the equilibrium condition and the constant, equilibrium term will be dropped.
- Only interactions between nearest neighbors are considered.

Therefore, the Hamiltonian reads

$$
\hat{H} = \frac{1}{2M_I} \sum_i \hat{p}_i^2 \; + \; \frac{M_I \omega^2}{8} \sum_{i,j} \left(u_i - u_j \right)^2 \delta_{i(j\pm 1)}
$$

$$
= \frac{1}{2M_I} \sum_i \hat{p}_i^2 \; + \; \frac{M_I \omega^2}{2} \sum_i \hat{u}_i^2 \; - \; \frac{M_I \omega^2}{2} \sum_i u_i u_{i+1}
$$

$$
= \hbar\omega \sum_i \left(a_i^+ a_i + \frac{1}{2} \right) - \frac{\hbar\omega}{4} \sum_i \left(a_i^+ + a_i \right) \left(a_{i+1}^+ + a_{i+1} \right), \quad (7.29)
$$

where the creation and annihilation operators[6] a_i^+, a_i are defined as in (3.29) for each site i. The strength parameter ω in the ion–ion potential may be interpreted as the frequency of each oscillator in the absence of coupling with other oscillators.

As in classical physics, the coupled oscillators may become uncoupled by means of a linear transformation

$$\hat{H} = \hbar \omega_k \left(\gamma_k^+ \gamma_k + \frac{1}{2} \right)$$

$$\gamma_k^+ = \sum_i (\lambda_{ki} a_i^+ - \mu_{ki} a_i), \qquad \sum_i (\lambda_{ki} \lambda_{li}^* - \mu_{ki} \mu_{li}^*) = \delta_{kl}. \qquad (7.30)$$

The uncoupling procedure is described at the end of the section. The resultant amplitudes λ_{ki}, μ_{ki} and the new frequencies ω_k are

$$\lambda_{ki} = \frac{1}{2} \left(\sqrt{\frac{\omega}{\omega_k N}} + \sqrt{\frac{\omega_k}{\omega N}} \right) \exp(i k r_i),$$

$$\mu_{ki} = \frac{1}{2} \left(\sqrt{\frac{\omega}{\omega_k N}} - \sqrt{\frac{\omega_k}{\omega N}} \right) \exp(i k r_i),$$

$$\omega_k = \frac{1}{\sqrt{2}} \omega k d, \qquad (7.31)$$

where the frequencies ω_k are proportional to the wave number k. If a cyclic chain is assumed ($r_{N+1} = r_1$, see Sect. 4.4.1)

$$k = k_n = \frac{2\pi n_k}{N d}, \qquad n_k = 0. \pm 1, \pm 2, \ldots. \qquad (7.32)$$

Thus, there are not only electrons and ions in a crystal but also extended periodic boson structures called phonons are present as well. According to (7.1), the phonon eigenstates and energies are given by[7]

$$\Psi = \prod_k \varphi_{n_k} = \prod_k \frac{1}{\sqrt{n_k!}} (\gamma_{n_k}^+)^{n_k} |0\rangle, \qquad (7.33)$$

$$E(n_k) = \sum_k \hbar w_k \left(n_k + \frac{1}{2} \right). \qquad (7.34)$$

These lattice vibrations have consequences on the thermodynamic properties of crystals, and in particular on the specific heat: because of the linear dependence of

---

[6] See also Sect. 7.8[†].

[7] See also Sect. 7.8[†].

frequency[8] on momentum, we can ignore the occupancy of other, finite frequency modes, if the thermal frequency $k_B T/\hbar$ is sufficiently small. To obtain the total phonon energy per unit volume V, we replace the phonon occupancies n_k in (7.34) by the thermal occupancy η_k given by the Bose–Einstein distribution (7.53)

$$
\begin{aligned}
u_{\text{phonon}} &= \frac{\hbar\alpha}{V} \sum_k k \left[\frac{1}{\exp\left(\frac{\hbar\alpha k}{k_B T}\right) - 1} + \frac{1}{2} \right] \\
&\rightarrow \frac{\hbar\alpha}{2\pi^2} \int_0^\infty \frac{k^3 dk}{\exp\left(\frac{\hbar\alpha k}{k_B T}\right) - 1} + \frac{\hbar\alpha}{2V} \sum_k k \\
&= \frac{\pi^2 (k_B T)^4}{30(\hbar\alpha)^3} + \frac{\hbar\alpha}{2V} \sum_k k.
\end{aligned}
\tag{7.35}
$$

Therefore, the phonon contribution to the specific heat at small T (well below room temperature) is proportional to T^3.

The Uncoupling of the Hamiltonian

The amplitudes λ_{ki}, μ_{ki} and the frequencies ω_k are determined by solving the harmonic oscillator equation

$$
[\hat{H}, \gamma_k^+] = \hbar\omega_k \, \gamma_k^+.
\tag{7.36}
$$

Using the last line of (7.29) with this equation, one obtains

$$
\begin{aligned}
&(\hbar\omega - \hbar\omega_k) \sum_i \lambda_{ki} a_i^+ + (\hbar\omega + \hbar\omega_k) \sum_i \mu_{ki} a_i \\
&= \frac{\hbar\omega}{4} \sum_i (\lambda_{ki} + \mu_{ki}) \left(a_{i-1}^+ + a_{i-1} + a_{i+1}^+ + a_{i+1} \right) \\
&= \frac{\hbar\omega}{4} \sum_i \left(\lambda_{k(i+1)} + \mu_{k(i+1)} + \lambda_{k(i-1)} + \mu_{k(i-1)} \right) \left(a_i^+ + a_i \right).
\end{aligned}
\tag{7.37}
$$

Since a_i^+, a_i represent independent degrees of freedom, their coefficients in the first line of (7.37) should equal those in the third line. This requirement yields N sets of two homogeneous linear equations

---

[8]This linearity also holds in three dimensions (sound waves).

$$\lambda_{ki} - \mu_{ki} = \frac{w_k}{\omega} \left(\lambda_{ki} + \mu_{ki} \right),$$

$$\lambda_{ki} + \mu_{ki} = -\frac{\omega^2}{2\omega_k^2}(\lambda_{k(i+1)} + \mu_{k(i+1)} + \lambda_{k(i-1)} + \mu_{k(i-1)} - 2\lambda_{ki} - 2\mu_{ki})$$

$$\approx -\frac{\omega^2 d^2}{2\omega_k^2} \frac{\mathrm{d}^2 \left(\lambda_{ki} + \mu_{ki} \right)}{(\mathrm{d} r_i)^2}. \tag{7.38}$$

The last equation implies the frequencies given in the last line of (7.31) and

$$\lambda_{ki} + \mu_{ki} = \mathcal{N} \exp(\mathrm{i} k r_i), \tag{7.39}$$

where $\mathcal{N}$ is a normalization constant. The normalization condition in (7.30) and the first of equations (7.38) yield the amplitudes (7.31).
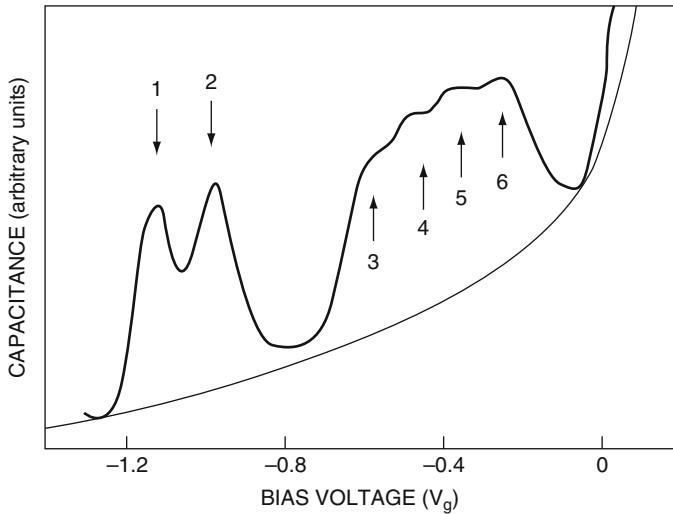
This method of uncoupling constitutes a particular application of the random-phase approximation, a standard procedure in many-body physics (Sect. 8.6.2[†]).

7.4.5[†] *Quantum Dots*

Quantum dots, also called artificial atoms, are small regions (from 1 to about 100 nm; 1 nm = 10^{-9} m) of one semiconductor material buried in another semiconductor material with a larger energy gap ΔE (Sect. 7.4.2[†]). They are made up by roughly 10^6 atoms. In addition, quantum dots contain a controlled number of electrons that display atomic-like spectra with very sharp discrete lines (like natural atoms do). However, unlike natural atoms, their energies can be strongly influenced by the size of the dot and other interactions with the surroundings.
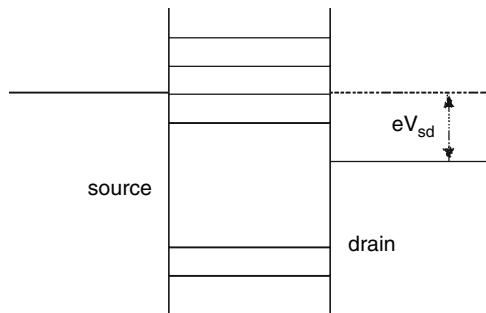
Electrons in a layer of GaAs are sandwiched between two layers of insulating AlGaAs, acting as tunnel barriers. One of these barriers is connected to the source lead, the other to the drain lead. The entire structure may also be linked to an insulated metal electrode which fixes the bias potential V_g.

The forces acting on the electrons inside the dot are difficult to estimate. However, it is possible to apply the concept of a central confining potential as in Sect. 7.3. When an electron enters or leaves the quantum dot there is a noticeable change in the capacitance of the dot, which can be measured. In Fig. 7.5 the capacitance is plotted against the voltage V_g. Each maxima denotes the loading of an additional electron to the dot. The first two electrons fill the lowest, spin degenerate states. The next shell displays four equally spaced maxima, which is consistent with a harmonic oscillator potential in two dimensions [Problem 13 of Chap. 6 and (7.45)]. Indeed, many properties of quantum dots can be accounted for by means of a parabolic confinement in the xy plane and assuming an oblate shape for the dot.

Fig. 7.5 Capacitance spectroscopy reveals quantum-dot electron occupancy and ground-state energies. (Reproduced with permission from [45])

Fig. 7.6 Discrete energy levels of a quantum dot are detected by varying V_{sd}. Every time a new discrete state is accessible there is a peak in d I/d V_{sd} [44]

Being finite-size systems, quantum dots can display shell effects similar to those discussed in Sect. 7.3. One can obtain the energy spectrum by measuring the tunneling current. The Fermi level in the source rises proportionally to a voltage V_{sd} relatively to the drain and to the energy levels of the dot. Additional current flows each time that the Fermi energy of the source rises above a level of the dot. Thus energy levels are measured by the voltages at which there are peaks in the curve representing d I/d V_{sd} against V_{sd}, where I is the tunneling current (Fig. 7.6).

Energy levels vary also in the presence of a magnetic field perpendicular to the GaAs layer. Very strong fields may produce Landau levels (Sect. 7.6.1[†]).

Quantum dots also display spin filtering capabilities for generating or detecting spin-polarized currents [45]. In one of such devices the spin state is mapped into a charge state as follows: the splitting between the energy levels is made so large that only the ground state can be occupied. Moreover, Coulomb repulsion ensures that

at most one electron is allowed. A magnetic field lifts the degeneracy between the spin-up and spin-down states by an amount larger than the thermal energy. Initially the Fermi level ϵ_F of an adjacent reservoir lies below the spin-up state and the dot is empty. The voltage is then adjusted so ϵ_F lies in between the two spin states. Thus an electron with spin up remains in the dot, while an electron with spin down leaves the dot. Subsequently, the charged state is measured. Once emptied, the dot can receive another electron with spin up from the reservoir.

This device constitutes a modern version of the Stern–Gerlach apparatus. It joins several advances in the electrical control of spins, including electrically controlled coupling between spins in quantum dots, quasi-one-dimensional quantum-dot arrays, etc. Since such devices could be self-contained in a chip (without the need of lasers and other optical elements) they could interface naturally with conventional electronic circuits. Thus they may be essential elements in future instrumentation for quantum information.

Another application is based on the emission frequency sensitivity to the size and composition of the dot. As a consequence, quantum dots have shown advantages over traditional organic dyes in modern biological analysis. They also allow for the use of blue lasers in modern DVD players.

7.5[†] Bose–Einstein Condensation

In 1924, Einstein realized the validity of the fact that as T increases (and remains below a critical value T_c), the ground state of a system of bosons (particles at rest) remains multiply occupied (see Sect. 7.7[†]) [46]. Any other single orbital, including the orbital of the second lowest energy, will be occupied by a relatively negligible number of particles. This effect is called Bose–Einstein condensation.[9] Its experimental realization was made possible by the development of techniques for cooling, trapping and manipulating atoms.[10]

In Einstein's original prediction, all bosons were supposed to be slowed down to zero momentum, which implies a macroscopic space, according to the uncertainty principle. However, any experimental set-up requires some confinement. The confining potential in the available magnetic traps for alkali atoms can be safely approximated by the quadratic form

$$V_{ext}(\boldsymbol{r}) = \frac{M\omega^2}{2}r^2. \qquad (7.40)$$

---

[9]The sources [47] have been used for this section.

[10]Einstein himself suggested H_2 and He^4 as possible candidates for B–E condensation. Only in 1938 the He^4 superfluid transition at 2.4 K was interpreted as a transition to the B–E condensate. However, this interpretation was marred by the presence of large residual interactions.

Neglecting the interaction between atoms implies that the Hamiltonian eigenvalues have the form (6.31), since we are considering a system composed of a large number ν of non-interacting bosons. The many-body ground state $\varphi(\boldsymbol{r}_1, \ldots, \boldsymbol{r}_\nu)$ is obtained by putting all the particles into the lowest single-particle state $\varphi_0(\boldsymbol{r})$:

$$\varphi(\boldsymbol{r}_1, \ldots, \boldsymbol{r}_\nu) = \prod_{i=1}^{i=\nu} \varphi_0(\boldsymbol{r}_i), \qquad \varphi_0(\boldsymbol{r}) = \left(\frac{M\omega}{\pi\hbar}\right)^{3/4} \exp(-r^2/2x_c^2). \quad (7.41)$$

The density distribution then becomes $\rho(\boldsymbol{r}) = \nu\,|\varphi_0(\boldsymbol{r})|^2$. While its value grows with ν, the size of the cloud is independent of ν and is fixed by the harmonic oscillator length x_c (3.28). It is typically of the order of $x_c \approx 1\ \mu\text{m}$ in today's experiments.

At finite temperatures, particles are thermally distributed among the available states. A rough estimate may be obtained by assuming $k_B T \gg \hbar\omega$. In this limit we may use a classical Boltzmann distribution

$$n(\boldsymbol{r}) = \exp\left(-M\omega^2 r^2/2k_B T\right), \quad (7.42)$$
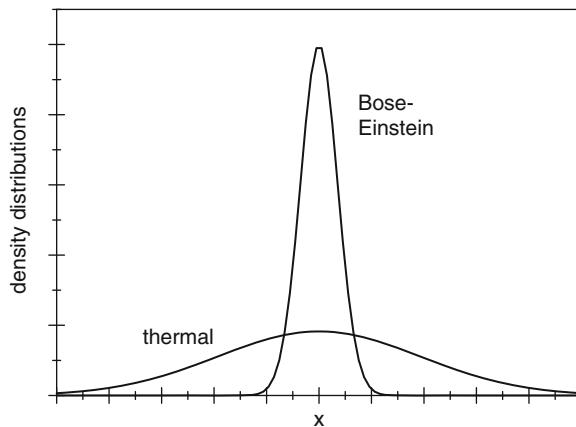
which displays the much broader width

$$\frac{k_B T}{M\omega^2} = x_c\frac{k_B T}{\hbar\omega} \gg x_c. \quad (7.43)$$

Therefore, the Bose–Einstein condensation in harmonic traps appears as a sharp peak in the central region of the density distribution. Figure 7.7 displays the density for 5,000 non-interacting bosons in a spherical trap at temperature $T = 0.9T_c$, where T_c is the critical temperature (see below). The central peak is the condensate, superimposed on the broader thermal distribution. The momentum distribution of the condensate is also Gaussian, having a width $\hbar/x_c$ (3.46). The momentum distribution of the thermal particles is broader, of the order of $(k_B T)^{1/2}$. In fact these two momentum distributions are also represented by the curves in Fig. 7.7, provided the correct units are substituted.

In 1995, rubidium atoms confined within a magnetic trap were cooled to the submicrokelvin regime by laser methods and then by evaporation [48]. The trap was suddenly turned off, allowing the atoms to fly away. By taking pictures of the cloud after various time delays, a two-dimensional momentum distribution of the atoms was constructed. As the temperature was lowered, the familiar Gaussian hump of the Maxwell–Boltzmann distribution was pierced by a rapidly rising sharp peak caused by atoms in the ground state of the trap, that is by the condensate.

By allowing the trap to have cylindrical symmetry, the average momentum along the short axis was double that along the other [see the harmonic oscillator predictions (3.46)]. In contrast, the momentum distribution is always isotropic for a classical gas, unless it is flowing.

Fig. 7.7 Comparison between the densities of the condensate and the thermal particles

The calculation of the critical temperature T_c involves concepts of statistical mechanics that lie beyond the scope of this discussion. The experimental results for the condensate fraction closely follow the thermodynamic limit [48]:

$$\frac{T}{T_c} = 1 - \left(\frac{v_0}{v}\right)^{1/3}.$$
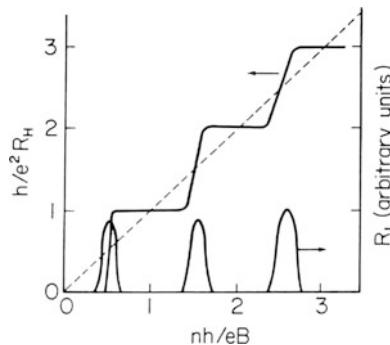
For 40,000 particles, T_c is approximately 3×10^{-7} K.

The first demonstration of the Bose–Einstein condensation involved 2,000 atoms. Today millions are being condensed.

Bose–Einstein condensation is unique because it is the only pure quantum mechanical phase transition: it takes place without any interaction between the particles. This field is presently full of activity: collective motion, condensation and damping times of the condensate, its interaction with light, collision properties, and effects of the residual interactions are just some of the themes that are currently under very intense theoretical and experimental study.

7.6† Quantum Hall Effects

A planar sample of conductive material is placed in a magnetic field perpendicular to its surface. An electric current I is made to pass from one end to the other by means of a potential V_L. The longitudinal resistivity is the ratio $R_L = V_L/I$. Because of the Lorentz force, more electrons accumulate on one side of the sample than on the other, thereby producing a measurable voltage V_H – the Hall voltage – across the sample. The ratio $R_H = V_H/I$ is called the Hall resistivity. It increases linearly with the magnetic field.

Fig. 7.8 The integer quantum Hall effect appears as plateaus in the Hall resistivity of a sample which coincide with the disappearance of the sample's electrical resistivity, as the magnetic field strength is varied [51]. (Reproduced with permission from Springer-Verlag)

However, in 1980 Klaus von Klitzing found that, for samples cooled to within 1 K and placed in strong magnetic fields, the Hall resistivity exhibits a series of plateaus, i.e. intervals in which the Hall resistivity appears not to vary at all with the magnetic field [49]. Figure 7.8 displays a diagram of the measured inverse Hall resistance $h/e^2 R_H$ as a function of the density of electrons n times the characteristic area of the problem (7.48). The longitudinal resistance is sketched as well. Where the Hall resistivity is constant, the longitudinal resistivity practically vanishes. Moreover, the resistivity is $R_H = h/e^2 n$, with an amazing accuracy of order 10^{-6}. Here h is Planck's constant, e is the electron charge and n is an integer (Fig. 7.8). This is even true for samples with different geometries and with different processing histories, as well as for a variety of materials. It is the integer quantum Hall effect.

In 1982 Daniel Tsui, Horst Störmer and Arthur Gossard discovered other plateaus at which n has specific fractional values (1/3, 2/5 and 3/7) [50]. This is the fractional quantum Hall effect.

7.6.1[†]   *Integer Quantum Hall Effect*

Consider the planar motion of an electron in an external, uniform, magnetic field perpendicular to the plane.[11] For the sake of simplicity we will study circular geometries, and thus choose the symmetric gauge $A_x = yB/2$, $A_y = -xB/2$. Replacing the momentum $\hat{\boldsymbol{p}}$ by the effective momentum $\hat{\boldsymbol{p}} - e\boldsymbol{A}$ [53] in the free particle Hamiltonian yields

$$\hat{H} = \frac{1}{2M}\hat{\boldsymbol{p}}^2 + \frac{e^2 B^2}{8M}\rho^2 + \frac{\mu_B B}{\hbar}\left(\hat{L}_z + 2\hat{S}_z\right). \tag{7.44}$$

---

[11]The main source of this section is [52].

The first two terms in (7.44) represent a two-dimensional harmonic Hamiltonian. The eigenvalues and eigenstates of the two-dimensional harmonic oscillator are (see Problem 13 in Chap. 6)

$$E_n = \hbar\omega(n+1), \qquad n = 0, 1, 2, \ldots, \qquad x_c = \sqrt{\hbar/M\omega}$$

$$\varphi_{nm_l}(\rho, \phi) = R_{n_\rho m_l}(u)\varphi_{m_l}(\phi), \ \rho = \sqrt{x^2 + y^2}, \ \phi = \tan^{-1}\frac{y}{x}, \ u = \rho/x_c$$

$$\varphi_{m_l}(\phi) = \frac{1}{\sqrt{2\pi}} \exp(im_l\phi), \qquad m_l = n, n-2, \ldots, -n \qquad (7.45)$$

$$R_{n_\rho m_l}(u) = N_{nm_l} \exp(-u^2/2)u^{m_l} f_{n_\rho m_l}(u^2), \qquad n_\rho = \frac{1}{2}(n - m_l).$$

The first two terms in (7.44) yield the frequency

$$\omega = -\frac{eB}{2M} = \frac{\mu_B B}{\hbar}. \qquad (7.46)$$

The term proportional to $\hat{L}_z$ arises from the cross product of the square of the effective momentum, and the term proportional to $\hat{S}_z$ arises from (5.22). Since the change in energy produced by increasing n by one unit is exactly compensated by decreasing the orbital angular momentum by one unit of $\hbar$, there are sets of degenerate states called Landau levels. In particular, the lowest Landau level is made up of radial nodeless states and values of $m_l = -n$. It has zero energy, since the spin term ($s_z = -\hbar/2$) compensates exactly for the zero point energy $\hbar\omega$ of the harmonic oscillator.

To keep electrons from flying apart, one adds a radial confining potential which does not alter the symmetry of the problem. Let us assume that all states of the first Landau level are occupied[12] up to and including a minimum angular momentum $|M_l|$. The expectation value of the density,

$$\sum_{n=0}^{n=|M_l|} |\varphi_{n(-n)}|^2 = \frac{2}{x_c^2} \exp\left(-u^2\right) \sum_{n=0}^{n=|M_l|} \frac{1}{n!}u^{2n}, \qquad (7.47)$$

is practically constant for $u \equiv \rho/x_c \ll \sqrt{|M_l|}$ and drops rapidly to zero around $\sqrt{|M_l|}$. This configuration is incompressible, since a compression would require the promotion of an electron to a higher Landau level.

Since the characteristic area of the problem is

$$\pi x_c^2 = \frac{\hbar\pi}{M\omega} = \frac{h}{|e|B}, \qquad (7.48)$$

---

[12]The Slater determinant for $|M_l|+1$ electrons moving in the first Landau level is written in (7.50).

the constant of proportionality between the number of electrons per unit area and the strength of the magnetic field depends only on Planck's constant and the charge of the electron.

However, there are impurities and, consequently, the single energy of a Landau level is spread out into a band. The states of the band belong to two classes: states near the bottom or the top of the band are localized states.[13] Near the center of each energy band are extended states, each one spreading out over a large space. They are the only ones that may carry current.

At very low temperatures, only states below the Fermi energy are occupied. Assume that the Fermi level is at the subband of localized states near the top of some Landau band. Now gradually increase the strength of the magnetic field, adjusting the current so that the Hall voltage remains constant. Since the number of states per unit area is proportional to the applied magnetic field [see (7.48)], the number of levels in each Landau state increases proportionately.

Many of the newly available states will be below the Fermi level, so electrons from higher energy localized states will drop to fill them. As a result, the Fermi level descends to a lower position. However, as long as it remains in the subband of high-energy localized states, all the extended states remain fully occupied. The amount of current flowing therefore remains constant and so does the Hall resistivity.

As the Fermi level descends through the subband of extended states, some of them are vacated. The amount of current flowing decreases, while the Hall resistivity increases.

Eventually, the extended states will be emptied and the Fermi level will enter the subband of low-energy localized states. If there is at least one full Landau band below the Fermi level, the extended states in that band will be able to carry a constant current. However, because the extended states in one band have been completely emptied, the number of subbands of extended states has been reduced by one, and the Hall resistance is larger than it was on the previous plateau. The current is proportional to the number of occupied subbands of extended states, and on each plateau an integral number of these subbands is filled.

The second striking feature of the quantized Hall effect is that current flows without resistance in the plateau region. Recall that, to dissipate power, an electron must make a transition to a state of lower energy, the excess energy being distributed within the lattice as vibrations or heat.

First we examine the regime between two plateaus. The Fermi energy varies slightly from point to point: the voltage measured at opposite sides of the sample gauges the difference between the Fermi energies at the two points. Thus, an electron can find itself in an extended state that is below the local Fermi energy in one region of space, but which extends into a region where its energy is above the local Fermi energy. The electron would thus be able to drop into a lower level, dissipating some energy into the lattice. This sample exhibits electrical resistance.

---

[13]Low (high) energy localized states arise around impurity atoms which have an excess (dearth) of positive charge.

If the Fermi energy is within the region of energy corresponding to localized states, there may also be empty states of lower energy. These states, however, are far apart in space, at distances much larger than the localization distance. Electrons cannot drop to lower states, and thus they cannot dissipate energy.

Within this model, localized states also act as a reservoir of electrons, so that, for finite ranges of magnetic field strengths, the extended states in each Landau band are either completely empty or completely filled. Without the reservoir, the width of the regions displaying an integer quantum Hall effect would be vanishingly small.

Therefore, a relatively simple model of independent electrons, moving under the influence of electric and magnetic fields, can account for the main properties of the integer quantum Hall effect. This model has some features in common with the band structure of metals that explains the existence of conductors and insulators (Sect. 7.4.2†).

The quantized Hall effect enables us to calibrate instruments with extreme accuracy as well as to measure fundamental physical constants more precisely than ever before.

7.6.2† *Fractional Quantum Hall Effect*

The fractional quantum Hall effect is seen only when a Landau level is partially filled. For instance, a plateau is seen when the lowest Landau level is approximately one-third full. In this case the Hall resistivity is equal to one-third of the square of the electron charge divided by Planck's constant.

The independent particle model previously used to explain the integer quantum Hall effect does not show any special stability when a fraction of the states is filled. To explain the fractional quantum Hall effect, we must consider the interaction between electrons (like everything associated with open shells).

It is helpful to write the total wave function of particles moving in a Landau level as a Slater determinant (7.11):

$$\Psi = \left(\frac{\sqrt{2}}{x_{\mathrm{c}}}\right)^{M_l+1} \frac{1}{\sqrt{(M_l+1)!}} \left(\prod_{n=0}^{n=M_l} \frac{1}{\sqrt{n!}}\right) \Phi(1, 2, \ldots, M_l+1), \qquad (7.49)$$

where

$$\Phi = \exp\left(-\frac{1}{2}\sum_{i=1}^{i=M_l+1}|z_i|^2\right) \begin{vmatrix} 1 & 1 & \cdots & 1 \\ z_1 & z_2 & \cdots & z_{M_l+1} \\ z_1^2 & z_2^2 & \cdots & z_{M_l+1}^2 \\ \vdots & \vdots & \ddots & \vdots \\ z_1^{M_l} & z_2^{M_l} & \cdots & z_{M_l+1}^{M_l} \end{vmatrix}$$

$$= \exp\left(-\frac{1}{2}\sum_{i=1}^{i=M_l+1}|z_i|^2\right)\prod_{i>j=0}^{i>j=M_l-1}(z_i - z_j). \tag{7.50}$$

Here $z \equiv u\exp(-i\phi)$.

In 1983, Robert Laughlin modified this wave function as follows [54]:

$$\Phi_\nu = \exp\left(-\frac{1}{2}\sum_{i=1}^{i=M_l+1}|z_i|^2\right)\prod_{i>j=0}^{i>j=M_l-1}(z_i - z_j)^\nu. \tag{7.51}$$

These wave states are exact ground states in the limit when electron–electron repulsions become infinitely short ranged. The exponent ν measures the fraction of filled states: the wave functions have the required stability when ν equals 1/3, 1/5, 1/7, 2/3, 4/5 or 6/7. The denominator in the fraction ν must be an odd number to satisfy the Pauli principle. A mechanism based on localized and extended states may also be invoked here but, instead of being applied to independent electrons, it must be used for quasi-particles, which may be described as fractionally charged anyons (see the first footnote 1 on p. 111). The topic of anyons lies beyond the scope of this text.

7.7[†]   Quantum Statistics

Differences between counting the number of states according to whether the particles are distinguishable or not and, in the latter case, whether they are bosons or fermions, have already appeared in the two-body case, as shown in Sect. 7.1. If three particles have to be distributed into three states, we may construct:
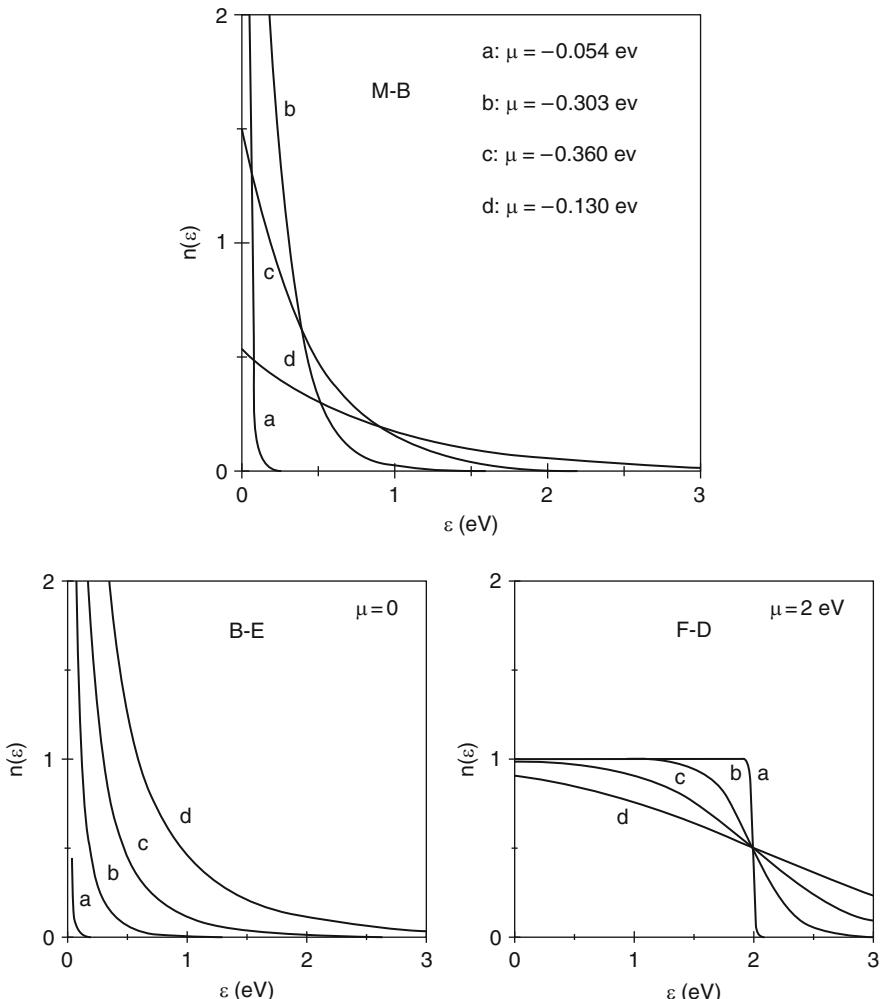
- One antisymmetric Slater determinant (7.11)
- Ten symmetric states [three states $\varphi_a^{(3)}$, six states $\varphi_a^{(2)}\varphi_b^{(1)}$ and one state $\varphi_a^{(1)}\varphi_b^{(1)}\varphi_c^{(1)}$ (7.9)]
- Sixteen states which are neither symmetric nor antisymmetric

Such differences lead to different occupation distributions $n(\epsilon)$ for the levels with energy ϵ.[14] Let us assume that:

1. The equilibrium distribution is the most probable distribution consistent with a constant number of particles and a constant energy.
2. The particles are identical.
3. The particles are distinguishable.
4. There is no restriction on the number of particles in any state.

---

[14]See [58], p. 417.

Fig. 7.9 Maxwell–Boltzmann (M–B), Bose–Einstein (B–E) and Fermi–Dirac (F–D) distribution functions. The value $n(\epsilon)$ gives the fraction of levels at a given energy which are occupied when the system is in thermal equilibrium. The curves correspond to (a) $T = 300\,\text{K}$, (b) $T = 1,000\,\text{K}$, (c) $T = 5,000\,\text{K}$ and (d) $T = 10,000\,\text{K}$

Given these assumptions, one derives the classical M–B distribution [Fig. 7.9 (M–B)]:

$$\eta(\epsilon) = \exp\left(-\frac{\epsilon - \mu}{k_B T}\right),\tag{7.52}$$

where μ is a constant fixing the number of particles.

In the quantum mechanical case, this distribution can only hold if the particles do not overlap. If this is not the case and, consequently, assumption 3 is removed, one obtains the B–E distribution [Fig. 7.9(B–E)], which applies to bosons [55]

$$\eta(\epsilon) = \left[\exp\left(\frac{\epsilon - \mu}{k_B T} \right) - 1 \right]^{-1}. \tag{7.53}$$

The occupancy of the ground state equals the total number of particles in the limit $T \to 0$. If we choose zero for the energy of the ground state,

$$\lim_{T \to 0} \eta(0) = \lim_{T \to 0} \left(1 - \frac{\mu}{k_B T} + \cdots - 1 \right)^{-1} \approx -\frac{k_B T}{\mu} \approx N, \qquad \mu = -\frac{k_B T}{N}. \tag{7.54}$$

Thus, in a boson system, the constant μ must lie below the ground state energy, if the occupations are to be non-negative numbers. In Fig. 7.9(B–E) it is assumed that $k_B T \ll N$.

Moreover, if assumption 4 is replaced by the condition that the number of particles in each level may be 0 or 1, the F–D distribution is derived [Fig. 7.9 (F–D)] [56, 57]

$$\eta(\epsilon) = \left[\exp\left(\frac{\epsilon - \mu}{k_B T} \right) + 1 \right]^{-1}. \tag{7.55}$$

In the case of an electron gas, the parameter μ may be approximated by the Fermi energy ϵ_F for $T \approx 0$ (Sect. 7.4.1). Thus $\mu \approx 3.23\,\text{eV}$ for the Na case.

At energies below $k_B T$, the number of particles per quantum state is greater for the B–E than for the M–B distribution. The opposite is true for the F–D distribution. For small temperatures, this last distribution only differs from a step function within a region of a few $k_B T$ around $\epsilon = \mu$. This fact can be exploited by expanding the integrand $g(\epsilon)\,\eta(\epsilon)$ around μ. The first terms in the resultant Sommerfeld expansion are

$$\int_{-\infty}^{\infty} g(\epsilon)\eta(\epsilon)\mathrm{d}\epsilon = \int_{-\infty}^{\mu} g(\epsilon)\mathrm{d}\epsilon + \frac{\pi^2}{6}(k_B T)^2 \left. \frac{\mathrm{d}g}{\mathrm{d}\epsilon} \right|_{\epsilon=\mu} + \mathcal{O}\left(\frac{k_B T}{\mu} \right)^4. \tag{7.56}$$

For values of $(\epsilon - \mu)/k_B T \gg 1$, the three distributions coincide.

7.8[†] Occupation Number Representation (Second Quantization)

The representation (3.37) of the harmonic oscillator states may be straightforwardly generalized to the case in which ν oscillators are present. The eigenstates and eigenvalues of the energy are [see (7.1)]

$$\varphi_{n_1, n_2, \ldots, n_\nu} = \prod_{p=1}^{p=\nu} \frac{1}{\sqrt{n_p!}} (a_p^+)^{n_p} \varphi_0, \qquad a_p \varphi_0 = 0,$$

$$E_{n_1,n_2,\ldots,n_\nu} = \sum_{p=1}^{p=\nu} E_p n_p, \tag{7.57}$$

where n_p is an eigenvalue of the operator $\hat{n}_p = a_p^+ a_p$ ($n_p = 0, 1, 2, \ldots$). We have disregarded the ground state energy.

The creation and annihilation operators corresponding to different subscripts commute with each other

$$[a_p, a_q] = \left[a_p^+, a_q^+\right] = 0, \qquad \left[a_p, a_q^+\right] = \delta_{pq}. \tag{7.58}$$

The n_p quanta that occupy the p-state are indistinguishable from one another. They are therefore bosons, and states $\varphi_{n_1,n_2,\ldots,n_\nu}$ constitute another representation of states (7.10). Note that it is much simpler to construct the vector state (7.57) than to apply the symmetrization operator $\hat{S}$ (7.8). Examples of the occupation number representation are given by phonons in lattice structures (Sect. 7.4.4[†]) and by the quantized radiation field (Sect. 9.8.2[†]).

One-body operators in many-body systems have been previously expressed as a sum of individual terms $\hat{Q} = \sum_i \hat{Q}_i$. In second quantization we may write $\hat{Q} = \sum_{q \cdot p} c_{qp} a_q^+ a_p$

$$\langle n_1, n_2, \ldots, (n_q + 1), (n_p - 1), \ldots, n_\nu | Q | n_1, n_2, \ldots, n_q, n_p \ldots n_\nu \rangle \tag{7.59}$$

$$= \langle (n_q + 1), (n_p - 1) | Q | n_q, n_p \rangle$$

$$= c_{qp} \sqrt{(n_q + 1)(n_p)}$$

$$= c_{qp} \quad \text{if} \quad n_p = 1, \ n_q = 0.$$

Therefore, $c_{qp} = \langle q | Q | p \rangle$ and thus

$$\hat{Q} = \sum_{qp} \langle q | Q | p \rangle a_q^+ a_p. \tag{7.60}$$

This expression makes no explicit reference to individual particles. A similar equivalence may be obtained for n-body operators. If $n = 2$,

$$\hat{Q} = \frac{1}{2} \sum_{\mu\nu\eta\zeta} \langle \varphi_\mu(1)\varphi_\nu(2) | v(1,2) | \varphi_\eta(1)\varphi_\zeta(2) \rangle a_\mu^+ a_\nu^+ a_\zeta a_\eta. \tag{7.61}$$

The operators $a_{lm_l}^+$ and $(-1)^{l-m_l} a_{l(-m_l)}$ have the same coupling properties as the spherical harmonics Y_{lm_l}.

Another important advantage of the second quantization formalism becomes apparent if the number of particles is not conserved. If an atom is prepared in an exited state, after a finite time the quantum state will be a superposition of a

component representing the initial state plus another component with the atom in a lower state and an emitted photon. The number of photons is not conserved.

It is natural to seek a similar formalism which may apply to fermions. A system of such particles can be described as a many-particle state vector that changes its sign with the interchange of any two particles. Since the required linear combination of products of one-particle states [Slater determinant (7.11)] can be uniquely specified by listing the singly occupied states, the formalism we seek must limit the eigenvalues of $\hat{n}_p$ to 0 and 1.

The desired modification consists in the replacement of commutators $[\hat{A}, \hat{B}]$ by anticommutators

$$\{\hat{A}, \hat{B}\} \equiv \hat{A}\hat{B} + \hat{B}\hat{A}. \tag{7.62}$$

The anticommutators of creation and annihilation operators read

$$\{a_p, a_q\} = \{a_p^+, a_q^+\} = 0, \qquad \{a_p^+, a_q\} = \delta_{pq}. \tag{7.63}$$

The eigenvalues of the number operators are obtained by constructing the operator equation

$$(\hat{n}_p)^2 = a_p^+ a_p a_p^+ a_p = a_p^+ (1 - a_p^+ a_p) a_p = a_p^+ a_p = \hat{n}_p. \tag{7.64}$$

Since both operators $(\hat{n}_p)^2$ and $\hat{n}_p$ are simultaneously diagonal, (7.64) is equivalent to the algebraic equation $n_p^2 = n_p$, which has two roots: 0 and 1. Fermions thus obey the exclusion principle. Within this limitation, the eigenstates and energies (7.57) are also valid for the case of fermions. Note that an interchange of two fermion creation operators changes the sign of the eigenststate [as happens for the Slater determinant (7.11)].

A state such as a closed shell, in which levels μ are occupied, may be represented as

$$\varphi_0 = \prod_\mu a_\mu^+ \, \varphi_{\text{vacuum}}. \tag{7.65}$$

φ_0 may be used as a redefined vacuum state. Thus $a_\eta^+ \varphi_0$ and $a_\eta^+ a_\mu \varphi_0$ represent a one-particle state and a particle-hole state, respectively.

Single-body and two-body operators are also constructed as in (7.60) and (7.61) within the fermion occupation number representation. If acting on products of fermion creation and annihilation operators, care must be taken with the number of permutations between the operators, to obtain consistent phases.

The operators a_{jm}^+ and $(-1)^{j-m} a_{j(-m)}$ have the same angular momentum coupling properties as states φ_{jm}.

Problems

Problem 1. Two particles with equal mass M are confined by a one-dimensional harmonic oscillator potential characterized by the length x_c. Assume that one is in the eigenstate $n = 0$ and the other in $n = 1$. Find the probability density for the relative distance $x = x_a - x_b$, the root mean square value of x, and the probability of finding the two particles within a distance of $x_c/5$ from each other if they are:

1. Non-identical particles
2. Identical bosons
3. Identical fermions

Hint: write the two-particle wave function in terms of the relative coordinate x and the center of mass coordinate $x_g = (x_a + x_b)/2$ and integrate the total probability density with respect to x_g.

Problem 2. Consider a He atom in which one electron is in the state $\varphi_{100\frac{1}{2}m_s}$ and the other in the state $\varphi_{21m_l\frac{1}{2}m_s}$.

1. Construct the possible two-electron states.
2. Split the energy of the allowed states in a qualitative manner by including a Coulomb repulsion between the electrons.

Problem 3. Couple two independent bosons, each carrying spin 2. What spin angular momenta are possible? [See the relations (5.34)].

Problem 4. State whether the spatial sector of a two-body vector state is symmetric or antisymmetric with respect to the interchange of the particles, if the spin sector is given by [see (5.30)]:

1. $[\varphi_{\frac{1}{2}}(1)\,\varphi_{\frac{1}{2}}(2)]_0^0$
2. $[\varphi_{\frac{1}{2}}(1)\,\varphi_{\frac{1}{2}}(2)]_m^1$
3. $[\varphi_1(1)\,\varphi_1(2)]_0^0$
4. $[\varphi_1(1)\,\varphi_1(2)]_m^1$
5. $[\varphi_1(1)\,\varphi_1(2)]_m^2$

Problem 5. What angular momenta are possible for two fermions constrained to move in a j-shell? A j-shell is constituted by the set of states which has the same quantum numbers, including j, with the exception of the projection m.

Problem 6. Couple the spin states of a deuteron ($s_d = 1$) and a proton ($s_p = 1/2$). What total spins are possible:

1. If we ignore the Pauli principle?
2. If the three nucleons move within the $N = 0$ harmonic oscillator shell and the Pauli principle is taken into account? (This is approximately the He^3 ground state.)

Problem 7. Show that a closed fermion j-shell carries zero angular momentum:

1. Using the Slater determinant (7.11)
2. Using the occupation number representation (7.57) plus the anticommutation relations (7.63)

Problem 8. Calculate the angular momentum j and the parity of odd nuclei with 1, 3, 7, 9, 21 and 39 protons. Assume that the Hamiltonian used in Problem 3 of Chap. 6 is valid.

Problem 9. 1. Calculate the magnetic moment of nuclei with 3, 7 and 9 protons, for states with $m = j$. Disregard the neutron contribution.
2. Do the same for neutrons.

Problem 10. Obtain the ratio v/c for:

1. An electron in the outer shell of the Pb atom ($Z = 82$)
2. A neutron in the outer shell of the Pb^{208} nucleus
3. An electron with the Fermi momentum in metal Na [see (7.22)]

Problem 11. Repeat the calculation of Sect. 7.4.1 for a two-dimensional gas model.

Problem 12. Obtain the ratio between the average energy per electron and the Fermi energy for one-, two- and three-dimensional gas models.

Problem 13. The semiconductor Cu_2O displays an energy gap of 2.1 eV. If a thin sheet of this material is illuminated with white light:

1. What is the shortest wavelength that gets through?
2. What color is it?

Problem 14. Consider the Fermi–Dirac distribution (7.55):

1. Find the temperature dependence of the difference $\mu - \epsilon_F$
   Hint: impose the conservation of the number of electrons n_F
2. Evaluate this difference for Na at room temperature.

Problem 15. Obtain the temperature dependence of the specific heat due to the phonons for high values of T.

Problem 16. Find the matrix elements $\langle ab|Q|ab \rangle$, $\langle bc|Q|ab \rangle$ and $\langle ac|Q|ab \rangle$ of the operator $\hat{Q} = \sum_{pq} q_{pq} a_p^+ a_q$, where a_p^+, a_p are fermion creation and annihilation operators and $p = a, b, c$. Assume that $q_{pq} = q_{qp}$.

Chapter 8
Approximate Solutions to Quantum Problems

The previous chapters may have left the (erroneous) impression that there is always an exact (and elegant) mathematical solution for every problem in quantum mechanics. In most cases there is not. One must resort to makeshift approximations, numerical solutions or combinations of both. In this chapter we discuss approximate methods that are frequently applied: perturbation theory, variational procedure, approximate matrix diagonalization, Hartree–Fock and random phase approximations. They are illustrated by means of applications to two-electron atoms, molecules, periodic potentials, etc.

8.1 Perturbation Theory

The procedure is similar to the one used in celestial mechanics, where the trajectory of a comet is first calculated by taking into account only the attraction of the sun. The (smaller) effect of planets is included in successive orders of approximation.

We divide the Hamiltonian $\hat{H}$, which we do not know how to solve exactly, into two terms. The first term, $\hat{H}_0$, is the Hamiltonian of a problem whose solution we know and which is reasonably close to the original problem; the second term, $\hat{V}$, is called the perturbation. Thus

$$\hat{H} = \hat{H}_0 + \lambda \hat{V}, \tag{8.1}$$

$$\hat{H}_0 \varphi_n^{(0)} = E_n^{(0)} \varphi_n^{(0)}. \tag{8.2}$$

The perturbation term has been multiplied by a constant λ that is supposed to be a number less than 1. The constant λ is helpful for keeping track of the order of magnitude of the different terms of the expansion that underlies the theory. Otherwise it has no physical meaning. It is replaced by 1 in the final expressions. We solve the eigenvalue equation

$$\hat{H}\Psi_n = E_n\Psi_n \tag{8.3}$$

by expanding the eigenvalues and the eigenstates in powers of λ and successively considering all terms corresponding to the same power of λ in (8.3):

$$E_n = E_n^{(0)} + \lambda E_n^{(1)} + \lambda^2 E_n^{(2)} + \cdots ,$$
$$\Psi_n = \varphi_n^{(0)} + \lambda\Psi_n^{(1)} + \lambda^2\Psi_n^{(2)} + \cdots . \tag{8.4}$$

The terms independent of λ yield (8.2). The terms proportional to λ give rise to the equation

$$\left(\hat{H}_0 - E_n^{(0)}\right)\Psi_n^{(1)} = \left(-\hat{V} + E_n^{(1)}\right)\varphi_n^{(0)}. \tag{8.5}$$

First, we take the scalar product of $\varphi_n^{(0)}$ with the states on each side of (8.5). The left-hand side vanishes because of (8.2). We thus obtain the first-order correction to the energy

$$E_n^{(1)} = \langle\varphi_n^{(0)}|V|\varphi_n^{(0)}\rangle. \tag{8.6}$$

Therefore, the leading order term correcting the unperturbed energy is the expectation value of the perturbation.

Next, we take the scalar product with $\varphi_p^{(0)}$ ($p \neq n$), so that

$$\left(E_p^{(0)} - E_n^{(0)}\right)\langle\varphi_p^{(0)}|\Psi_n^{(1)}\rangle = -\langle\varphi_p^{(0)}|V|\varphi_n^{(0)}\rangle. \tag{8.7}$$

Using the states $\varphi_p^{(0)}$ as basis states, we expand

$$\Psi_n^{(1)} = \sum_{p \neq n} c_p^{(1)}\varphi_p^{(0)}, \qquad c_p^{(1)} = \frac{\langle\varphi_p^{(0)}|V|\varphi_n^{(0)}\rangle}{E_n^{(0)} - E_p^{(0)}}. \tag{8.8}$$

The still missing amplitude $c_n^{(1)}$ is determined from the normalization condition: since both Ψ_n and $\varphi_n^{(0)}$ are supposed to be normalized to unity, the terms linear in λ are

$$0 = \langle\Psi_n|\Psi_n\rangle - \langle\varphi_n^{(0)}|\varphi_n^{(0)}\rangle = \lambda\left[\langle\Psi_n^{(1)}|\varphi_n^{(0)}\rangle + \langle\varphi_n^{(0)}|\Psi_n^{(1)}\rangle\right] = 2\lambda\,\mathrm{Re}\,(c_n^{(1)}). \tag{8.9}$$

Therefore, the first-order coefficient $c_n^{(1)}$ disappears, since we can make it real by changing the (arbitrary) phase of $\varphi_n^{(0)}$.

Equations (8.6) and (8.8) determine the first-order changes in the energies and state vectors in terms of matrix elements of the perturbation with respect to the basis of zero-order states. The convergence of perturbation theory requires that $|c_p^{(1)}|^2 \ll 1$, i.e. the matrix element of the perturbation between two states should be smaller than the unperturbed distance between these states. In particular, perturbation theory cannot be applied if there are non-vanishing matrix elements

between degenerate states. In these cases, we must resort to either variational (Sect. 8.2) or diagonalization procedures (Sect. 8.5).

The second-order correction to the energy is given by

$$E_n^{(2)} = \sum_{p \neq n} \frac{|\langle \varphi_p^{(0)} | V | \varphi_n^{(0)} \rangle|^2}{E_n^{(0)} - E_p^{(0)}}. \tag{8.10}$$

This perturbation theory is called the Raleigh–Schrödinger perturbation theory. Its apparent simplicity disappears in higher orders of perturbation, due to the increase in the number of contributing terms. A formal simplification may be achieved by summing up partial series of terms. For instance, in the Brillouin–Wigner perturbation theory, one replaces the unperturbed energy $E_n^{(0)}$ of the state n by the exact energy E_n in the denominators. For the case of the energy expansion, one obtains

$$E_n = E_n^{(0)} + \langle \varphi_n^{(0)} | V | \varphi_n^{(0)} \rangle + \sum_{p \neq n} \frac{|\langle \varphi_p^{(0)} | V | \varphi_n^{(0)} \rangle|^2}{E_n - E_p^{(0)}} + \cdots$$

$$= E_n^{(0)} + \langle \varphi_n^{(0)} | V | \varphi_n^{(0)} \rangle + \sum_{p \neq n} \frac{|\langle \varphi_p^{(0)} | V | \varphi_n^{(0)} \rangle|^2}{E_n^{(0)} - E_p^{(0)}}$$

$$- \sum_{p \neq n} \frac{|\langle \varphi_p^{(0)} | V | \varphi_n^{(0)} \rangle|^2 \langle \varphi_n^{(0)} | V | \varphi_n^{(0)} \rangle}{\left(E_n^{(0)} - E_p^{(0)} \right)^2} + \cdots. \tag{8.11}$$

The last term appears as a third-order term in the Raleigh–Schrödinger perturbation theory. It does not exist[1] in the Brillouin–Wigner expansion, since it has been taken into account through the replacement in the denominator of the second-order term (8.10). However, the advantage of reducing the number of terms may be compensated by a decrease in the convergence of the perturbation expansion, associated with the nature of the partial summations. Moreover, different powers of λ may be present in many terms of the Brillouin–Wigner series.

There is an elegant and useful formulation of perturbation theory conceived by Feynman. This uses diagrams carrying both a precise mathematical meaning and a description of the processes involved [59]. The "finest hour" of perturbation theory is represented by the calculation of the gyromagnetic electron value to nine significant figures, using quantum electrodynamics (see Sect. 5.2.2).

The ground state energy of the He atom is calculated using perturbation theory in Sect. 8.3.

---

[1] One can prove that the Brillouin–Wigner expansion does not contain terms in which the state $\varphi_n^{(0)}$ appears in the numerator as an intermediate state.

8.2   Variational Procedure

This approximation may be considered as the inverse of the perturbation procedure: instead of working with a fixed set of unperturbed states, one guesses a trial state Ψ, which may be expanded in terms of the basis set of eigenstates φ_E of the Hamiltonian ($\Psi = \sum_E c_E \varphi_E$):

$$\langle \Psi | H | \Psi \rangle = \sum_E E |c_E|^2 \geq E_0 \sum_E |c_E|^2 = E_0, \qquad (8.12)$$

where E_0 is the ground state energy. The state Ψ may depend on some parameter, and the expectation value of the Hamiltonian is minimized with respect to this parameter. One thus obtains an upper limit for the ground state energy of the system.

The fact that the energy is an extremum guarantees that if the trial wave function is wrong by something of the order of δ, the variational estimate of the energy is off by something of the order δ^2. So one can be rewarded with a good energy estimate, even though the initial wave function may be only a fair guess.

The ground state energy obtained in first-order perturbation theory $E_0^{(0)} + \langle \varphi_0^{(0)} | V | \varphi_0^{(0)} \rangle$ is an expectation value of the total Hamiltonian and is thus equivalent to a non-optimized variational calculation.

8.3   Ground State of the He Atom

This three-body problem may be reduced to a two-body problem by again considering a very massive nucleus. However, even the remaining problem is difficult to solve because of the presence of the Coulomb repulsion V between the two electrons. The total Hamiltonian is $\hat{H}_0 + V$, where

$$\hat{H}_0 = -\frac{\hbar^2}{2M} (\nabla_1^2 + \nabla_2^2) - \frac{Ze^2}{4\pi\epsilon_0} \left(\frac{1}{r_1} + \frac{1}{r_2} \right), \qquad V = \frac{e^2}{4\pi\epsilon_0 r_{12}}. \qquad (8.13)$$

Here $r_{12} = |\mathbf{r}_1 - \mathbf{r}_2|$ is the distance between the electrons.

We know how to solve the problem of two electrons moving independently of each other in the Coulomb potential of the He nucleus. Because the ground state energy of a hydrogen-like atom is proportional to Z^2 and there are two electrons, the unperturbed energy is $8E_H$, where E_H is the energy of the electron in the H atom. The antisymmetrized two-electron state vector of the ground state in the He atom is discussed in Sect. 7.2. Using this state, the first-order correction to the energy is (Sect. 8.7*)

$$E_{\text{g.s.}}^{(1)} = \left\langle \varphi_{\text{g.s.}} \left| \frac{e^2}{4\pi\epsilon_0 r_{12}} \right| \varphi_{\text{g.s.}} \right\rangle = -\frac{5}{2} E_H. \qquad (8.14)$$

Therefore, the total energy becomes $5.50E_H$, which constitutes an improved approximation to the experimental result $5.81E_H$ compared with the unperturbed value $8E_H$.

As mentioned in Sect. 8.2, one may improve the predictions for the ground state by a variational calculation. In this case we may write the expectation value of the kinetic energy, of the potential energy and the Coulomb repulsion as functions of the parameter Z^* entering the wave function. The value $Z = 2$ is kept in the Hamiltonian:

$$\langle \varphi_{\text{g.s.}} | H | \varphi_{\text{g.s.}} \rangle_{Z^*} = -2(Z^*)^2 E_H + 4ZZ^* E_H - \frac{5}{4} Z^* E_H. \qquad (8.15)$$

Minimization with respect to Z^* yields the effective value $Z^* = 1.69$ for He (instead of 2), which is an indication that the electrons mutually screen the nuclear attraction. The final result is $\langle \varphi_{\text{g.s.}} | H | \varphi_{\text{g.s.}} \rangle_{Z=1.69} = 5.69E_H$, and this is in even better agreement with the experimental value than the first-order perturbation result.
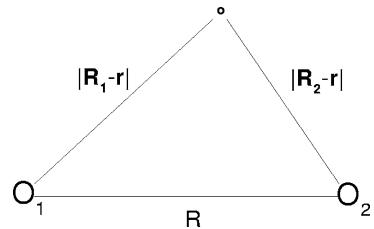
To apply the variational procedure to excited states, one must ensure their orthogonality with lower energy states, for the resulting value of the minimization parameter.

8.4 Molecules

Molecules are made up of nuclei and electrons. The theoretical description of this many-body system is facilitated by the very different masses of the two constituents, which allows us to decouple their respective motions. The procedure is called the Born–Oppenheimer approximation. In principle, it is possible to begin by solving the problem of motion of electrons subject to the (static) field of the nuclei and to the field of other electrons. In this first step, the nuclear coordinates $\boldsymbol{R}_i$ are treated as parameters. Minimization of the energy $W(\boldsymbol{R}_i)$ with respect to these parameters yields their equilibrium values. A subsequent step consists in allowing small departures of the nuclei from their equilibrium position and using the associated increase in the energy W as the restoring force for the oscillatory motion. Finally, the molecules may also perform collective rotations without changing the relative positions of the electrons and the nuclei.

8.4.1 Intrinsic Motion: Covalent Binding

We illustrate the procedure for the case of the molecular hydrogen ion H_2^+. Figure 8.1 represents the two protons 1 and 2 and the electron. The assumption that the protons are at rest simplifies the Hamiltonian to

Fig. 8.1 The hydrogen ion

$$\hat{H} = -\frac{\hbar^2}{2M}\nabla^2 - \frac{e^2}{4\pi\epsilon_0|\boldsymbol{r}-\boldsymbol{R}_1|} - \frac{e^2}{4\pi\epsilon_0|\boldsymbol{r}-\boldsymbol{R}_2|} + \frac{e^2}{4\pi\epsilon_0 R}, \qquad (8.16)$$

where $R = |\boldsymbol{R}_1 - \boldsymbol{R}_2|$. Although in this particular case, exact numerical solutions may be obtained by solving the Schrödinger equation in elliptical coordinates, it is more instructive to approximate the solution by means of a variational procedure.

If the distance R is very large, the two (degenerate) solutions describe a H atom plus a dissociated proton. The two orbital wave functions are

$$\varphi_1 = \varphi_{100}(|\boldsymbol{r}-\boldsymbol{R}_1|), \qquad \varphi_2 = \varphi_{100}(|\boldsymbol{r}-\boldsymbol{R}_2|). \qquad (8.17)$$

Note that such wave functions are orthogonal only for very large values of R. In fact, their overlap is $\langle 1|2\rangle = 1$ for $R = 0$.

The requirement of antisymmetry between the two protons must be taken into account. As in Sect. 7.2, the spin of the two protons may be coupled to 1 (symmetric spin states) or to 0 (antisymmetric spin states). The corresponding spatial wave functions should thus be antisymmetric and symmetric, respectively:
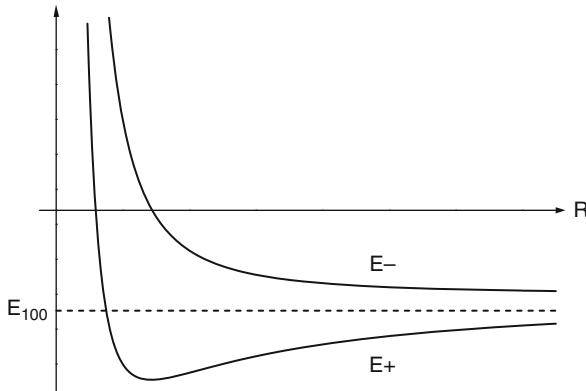
$$\varphi_{\mp} = \frac{\varphi_1 \mp \varphi_2}{\sqrt{2(1 \mp \langle 1|2\rangle)}}. \qquad (8.18)$$

The energy to be minimized with respect to the distance R is

$$\begin{aligned}
E_{\pm}(R) &= \langle\pm|H|\pm\rangle \\
&= E_{100} + \frac{e^2}{4\pi\epsilon_0 R} - \frac{e^2}{4\pi\epsilon_0(1\pm\langle 1|2\rangle)}\left\langle 2\left|\frac{1}{|\boldsymbol{r}-\boldsymbol{R}_1|}\right|2\right\rangle \\
&\quad \mp \frac{e^2}{4\pi\epsilon_0(1\pm\langle 1|2\rangle)}\left\langle 1\left|\frac{1}{|\boldsymbol{r}-\boldsymbol{R}_1|}\right|2\right\rangle,
\end{aligned} \qquad (8.19)$$

which has the limits

$$\lim_{R\to 0} E_{\pm} \to \infty, \qquad \lim_{R\to\infty} E_{\pm} = E_{100}. \qquad (8.20)$$

Fig. 8.2 Lowest energies of the hydrogen ion as a function of the distance between protons

Since the matrix element in the third line of (8.19) is positive, we conclude that the energy corresponding to the spatially symmetric wave function lies lowest. In fact, the two curves are plotted in Fig. 8.2. Only the energy corresponding to φ_+ displays a minimum. This may be interpreted as being due to the build-up of the electron density between the two nuclei, which allows for the screening of the Coulomb repulsion. This type of binding is called covalent binding.[2]

8.4.2 Vibrational and Rotational Motions

We consider here the somewhat more general case of a diatomic molecule with masses M_1 and M_2, respectively. First we perform the well-known separation between the relative and center of mass operators:

$$\hat{R} = \hat{R}_1 - \hat{R}_2, \qquad \hat{R}_g = \frac{M_1}{M_g}\hat{R}_1 + \frac{M_2}{M_g}\hat{R}_2,$$
$$\hat{P} = \frac{M_2}{M_g}\hat{P}_1 - \frac{M_1}{M_g}\hat{P}_2, \qquad \hat{P}_g = \hat{P}_1 + \hat{P}_2. \tag{8.21}$$

The inversion of definitions (8.21) yields the kinetic energy

$$\frac{\hat{P}_1^2}{2M_1} + \frac{\hat{P}_2^2}{2M_2} = \frac{\hat{P}_g^2}{2M_g} + \frac{\hat{P}^2}{2\mu}. \tag{8.22}$$

Here $M_g = M_1 + M_2$ is the total mass and $\mu \equiv M_1 M_2 / M_g$ is the reduced mass.

---

[2]See also the example in Sect. 3.2.

If the potential energy $V(R)$ depends only on the distance between the ions, the center of mass moves as a free particle. This problem has already been discussed in Sect. 4.3. The kinetic energy associated with the relative motion may be expressed in spherical coordinates, as in (6.1), with the substitution $M \to \mu$.

Let us split the relative Hamiltonian into rotational and vibrational contributions, viz.,

$$\hat{H} = \hat{H}_{\text{rot}} + \hat{H}_{\text{vib}},$$

$$\hat{H}_{\text{rot}} = \frac{1}{2\mu R^2} \hat{\boldsymbol{L}}^2, \tag{8.23}$$

$$\hat{H}_{\text{vib}} = -\frac{\hbar^2}{2\mu} \left(\frac{d^2}{dR^2} + \frac{2}{R} \frac{d}{dR} \right) + V(R). \tag{8.24}$$

We now assume that the interactions between the ions stabilize the system at the relative distance R_0. The difference $y = R - R_0$ will be such that $|y| \ll R_0$.
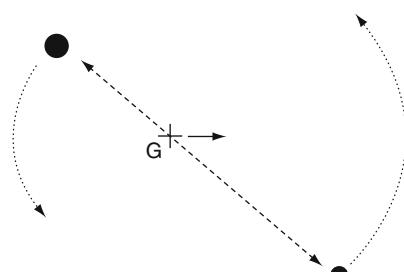
Rotational Motion

The Hamiltonian for the rotational motion may be approximated as (see Fig. 8.3)

$$\hat{H}_{\text{rot}} = \frac{1}{2\mathcal{I}} \hat{L}^2, \qquad \mathcal{I} = \mu R_0^2, \tag{8.25}$$

where $\mathcal{I}$ is the moment of inertia. The eigenfunctions are labeled by the quantum numbers l, m_l (Sect. 5.1.2). The energies are obtained by replacing the operator $\hat{\boldsymbol{L}}^2$ in (8.25) by its eigenvalues $\hbar^2 l(l + 1)$. The photon energy corresponding to the transition between neighboring states increases linearly with l, so that

$$\Delta(l \to l - 1) = \frac{\hbar^2}{\mathcal{I}} l. \tag{8.26}$$

Fig. 8.3 Vibrational (*dashed line*), rotational (*dotted lines*) and translation of the center of mass G (*continuous line*) of a diatomic molecule

Vibrational Motion

If the stabilization at $R \approx R_0$ is sufficiently good we may extend the domain of the radial coordinate from 0 to $-\infty$, since the wave function should be increasingly small for negative values of R. Simultaneously, the R^2 factor in the volume element may be eliminated from the integrals by the substitution $\Psi(R) \to \Phi(R)/R$. In such a case the radial Schrödinger equation transforms into a linear equation of the type seen in Chap. 4:

$$-\frac{\hbar^2}{2\mu}\left(\frac{d^2}{dR^2} + \frac{2}{R}\frac{d}{dR}\right)\Psi + V(R)\Psi = E\Psi \longrightarrow -\frac{\hbar^2}{2\mu}\frac{d^2}{dR^2}\Phi + V(R)\Phi = E\Phi,$$

(8.27)

with the boundary conditions $\Phi(\pm\infty) = 0$.

Finally, the Taylor expansion of the potential around the equilibrium position R_0 and the replacement of the coordinate R by $y = R - R_0$ yield the harmonic oscillator Hamiltonian discussed in Sects. 3.3 and 4.2 (see Fig. 8.3)

$$\left[-\frac{\hbar^2}{2\mu}\frac{d^2}{dy^2} + \frac{1}{2}\left.\frac{d^2V(R)}{dR^2}\right|_{R=R_0}y^2\right]\Phi = \left[E - V(R_0)\right]\Phi.$$

(8.28)

The vibrational states are equidistant from each other (Fig. 3.2). The photon spectrum displays the single frequency

$$\Delta(N \to N - 1) = \hbar\omega = \hbar\sqrt{\frac{1}{\mu}\left.\frac{d^2V(R)}{dR^2}\right|_{R=R_0}}.$$

(8.29)

8.4.3 Characteristic Energies
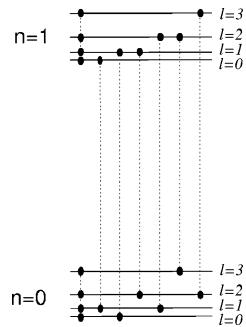
The diatomic molecule is the simplest illustration of a general feature: the breaking of the spherical symmetry produced by the shape of the intrinsic system generates rotational degrees of freedom; if the amount of this breaking is measured by a minimization parameter (the distance R_0), there appear vibrational degrees of freedom around this value.

The intrinsic motion of electrons and the vibrational and rotational motion of nuclei are associated with different characteristic energies. The order of magnitude for intrinsic transitions should be similar to the excitation energies in atoms

$$E_{\text{intr}} \approx -E_H = \frac{\hbar^2}{2a_0^2M},$$

(8.30)

since the same Coulomb interaction and similar interparticle distances are present. Here a_0 is the Bohr radius (Table 6.1). The potential energy of the vibrational motion

Fig. 8.4 Vibrational and
rotational excitations of a
molecule. *Dotted lines*
represent allowed transitions,
according to the definition
(9.71)

originates also in the Coulomb potential and thus should be of the same order of
magnitude as E_{intr}

$$E_{\text{vib}} = \hbar \sqrt{\frac{E_{\text{intr}}}{2a_0^2 \mu}} \approx \frac{\hbar^2}{a_0^2 \sqrt{2M\mu}} \approx \sqrt{\frac{M}{M_p}} E_{\text{intr}} \tag{8.31}$$

Rotational energies are given by (8.26)

$$E_{\text{rot}} \approx \frac{\hbar^2}{2a_0^2 \mu} \approx \frac{M}{M_p} E_{\text{intr}}. \tag{8.32}$$

Since the ratio between the electron and the proton masses $M/M_{\text{p}} \approx 1/2,000$
(see Table A.1), the transitions between vibrational states occupy an intermediate
energy range compared to those corresponding to intrinsic electron transitions or
to transitions between rotational states. Therefore, the molecular spectrum displays
vibrational states on top of each intrinsic excitation and rotational states on top of
each vibrational state (see Fig. 8.4). The electromagnetic radiation associated with
transitions between intrinsic, vibrational and rotational states appears, successively,
in the visible, infrared and radiofrequency regions of the optical spectrum.

As the energies of the rotational and vibrational excitations increase, the
approximations become less reliable:

- Terms that are functions of y will appear in the rotational Hamiltonian, coupling
  the rotational and vibrational motion
- Higher order terms in the Taylor expansion of the potential become relevant

8.5   Approximate Matrix Diagonalizations

If the conditions for applying perturbation theory are not satisfied, we may resort to
a diagonalization procedure. This is obviously necessary if there are degenerate or
close-lying states. This is the case if two or more particles are added to a closed shell,

whether it be atomic or nuclear. The size of the matrix to be diagonalized may be reduced due to physical considerations, for example, when we use the symmetries of the Hamiltonian. If we are only interested in the ground state and neighboring states, we may also simplify the problem by taking into account only those states which are close in energy to the ground state.

It is also possible to include those contributions to the matrix elements of the Hamiltonian to be diagonalized that arise from states not included in the diagonalization. One may use either the technique of folded diagrams (a generalization of Raleigh–Schrödinger perturbation theory) [61] or the Bloch–Horowitz procedure (an extension of the Brillouin–Wigner expansion) [62].

An alternative procedure consists in simplifying the expressions for the matrix elements. This includes eliminating many of them (see Problem 12). In such cases, good insight is required to avoid distorting the physical problem.

8.5.1[†]   *Approximate Treatment of Periodic Potentials*
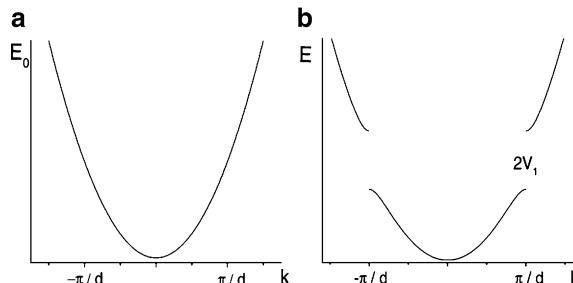
This example illustrates the interplay between exact diagonalization and perturbation theory that can be applied in more complicated situations. We treat the same problem as in Sect. 4.6[†], but in the limit of a small periodic potential $V(x)$.

We choose the free-particle Hamiltonian $H_0 = \frac{1}{2M}\hat{p}^2$ as zero-order Hamiltonian. The unperturbed energies are given in Fig. 8.5a, as a function of the wave number k. If $V(x) = V(x + d)$, a Fourier transform of the potential yields

$$V(x) = \sum_n V_n, \qquad V_n = v_n \exp\left(\frac{i2\pi nx}{d}\right), \qquad n = 0, \pm 1, \pm 2, \dots \quad (8.33)$$

Therefore, the non-vanishing matrix elements of the perturbation are

$$\langle k'|V_n|k\rangle = v_n, \qquad \text{if } k' - k = \frac{2\pi n}{d}, \quad (8.34)$$

Fig. 8.5 Bands in periodic potentials. The unperturbed parabolic energies are given as functions of k in (**a**). The eigenvalue E_- is plotted in the interval $0 \le |k| \le \frac{\pi}{d}$ and E_+ for $\frac{\pi}{d} \le |k|$ in (**b**)

and the Hamiltonian matrix is of the form[3]

$$
\begin{pmatrix}
\cdots & \cdots & \cdots & \cdots & \cdots & \cdots \\
\cdots & \frac{\hbar^2}{2M}\left(k - \frac{4\pi}{d}\right)^2 & v_1 & v_2 & v_3 & \cdots \\
\cdots & v_1 & \frac{\hbar^2}{2M}\left(k - \frac{2\pi}{d}\right)^2 & v_1 & v_2 & \cdots \\
\cdots & v_2 & v_1 & \frac{\hbar^2}{2M}k^2 & v_1 & \cdots \\
\cdots & v_3 & v_2 & v_1 & \frac{\hbar^2}{2M}\left(k + \frac{2\pi}{d}\right)^2 & \cdots \\
\cdots & \cdots & \cdots & \cdots & \cdots & \cdots
\end{pmatrix}.
$$

$$(8.35)$$

We concentrate on the non-diagonal terms v_1. However small, they cannot be treated in perturbation theory, because they connect degenerate states: the state with $k = \frac{\pi}{d}$ has the same unperturbed energy as the state with $k' = k - \frac{2\pi}{d} = -\frac{\pi}{d}$. Thus, we must first proceed to make a diagonalization between degenerate (or quasi-degenerate) states, i.e. we must put to zero the determinant

$$
\begin{vmatrix}
\frac{\hbar^2}{2M}\left(k - \frac{2\pi}{d}\right)^2 - E & v_1 \\
v_1 & \frac{\hbar^2}{2M}k^2 - E
\end{vmatrix} = 0.
$$

$$(8.36)$$

The eigenvalues

$$
E_{\pm} = \frac{\hbar^2}{2M}\left(k^2 - k\frac{2\pi}{d} + \frac{2\pi^2}{d^2} \pm \sqrt{\frac{4\pi^2}{d^2}\left(k - \frac{\pi}{d}\right)^2 + \left(\frac{2Mv_1}{\hbar^2}\right)^2}\right) \quad (8.37)
$$

are plotted as functions of k in Fig. 8.5b. There are no states in the interval $\frac{1}{2M}\left(\frac{\hbar\pi}{d}\right)^2 - v_1 \le E \le \frac{1}{2M}\left(\frac{\hbar\pi}{d}\right)^2 + v_1$. A gap of size $2v_1$ appears in the spectrum, pointing to the existence of two separate bands.

In the region $|k| \approx \frac{\pi}{d}$, the remaining non-diagonal terms v_n may be treated as perturbations, if they are sufficiently small. Unfortunately, they usually are not so in realistic cases.

8.6   Independent-Particle Approximations

8.6.1[†]   *The Hartree–Fock Approximation*

On several occasions we have used with good results a product of single-particle states to represent the ground state of many-fermion problems (atoms, nuclei, metals, etc.)

---

[3]We disregard v_0 since it only affects the zero-point energy.

$$\varphi_0 = \prod_h a_h^+ |\text{vacuum}\rangle, \tag{8.38}$$

where h denotes occupied states. Of course this can only be an approximation if the Hamiltonian includes n-body interactions, with $n > 1$. The Hartree–Fock procedure determines the best single particle set to be used in such cases. It consists on the replacement of some (large) one-body operators by their expectation values, thus neglecting their fluctuations.

Let us consider a system of identical fermions within the formalism of second quantization. The Hamiltonian is

$$\hat{H} = \sum_{kj}\langle k|H_1|j\rangle c_k^+ c_j + \frac{1}{2}\sum_{kljm}\langle kl|H_2|jm\rangle c_k^+ c_l^+ c_m c_j, \tag{8.39}$$

where $\hat{H}_\nu$ contains ν-body terms (ν=1,2). States (8.38) are eigenstates of an independent particle Hamiltonian

$$\hat{H}_{\text{HF}} = \sum_i \epsilon_i a_i^+ a_i. \tag{8.40}$$

The two sets of single-fermion creation operators are related through a transformation

$$a_i^+ = \sum_j \lambda_{ij} c_j^+. \tag{8.41}$$

To find the Hartree–Fock single-particle energies ϵ_i and the amplitudes λ_{ij}, we calculate the commutators

$$[\hat{H}_{HF}, a_i^+] = \sum_k \epsilon_i \lambda_{ik} c_k^+ \tag{8.42}$$

$$[\hat{H}, a_i^+] = \sum_q \lambda_{iq}\left[\sum_k \langle k|H_1|q\rangle c_k^+ + \frac{1}{2}\sum_{klj}(\langle kl|H_2|qj\rangle - \langle kl|H_2|jq\rangle)c_k^+ c_l^+ c_j\right]$$

$$= \sum_{qk} \lambda_{iq} c_k^+ \left[\langle k|H_1|q\rangle + \sum_{lj}(\langle kl|H_2|qj\rangle - \langle kl|H_2|jq\rangle)c_l^+ c_j\right]$$

$$\approx \sum_{qk} \lambda_{iq} c_k^+ \left[\langle k|H_1|q\rangle + \sum_h(\langle kh|H_2|qh\rangle - \langle kh|H_2|hq\rangle)\right]. \tag{8.43}$$

In deriving the last line, we have replaced the operator $c_l^+ c_j \to \delta_{lj}$ if $l = j = h$ (h = occupied state). Equating the coefficients of c_k^+ from (8.42) and (8.43) yields the eigenvalue matrix equations (3.11)

$$\epsilon_i \, \lambda_{ik} = \sum_q \left[\langle k|H_1|q\rangle \, + \, \sum_h (\langle kh|H_2|qh\rangle - \langle kh|H_2|hq\rangle) \right] \lambda_{iq}, \qquad (8.44)$$

which we know how to solve to obtain energies and amplitudes.

However, the replacement of $c_l^+ c_j$ by δ_{lj} would be a good approximation for the number operator acting on the ground state (8.38), only if the set c_j^+ of creation operators is the same as the set a_i^+ appearing in (8.38). In general, this is not the case, since the initial guess may be arbitrary, aside from some boundary conditions [see, for instance (7.13)]. We iterate the previous process, starting now from the new set a_i defined by the transformation (8.41) with the amplitudes λ_{ik} just obtained from (8.44), until convergence to a unique set is obtained.

The matrix elements of $\hat{H}_2$ in (8.44) can be interpreted as due to the one-body potential produced by all the particles in occupied states. The second contribution of $\hat{H}_2$ is due to the antisymmetry of the fermion state (8.38) and is called the exchange term. The Hartree approximation is obtained by neglecting this last contribution.

The lowest excited states $\varphi_{ph} = a_p^+ a_h \varphi_0$ are obtained by promoting a particle from an occupied state h to an empty state p. Their excitation energy is given by the difference $\epsilon_p - \epsilon_h$. The matrix elements between the ground and particle-hole states vanish

$$\langle ph|H|0\rangle = 0. \qquad (8.45)$$

8.6.2[†]   *The Random–Phase Approximation (RPA)*

Products of fermion operators may act as bosons. In particular, the commutation of the products

$$\gamma_{ph}^+ \equiv a_p^+ a_h, \qquad (8.46)$$

used in the last paragraph of the Hartree–Fock subsection, is

$$[a_h^+ a_p, a_{p'}^+ a_{h'}] = \delta_{p'p} \, a_h^+ a_{h'} \, - \, \delta_{h'h} \, a_{p'}^+ a_p \approx \delta_{p'p} \, \delta_{h'h}$$

$$[a_p^+ a_h, a_{p'}^+ a_{h'}] = [a_h^+ a_p, a_{h'}^+ a_{p'}] = 0, \qquad (8.47)$$

where we have used the same approximation $a_h^+ a_{h'} \approx \delta_{h'h}$ involved in the Hartree–Fock case. Therefore, the set of operators $\gamma_{ph}^+, \gamma_{ph}$ obey boson commutation relations (within the approximation).

The Hamiltonian (8.40) may be written as

$$\hat{H}_{\mathrm{HF}} \approx \sum_{ph} e_{ph} \gamma_{ph}^+ \gamma_{ph}, \qquad e_{ph} = \epsilon_p - \epsilon_h, \qquad (8.48)$$

as can be verified by commuting both sides with γ_{ph}^+ or with γ_{ph}.

In addition to the terms in the Hamiltonian determining $\hat{H}_{\mathrm{HF}}$, there are residual contributions of $\hat{H}$. Some of them may be expressed in terms of the bosons (8.46) and thus, they represent (quadratic) boson interactions:

$$\hat{H}_{2b} = \frac{1}{2} \sum_{(ph),(p'h')} \left(\langle ph'|H_2|hp' \rangle \gamma_{ph}^+ \gamma_{p'h'} + \langle pp'|H_2|hh' \rangle \gamma_{ph}^+ \gamma_{p'h'}^+ \right) + \text{h.c.} \tag{8.49}$$

The objective now is to obtain a set of uncoupled bosons, giving rise to the Hamiltonian

$$\hat{H}_b \equiv \sum_n \hbar \omega_n \Gamma_n^+ \Gamma_n = \hat{H}_{\mathrm{HF}} + \hat{H}_{2b}. \tag{8.50}$$

The procedure is similar to that used in the Hartree–Fock case. One starts by defining the boson transformation [which plays a similar role to (8.41)]

$$\Gamma_n^+ = \lambda_{n,(ph)} \gamma_{ph}^+ - \mu_{n,(ph)} \gamma_{ph}. \tag{8.51}$$

Subsequently, we equate the terms proportional to γ_{ph}^+ and to γ_{ph} in the commutation of both sides of (8.50) with the uncoupled bosons Γ_n^+. One obtains a set of 2ν linear equations, ν being the number of possible pairs (ph)

$$\begin{pmatrix} A & B \\ -B^* & -A^* \end{pmatrix} \begin{pmatrix} \lambda_n \\ \mu_n \end{pmatrix} = \omega_n \begin{pmatrix} \lambda_n \\ \mu_n \end{pmatrix}, \tag{8.52}$$

where

$$\langle p'h'|A|ph \rangle = e_{ph} \delta_{p'p} \delta_{h'h} + \langle p'h|H_2|h'p \rangle$$
$$\langle p'h'|B|ph \rangle = \langle p'p|H_2|h'h \rangle. \tag{8.53}$$

The solution is symmetrical between positive and negative values of ω_n and an interchange between λ_n and μ_n^*. Only the positive energies are considered

It is usually convenient to further limit the possible pairs (ph) by requiring, for instance, that the bosons carry a definite momentum or angular momentum, parity, etc.

Although the RPA modes constitute simple boson excitations, they have a complicated (collective) structure from the point of view of the original constituents of the system (electrons, ions, nuclei, etc.). They may occupy regions of the spectrum that cannot be simply covered by particle-hole excitations (8.48). See, for instance, Sects. 7.4.4[†], 8.4.2 and 10.1.6[†].

The RPA excitation spectrum replaces the HF particle-hole spectrum. It is expected to be more accurate, since it takes into account residual interactions (8.49) not included in (8.48). However, if many bosons γ_{ph}^+ (8.46) become admixed in the ground state through the RPA correlations, the approximation (8.47) becomes

less valid. Corrections to the Hartree approximation + RPA lie beyond the scope of
this text.

8.7*   Matrix Elements Involving the Inverse
of the Interparticle Distance

Although the integrals involved may be found in tables, we calculate them explicitly
as a quantum mechanical exercise. The inverse of the distance between two particles
may be expressed as

$$\frac{1}{r_{12}} = \frac{1}{r_2} \sum_l \left(\frac{r_1}{r_2}\right)^l P_l(\cos\alpha_{12}), \qquad r_1 < r_2. \tag{8.54}$$

Here P_l is the Legendre polynomial of order l (Sect. 5.5*), a function of the angle
α_{12} subtended by the two vectors r_1, r_2. It may be expressed by coupling two
spherical harmonics to zero angular momentum (5.66).

Next, we evaluate matrix elements such as

$$\left\langle n_1 l_1 m_1 n_2 l_2 m_2 \left| \frac{1}{r_{12}} \right| n_1 l_1 m_1 n_2 l_2 m_2 \right\rangle$$

$$= N_{n_1 l_1}^2 N_{n_2 l_2}^2 \int_0^\infty |R_{n_1 l_1}(1)|^2 r_1^2 dr_1 \int_0^\infty |R_{n_2 l_2}(2)|^2 r_2^2 dr_2$$

$$\times \int_0^{4\pi} |Y_{l_1 m_1}(1)|^2 d\Omega_1 \int_0^{4\pi} |Y_{l_2 m_2}(2)|^2 d\Omega_2 / r_{12}$$

$$= N_{n_1 l_1}^2 N_{n_2 l_2}^2 \sum_l \frac{4\pi}{2l+1} \int_0^\infty |R_{n_1 l_1}(1)|^2 r_1^2 dr_1$$

$$\times \left[\frac{1}{r_1^{l+1}} \int_0^{r_1} |R_{n_2 l_2}(2)|^2 r_2^{l+2} dr_2 + r_1^l \int_{r_1}^\infty |R_{n_2 l_2}(2)|^2 r_2^{1-l} dr_2 \right]$$

$$\times \sum_{m_l=-l}^{m_l=l} (-1)^{l-m_l} \langle Y_{l_1 m_1} | Y_{l m_l} | Y_{l_1 m_1} \rangle \langle Y_{l_2 m_2} | Y_{l(-m_l)} | Y_{l_2 m_2} \rangle. \tag{8.55}$$

The angular integrals restrict the values of l in the summation (see Problem 5 in
Chap. 5). If at least one of the particles is in an s state, only one l term survives. If
both particles are in s states,

$$\left\langle n_1 00 n_2 l_2 m_2 \left| \frac{1}{r_{12}} \right| n_1 00 n_2 l_2 m_2 \right\rangle = N_{n_1 0}^2 N_{n_2 l_2}^2 \int_0^\infty |R_{n_1 0}(1)|^2 r_1^2 dr_1$$

$$\times \left[\frac{1}{r_1} \int_0^{r_1} |R_{n_2 l_2}(2)|^2 r_2^2 dr_2 + \int_{r_1}^\infty |R_{n_2 l_2}(2)|^2 r_2 dr_2 \right],$$

(8.56)

which yields the value (8.14) for $n_1 = n_2 = 1$.

Problems

Problem 1. 1. Obtain the expression for the second-order correction to the energy in perturbation theory and show that this correction is always negative for the ground state.

2. Calculate the second-order correction to the eigenstate.

Problem 2. Assume that the zero-order Hamiltonian and the perturbation are given by the matrices

$$\hat{H}_0 = \begin{pmatrix} 5 & 0 & 0 \\ 0 & 2 & 0 \\ 0 & 0 & -1 \end{pmatrix}, \qquad \hat{V} = \begin{pmatrix} 0 & c & 0 \\ c & 0 & 0 \\ 0 & 0 & 2c \end{pmatrix}.$$

1. Calculate the first-order perturbation corrections to the energies.
2. Calculate the second-order perturbation corrections to the energies.
3. Obtain the first-order corrections to the vector states.
4. Obtain the second-order corrections to the vector states.
5. Expand the exact energies in powers of c and compare the results with those obtained in perturbation theory:

$$(1 + x)^{1/2} = 1 + \frac{1}{2}x - \frac{1}{8}x^2 + \frac{1}{16}x^3 - \cdots .$$

Problem 3. 1. Calculate the first- and second-order corrections to the ground state energy of a linear harmonic oscillator if a perturbation $V(x) = kx$ is added, and compare with the exact value.

2. Do the same if the perturbation is $V(x) = bx^2/2$.

Problem 4. 1. Calculate the lowest relativistic correction to the ground state energy of a linear harmonic oscillator. Hint: expand the relativistic energy $\sqrt{M^2 c^4 + c^2 p^2}$ in powers of p/Mc.

2. Obtain the order of magnitude of the ratio between the relativistic correction and the non-relativistic value in the molecular case.

Problem 5. Obtain the vector state up to second order in the Brillouin–Wigner perturbation theory. Compare with the results (8.8) and Problem 1.

Problem 6. Show that the Brillouin–Wigner perturbation theory already yields the exact results (3.19) in second order, for a Hamiltonian of the form (3.18). Hint: use

$$E_a = \langle a|H|a \rangle + \frac{|\langle a|H|b \rangle|^2}{E_a - \langle b|H|b \rangle}.$$

Problem 7. Minimize the ground state energy by taking the mass as the variation in the lowest harmonic oscillator state and using the harmonic oscillator potential plus the relativistic kinetic energy as Hamiltonian. Include as many powers of p^2/M^2c^2 in the latter as are necessary to obtain an improvement over the perturbation results of Problem 5:

1. Write the expectation value of the Hamiltonian as a function of M^*/M.
2. Write the minimization condition.
3. Solve this equation in powers of $\hbar\omega/Mc^2$.
4. Expand the energies in powers of $\hbar\omega/Mc^2$.

Problem 8. Calculate the perturbation correction for the two $1s2p$ electron states in the He atom. Explain why perturbation theory may be used in spite of the existing degeneracies.

Problem 9. 1. In units of E_H, calculate the first-order perturbation correction for the ground state energy of the He atom, the ionized Li atom and the doubly ionized Be atom.
2. Obtain the variational energies using the effective number of electrons Z^* as the variational parameter.
3. Compare with the experimental values: -79 eV (He), -197 eV (Li$^+$), -370 eV (Be^{++}).

Problem 10. Substitute $R \rightarrow R_0 + y$ in the rotational Hamiltonian (8.23) and expand the Hamiltonian in powers of y up to quadratic order. Calculate the correction for the energy in perturbation theory, using the product of the rotational and vibrational bases as an unperturbed basis

$$(1 + a)^{-2} = 1 - 2a + 3a^2 + \cdots.$$

Problem 11. Two He atoms are attracted by a Van der Waals potential $V(R) = 4\epsilon \left[\left(\frac{\sigma}{\kappa} \right)^1 2 - \left(\frac{\sigma}{\kappa} \right)^6 \right]$, with $\epsilon = 8.75 \times 10^{-4}$ eV and $\sigma = 2.56$ Å. Find

1. The energy ϵ_0 and separation distance R_0 at equilibrium.
2. The characteristic vibrational energy $\hbar\omega$.
3. The characteristic rotational energy $\hbar^2/2\mu\, R_0^2$.

Problem 12. A hydrogen atom is subject to a constant electric field in the z-direction (Stark effect):

1. Construct the matrix of the perturbation for the $n = 2$ state and diagonalize this matrix.
2. Do the same for the $N = 2$ states of the harmonic oscillator potential.

Problem 13. Consider N fermions interacting through $V = \frac{\zeta}{4} \sum_{i,j} (x_i - x_j)^2$:

1. Write the Hamiltonian H in second quantization form.
2. Write the Hartree Hamiltonian H_{H} and the residual interaction V'. Find the Hartree frequency ω_{H}.
3. Write the RPA Hamiltonian H_{RPA} and find the root ω_{RPA} ($N \gg 1$).
4. Which symmetry is carried by the original Hamiltonian H and is violated by H_{H} (see Chap. 10).

Chapter 9
Time Dependence in Quantum Mechanics

Up to now we have only considered static situations (except for the reduction of the state vector when a measurement takes place). We now discuss the time dependence of the state vector, which requires a new principle. The resultant time-dependent Schrödinger equation is solved exactly for simple (spin) cases and in perturbation theory. The notion of transition probability yields physical meaning to non-diagonal matrix elements and allows us to present the energy–time uncertainty relation, together with the concept of mean lifetime (Sect. 9.5).

In Chap. 1 we stressed the fact that the main reason for the development of quantum mechanics was the instability of the hydrogen atom under classical mechanics and electromagnetism. Thus, an exposition of quantum mechanics cannot be deemed complete without showing that this original crisis has been solved. This task requires an introduction to quantum electrodynamics (QED). The concepts of induced and spontaneous emission, laser optics and selection rules appear along the exposition.

9.1 The Time Principle

In the first place we stress the fact that in quantum mechanics, time is taken to be a parameter, not an observable. Although there is an evolution operator, there is no such thing as a time operator.[1]

---

[1]As Jun John Sakurai points out: "Ironically, in the historical development of wave mechanics both L. de Broglie and E. Schrödinger were guided by a kind of covariant analogy between energy and time on the one hand and momentum and position (spatial coordinate) on the other. Yet when we now look at quantum mechanics in its finished form, there is no trace of a symmetrical treatment between time and space. The relativistic quantum theory of fields does treat the time and space coordinates on the same footing, but it does so at the expense of demoting position from the status of being an observable to that of being just a parameter." [63], Chap. 2. Nevertheless, and

Assume that the system is represented at time t by the time-dependent state vector $\Psi(t)$. At time $t' > t$, the system will evolve in accordance with

$$\Psi(t') = \mathcal{U}(t', t)\Psi(t), \tag{9.1}$$

where $\mathcal{U}(t', t)$ is called the evolution operator. This operator satisfies the conditions of being unitary and

$$\lim_{t' \to t} \mathcal{U}(t', t) = 1. \tag{9.2}$$

Therefore, if $t' = t + \Delta t$,

$$\Psi(t + \Delta t) = \mathcal{U}(t + \Delta t, t)\Psi(t)$$
$$= \left[1 + \frac{\partial}{\partial t'} \mathcal{U}(t', t) \Big|_{t'=t} \Delta t + \cdots \right] \Psi(t),$$

$$\frac{\partial}{\partial t} \Psi(t) = \frac{\partial}{\partial t'} \mathcal{U}(t', t)|_{t'=t} \Psi(t). \tag{9.3}$$

A new quantum principle must be added to those stated in Chaps. 2 and 7.

Principle 5. *The operator yielding the change of the state vector over time is proportional to the Hamiltonian*

$$\frac{\partial}{\partial t'} \mathcal{U}(t', t)|_{t'=t} = -\frac{i}{\hbar} \hat{H}(t). \tag{9.4}$$

Note the following consequences:

- The time evolution of the system is determined by the first-order linear equation

$$i\hbar \frac{\partial}{\partial t} \Psi(t) = \hat{H} \Psi(t). \tag{9.5}$$

This is called the time-dependent Schrödinger equation. It is valid for a general state vector, and it is independent of any particular realization of quantum mechanics.
- The evolution is deterministic, since the state vector is completely defined once the initial state is fixed (quantum indeterminacy pertains to measurement processes).
- The evolution is unitary (i.e. the norm of the states is preserved).

---

although the commutation relation $[\hat{x}, \hat{p}]$ has been postulated in the present text, it has also been derived in the non-relativistic limit of Lorentz transformations [18], thus suggesting a deeper link between relativity and quantum mechanics.

- The evolution of the system is reversible.
- The evolution satisfies the composition property

$$\mathcal{U}(t'-t) = \mathcal{U}(t'-t'')\mathcal{U}(t''-t) \qquad (t' > t'' > t). \tag{9.6}$$

- If $[\hat{H}(\tau_1), \hat{H}(\tau_2)] = 0$, the evolution operator is

$$\mathcal{U}(t',t) = \exp\left[-\frac{\mathrm{i}}{\hbar}\int_t^{t'} \hat{H}(\tau)\,\mathrm{d}\tau\right]. \tag{9.7}$$

In the case of a time–independent Hamiltonian satisfying the eigenvalue equation $\hat{H}\varphi_i = E_i\varphi_i$, the solution to the differential equation (9.5) may be found using the method for separation of variables. Hence,

$$\varphi_i(t) = f(t)\varphi_i, \qquad \mathrm{i}\hbar\frac{\mathrm{d}f}{\mathrm{d}t} = E_i f \to f = \exp(-\mathrm{i}E_i t/\hbar) \tag{9.8}$$

and thus,

$$\varphi_i(t) = \varphi_i \exp\left(-\frac{\mathrm{i}}{\hbar}E_i t\right). \tag{9.9}$$

We expect the solutions of a time-independent Hamiltonian to be independent of time. However, as usual, this requirement can only be enforced up to a phase. This is consistent with the result (9.9).

The constant of proportionality $-\mathrm{i}/\hbar$ chosen in (9.4) ensures that the time-dependent wave function for a free particle with energy $E = \hbar\omega$ is a plane wave, as expected [see (4.32)]:

$$\varphi_{\pm k}(x,t) = A\exp\left[\mathrm{i}(\pm kx - \omega t)\right]. \tag{9.10}$$

If the Hamiltonian is time independent and the state is represented at time $t = 0$ by the linear combination (2.6) of its eigenstates,

$$\Psi(t = 0) = \sum_i c_i\varphi_i, \tag{9.11}$$

(9.9) implies that at time t the state has evolved into[2]

$$\Psi(t) = \sum_i c_i\varphi_i\exp\left[-\frac{\mathrm{i}}{\hbar}E_i\,t\right]. \tag{9.12}$$

---

[2]The evolution is valid only for the Hamiltonian basis. Therefore, the expression $\Psi(t) = \sum_i c_i\varphi_i\exp(-\mathrm{i}q_i t/\hbar)$ makes no sense if φ_i, q_i are not eigenstates and eigenvalues of the Hamiltonian.

The relation $[\hat{Q}, \hat{H}] = 0$ implies a conservation law. If the system is initially in an eigenstate of the operator $\hat{Q}$ it remains so during its time evolution.

9.2 Time Dependence of Spin States

9.2.1 Larmor Precession

To begin with we give a simple but non-trivial example of a solution to (9.5). We use as Hamiltonian the interaction (5.15), with the magnetic field directed along the z-axis. The evolution operator (9.7) is given by

$$\mathcal{U}_z(t, 0) = \exp[-i\hat{H}_z t/\hbar] = \begin{pmatrix} \exp[i\omega_{\mathrm{L}} t/2] & 0 \\ 0 & \exp[-i\omega_{\mathrm{L}} t/2] \end{pmatrix}$$

$$\hat{H}_z = -\omega_{\mathrm{L}}\, \hat{S}_z, \tag{9.13}$$

where $\omega_{\mathrm{L}} \equiv \mu_\nu\, g_s\, B/\hbar$ is called the Larmor frequency [see (5.22)]. We have used (5.21) in the expansion of the exponential in (9.13).

The time evolution is given by

$$\Psi(t) = \begin{pmatrix} c_\uparrow(t) \\ c_\downarrow(t) \end{pmatrix} = \mathcal{U}_z(t, 0) \begin{pmatrix} c_\uparrow(0) \\ c_\downarrow(0) \end{pmatrix}. \tag{9.14}$$

If the state of the system is an eigenstate of the operator $\hat{S}_z$ at $t = 0$, it remains so forever and (9.14) is just a particular case of (9.9). However, if at $t = 0$ the spin points in the positive x-direction [initial values: $c_\uparrow = c_\downarrow = 1/\sqrt{2}$, see (3.21)], then

$$\Psi(t) = \frac{1}{\sqrt{2}} \begin{pmatrix} 1 \\ 1 \end{pmatrix} \cos\frac{\omega_{\mathrm{L}} t}{2} + i\frac{1}{\sqrt{2}} \begin{pmatrix} 1 \\ -1 \end{pmatrix} \sin\frac{\omega_{\mathrm{L}} t}{2}. \tag{9.15}$$

The probability of finding the system with spin aligned with the x-axis (or in the opposite direction) is $\cos^2(\omega_{\mathrm{L}} t/2)$ [or $\sin^2(\omega_{\mathrm{L}} t/2)$].

The expectation values of the spin components are

$$\langle\Psi|S_x|\Psi\rangle = \frac{\hbar}{2}\cos(\omega_{\mathrm{L}} t), \qquad \langle\Psi|S_y|\Psi\rangle = -\frac{\hbar}{2}\sin(\omega_{\mathrm{L}} t), \qquad \langle\Psi|S_z|\Psi\rangle = 0. \tag{9.16}$$

The spin precesses around the z-axis (the magnetic field axis), with the Larmor frequency ω_{L} in the clockwise direction ($x \to -y$). It never aligns itself with the z-axis. Unlike the case in which a definite projection of the angular momentum along the z-axis is well defined (see the discussion of Fig. 5.1 in Sect. 5.1.1), we are describing a true precession here, which is obtained at the expense of the determination of S_z.

If $t \ll 1/\omega_{\mathrm{L}}$, we speak of a transition from the initial state $\varphi_{S_x = \hbar/2}$ to the final state $\varphi_{S_x = -\hbar/2}$ with the probability $\omega_{\mathrm{L}}^2 t^2/4$. In this case, the probability per unit time is linear in time.

If the z-direction is substituted by the x-direction in the Hamiltonian (9.13), we obtain the transformation

$$\mathcal{U}_x(t,0) = \begin{pmatrix} \cos \omega_{\mathrm{L}} t/2 & i \sin \omega_{\mathrm{L}} t/2 \\ i \sin \omega_{\mathrm{L}} t/2 & \cos \omega_{\mathrm{L}} t/2 \end{pmatrix}. \tag{9.17}$$

9.2.2 Magnetic Resonance

We now add a periodic field along the x- and y-directions, of magnitude B' and frequency ω, to the constant magnetic field of magnitude B pointing along the z-axis. The Hamiltonian reads

$$\hat{H} = -\mu_s B \hat{S}_z - \mu_s B' \left(\cos \omega t \, \hat{S}_x - \sin \omega t \, \hat{S}_y \right)$$

$$= -\frac{1}{2} \mu_s \hbar \begin{pmatrix} B & B' \exp(i\omega t) \\ B' \exp(-i\omega t) & -B \end{pmatrix}. \tag{9.18}$$

Since this Hamiltonian does not commute with itself at different times, we cannot use the evolution operator (9.7). We must solve instead the differential equation (9.5) for the amplitudes $c_i(t)$. Although the solution may be worked out analytically for any value of ω, it turns out that the maximum effect is obtained if this frequency equals the Larmor frequency ω_{L}. We make this assumption in the derivation below. We also set $\omega' \equiv \mu_s B'$.
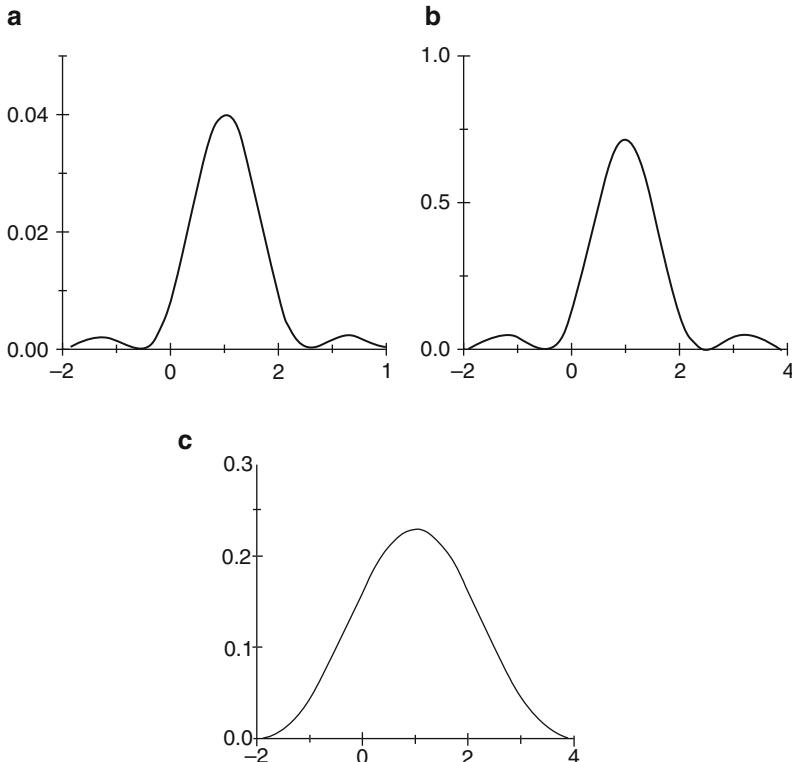
We try a solution of the form (9.14), but with time-dependent amplitudes:

$$\begin{pmatrix} b_\uparrow(t) \\ b_\downarrow(t) \end{pmatrix} = \begin{pmatrix} \exp[i\omega t/2] \, c_\uparrow(t) \\ \exp[-i\omega t/2] \, c_\downarrow(t) \end{pmatrix}, \quad \begin{pmatrix} \dot{b}_\uparrow \\ \dot{b}_\downarrow \end{pmatrix} = \frac{i}{2}\omega' \begin{pmatrix} b_\downarrow \\ b_\uparrow \end{pmatrix}. \tag{9.19}$$

The solution to the last equation is

$$\begin{pmatrix} b_\uparrow \\ b_\downarrow \end{pmatrix} = \begin{pmatrix} \cos \dfrac{\omega' t}{2} & \sin \dfrac{\omega' t}{2} \\ i \sin \dfrac{\omega' t}{2} & -i \cos \dfrac{\omega' t}{2} \end{pmatrix} \begin{pmatrix} b_\uparrow(0) \\ b_\downarrow(0) \end{pmatrix}. \tag{9.20}$$

This result ensures the occurrence of the spin flip: a spin pointing up (down) will eventually point down (up), i.e. it will be flipped. The probabilities that the initial spin is maintained or flipped are (Fig. 9.1)

Fig. 9.1 Probability of a spin flip according to (9.22). Values of ω/ω_L are represented on the horizontal axis, while probabilities are indicated on the vertical axis. The resonant behavior for $\omega = \omega_L$ is apparent. The parameters are $t\omega_L = 4$, $\omega'/\omega_L = 1/10$ (**a**); $t\omega_L = 4$, $\omega'/\omega_L = 1/2$ (**b**) and $t\omega_L = 2$, $\omega'/\omega_L = 1/2$ (**c**). The comparison between the last two graphs anticipates the complementary relation between time and energy [see (9.35) and Sect. 9.5]

$$P_{\uparrow\to\uparrow} = P_{\downarrow\to\downarrow} = \cos^2\left(\frac{1}{2}\omega't\right),$$

$$P_{\uparrow\to\downarrow} = P_{\downarrow\to\uparrow} = \sin^2\left(\frac{1}{2}\omega't\right). \tag{9.21}$$

For an arbitrary relation between ω and ω_L, the probability of a spin flip is given by

$$P_{\uparrow\to\downarrow}(t) = \frac{(\omega')^2}{(\omega - \omega_L)^2 + (\omega')^2} \sin^2\left[\frac{1}{2}t\sqrt{(\omega - \omega_L)^2 + (\omega')^2}\right]. \tag{9.22}$$

This equation expresses a typical resonance phenomenon (hence the name magnetic resonance): if $\omega \approx \omega_L$, a very weak field B' produces large effects (Fig. 9.1). One cannot treat the interaction with the sinusoidal field as a small perturbation.

This would require $|\omega'| \ll |\omega - \omega_L|$, a condition violated in the neighborhood of resonance.

Nuclear magnetic resonance (NMR) is an essential part of processes involving the alignment of spins. It has applications in many branches of physics, such as measuring magnetic moments of particles, including elementary particles, and determining properties of condensed matter. It is also an important tool in quantum computing.

In medicine, NMR is called magnetic resonance imaging (MRI). It is the result of three contributing quantum technologies:

- The patient is placed in a large magnetic field that is produced without heating, by means of superconducting coils (Sect. 10.1).
- The evolution of spins of the hydrogen atoms in our body is affected by both static and modulated fields, as described above.
- The signals picked by detection coils are transformed into images by computers employing hardwares based on transistor technologies (Sect. 7.4.3[†]).

An enormous amount of information is obtained from the medium. For instance, the brain activity can be directly observed through changes in the magnetic environment produced by the flux of blood.

9.3 Sudden Change in the Hamiltonian

We consider a time-dependent Hamiltonian $\hat{H}$ such that $\hat{H} = \hat{H}_0$ for $t < 0$ and $\hat{H} = \hat{K}_0$ for $t > 0$, where $\hat{H}_0$ and $\hat{K}_0$ are time-independent Hamiltonians. We know how to solve the problem for these two Hamiltonians:

$$\hat{H}_0 \varphi_i = E_i \varphi_i, \qquad \hat{K}_0 \phi_i = \epsilon_i \phi_i. \tag{9.23}$$

The system is initially in the state $\varphi_i \exp(-iE_i t/\hbar)$. For $t > 0$, the solution is given by the superposition

$$\Psi = \sum_k c_k \phi_k \exp(-i\epsilon_k t/\hbar), \tag{9.24}$$

where the amplitudes c_k are time independent, as is $\hat{K}_0$.

The solution must be continuous in time to satisfy a differential equation. Therefore, at $t = 0$,

$$\varphi_i = \sum_k c_k \phi_k \longrightarrow c_k = \langle \phi_k | \varphi_i \rangle. \tag{9.25}$$

The transition probability is given by

$$P_{\varphi_i \to \phi_k} = |c_k|^2. \tag{9.26}$$

9.4   Time-Dependent Perturbation Theory

If the Hamiltonian includes both a time-independent term $\hat{H}_0$ and a time-dependent contribution $\hat{V}(t)$, one may still use the expansion (9.12), but with time-dependent amplitudes $[c_i = c_i(t)]$. In that case, the Schrödinger equation for the Hamiltonian $\hat{H}_0 + \hat{V}$ is equivalent to the set of coupled equations

$$i\hbar \sum_i \dot{c}_i \varphi_i \exp(-iE_i t/\hbar) = \hat{V} \sum_i c_i \varphi_i \exp(-iE_i t/\hbar). \tag{9.27}$$

The scalar product with φ_k yields

$$i\hbar \dot{c}_k = \sum_i c_i \langle k|V|i \rangle \exp(i\omega_{ki} t), \qquad \omega_{ki} = \frac{E_k - E_i}{\hbar}, \tag{9.28}$$

where ω_{ki} is the Bohr frequency. This set of coupled equations must be solved together with boundary conditions, such as the value of the amplitudes c_i at $t = 0$. The formulation of the time-dependent problem in terms of the coupled amplitudes $c_i(t)$ is attributed to Dirac.

The set of coupled equations (9.28) is not easier to solve than (9.5). Therefore, one must resort to a perturbation treatment. As in Sect. 8.1, we multiply the perturbation $\hat{V}(t)$ by the unphysical parameter λ ($0 \leq \lambda \leq 1$) and expand the amplitudes

$$c_k(t) = c_k^{(0)} + \lambda c_k^{(1)}(t) + \lambda^2 c_k^{(2)}(t) + \cdots . \tag{9.29}$$

We impose the initial condition that the system be in the state $\varphi_i^{(0)}(t)$ at $t = 0$. This condition is enforced through the assignment $c_k^{(0)} = \delta_{ki}$, which accounts for terms independent of λ in (9.28).

The perturbation is applied at $t = 0$. Our aim is to calculate the probability of finding the system in another unperturbed eigenstate $\varphi_k^{(0)}$ at time t. The terms linear in λ yield

$$\dot{c}_k^{(1)} = -\frac{i}{\hbar} \langle k|V|i \rangle \exp(i\omega_{ki} t). \tag{9.30}$$

Therefore, the transition amplitudes are given by

$$c_k^{(1)}(t) = -\frac{i}{\hbar} \int_0^t \langle k|V|i \rangle \exp(i\omega_{ki} \tau) d\tau. \tag{9.31}$$

The transition probability between the initial state i and the final state k, induced by the Hamiltonian $\hat{V}(t)$, is given in first-order of perturbation theory as

$$P_{i \to k}^{(1)}(t) = \left| c_k^{(1)} \right|^2 . \tag{9.32}$$

9.5 Energy–Time Uncertainty Relation
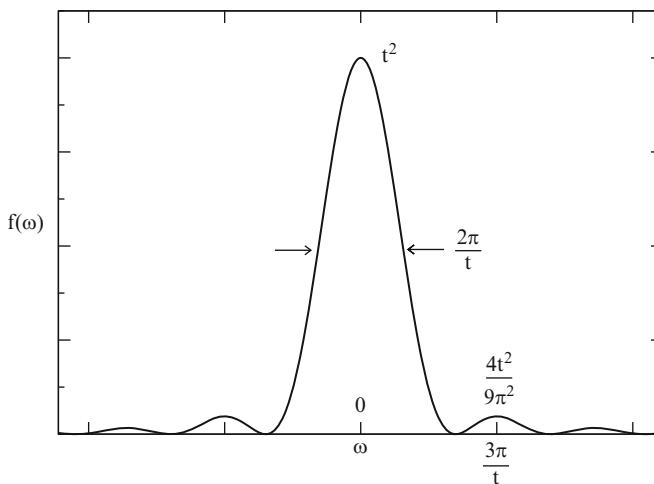
Consider matrix elements of the perturbation $\langle k|V|i\rangle$ which do not depend on time in the interval $(0, t)$, and otherwise vanish. The first-order amplitude and transition probabilities (9.31) and (9.32) are given by

$$c_k^{(1)} = -\frac{\langle k|V|i\rangle}{\hbar\omega_{ki}} \left[\exp(i\omega_{ki}t) - 1\right], \tag{9.33}$$

$$P_{i \to k}^{(1)} = \left|\frac{\langle k|V|i\rangle}{\hbar\omega_{ki}}\right|^2 4\sin^2(\omega_{ki}t/2). \tag{9.34}$$

The result (9.34) is common to many first-order transition processes. Therefore, we discuss it in some detail:

- If the final states φ_k belong to a continuous set, the transition probability is proportional to the function $f(\omega) = (4/\omega^2)\sin^2(\omega t/2)$ plotted in Fig. 9.2. The largest peak at $\omega = 0$ has a height proportional to t^2, while the next highest, at $\omega \approx 3\pi/t$, is smaller by a factor of $4/9\pi^2 \approx 1/20$. Therefore, practically all transitions take place for frequencies lying within the central peak, which is characteristic of the phenomena of resonance. The secondary peaks are associated with diffraction processes.
- The total probability is obtained by integrating over the frequencies. Assuming that the matrix element is not changed within the frequency interval of the main peak, and approximating the surface of the latter by the area of an isosceles triangle of height t^2 and half-base $2\pi/t$, we conclude that the total probability

Fig. 9.2 The function $f(\omega)$ as a function of the frequency ω

increases linearly with time and that the probability per unit interval of time is constant.

- The energy of an initially excited atomic state may be obtained from the frequency of the photon resulting from de-excitation of this state (Sect. 9.8.4†). Therefore, the spread shown in Fig. 9.2 changes the notion of the eigenvalue in the case of an unstable state. Instead of a sharp energy, the existence of the spread is associated with an indeterminacy in the energy on the order of

$$\Delta E \geq \hbar \frac{2\pi}{t}. \tag{9.35}$$

This inequality is a manifestation of the uncertainty as applied to energy and time. There is a similar uncertainty if the energy of the excited states is obtained via a process of absorption of electromagnetic radiation.

This time–energy relation was anticipated in the caption of Fig. 9.1.

- It would be wrong to conclude from (9.35) that energy is not conserved at the microscopic quantum scale, since such conservation principle does not hold for a time-dependent Hamiltonian. What enters in (9.35) is the difference between eigenvalues of the unperturbed Hamiltonian.
- Non-diagonal matrix elements $\langle k|V|i\rangle$ acquire physical meaning, since they can be measured through transition rates.
- If there is a continuum of final states, we are interested in summing up the probabilities over the set K of these final states ($k \in K$):

$$P_{i\to K}^{(1)} = \int_{E_i-\Delta E/2}^{E_i+\Delta E/2} P_{i\to k}^{(1)} \rho(E_k)\mathrm{d}E_k, \tag{9.36}$$

where $\rho(E_k)$ is the density of the final states.[3] Assuming that both $|\langle k|V|i\rangle|^2$ and $\rho(E_k)$ remain constant during the interval ΔE, and that most of the transitions take place within this interval, then

$$P_{i\to K}^{(1)} \approx \frac{4}{\hbar^2}|\langle k|V|i\rangle|^2\rho(E_k)\int_{-\infty}^{\infty}\mathrm{d}E_k\frac{\sin^2\omega_{ki}t/2}{\omega_{ki}^2} = \frac{2\pi t}{\hbar}|\langle k|V|i\rangle|^2\rho(E_k). \tag{9.37}$$

The expression for the transition per unit time is called the Fermi golden rule:

$$\frac{\mathrm{d}P_{i\to K}^{(1)}}{\mathrm{d}t} = \frac{2\pi}{\hbar}|\langle k|V|i\rangle|^2\rho(E_k). \tag{9.38}$$

So far, the transition probability $\mathrm{d}P/\mathrm{d}t$ per unit time has been calculated for a single system. If there are $\mathcal{N}$ similar systems present (for instance, $\mathcal{N}$ atoms), one cannot ascertain when a particular system will decay. If $\mathrm{d}P/\mathrm{d}t$ is time-independent

---

[3]The density of states is given in (7.21) for the free particle case. A similar procedure is carried out for photons in (9.60).

(as in (9.38)), the total rate of change is given by

$$\frac{d\mathcal{N}}{dt} = -\mathcal{N}\frac{dP}{dt}.$$ (9.39)

Therefore,

$$\mathcal{N} = \mathcal{N}_0 \exp\left(-\frac{dP}{dt}t\right) = \mathcal{N}_0 \exp(-t/\tau), \qquad \tau = \left(\frac{dP}{dt}\right)^{-1}.$$ (9.40)

The constant τ is called the mean lifetime. It is the time required for the reduction of the size of the population by a factor of $1/e$ and thus it is a measure of the the time Δt at which the decay takes place. The energy–time uncertainty relation is written in analogy[4] with (2.37)

$$\Delta t\, \Delta E \geq \hbar.$$ (9.41)

A short mean lifetime implies a broad peak, and vice versa.

9.6[†]   **The Heisenberg Picture**

So far, the expectation value of an operator $\hat{Q}$ not depending explicitly on time only depends on the time evolution of the state vector (Sect. 9.1). There is an alternative description – the Heisenberg picture – in which the state vector is frozen at, for instance, $t = 0$, and the operator evolves as

$$\hat{Q}^{(H)}(t) = \hat{\mathcal{U}}^+(t)\, \hat{Q}^{(S)}\, \hat{\mathcal{U}}(t),$$ (9.42)

where the superscripts (H) and (S) stand for Heisenberg and Schrödinger, respectively. We can easily verify that both pictures yield the same expectation value of the operator

$$\langle \Psi(t)|Q^{(S)}|\Psi(t)\rangle = \langle \Psi(0)|\mathcal{U}^+(t)Q^{(S)}\mathcal{U}(t)|\Psi(0)\rangle = \langle \Psi(0)|Q^{(H)}|\Psi(0)\rangle.$$ (9.43)

The time derivative of the Heisenberg version of the operator yields

$$\begin{aligned}\frac{d\,\hat{Q}^{(H)}}{dt} &= \frac{d\hat{\mathcal{U}}^+(t)}{dt}\,\hat{Q}^{(S)}\hat{\mathcal{U}}(t) + \hat{\mathcal{U}}^+\,\hat{Q}^{(S)}\frac{d\hat{\mathcal{U}}(t)}{dt}\\ &= \frac{i}{\hbar}\hat{\mathcal{U}}^+(t)\,\hat{H}\,\hat{Q}^{(S)}\hat{\mathcal{U}}(t) - \frac{i}{\hbar}\hat{\mathcal{U}}^+\hat{Q}^{(S)}\hat{H}\hat{\mathcal{U}}(t)\\ &= -\frac{i}{\hbar}\,[\hat{Q}^{(H)}, \hat{H}],\end{aligned}$$ (9.44)

where (9.7) has been used. This is the Heisenberg equation of motion.

---

[4]However, it has a different origin (see footnote 1).

9.7[†]   Time-Reversal Symmetry

The quantum mechanical version of the time-reversal operation is characterized, in the case of one particle, by the transformation $\hat{\Theta}$ of the position, momentum and spin operators

$$\hat{x}'_i = \hat{\Theta}\,\hat{x}_i\,\hat{\Theta}^{-1} = \hat{x}_i,$$

$$\hat{p}'_i = \hat{\Theta}\,\hat{p}_i\,\hat{\Theta}^{-1} = -\hat{p}_i,$$

$$\hat{S}'_i = \hat{\Theta}\,\hat{S}_i\,\hat{\Theta}^{-1} = -\hat{S}_i. \tag{9.45}$$

Thus, the time-reversal operation should more appropriately be called motion-reversal. A Hamiltonian such as $\hat{P}^2/2M + V(x)$ is invariant under this transformation.

Since a unitary transformation preserves relations between operators, the time-reversal transformation cannot be unitary. For instance,

$$[\hat{x}_i, \hat{p}_i] = -[\hat{x}'_i, \hat{p}'_i]. \tag{9.46}$$

It is possible, however, to write $\hat{\Theta}$ as a product of a unitary transformation $\hat{\mathcal{U}}_\tau$ times an operation $\hat{K}$ defined as the complex conjugation of all c-numbers. This is called an *antiunitary* transformation. Therefore,

$$\hat{\Theta}\,\varphi_i = \hat{\mathcal{U}}_\tau\,\hat{K}\,\varphi_i = \sum_{i'}\langle i'|i\rangle^*\,\hat{\mathcal{U}}_\tau\,\varphi_{i'}. \tag{9.47}$$

If $[\hat{\Theta}, \hat{H}] = 0$, the Hamiltonian eigenstates φ_i and $\hat{\Theta}\,\varphi_i$ correspond to the same eigenvalue E_i, no mater how complicated the potential may be. For instance, if the central potential is not spherically symmetric, the $2J + 1$ degeneracy disappears, but the levels still display the twofold *Kramers degeneracy* $(m, -m)$, due to the time-reversal symmetry.

The universal validity of the time-reversal invariance is still not a closed subject.

9.8[†]   Quantum Electrodynamics for Newcomers

In Chap. 1, we stated that the most relevant manifestation of the crisis in physics that took place at the beginning of the twentieth century was the (classical) instability of the motion of an electron circling around the nucleus. To show that quantum mechanics does indeed solve this problem, we must use that beautiful extension of quantum mechanics called quantum electrodynamics. In the following we present a very brief introduction to QED.

We first consider the electromagnetic field in the absence of charges (light waves). A quadratic expression for the energy is obtained in terms of canonical variables. Subsequently, the theory is quantized by replacing such variables with operators satisfying the relation (2.15) (or an equivalent). In the next step, we consider the interaction between particles and the electromagnetic field. Finally, we solve the ensuing time-dependent problem applying perturbation theory.

9.8.1[†]   *Classical Description of the Radiation Field*

In the absence of charges, the classical electromagnetic vector potential $A(r,t)$ satisfies the equation

$$\nabla^2 A = \frac{1}{c^2}\frac{\partial^2 A}{\partial t^2}. \tag{9.48}$$

The vector A may be written as the sum of a transverse and a longitudinal component. The latter can be included within the particle Hamiltonian, since it is responsible for the Coulomb interaction and does not cause the radiation field. The transverse component $A_t(r,t)$ satisfies the equation

$$\mathrm{div}\,A_t = 0. \tag{9.49}$$

It may be expanded in terms of a complete, orthonormal set $A_\lambda(r)$ of functions of the coordinates:

$$A_t = \sum_\lambda c_\lambda(t)A_\lambda, \tag{9.50}$$

$$\int_{L^3} A_\lambda^* A_{\lambda'}\,\mathrm{d}V = \delta_{\lambda,\lambda'}, \tag{9.51}$$

where we assume a large volume L^3 enclosing the field. Insertion of (9.50) in (9.48) and separation of variables yield the two equations

$$\frac{\mathrm{d}^2}{\mathrm{d}t^2}c_\lambda + \omega_\lambda^2 c_\lambda = 0, \tag{9.52}$$

$$\nabla^2 A_\lambda + \frac{\omega_\lambda^2}{c^2}A_\lambda = 0, \tag{9.53}$$

where ω_λ is introduced as a separation constant. The solution to the oscillator equation (9.52) is

$$c_\lambda = \eta_\lambda \exp(-i\omega_\lambda t), \tag{9.54}$$

with η_λ independent of time. A solution to (9.53) is given by the three-dimensional generalization (7.17) of (4.43). Periodic boundary conditions are assumed, so that

$$A_\lambda = \frac{1}{L^{3/2}} \boldsymbol{v}_\lambda \exp(\mathrm{i}\boldsymbol{k}_\lambda \cdot \boldsymbol{r}), \qquad k_{\lambda i} = 2\pi n_{\lambda i}/L. \tag{9.55}$$

There are two independent directions of polarization $\boldsymbol{v}_\lambda$, since (9.49) implies $\boldsymbol{v}_\lambda \cdot \boldsymbol{k}_\lambda = 0$.

We construct the electric field

$$\boldsymbol{E} = -\frac{\partial}{\partial t}\boldsymbol{A}_t = \mathrm{i}\sum_\lambda \omega_\lambda c_\lambda \boldsymbol{A}_\lambda. \tag{9.56}$$

The total field energy is expressed as

$$\begin{aligned}
U &= \frac{1}{2}\int_{L^3} \left(\epsilon_0|\boldsymbol{E}|^2 + \mu_0|\boldsymbol{B}|^2\right)\mathrm{d}V = \int_{L^3}\epsilon_0|\boldsymbol{E}|^2\mathrm{d}V \\
&= \epsilon_0 \sum_\lambda \omega_\lambda^2 c_\lambda^* c_\lambda \\
&= \sum_\lambda \hbar\omega_\lambda a_\lambda^* a_\lambda, \tag{9.57}
\end{aligned}$$

where the substitution

$$c_\lambda = c\sqrt{\frac{\hbar}{\epsilon_0\omega_\lambda}}a_\lambda$$

has been made. Note that since the vector field has dimension $\mathrm{k\,m\,s^{-1}\,C^{-1}}$, the amplitudes c_λ have dimension $\mathrm{k\,m^{5/2}\,s^{-1}\,C^{-1}}$ and the amplitudes a_λ are dimensionless.

9.8.2[†]   *Quantization of the Radiation Field*

We have obtained an expression for the energy of the radiation field that is quadratic in the amplitudes a_λ^*, a_λ. Quantization is achieved by replacing these amplitudes by the creation and annihilation operators a_λ^+, a_λ, satisfying the commutation relations (3.31) and (7.58). We thus obtain the Hamiltonian[5]

$$\hat{H} = \sum_\lambda \hbar\omega_\lambda\, a_\lambda^+ a_\lambda\,. \tag{9.58}$$

---

[5]We ignore the ground state energy of the radiation field.

This Hamiltonian implies that:

- The radiation field is made up of an infinite number of oscillators. The state of the radiation field is described by all the occupation numbers n_λ.
- The oscillators are of the simple, boson, harmonic type introduced in (3.29) and used in Sects. 7.4.4[†] and 7.8[†], if the quantum radiation field is in a stationary state without residual interactions.
- In agreement with Einstein's 1905 hypothesis, each oscillator has an energy which is a multiple of $\hbar\omega_\lambda$. The energy of the field is the sum of the energies of each oscillator.
- Since the radiation field is a function defined at all points of space and time, the number of canonical variables needed for its description is necessarily infinite. However, by enclosing the field within the volume L^3, we have succeeded in transforming this infinity into a denumerable infinity.
- In the absence of any interaction between particles and radiation field, vector states may be written as products of the two Hilbert subspaces, and the energy $E_{b,n_1,n_2,...}$ is the sum of particle and radiation terms [see (7.1)]

$$\Psi_{b,n_1,n_2,...} = \varphi_b(\text{particles}) \times \Pi_\lambda \frac{1}{\sqrt{n_\lambda!}} (a_\lambda^+)^{n_\lambda} \varphi_0,$$

$$E_{b,n_1,n_2,...} = E_b + \sum_\lambda \hbar\omega_\lambda n_\lambda. \tag{9.59}$$

- The number of states up to a certain energy $n(E_\lambda)$ and per unit interval of energy $\rho(E_\lambda)$ for each independent direction of polarization is[6]

$$n(E_\lambda) = \frac{L^3 k_\lambda^3}{6\pi^2} = \frac{L^3 E_\lambda^3}{6\pi^2\hbar^3 c^3}, \qquad \rho(E_\lambda) = \frac{\partial n}{\partial E_\lambda} = \frac{L^3\omega_\lambda^2}{2\pi^2\hbar c^3}. \tag{9.60}$$

- The Hermitian, quantized, vector potential reads

$$\hat{A}_t = \frac{1}{2}\sum_\lambda \sqrt{\frac{\hbar}{\epsilon_0 L^3\omega_\lambda}} \Big[a_\lambda \boldsymbol{v}_\lambda \exp(i\boldsymbol{k}_\lambda \cdot \boldsymbol{r}) + a_\lambda^+ \boldsymbol{v}_\lambda \exp(-i\boldsymbol{k}_\lambda \cdot \boldsymbol{r}) \Big]. \tag{9.61}$$

- We may be only interested in the polarization states of the photon, ignoring wavelength and direction of motion. A complete description of this system requires only two basis states, as in the case of spin. The analogous to the Stern–Gerlach device is a calcite crystal: a beam of monochromatic light passing through this crystal will produce two parallel emergent beams with the same

---

[6]These expressions have been derived using a similar procedure to the one used to obtain (7.21). A factor of 2, which was included in (7.21) due to spin, is not needed in (9.60). It reappears in (9.66), where the two directions of polarization are taken into account.

frequency and polarization axis perpendicular to each other. Most of the thought quantum experiments have become real laboratory experiments through the use of polarized photons.

9.8.3[†]   *Interaction of Light with Particles*

In the presence of an electromagnetic field, the momentum $\hat{\boldsymbol{p}}$ of the particles[7] is replaced in the Hamiltonian by the effective momentum [53]

$$\hat{\boldsymbol{p}} \longrightarrow \hat{\boldsymbol{p}} - e\hat{\boldsymbol{A}}_t, \tag{9.62}$$

$$\frac{1}{2M}\hat{\boldsymbol{p}}^2 \longrightarrow \frac{1}{2M}\hat{\boldsymbol{p}}^2 + \hat{V} + \cdots, \qquad \hat{V} = \sqrt{\frac{\alpha 4\pi\epsilon_0 \hbar c}{M^2}}\,\hat{\boldsymbol{A}}_t \cdot \hat{\boldsymbol{p}}. \tag{9.63}$$

The various ensuing processes may be classified according to the associated power of the fine structure constant α. The smallness of α (Table A.1) ensures the convergence of perturbation theory. The linear, lowest order processes require only the perturbation term $\hat{V}$. This causes transitions in the unperturbed system, particle $+$ radiation, by changing the state of the particle and simultaneously increasing or decreasing the number of field quanta by one unit (emission or absorption processes, respectively).

We apply the perturbation theory developed in Sects. 9.4 and 9.5. Since the radiation field has a continuous spectrum, a transition probability per unit time (9.38) is obtained.

According to (9.61) and (9.63), the matrix elements of the perturbation read

$$\langle b(n_\lambda + 1)|V|an_\lambda\rangle = K_\lambda \sqrt{n_\lambda + 1},$$
$$\langle b(n_\lambda - 1)|V|an_\lambda\rangle = K_\lambda \sqrt{n_\lambda}, \tag{9.64}$$

where K_λ is given by

$$
\begin{aligned}
K_\lambda &= \frac{\hbar}{M}\sqrt{\frac{\alpha\pi c}{L^3\omega_\lambda}}\,\langle b\,|(\boldsymbol{v}_\lambda \cdot p)\exp(\pm i\boldsymbol{k}_\lambda \cdot r)|\,a\rangle \\
&\approx \frac{\hbar}{M}\sqrt{\frac{\alpha\pi c}{L^3\omega_\lambda}}\,\langle b|\boldsymbol{v}_\lambda \cdot p|a\rangle \\
&= i\hbar\omega_\lambda\sqrt{\frac{\alpha\pi c}{L^3\omega_\lambda}}\,\langle b|\boldsymbol{v}_\lambda \cdot \boldsymbol{r}|a\rangle. \tag{9.65}
\end{aligned}
$$

---

[7]$[\hat{\mathbf{p}}, \hat{\mathbf{A}}_t] = 0$ because of (9.49).

We have neglected the exponential within the matrix element, on the basis of the estimate $\langle k_\lambda r \rangle \approx \omega_\lambda a_0/c = O(10^{-4})$, for $\hbar\omega_\lambda \approx 1\,\text{eV}$. The third line is derived using the relation $\hat{p} = (iM/\hbar)[\hat{H}, \hat{x}]$ (Problem 9 of Chap. 2).

We next work out the product appearing in the golden rule (9.38):

$$
\begin{aligned}
\frac{2\pi}{\hbar}|K_\lambda|^2\,\rho(E_\lambda) &= \frac{\alpha|\omega_\lambda|^3}{c^2}\,|\langle b|\boldsymbol{v}_\lambda \cdot \boldsymbol{r}|a\rangle|^2 \\
&\longrightarrow \frac{2\alpha|\omega_\lambda|^3}{3c^2}\,|\langle b|\boldsymbol{r}|a\rangle|^2\,,
\end{aligned} \tag{9.66}
$$

where we have summed over the two final polarization directions and averaged over them.

9.8.4† *Emission and Absorption of Radiation*

The transition probabilities per unit time are given by
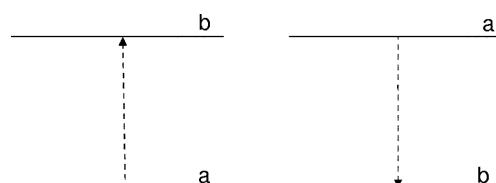
$$
\frac{\mathrm{d}P^{(1)}_{an_\lambda \to b(n_\lambda-1)}}{\mathrm{d}t} = \frac{2\alpha|\omega_\lambda|^3}{3c^2}\,|\langle b|\boldsymbol{r}|a\rangle|^2\,\bar{n}_\lambda, \tag{9.67}
$$

$$
\frac{\mathrm{d}P^{(1)}_{an_\lambda \to b(n_\lambda+1)}}{\mathrm{d}t} = \frac{2\alpha|\omega_\lambda|^3}{3c^2}\,|\langle b|\boldsymbol{r}|a\rangle|^2\,(\bar{n}_\lambda + 1), \tag{9.68}
$$

for absorption and emission processes, respectively. Here $\bar{n}_\lambda$ is the average number of photons of a given frequency (Fig. 9.3).

Fundamental consequences can be extracted from (9.67) and (9.68):

- The probability of absorbing a photon is proportional to the intensity of the radiation field present before the transition. This intensity is represented by $\bar{n}_\lambda$. This is to be expected. However, the probability of emission consists of two terms: the first one also depends on the intensity of the radiation field (induced emission); the second term, independent of the field intensity, allows the atom to decay from an excited state in vacuo (spontaneous emission).

Fig. 9.3 The absorption process (9.67) (*left*) and the emission process (9.68) (*right*) of electromagnetic radiation. Labels **a,b** denote particle states

- The mean lifetime of the excited state φ_{210} in the hydrogen atom ($\hbar\omega = 10.2\,\text{eV}$) may be obtained[8] from (9.68) and (9.40). The result yields $\tau = 0.34 \times 10^{-9}$ s. Does this represent a short or a long time? In fact it is a long time, since this mean lifetime has to be compared with the period of the emitted radiation $\mathcal{T} = 2\pi/\omega = 0.41 \times 10^{-15}$ s. The mean lifetime is associated with a spread in energy of 1.23×10^{-5} eV, which is much smaller than the excitation energy. We can see now how effectively the great crisis of early twentieth century physics was resolved.

- The ratio $(\bar{n}_\lambda + 1)/\bar{n}_\lambda$ is needed to preserve the correct thermal equilibrium of the radiation with a gas: in a gas at temperature T, the number of atoms in the states a, b is given by $\exp(-E_a/k_\text{B}T)$ and $\exp(-E_b/k_\text{B}T)$, respectively. The condition for equilibrium is

$$P_\text{emission} \exp(-E_a/k_\text{B}T) = P_\text{absorption} \exp(-E_b/k_\text{B}T), \qquad (9.69)$$

which yields

$$\bar{n}_\lambda = 1/\left[\exp(\hbar\omega_{ab}/k_\text{B}T) - 1\right]. \qquad (9.70)$$

From this deduction of Planck's law, Einstein showed the need for spontaneous and induced emission in quantum theory [64].

9.8.5[†] *Selection Rules*

We now focus our attention on the particle matrix elements. The transition probabilities are also proportional to the squared modulus of the matrix elements $|\langle b|\boldsymbol{r}|a\rangle|^2$. Therefore, transition rates give information about the value of non-diagonal matrix elements. (Since Chap. 2, we know that diagonal matrix elements represent averages obtained in measurements of the eigenvalues of physical observables.)

Let l_b, π_b (l_a, π_a) be the orbital angular momentum and parity quantum numbers of the final (initial) state. Conservation of angular momentum requires the orbital angular momentum of the final state to equal the vector sum of the initial angular momentum and that of the radiation (see Sect. 5.3.1). The latter manifests itself through the operator $\hat{\boldsymbol{r}}$ in (9.68), which can be expressed as a sum of terms proportional to the spherical harmonics Y_{1m_l}. Therefore, the matrix elements must satisfy the selection rule $l_a + 1 \geq l_b \geq |l_a - 1|$ (5.33), or $\Delta l = 0, \pm 1$.

---

[8]An order of magnitude of τ may be obtained by equating the rate of radiation of an oscillating classical dipole with the ratio between the emitted energy $\hbar\omega$ and the mean lifetime

$$\frac{\omega^4 D_0}{3c^2} = \frac{\hbar\omega}{\tau} \longrightarrow \tau = \frac{3\hbar c^2}{\omega^3 D_0}.$$

The amplitude of the dipole oscillation is approximated by $D_0 \approx -ea_0$. If the transition energy is assumed to be 10 eV, we obtain an estimated value $\tau = O(10^{-10}$ s).

Since the operator r is odd under the parity operation (5.12), the non-vanishing of this matrix element also requires the initial and final states to carry a different parity, $\pi_a \pi_b = -1$. The combination of the conservation rules associated with orbital angular momentum and parity is condensed in the selection rule

$$\Delta l = \pm 1, \tag{9.71}$$

which defines allowed transitions (see, for instance, Fig. 8.4).

Forbidden (i.e. non-allowed) transitions may also occur, but are much weaker than the allowed ones. Their relative intensity may be estimated on the basis of the expectation value of the neglected terms in (9.65).

Let us now consider the final (initial) angular momentum j_b (j_a) with projection m_b (m_a)

$$\frac{3}{4\pi}|\langle j_b m_b|\mathbf{r}|j_a m_a\rangle|^2 = \sum_\mu |\langle j_b m_b|r\,Y_{1\mu}|j_a m_a\rangle|^2$$

$$= \frac{1}{2j_b + 1}|\langle j_b||r\,Y_1||j_a\rangle|^2 \sum_\mu c\big(j_a m_a; 1\mu; j_b m_b\big)^2$$

$$= \frac{1}{2j_a + 1}|\langle j_b||r\,Y_1||j_a\rangle|^2 \sum_\mu c\big(j_b(-m_b); 1\mu; j_a(-m_a)\big)^2, \tag{9.72}$$

where we have successively applied (5.65), the definition (5.49) of the reduced matrix element and the last one of equations (5.34). In general we must sum over all possible final projections m_b. If this is the case, the first of equations (5.36) yields

$$\sum_{m_b}|\langle j_b m_b|\mathbf{r}|j_a m_a\rangle|^2 = \frac{4\pi}{3}\frac{|\langle j_b||r\,Y_1||j_a\rangle|^2}{2j_a + 1}, \tag{9.73}$$
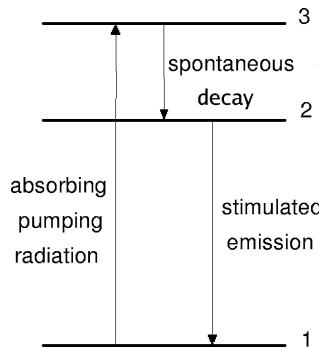
which is independent of the initial projection m_a and of other geometrical terms (such as Wigner coefficients).

9.8.6[†]   *Lasers and Masers*

The first material used to produce laser light[9] was ruby [65]. The ions undergoing laser transitions are Cr^{3+}, an impurity in the Al_2O_3 crystal.

---

[9]Laser, light amplification by stimulated emission of radiation; maser, microwave amplification by stimulated emission of radiation. These two devices differ in the range of electromagnetic frequency in which they operate.

Fig. 9.4 Schematic representation of the levels of a ruby laser

Figure 9.4 schematizes the three relevant levels of Cr. At room temperature the population of state 2 is much smaller than that of state 1, since $E_2 - E_1 \gg kT$ (see Sect. 7.7[†]). A population inversion is achieved by means of auxiliary radiation (pumping radiation) exciting many atoms into higher energy states 3 (actually into two excited bands), from which they spontaneously decay into the state 2 (or back to 1) within 10^{-7} s. Since the spontaneous lifetime of state 2 is rather large (10^{-3} s), a considerable fraction of the population of state 1 is transferred to state 2 ($\geq 1/2$).

Some of the photons spontaneously emitted in the decay of state 2 are reflected back and forth between a completely reflecting and a partially reflecting surface of the crystal. Thus a standing electromagnetic wave is built. Its intensity increases very rapidly through induced emission of further photons, simultaneously with the depopulation of state 2. A pulse of laser light crosses over the partially reflecting surface. The main characteristics of this emitted light are:

- Extreme monochromaticity.
- Large power per unit area of cross section (more than 10^9 times the one obtained from conventional light sources).
- Extreme coherence. The phase of the light emitted from one atom is related to that from each other atom. As a consequence, the phase difference between the laser light beam will stay constant at two different points (the points may be separated as much as 100 km). On the contrary, light spontaneously emitted is incoherent.

Laser light is playing an ever increasing role in many scientific and technological applications: precise determinations of length and time, CD players and readers, non-linear optics, hot fusion, etc. In communications, laser light allows to transport 10^{12} information units per second through a single optical fiber across the oceans.

Problems

Problem 1. At $t = 0$, a state is given by the linear combination of the two lowest states of a linear, infinite square well potential of width a :

$$\Psi(t = 0) = \frac{1}{\sqrt{3}}\varphi_1 - i\sqrt{\frac{2}{3}}\varphi_2.$$

1. Write the wave function at time t.
2. Calculate the probability of finding the particle in the second half of the well.

Problem 2. Use the time-dependent Schrödinger equation to show that Newton's second law is obeyed on average in quantum mechanics (Ehrenfest theorem). Hint: calculate

$$\frac{d\langle\Psi(t)|p|\Psi(t)\rangle}{dt},$$

as in (4.15).

Problem 3. In the state (9.15), calculate the amplitude of the eigenstate of the operator $\hat{S}_y$, with spin pointing in the positive direction.

Problem 4. Write the evolution operator for a Hamiltonian $-\boldsymbol{\mu} \cdot \boldsymbol{B}$ if the magnetic field points to the same direction as vector $\mathbf{n}$ ($|\mathbf{n}| = 1$).

Problem 5. A particle is in the ground state of an infinite linear square well potential. What is the probability of finding it in the $n = 1, 2, 3$ states when the wall separation is suddenly doubled by displacing the right wall?

Problem 6. Calculate the probability of a spin flip in the first order of perturbation theory. Assume the Hamiltonian (9.18) and $|\omega'/(\omega - \omega_L)| \ll 1$. Compare with the exact result (9.22).

Problem 7. A particle in the ground state of a linear harmonic oscillator interacts with a projectile through an interaction of the form $V_0\delta(u - vt/x_c)$.

1. Express the amplitude for the transition to the first excited state as an integral over the time interval $t_1 \le t \le t_2$.
2. Calculate the probability of this transition for $t_1 = -\infty$, $t_2 = \infty$.

Problem 8. The Hamiltonian

$$\hat{V}(t) = \frac{V_0}{\hbar^2}\hat{\boldsymbol{S}}_1 \cdot \hat{\boldsymbol{S}}_2 \cos(\omega t)$$

acts on a two-spin system. Find the time-dependent solution if:

1. The system has $m_s = 0$.
   Hint: try $\Psi(t) = \cos\theta \exp(i\phi)\chi_0^1 + \sin\theta \exp(-i3\phi)\chi_0^0$.
2. The system is in the Bell state $\Psi_{B_0} = \frac{1}{\sqrt{2}}\left[\varphi_\uparrow(1)\varphi_\uparrow(2) + \varphi_\downarrow(1)\varphi_\downarrow(2)\right]$.

Problem 9. What is the probability of exciting a linear harmonic oscillator from the ground state to the first excited state, assuming that a perturbation $V = Kx$, acting for an interval t, is added to the oscillator Hamiltonian?

Problem 10. 1. Obtain the expression for the second-order amplitudes $c_k^{(2)}(t)$ if the perturbation is constant in time.
2. Calculate the probability of a transition to the second excited state for the same case as in Problem 9.

Problem 11. 1. Interpret the ratio $2\Delta E\,\Delta l/\hbar c$, where Δl is the length of the system.
2. Calculate this ratio for the "giant resonance" ($\Delta E \approx 4\,\text{MeV}$) and for a slow neutron resonance ($\Delta E \approx 0.1\,\text{eV}$) in the case of a nucleus with $A \approx 100$. (See Problem 7, Chap. 6).
3. Do the same for a meson with a spread of $200\,\text{MeV}$ (proton size $\approx 10^{-17}\,\text{m}$).

Problem 12. Calculate the ratio between the populations of the states φ_{210} and φ_{310} if hydrogen atoms in their ground state are illuminated with white light.

Problem 13. 1. Calculate the ratio between the intensities of photons de-exciting the state φ_{310} of the hydrogen atom.
2. Calculate the mean lifetime of this state.
3. Calculate the width of this state.

Problem 14. Consider the transition $\varphi_{n,l=n-1} \to \varphi_{n-1,n-2}$ via the dipole operator $Q_{1\mu} = \sqrt{\frac{4\pi}{3}}\, rY_{1\mu}$ in a Rydberg atom. In the limit of large n, obtain

1. The reduced matrix element for the transition.
2. The mean lifetime τ for the $(n, n-1 \to n-1, n-2)$ transition.
3. The ratio between this lifetime and $\tau(2, 1 \to 1, 0)$.

Chapter 10
Broken Symmetries

We have discussed several problems in which the symmetry of the Hamiltonian constitutes an essential tool in the construction of the (factorized) eigenstates. In these cases, the ground state φ_0 is annihilated by the generators of the transformation associated with that symmetry. For instance, in the case of the hydrogen atom, $[\hat{H}, \hat{L}_i] = 0$ and $\hat{L}_i \varphi_0 = 0$. We say that the states carry the same symmetry as the Hamiltonian.

In the present chapter, we study situations in which this is not the case. In fact, the description with broken symmetries permeates an important fraction of today physics: ferromagnetism; superconductivity and superfluidity (condensed matter physics, nuclei, neutron stars); Hartree–Fock description (atomic and nuclear physics); molecules; quadrupole deformed nuclei; theory of electro-weak interactions and quantum chromodynamics (field theory, cosmology); etc.

The chapter is divided into two main sections. In the first one, we present the treatment of superconducting and superfluid systems by Bardeen, in collaboration with Leon N. Cooper and John R. Schrieffer. The BCS theory [66] constitutes a relevant illustration of a description based on the approximation of broken symmetries. Superconducting systems are macroscopic manifestations of quantum mechanics, and thus bear relevance in the diffuse limit between classical and quantum descriptions of nature. In addition, they display an increasing number of technical applications ranging from the transmission of electric currents without losses to the most accurate determination of the ratio $e/\hbar$.

In the second section of the chapter, we delve deeper into the concept of broken symmetry by means of a very simple mechanical example. Corrections to this approximation demand the appearance of additional degrees of freedom, the collective variables, which become compensated by the existence of constraints. Little attention, if any, is paid in quantum textbooks to the problem of quantization with constraints, an area where great progress has been made over the last 35 years [67]. This subject is not only of paramount importance in gauge field theories [68], but it also has applications in quantum mechanics, as in the description of many-body systems from moving frames of reference [69]. Moreover, the problem is conceptually significant in terms of properties of Hilbert spaces. Although we

are here restricted to present just an outline of the BRST procedure, we hope that the reader may get some feeling of this elegant method developed by C. Becchi, A. Rouet, R. Stora and I.V. Tyutin [67] (Sects. 10.2.2–10.2.4[†]).

Quantization with constraints and superconductivity are two subjects which are seldom explained together. However, although the formalism describing superconductivity has more complexity than the one employed in Sect. 10.2, the underlying mechanism of broken symmetry is similar in both cases. Moreover, the collective sector that appears as a consequence of the BRST formalism provides a phase to the BCS solution which becomes relevant in processes involving the transference of pairs of particles (e.g. Josephson junctions).

10.1   The BCS Theory of Superconductivity

In many cases for which the exact eigenstates with the correct symmetry are difficult to obtain, it is a good approximation to use solutions involving a breakdown of symmetries. In this section we present superconductivity as an illustration of a broken symmetry. The formalism applies as well to nuclear superfluidity.

Heike Kamerlingh Onnes discovered in 1911 that, below a certain temperature, most metals conduct electricity without any resistance [70]. It took almost 50 years until Bardeen, Cooper and Schrieffer developed an adequate microscopic description for the quantum state of electrons in a metal, subject to attractive interactions. They were able to explain the behavior of all superconducting materials known at the time when the theory was developed [66]. Those materials are known today as low critical temperature superconductors. The magnetic response of the superconductors as well as the formal discussion of a possible microscopic theory for the superconductivity found in copper oxide superconductors (high critical temperature superconductors) is not the subject of this introduction.

10.1.1[†]   *The Conjugate Variable to the Number of Particles*

We consider now the case of the *gauge* symmetry,[1] associated with the number of particles N. For all systems treated so far, the number of particles has been a conserved quantity and its conjugate variable has been ignored. In fact, it has been completely undetermined, as in (10.38). Thus, we start by looking for the conjugate variable θ to the number of particles. This variable does exist, as can be verified for the boson case within the harmonic description.

According to (3.42), the number of bosons $\hat{N} = a^+ a$ is given by $\frac{\hat{H}}{\hbar\omega} - \frac{1}{2}$. The corresponding classical expression is

---

[1]The use of the word *gauge* is explained in footnote 5.

$$N = \frac{1}{2\hbar} \left(\frac{1}{M\omega} p^2 + M\omega \, x^2 \right). \tag{10.1}$$

If the gauge angle is defined as

$$\theta = -\tan^{-1} \frac{p}{M\omega \, x}, \tag{10.2}$$

the (classical) Poisson bracket has the value

$$\{\theta, \hbar N\}_{\text{PB}} = \hbar \left(\frac{\partial \theta}{\partial x} \frac{\partial N}{\partial p} - \frac{\partial \theta}{\partial p} \frac{\partial N}{\partial x} \right) = 1. \tag{10.3}$$

Therefore, according to Dirac's relation (2.48), the commutator

$$[\hat{\theta}, \hbar \hat{N}] = i\hbar \tag{10.4}$$

holds. Indeed, the operator $\hbar \hat{N}$ plays the same role as a two-dimensional angular momentum, with the angle $\hat{\theta}$ being its conjugate variable.

In analogy to (4.7) and (5.37), we may also construct an operator generating rotations in gauge space

$$\mathcal{R}(\theta) = \exp(i \, \theta \hat{N})$$
$$\mathcal{R}(\theta) \, a^+ \, \mathcal{R}(-\theta) = \exp(i\theta) \, a^+. \tag{10.5}$$

We now turn our attention to the fermion case. From hereon a^+ denotes the creation of a fermion. A pair of fermions acts like a boson,[2] since changing the position of the pair does not produce a change of the wave function. Thus, to preserve (10.5) for the case of fermion pairs, we infer for the single fermion

$$\mathcal{R}(\theta) = \exp(i \, \theta \hat{N}_\pi)$$
$$\mathcal{R}(\theta) \, a^+ \, \mathcal{R}(-\theta) = \exp(i\theta/2) \, a^+, \tag{10.6}$$

where $\hat{N}_\pi$ is the operator corresponding to the number of pairs of fermions.[3]

Operators with the same number of single-fermion creation and annihilation operators behave like scalars under gauge transformations; operators with two more creation than annihilation operators behave as bosons do in (10.5)

$$\mathcal{R}(\theta) \, a_1^+ a_2 \, \mathcal{R}(-\theta) = a_1^+ a_2$$
$$\mathcal{R}(\theta) \, a_1^+ a_2^+ \, \mathcal{R}(-\theta) = \exp(i\theta) \, a_1^+ a_2^+. \tag{10.7}$$

---

[2] We have used already a similar substitution in (8.46).

[3] The factor $1/2$ in the r.h.s. of (10.6) plays a similar role as the same factor in the rotation of spin states (5.26).

10.1.2† *The Monopole Pairing Operator and the Hamiltonian*

Two identical fermions may be created at the same point of space if they are in a singlet-spin state. The associated operator in the x-representation is

$$\Gamma_{x,0}^+ = \frac{1}{\sqrt{2}} \sum_{n,n'} \langle x|n\rangle \langle x|n'\rangle \sum_{m_s=\pm\frac{1}{2}} a_{n,m_s}^+ a_{n',-m_s}^+ , \qquad (10.8)$$

see Sect. 11.1†. We consider the case for which the creation of two particles at the same point is homogeneous over all space (monopole pairing). If intermediate momentum eigenstates are used, the total operator for creating two particles at the same point is

$$\hat{P}^+ = \int \mathrm{d}x \, \Gamma_{x,0}^+ = \frac{1}{\sqrt{2}} \sum_{p,p'} \int \mathrm{d}x \, \langle x|p\rangle \langle x|p'\rangle \sum_{m_s=\pm\frac{1}{2}} a_{p,m_s}^+ a_{p',-m_s}^+$$

$$= \frac{1}{\sqrt{2}} \sum_{p>0} \sum_{m_s=\pm\frac{1}{2}} a_{p,m_s}^+ a_{-p,-m_s}^+$$

$$\rightarrow \sum_{p>0} a_p^+ a_{-p}^+ . \qquad (10.9)$$

We have used (11.7) for the overlaps $\langle x|p\rangle$ and (11.6) for the delta function. The explicit dependence on spin has been omitted in the last line, for the sake of simplicity. The notation $p > 0$ indicates that the sum includes only a single term for each (degenerate) pair of momentum states $(p, -p)$. In the nuclear case the momentum representation may be replaced by eigenstates of the Woods–Saxon potential (7.15), which can also be paired in time-reversed states (Sect. 9.7†).

A simplified, schematic Hamiltonian may be written as

$$\hat{H} = \hat{H}_{sp} + \hat{H}_{tb}$$

$$\hat{H}_{sp} = \sum_{p>0} \epsilon_p \left(a_p^+ a_p + a_{-p}^+ a_{-p} \right)$$

$$\hat{H}_{tb} = -g \, \hat{P}^+ \hat{P} . \qquad (10.10)$$

It turns out that there is a net effective attraction between the electrons, due to the interactions between the electrons with the vibrations of the ions in the lattice. Thus the strength $g > 0$. However, this attraction is very weak, and only a tiny thermal agitation is needed to destroy it. In the nuclear case there is a natural attraction between nucleons without invoking other processes.

The two-body term $\hat{H}_{tb}$ allows pairs of nearby particles to jump from one momentum state to the other, thus generating correlations in their motion. It is

called a *contact* interaction because the leap only takes place if they are at the same place. Consistently, a delta force also displays fairly constant matrix elements for the jump of pairs of particles.[4] The expression (10.10) has the advantage over a delta interaction that it has a simpler expression, due to the fact that it is written in a separable form. Nevertheless, in spite of its simplifications, this Hamiltonian is still difficult to solve (but for special cases as those described in Problems 1 and 2). Therefore, we resort to approximations. However, see Ref. [132].

Note that the Hamiltonian (10.10) is a scalar under gauge transformations (10.6).

There are also normal electrons (not bound in pairs), moving around the metal in an ordinary way. We disregard this complication here.

10.1.3[†]   *The BCS Hamiltonian*

We have mentioned that a pair of fermions acts like a boson. In a system with $N \gg 1$ bosons, the creation of all of them in a single state is favored over their distribution in different states, since the amplitude for creating a new pair is proportional to $\sqrt{N+1}$ (3.35). The essential feature of the superconducting phase is the presence of many bosons (i.e. pairs of bound electrons) in a single quantum state. This is called a condensate.

The mean-field approximation is a straightforward extension of the Hartree–Fock treatment (Sect. 8.6.1[†]). It is also obtained by using a representation in which large matrix elements of some operator become expectation values, ignoring their quantum fluctuations. In the superconducting case this operator is P^+, which bears some relation with the persistance of currents. Thus,

$$\hat{P}^+ \rightarrow \langle 0|P^+|0\rangle = \sum_{p>0}\langle 0|a_p^+ a_{-p}^+|0\rangle = \frac{\Delta}{g}\exp(i\theta), \qquad (10.11)$$

where the (real) modulus is given in units of the interaction strength. Thus, we require that $\Delta/g \gg 1$.

The phase angle θ of the condensate represents the orientation of the system in gauge space. Since it is conjugate to the number of bosons in the condensate, it is completely undefined [as in (10.38)] for systems with a definite number of pairs of particles. The choice of a particular value of θ in (10.11) implies that:

- The original symmetry of the Hamiltonian is broken in the state φ_0.
- The number of pairs of particles becomes ill defined. This is consistent with the fact that the expectation value of an operator creating two particles is different from zero.

---

[4]There are also cases of superconductivity for which other components of the interaction have to be introduced.

- We may request that at least the average number of pairs of particles has a prescribed value A_π. Thus, we add to the Hamiltonian (10.10) a term changing the origin of single-particle energies, which has a vanishing expectation value

$$-2\mu\,(\hat{N}_\pi - A_\pi)\,;\qquad A_\pi \equiv \langle 0|N_\pi|0\rangle. \qquad (10.12)$$

The (pair-degenerate) single-particle energies ϵ_p become replaced by $\epsilon_p - \mu$. The constant μ is used to fix the average number of particles to the number $2A_\pi$, and plays a similar role as the Fermi energy in normal systems (see Sect. 7.7†). It is called a Lagrange multiplier.

In the following we choose $\theta = 0$. However, since this option is arbitrary,[5] physical results should not depend on it.

The monopole pairing operator can be written as

$$\hat{P}^+ = \frac{\Delta}{g} + \left(\hat{P}^+ - \frac{\Delta}{g}\right), \qquad (10.13)$$

where the first term on the right hand side is supposed to be much larger than the term between parenthesis. The BCS Hamiltonian is obtained by expanding $\hat{H}_{\text{tb}}$ in powers of Δ/g. To leading orders,[6]

$$\hat{H} \to \hat{H}_{\text{BCS}} = 2\mu A_\pi - \frac{\Delta^2}{g}$$
$$+ \sum_{p>0}\left[(\epsilon_p - \mu)\left(a_p^+ a_p + a_{-p}^+ a_{-p}\right) - \Delta\left(a_p^+ a_{-p}^+ + a_{-p}a_p\right)\right]. \qquad (10.14)$$

Since this Hamiltonian is only quadratic in the fermion creation and annihilation operators, it is easy to diagonalize. We use the transformation

$$\alpha_{\pm p}^+ = U_p a_{\pm p}^+ \mp V_p a_{\mp p}. \qquad (10.15)$$

The operators $\alpha_{\pm p}^+$ create excitations called quasi-particles. They carry good momentum $\pm p$, since the annihilation of an entity carrying momentum $\mp p$ implies the creation of the momentum $\pm p$. The normalization condition implies

$$U_p^2 + V_p^2 = 1. \qquad (10.16)$$

---

[5]The word *gauge* is used in this chapter by the similarity with electromagnetic theory, where a gradient may be added to the vector potential without altering the physical results.

[6]Parts of the residual terms in $\hat{H} - \hat{H}_{\text{BRST}}$ are taken into account in Sect. 10.1.5†.

The diagonalization amounts to insure the vanishing of the terms creating two-quasi-particles in (10.14). Inversion of (10.15) and replacement in $\hat{H}_{\mathrm{BCS}}$ yields the equations

$$2U_pV_p = \frac{\Delta}{E_p} \quad \text{and} \quad U_p^2 - V_p^2 = \frac{\epsilon_p - \mu}{E_p}, \tag{10.17}$$

which determine the ground state energy W, the quasi-particle excitation energies E_p, and the amplitudes U_p, V_p.

$$\hat{H}_{\mathrm{BCS}} = W + \sum_{p>0} E_p \left(\alpha_p^+ \alpha_p + \alpha_{-p}^+ \alpha_{-p} \right) \tag{10.18}$$

$$W = 2 \sum_{p>0} \epsilon_p V_p^2 - \frac{\Delta^2}{g} \; ; \qquad E_p = \sqrt{(\epsilon_p - \mu)^2 + \Delta^2} \; ;$$

$$U_p = \frac{1}{\sqrt{2}} \left(1 + \frac{\epsilon_p - \mu}{E_p} \right)^{1/2} \; ; \qquad V_p = \frac{1}{\sqrt{2}} \left(1 - \frac{\epsilon_p - \mu}{E_p} \right)^{1/2} .$$

The Hamiltonian $\hat{H}_{\mathrm{BCS}}$ describes a system of independent quasi-particles. The condensate provides an energy of order Δ to each single-particle excitation energy $|\epsilon_p - \mu|$, and an extra contribution to the binding energy.

In the limit $\Delta \to 0$, $V_p = 1$ (0) and $U_p = 0$ (1) for single-particle energies $(\epsilon_p - \mu) < 0$ (> 0). For a normal system, V_p drops abruptly from 1 to 0 at the Fermi level, while in superconducting systems there is a diffuseness of the Fermi energy extending over a range of size Δ. The BCS solution is able to describe solutions ranging from a cylindrically symmetric vacuum (completely undetermined θ) to a vacuum which does not display this symmetry.

There are still two parameters in this solution, Δ and μ, which must be determined. This is accomplished by making use of the following two requirements:

- The expectation value (10.11) and the first of requirements (10.17) yield the self-consistent condition

$$\frac{2}{g} = \sum_{p>0} \frac{1}{E_p}. \tag{10.19}$$

  A solution with a non-vanishing Δ is always obtained for sufficiently large values of g.
- The requirement that the average number of the pair of particles corresponds to a certain prefixed value A_π is written as

$$\frac{1}{2} \left\langle 0| \sum_p a_p^+ a_p |0 \right\rangle = \sum_{p>0} V_p^2 = A_\pi. \tag{10.20}$$

10.1.4[†]   *The Ground State*

The ground state φ_0 represents the vacuum of quasi-particles ($\alpha_p \varphi_0 = 0$). In terms of particles, it is given by

$$\varphi_0 = \prod_{p>0} \left(U_p + V_p a_p^+ a_{-p}^+ \right) |\rangle, \tag{10.21}$$

where $|\rangle$ is the true vacuum of particles.

The matrix elements for the creation and the destruction of a particle between the ground state and the states $\alpha_p^+ \varphi_0$ are given by

$$\langle \alpha_p^+ | a_p^+ | 0 \rangle = U_p, \qquad \langle \alpha_p^+ | a_p | 0 \rangle = -V_p. \tag{10.22}$$

Therefore, U_p^2 (V_p^2) in (10.18) is the probability that the particle state p is empty (occupied).

The expectation value of the operator creating a pair of particles is

$$\langle 0 | a_p^+ a_{-p}^+ | 0 \rangle = U_p V_p = \frac{\Delta}{2 E_p} \leq \frac{1}{2}. \tag{10.23}$$
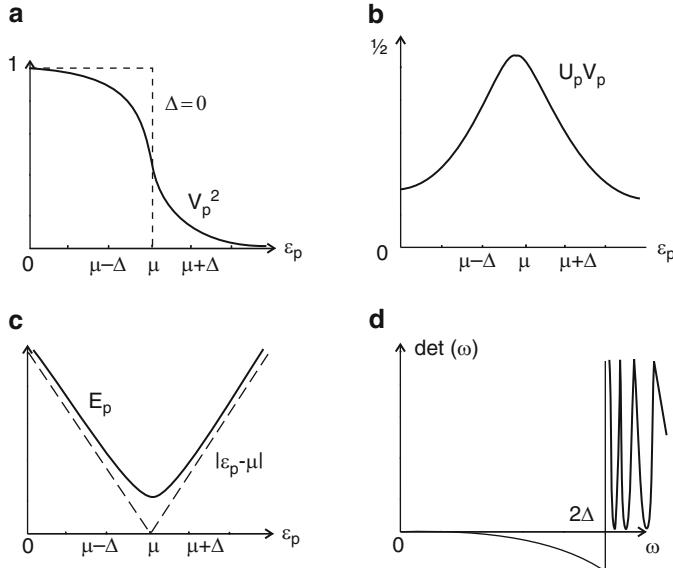
This expectation number is larger for states within the gap ($|\epsilon_p - \mu| << \Delta$) and decreases for distant states ($|\epsilon_p - \mu| >> \Delta$). Replacement of (10.23) in (10.19) yields the ratio Δ/g. It is a large number (as required), since all contributions to the sum (10.11) have the same sign.

As an illustration, let us consider the case of 19 pairs of particles allowed to move in 38 single-particle equidistant levels. The distance between consecutive levels will be the unit of energy. For $g = 0.456$, (10.19) and (10.20) yield the parameters $\Delta = 4.50$ and $\mu = 19.50$. The quasi-particle energies E_p are compared with the particle excitation energies $|\epsilon_p - \mu|$ in Fig. 10.1c. The occupation probabilities V_p^2 are represented in Fig. 10.1a and the amplitudes $U_p V_p$ in Fig. 10.1b.

The particles constituting a pair are not very close in real space, in spite of the fact that a contact interaction has been used: the mean value of this distance is somewhat larger than the average distance between different pairs of particles. This is due to the fact that, in the condensate, there are many pairs of particles occupying the same state.

10.1.5[†]   *The Excitation Spectrum*

The ground state (10.21) displays an even number of particles. In fact, although the transformation (10.15) to quasi-particles does not conserve the number of particles, it preserves the parity in the number of particles. Systems with an even number of particles are represented by states with an even number of quasi-particles, including

Fig. 10.1 Occupation probabilities V_p^2 (**a**); amplitudes $U_p V_p$ (**b**); and quasi-particle energies E_p (**c**), as functions of the particle energies ϵ_p. The determinant $\det(\omega)$ is represented as a function of ω in (**d**) [see (10.29)]

the vacuum state φ_0. Odd systems are in correspondence with states with an odd number of quasi-particles, like $\alpha_p^+ \varphi_0$.

Therefore, the lowest excited states of an even system consists of two quasi-particle states $\alpha_{p_1}^+ \alpha_{p_2}^+ \varphi_0$, with energies $E_{p_1} + E_{p_2} \geq 2\Delta$. Thus, the spectrum displays a gap in the vicinity of the ground state.

In a normal conductor, resistance originates from the heat produced by collisions of the moving electrons with the ionic lattice. In a superconductor, the current is due to pairs of electrons moving together, each pair with a non-vanishing center of mass momentum. These pairs form a highly collective quantum condensate: breaking a pair requires a change of energy of all other pairs, which is of order of the gap (≈ 2.7 meV for Nb). Thus, resistance is suppressed.

However, since there is no restoring force in the θ angular direction, we should expect the existence of a zero frequency boson, which appears to be precluded by the existence of a gap. Nevertheless, we have seen in Sect. 8.6.2[†] that low energy bosons may appear as RPA excitations of the ground state in fermion systems. In the following, we search for this type of excitations in the superconducting case.

We again take advantage of the fact that a pair of fermion operators acts in many respects as a boson, and make the replacement

$$\alpha_p^+ \alpha_{-p}^+ \rightarrow \gamma_p^+ ; \quad [\gamma_p, \gamma_{p'}^+] = \delta_{pp'}. \tag{10.24}$$

We now focus our attention on states of the form $\alpha_p^+ \alpha_{-p}^+ \varphi_0 \rightarrow \gamma_p^+ \varphi_0$, with energies $2E_p$.

In addition to the BCS Hamiltonian (10.14), there are residual interactions that are quartic products of quasi-particle operators. We select those terms which allow for the replacement of the two pairs of fermions, $\alpha_p^+ \alpha_{-p}^+$ and $\alpha_{-p} \alpha_p$, by the bosons (10.24), and thus, become quadratic in these boson operators.[7] We also obtain the operator associated with the number of pairs of particles

$$\hat{H}_b = W + \sum_{p>0} 2E_p \gamma_p^+ \gamma_p - g \sum_{p,p'>0} (U_p^2 \gamma_p^+ - V_p^2 \gamma_p)(-V_{p'}^2 \gamma_{p'}^+ + U_{p'}^2 \gamma_{p'})$$

$$(\hat{N}_\pi)_b = A_\pi + \sum_{p>0} U_p V_p (\gamma_p^+ + \gamma_p). \tag{10.25}$$

We carry below the uncoupling of the bosons γ_p^+, γ_p in $\hat{H}_b$, and we find that a zero frequency root $\omega_0 = 0$ is always present (Fig. 10.1d). The associated creation operator $\Gamma_0^+ (= \Gamma_0)$ is proportional to the boson term of the operator[8] $\hat{N}_\pi$ in the last line of (10.25).

The Uncoupling of the Hamiltonian (10.25) and the Presence of the Zero-Frequency Excitation

The procedure is completely similar to the one applied in the RPA (Sect. 8.6.2[†]). We perform the linear transformation

$$\Gamma_\nu^+ = \sum_{p>0} (\lambda_{\nu p} \gamma_p^+ - \mu_{\nu p} \gamma_p). \tag{10.26}$$

Use is made of the commutation

$$[\hat{H}_b, \Gamma_\nu^+] = \sum_{p>0} \left(\lambda_{\nu p} 2E_p - \Lambda_{\nu 1} V_p^2 - \Lambda_{\nu 2} U_p^2 \right) \gamma_p^+$$

$$+ \sum_{p>0} \left(\mu_{\nu p} 2E_p + \Lambda_{\nu 1} U_p^2 + \Lambda_{\nu 2} V_p^2 \right) \gamma_p \tag{10.27}$$

$$\Lambda_{\nu 1} \equiv g \sum_{p>0} (\lambda_{\nu p} V_p^2 - \mu_{\nu p} U_p^2), \qquad \Lambda_{\nu 2} \equiv g \sum_{p>0} (\lambda_{\nu p} U_p^2 - \mu_{\nu p} V_p^2).$$

---

[7]It can be shown that the remaining terms only yield higher order contributions in perturbation theory [69].

[8]The applicability of the BRST procedure (Sect. 10.2.1) also requires the existence of a zero frequency boson. The generator $\hat{N}_\pi$, together with the angle θ, are incorporated into the unphysical sector, as in Sect. 10.2.4[†].

The amplitudes λ_{vp}, μ_{vp} are obtained from the condition that the coefficients of the operators γ_p^+ and γ_p vanish in the harmonic equation $[\hat{H}_b, \Gamma_v^+] - \omega_v \Gamma_v^+ = 0$. One obtains

$$\lambda_{vp} = \frac{\Lambda_{v1} V_p^2 + \Lambda_{v2} U_p^2}{2E_p - \hbar\omega_v}, \qquad \mu_{vp} = -\frac{\Lambda_{v1} U_p^2 + \Lambda_{v2} V_p^2}{2E_p + \hbar\omega_v}. \tag{10.28}$$

Introduction of (10.28) into the definitions on the last line of (10.27) yields two linear, homogeneous, coupled equations, which should have a null determinant

$$0 = \Lambda_{v1}\left(A - \frac{1}{g}\right) + \Lambda_{v2} C ; \qquad 0 = \Lambda_{n1} C + \Lambda_{n2}\left(B - \frac{1}{g}\right)$$

$$\det(\omega) = \left(A - \frac{1}{g}\right)\left(B - \frac{1}{g}\right) - C^2, \tag{10.29}$$

where

$$A = \sum_{p>0}\left(\frac{V_p^4}{2E_p - \hbar\omega} + \frac{U_p^4}{2E_p + \hbar\omega}\right); \qquad B = \sum_{p>0}\left(\frac{U_p^4}{2E_p - \hbar\omega} + \frac{V_p^4}{2E_p + \hbar\omega}\right)$$

$$C = 4\sum_{p>0}\frac{U_p^2 V_p^2 E_p}{4E_p^2 - \hbar^2\omega^2}. \tag{10.30}$$

The Hamiltonian $\hat{H}_b$ may be expressed in terms of the bosons (10.26)

$$\hat{H}_b = W - g\sum_{p>0}V_p^4 + \sum_v \hbar\omega_v \Gamma_v^+ \Gamma_v, \tag{10.31}$$

where the frequencies ω_v are given by the roots of the equation $\det(\omega) = 0$. The determinant is represented in Fig. 10.1d as a function of ω, using the same parameters as in Figs. 10.1a–c. Poles appear at each unperturbed excitation value $2E_p$: there are none within the gap 2Δ and become compressed just above the gap; they are separated by twice the distance between consecutive levels for higher states.

The roots ω_v display a density similar to that of the poles (they are completely intermixed), but for the root $\omega_0 = 0$, which is present at the origin. Using the normalization condition (10.16) and the self-consistency requirement (10.19), it is simple to show that there is always a zero frequency root, independently of the single-particle spectrum and of the number of pairs of particles. Moreover, the relative amplitudes of the (coupled) bosons $\gamma_p^+ + \gamma_p$ for this root are proportional to $U_p V_p$, and thus $\Gamma_0^+ + \Gamma_0$ is proportional to the boson term in $\hat{N}_\pi$ (10.25).

10.1.6† *Collective sector. Rotational Bands. Josephson Junctions*

The breaking of rotational invariance is always associated with the occurrence of rotational degrees of freedom. The simplest example is given by the diatomic molecule (see Sect. 8.4.3).

The intrinsic motion is described relative to the body-fixed coordinate frame $\theta = 0$. The orientation of the body-fixed frame relative to the laboratory frame is determined by the collective azimuthal angle ϕ. The separation of motion into intrinsic and rotational components yields the product state

$$\Psi_{n_\nu, A_\pi} = \frac{1}{\sqrt{2\pi}} \exp(iA_\pi \phi) \prod_{\nu \neq 0} \frac{1}{\sqrt{n_\nu!}} \left(\Gamma_\nu^+ \right)^{n_\nu} \varphi_0, \tag{10.32}$$

where A_π is the number of pairs of particles. In the present subsection, the relevance of the presence of the collective eigenvector $\exp(iA_\pi \phi / \sqrt{2\pi})$ (5.60) in the description of a superconductor is emphasized.

The product states (10.32) constitute an approximation, since there appear more degrees of freedom than the original ones. One consequence is that overcompleteness and Pauli violations are included in (10.32). However, a legitimation of these states is presented in Sect. 10.2.

States with the same number n_ν of finite frequency bosons can be grouped into "rotational" bands made up from systems with different numbers of pairs of particles. In particular, the set of ground states of even systems constitutes a rotational band. The associated rotational energies can be obtained as in (10.65).

Since φ_0 is a valid description of the ground state in the intrinsic system, any operator must be transformed to this system before operating within states (10.32). For instance, using (10.7)

$$\langle n_\nu = 0, A_\pi' | \mathcal{R}^{-1}(\phi) \, P^+ \, \mathcal{R}(\phi) | n_\nu = 0, A_\pi \rangle$$

$$= \frac{\langle 0 | P^+ | 0 \rangle}{2\pi} \int_0^{2\pi} d\phi \, \exp[i(-A_\pi' + 1 + A_\pi)]$$

$$= \frac{\Delta}{g} \delta_{A_\pi', A_\pi + 1}. \tag{10.33}$$

The presence of the collective sector in (10.32) ensures the conservation of the number of particles, which the intrinsic state φ_0 by itself does not. Moreover, (10.33) is the large matrix element of the transfer operator connecting consecutive members of the ground state band.

A Josephson junction [71] is made up from two superconductors separated by a thin layer of insulating material. We assume, for simplicity, that the two superconductors are made of the same material and that the junction is symmetrical.

A potential difference V may exist between the two sides of the insulating barrier. Therefore, there appears a difference between the Fermi energies of the two superconductors $\mu_1 - \mu_2 = eV$, where e is the electron charge. The Lagrange

multipliers are related to the angular frequencies by the canonical equation through the term (10.12) included in $\hat{H}_{BCS}$,

$$\dot{\phi} = \frac{\partial H_{BCS}}{\hbar \, \partial A_\pi} = \frac{2}{\hbar} \mu. \tag{10.34}$$

Thus, one obtains

$$\dot{\phi}_1 - \dot{\phi}_2 = \frac{2}{\hbar} eV$$

$$\phi_1 - \phi_2 = \frac{2}{\hbar} eV (t - t_0) + \delta_0 \tag{10.35}$$

Our aim is to find the probability amplitude for the electrons to jump across the junction. This tunneling can be represented by a symmetrical coupling that destroys a pair on one side of the barrier and creates another on the other side ([38], Chap. 6)

$$\hat{H}_{coup} = K \, \cos{(\phi_1 - \phi_2)}, \tag{10.36}$$

where K is a constant determining the intensity of the tunneling. The presence of (10.36) prevents the separate conservation of $(A_\pi)_1$ and $(A_\pi)_2$. In fact, the canonical equations $(\dot{A}_\pi)_i = -\frac{\partial H}{\partial \phi_i}$ yield the current J from superconductor 1 to 2

$$J \propto (\dot{A}_\pi)_1 = -(\dot{A}_\pi)_2 = -\frac{\partial H_{coup}}{\hbar \partial \phi_1}$$

$$= J_0 \, \sin{(\phi_1 - \phi_2)} = J_0 \, \sin{\left(\frac{2eV}{\hbar} (t - t_0) + \delta_0 \right)} \tag{10.37}$$

The current J_0 is the maximum current that can be passed by the junction. It is proportional to the coupling strength K.

- dc Josephson current: with no applied dc voltage, a dc current flows across the junction, with a value between J_0 and $-J_0$ depending on the phase shift δ_0
- ac Josephson current: with a dc voltage applied across the junction, an ac current oscillates with frequency $\omega = 2eV/\hbar$. Thus, a photon of energy $\hbar\omega = 2eV$ is emitted or absorbed each time that a pair crosses the junction. Note the factor 2, which reflects the fact that it is a pair of electrons that crosses. A very precise measure of the ratio $e/\hbar$ is obtained by measuring voltage and frequency.

10.2   Quantization with Constraints

10.2.1   Constraints

Let us consider a very simple system of one particle constrained to move along a circumference of radius r_0, in real space. Thus, as in the BCS case, there is an initial

circular symmetry. The fact that one takes place in gauge space, and the other in real space, is immaterial. On the other hand, this toy model is much simpler to handle, because any other degree of freedom is gone, but the rotation along the angular coordinate θ.

The Hamiltonian and eigenstates are given by

$$\hat{H} = \frac{\hat{L}^2}{2M r_0^2}, \qquad \varphi_m(\theta) = \frac{1}{\sqrt{2\pi}} \exp(im\theta), \qquad (10.38)$$

where $\hbar m$ is the eigenvalue of the angular momentum $\hat{L}$ and the conjugate angle θ is completely undetermined ($0 \leq \theta \leq 2\pi$). In particular, the ground state satisfies the relation $\hat{L}\varphi_0 = 0$.

However, other descriptions are also possible. For instance, from a rotating frame of reference. In this case, states $\varphi(\theta)$ carry less symmetry than the circular symmetry associated both with the Hamiltonian and with the eigenstates (10.38). We say that there has been a breakdown of symmetry.

Moreover, this description requires the inclusion of the angle ϕ specifying the orientation of the moving frame relative to the laboratory. Hence, we have an overcomplete set of degrees of freedom, namely the two angles θ and ϕ.

We call *intrinsic*, the coordinates of a system that are referred to a rotating frame of reference. The motion of the moving frame relative to the laboratory is described by means of *collective* coordinates. Therefore, in this problem:

- The rotations of the system are generated by the intrinsic angular momentum $\hat{L}$ (5.37). There is also a collective angular momentum $\hat{I}$, the generator of rotations of the moving frame.
- The classical set of equations defining the momenta in terms of partial derivatives of the Lagrange function $\mathcal{L}$ cannot be solved in this case. This failure is due to the fact that this function does not contain information about the frame itself. For instance, in the case of one particle allowed to move on a circumference of radius r_0, the Lagrange function may be expressed in terms of the angular velocities $\dot{\theta}$ and $\dot{\phi}$ (Fig. 10.2):

$$\mathcal{L} = \frac{\mathcal{J}}{2} \left(\dot{\theta} + \dot{\phi} \right)^2. \qquad (10.39)$$

Here $\theta = \tan^{-1}(y/x)$ and $\mathcal{J} = M r_0^2$ is the moment of inertia. From the equations
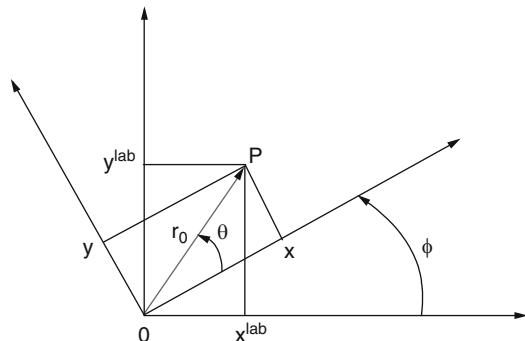
$$L = \frac{\partial \mathcal{L}}{\partial \dot{\theta}} \qquad \text{and} \qquad I = \frac{\partial \mathcal{L}}{\partial \dot{\phi}},$$

one obtains the orbital angular momentum L and the constraint $L = I$:

$$L = \mathcal{J} \left(\dot{\theta} + \dot{\phi} \right), \qquad (10.40)$$

$$f \equiv L - I = 0. \qquad (10.41)$$

Fig. 10.2 Intrinsic (x, y) and laboratory $(x^{\mathrm{lab}}, y^{\mathrm{lab}})$ coordinates of a generic point P. The two sets of coordinates are related by a rotation. Reproduced from Fig. 1 of the second of Refs. [69], with authorization from A.A.P.T

Equation (10.41) expresses the obvious fact that if the particle is rotated through an angle relative to the moving frame, the corresponding description should be completely equivalent to the one obtained by rotating the moving frame in the opposite direction. This constitutes a mechanical analogue of a gauge invariance. The quantity f is the classical generator of transformations within the gauge space associated with this simple model. It transforms a given physical trajectory into an equivalent one described from another frame. To choose a gauge means to select only one of these equivalent trajectories.

- Our aim is to quantize this classical model. The following commutation relations hold:

$$[\hat{\theta}, \hat{L}] = [\hat{\phi}, \hat{I}] = i\hbar. \tag{10.42}$$

Since we have artificially enlarged the vector space, we must expect the presence of unphysical states and operators, in addition to physical ones. The constraint (10.41) is equivalent to the quantum mechanical conditions

$$\hat{f}\varphi_{\mathrm{ph}} = 0, \qquad \hat{f}\varphi_{\mathrm{unph}} \neq 0,$$
$$[\hat{f}, \hat{O}_{\mathrm{ph}}] = 0, \qquad [\hat{f}, \hat{O}_{\mathrm{unph}}] \neq 0, \tag{10.43}$$

where the labels "ph" and "unph" indicate physical and unphysical states or operators. Except in simple cases, this separation is by no means a trivial operation.

- Since the problem displays circular symmetry, there is no restoring force in the intrinsic angular direction. Therefore, we expect a zero energy state created by an operator proportional to the generator $\hat{L}$. Consequently, "infrared divergences" may prevent the applicability of perturbation theory.

10.2.2   Outline of the BRST Solution

The most natural thing to do would be to use the constraint (10.41) to reduce the number of variables to the initial number. However, progress has been made in the

opposite direction, i.e. by enlarging the number of variables and introducing a more powerful symmetry.

The collective subspace is given by the eigenfunctions of the orbital angular momentum in two dimensions (5.60):

$$\varphi_m(\phi) = \frac{1}{\sqrt{2\pi}} \exp(im\phi). \tag{10.44}$$

The collective coordinate ϕ, which was introduced in Sect. 10.2.1 as an artifact associated with the existence of the moving frame, has been raised to the status of a real degree of freedom.

Since this problem has only one real degree of freedom, and since this role is taken by the collective angle, all others are unphysical. There must therefore be a trade-off: the intrinsic coordinate θ has to be transferred to the unphysical subspace.

In the BRST procedure, this unphysical subspace is also integrated with auxiliary fields [67]. All effects of the unphysical degrees of freedom on any physical observable must cancel out. Moreover, the degree of freedom $(\hat{\theta}, \hat{L})$ acquires a finite frequency through its mixture with the other spurious fields, and perturbation theory becomes feasible.

Quite generally, the total zero-order state may be factorized into three terms:

- A collective term carrying a representation of the degrees of freedom corresponding to the symmetry that is being restored: $\frac{1}{\sqrt{2\pi}}\exp(im\phi)$ for two dimensional rotations (10.44); $\sqrt{\frac{2I+1}{8\pi^2}} D^I_{MK}$ for three dimensional rotations (5.43); $\frac{1}{\sqrt{V}}\exp(i\mathbf{p}\cdot\mathbf{r}/\hbar)$ for translations (7.17); etc..
- A term representing the physical intrinsic degrees of freedom. For instance, had a radial potential $\frac{1}{2}M\omega^2(r - r_0)^2$ been added to the Hamiltonian, a harmonic oscillator would describe the (real) motion along the radial direction.
- An unphysical term including the degrees of freedom associated with the broken symmetries in the intrinsic system, plus the auxiliary fields that have been introduced.

The reader may believe these conclusions and proceed to Sect. 10.3 if he or she does not wish to get involved with the somewhat abstract BRST manipulations.

Note that the BRST procedure can be applied in particular to the BCS solution (Sect. 10.1), which displays all the necessary features:

1. There is an initial circular symmetry (in gauge space).
2. This symmetry is destroyed in the chosen, arbitrary frame ($\theta = 0$).
3. There is a large parameter measuring the deformation in gauge space (Δ/g). It plays the same role as r_0 in the toy model. Eventually, a perturbation expansion in inverse powers of this parameter becomes possible.
4. There is a zero frequency boson associated with the generator of rotations in gauge space ($\hat{N}_\pi$).

Thus, (10.32) becomes completely justified.

10.2.3[†] *A Presentation of the BRST Symmetry for the Abelian Case*

An elementary presentation of the quantum mechanical BRST method is given in the second of references [69]. In the following, we follow this presentation.

- A new symmetry requires additional degrees of freedom. Thus, the gauge symmetry implied the existence of both intrinsic and collective coordinates (10.40). The BRST enlarged space is obtained through further inclusion of a new boson degree of freedom,[9] with an associated constraint,

$$[\hat{\mu}, \hat{B}] = i, \qquad \hat{B}\, \varphi_{\text{ph}} = 0, \tag{10.45}$$

and of two new fermion variables η and $\bar{\eta}$, called ghosts, with their conjugate partners π and $\bar{\pi}$

$$\{\eta, \pi\} = \{\bar{\eta}, \bar{\pi}\} = 1. \tag{10.46}$$

All other anticommutators vanish. The ghosts carry zero angular momentum.

- The generator $\hat{\Omega}$ of BRST transformations is a linear function of the two constraints (10.43) and (10.45)

$$\hat{\Omega} = -\eta \hat{f} + \bar{\pi} \hat{B}. \tag{10.47}$$

It is a nilpotent ($\hat{\Omega}^2 = 0$) and Hermitian ($\hat{\Omega}^+ = \hat{\Omega}$) operator, which annihilates physical states and commutes with physical operators [see (10.43)]

$$\hat{\Omega}\, \varphi_{\text{ph}} = 0, \qquad [\hat{\Omega}, \hat{Q}_{\text{ph}}] = 0. \tag{10.48}$$

- However, there is a set of unphysical states and operators satisfying similar properties, namely

$$\varphi_{\chi} = \hat{\Omega}\, \varphi_{\text{unph}}, \qquad \hat{Q}_{\chi} = \{\hat{\Omega}, \hat{Q}_{\text{unph}}\}. \tag{10.49}$$

Therefore, we must act within the composite subspace $\varphi_{\text{ph}} + \varphi_{\chi}$ with the set of operators $\hat{Q}_{\text{ph}} + \hat{Q}_{\chi}$. States φ_{χ} have zero norm. Fortunately, the enlargement of space and of the set of operators does not change the values of the matrix elements, since

$$(\langle \text{ph}| + \langle \chi|)(Q_{\text{ph}} + Q_{\chi})(|\text{ph}\rangle + |\chi\rangle) = \langle \text{ph}|Q_{\text{ph}}|\text{ph}\rangle. \tag{10.50}$$

---

[9]The boson term $\hat{\mu}$ may include a constant value that plays the role of the Lagrange multiplier (10.12) in the previous section. We use $\hbar = 1$ in Sects. 10.2.3 and 10.2.4.

This statement may be verified term by term. For instance,

$$\langle\chi|Q_\chi|\text{ph}\rangle = \langle\text{unph}|\Omega^2\,Q_{\text{unph}}|\text{ph}\rangle + \langle\chi|Q_{\text{unph}}\,\Omega|\text{ph}\rangle = 0 + 0. \quad (10.51)$$

- We construct the BRST Hamiltonian by adding to the Hamiltonian $\hat{H}$ a $\hat{Q}_\chi$ operator

$$\hat{H}_{\text{BRST}} = \hat{H} + \{\hat{\rho}, \hat{\Omega}\} \quad (10.52)$$

For any choice of the operator $\hat{\rho}$, $\hat{H}_{\text{BRST}}$ yields the same physical eigenvalues as the original $\hat{H}$. The selection of $\hat{\rho}$ is equivalent to the selection of a gauge. One possible choice is motivated by an analogy with the covariant gauge in Yang–Mills theory

$$\hat{\rho} = \pi\hat{\mu} + \bar{\eta}\left(\hat{\theta} - \frac{1}{2\mathcal{I}}\hat{B}\right)$$

$$\hat{H}_{\text{BRST}} = \hat{H} - \hat{\mu}\hat{f} + i\pi\bar{\pi} + \hat{B}\hat{\theta} - \frac{1}{2\mathcal{I}}\hat{B}^2 + \eta\bar{\eta}\,[\hat{\theta}, \hat{L}], \quad (10.53)$$

where $\mathcal{I} = Mr_0^2$ is the moment of inertia and $\hat{\theta}$ is a function of the intrinsic coordinates which does not commute with $\hat{L}$. It may well be the conjugate angle, but this is not necessary. Since $\hat{H}_{\text{BRST}}$ does not commute with $\hat{L}$ (unlike $\hat{H}$), the microscopic circular symmetry is lost. Microscopic invariance is replaced by a macroscopic collective invariance.

10.2.4[†]   *Application of the BRST Formalism to the Abelian Toy Model*

The previous subsection displays a quite general presentation of the BRST formalism as applied to Abelian transformations. We return now to the toy model described in Sect. 10.2.1. We may choose the classical, "deformed" solution $x = r_0$, $y = 0$ as the starting point for the motion in the intrinsic system. The radius r_0 constitutes the large distance of the problem, the *order parameter*. Thus, the leading contribution to the particle angular momentum is $\hat{L}^{(0)} = r_0\,\hat{p}_y$. It is convenient to choose $\hat{\theta}$ as the conjugate variable to this leading order term: $\hat{\theta} = \hat{y}/r_0$. This choice fixes the particle to the moving x-axis. Thus, $\hat{H}_{\text{BRST}}$ (10.53) may be written as

$$\hat{H}_{\text{BRST}} = \hat{H}_b + \hat{H}_g + \hat{H}_c + \hat{H}_x$$

$$\hat{H}_b = \frac{1}{2M}\hat{p}_y^2 - r_0\hat{\mu}\hat{p}_y + \frac{1}{r_0}\hat{B}\hat{y} - \frac{1}{2\mathcal{I}}\hat{B}^2$$

$$\hat{H}_g = i\pi\bar{\pi} + i\eta\bar{\eta}$$

$$\hat{H}_c = \hat{\mu}\,\hat{I}$$

$$\hat{H}_x = \frac{1}{2M}\hat{p}_x^2 + \frac{1}{r_0}(\hat{x} - r_0)\,\eta\,\bar{\eta} + \hat{\mu}\,[(\hat{x} - r_0)\hat{p}_y - \hat{y}\hat{p}_x]. \quad (10.54)$$

As usual in field theory, we proceed to diagonalize the quadratic Hamiltonian to define a basis of independent bosons and fermions. By completing squares, we obtain for $\hat{H}_b$

$$\hat{H}_b = \frac{1}{2M}(\hat{p}_y - Mr_0\hat{\mu})^2 + \frac{M}{2}\hat{y}^2 - \frac{1}{2\mathcal{I}}\left(\hat{B} - Mr_0 y\right)^2 - \frac{\mathcal{I}}{2}\hat{\mu}^2$$

$$= \Gamma_1^+\Gamma_1 - \gamma_0^+\gamma_0, \quad (10.55)$$

where

$$\Gamma_1^+ = \frac{1}{\sqrt{2M}}(\hat{p}_y - Mr_0\hat{\mu}) + \mathrm{i}\frac{M}{2}\hat{y}$$

$$\gamma_0^+ = -\mathrm{i}\frac{1}{\sqrt{2\mathcal{I}}}(\hat{B} - Mr_0\hat{y}) + \sqrt{\frac{\mathcal{I}}{2}}\hat{\mu}$$

$$[\Gamma_1, \Gamma_1^+] = [\gamma_0, \gamma_0^+] = 1. \quad (10.56)$$

Thus, $\hat{H}_b$ has been written in terms of two uncoupled oscillators, with frequencies ± 1. We can overcome this last inconvenience through the replacement $\gamma_0^+ \to \Gamma_0$, $\gamma_0 \to \Gamma_0^+$. Therefore,

$$\hat{H}_b = \Gamma_1^+\Gamma_1 - \Gamma_0^+\Gamma_0 + 1 \quad (10.57)$$

$$[\Gamma_0^+, \Gamma_0] = 1. \quad (10.58)$$

If the new vacuum state is annihilated by Γ_0, all excitations of $\hat{H}_b$ become positive, at the expense of working with the anomalous metric (10.58).[10]

The ghost sector may be written as

$$\hat{H}_g = \bar{a}a - \bar{b}b - 1$$

$$a = \mathrm{i}\bar{b}^+ = \frac{1}{\sqrt{2}}(\bar{\pi} - \mathrm{i}\eta), \quad b = -\mathrm{i}\bar{a}^+ = \frac{1}{\sqrt{2}}(\pi + \mathrm{i}\bar{\eta}). \quad (10.59)$$

Note that

$$\{\bar{a}, a\} = \{\bar{b}, b\} = 1, \quad \text{but } \bar{a} \neq a^+ \; ; \; \bar{b} \neq b^+. \quad (10.60)$$

---

[10]This metric has been also employed for the boson associated with the Lagrange multiplier, for instance in QED.

Therefore, the quadratic Hamiltonian of the unphysical sector,

$$\hat{H}^{(2)}_{\text{unph}} = \Gamma_1^+ \Gamma_1 - \Gamma_0^+ \Gamma_0 + \bar{a}a + \bar{b}b, \tag{10.61}$$

is a supersymmetric Hamiltonian with a characteristic energy equal to unit. Some interesting features of this Hamiltonian are:

- The eigenvectors define the subspace

$$\varphi_{n_1,n_0,n_a,n_b} = \frac{1}{\sqrt{n_1! \, n_0!}} \, (\Gamma_1^+)^{n_1} \, (\Gamma_0^+)^{n_0} \, (\bar{a})^{n_a} \, (\bar{b})^{n_b} \, \varphi_0, \tag{10.62}$$

  with $n_1, n_0 = 0, 1, 2, \ldots$ and $n_a, n_b = 0, 1$.
- The vacuum state is annihilated by the operators Γ_1, Γ_0, a, b and thus, by the quadratic term in the $BRST$ generator (10.47)

$$\hat{\Omega}^{(2)} = -\mathrm{i}(\Gamma_1^+ + \Gamma_0^+)a - (\Gamma_1 + \Gamma_0)\bar{b}. \tag{10.63}$$

  Therefore, this vacuum is a physical state, according to (10.43). In fact, it is the only one among the whole set of states (10.62). Moreover, the system displays the BRST symmetry ($[\hat{\Omega}, \hat{H}_{\text{BRST}}] = 0$; $\quad \hat{\Omega} \, \varphi_0 = 0$).
- The cancelation of unphysical effects would not be possible if all states (10.62) were ordinary states in Hilbert space. However, the unusual relations (10.58) and (10.60) are well defined and may be used without problems.
- As a consequence of the circular symmetry, the Hamiltonian $\hat{H}$ does not display a restoring force in the y-direction. However, this symmetry is lost for $\hat{H}_{\text{BRST}}$ in the intrinsic frame and, as a consequence, all unphysical degrees of freedom have acquired a finite frequency [see (10.61)]. Perturbation theory becomes feasible.
- The coupling term $\hat{H}_c$ in (10.54) can be obtained from the second equation (10.56)

$$\hat{H}_c = \frac{\hat{I}}{\sqrt{2\mathcal{I}}}(\Gamma_0^+ + \Gamma_0) \tag{10.64}$$

Since this term is small $[\mathcal{O}\,(1/r_0)]$, it can be treated in perturbation theory. The second-order contribution has the value

$$\Delta E^{(2)} = -\hat{I}^2 \, {}_{\text{unph}}\langle 0|\mu|n_0 = 1\rangle\langle n_0 = 1|\mu|0\rangle_{\text{unph}} = \frac{\hat{I}^2}{2\mathcal{I}}, \tag{10.65}$$

where (10.56) and (10.58) have been used. Second-order perturbation theory yields a positive contribution to the energy of the ground state due to the unusual metric (10.58). It agrees with the exact result in the present case. The associated eigenfunctions are given by (10.44). The spectrum displays a physical collective rotation given by (10.44) and (10.65).

- The presence of $\hat{H}_x$ allows for radial motion (or motion along the x-axis in the intrinsic frame). The spectrum also displays physical, intrinsic, finite-frequency modes.
- There are unphysical excitations described by the excited states of (10.62).
- The BRST treatment is something of an overkill for the Abelian model. In fact, the ghosts are uncoupled from the start. Their role is much more significative for non-Abelian transformations. "Nevertheless, through the Abelian calculation, we have been able to discuss properties of the BRST procedure that continue to be present in the non-Abelian case, such as the BRST symmetry, the existence of the zero-norm subspace, the construction of the unphysical subspace, and the feasibility of the perturbation expansion" [69]. Moreover, statements in Sect. 10.2.2 have been substantiated.

10.3 Generalizations

Symmetry breaking is common in physics.

The treatment of the two examples presented in this chapter has in common the fact that, although the generators of the transformations commute with the Hamiltonian ($[\hat{L}, \hat{H}] = [\hat{N}, \hat{H}] = 0$), the ground states are represented by states which are not annihilated by the generators. As a consequence, the states $\hat{L}\varphi_0$ and $\hat{N}\varphi_0$ have the same energy as the ground state configuration φ_0. There are many degenerate ground states. We speak of a *hidden symmetry*.

In finite systems one of these configurations may tunnel through to other configurations, so the true ground state becomes a superposition of degenerate states. One consequence is that the lost symmetry is retrieved at the collective level in the form of rotational bands, as indicated after (10.32).

For instance, in many nuclear species it is convenient to extend the spherical shell-model (Sect. 7.3.2) by including a quadrupole term in the single-particle potential $V_2 \propto r^2 Y_{20}(\theta)$ [38]. In this case, the large number measuring the deformation is the expectation value of the quadrupole operator $\langle 0| \sum_h r_h^2 Y_{20}(\theta_h)|0\rangle$. As a consequence, φ_0 is not longer an eigenstate of the angular momentum $\hat{I}$ with null eigenvalue. The associated degeneracy manifests itself in the form of low-lying rotational bands,[11] with characteristic energies $(\hbar^2/2\mathcal{I})I(I+1)$ and eigenstates $D_{MK}^I \varphi_\nu$ (Sect. 5.3.2[†]).

One also finds zero-energy bosons in infinite deformed systems, which are related to the one found in subsection 10.1.5[†]. They are called Goldstone bosons. Moreover, they may materialize as very light particles, like the pion. However, the procedure based on collective variables is not applied to those cases, since it may take an infinite amount of time to get across all configurations.

---

[11]Similar effects appear in the case of the (non-spherical) diatomic molecule (Sect. 8.4.2).

A second generalization concerns the generation of energy, a consequence similar to the increase of the single-particle energy $|\epsilon_p - \mu|$ by an amount of $\mathcal{O}(\Delta)$. Most of the mass of hadrons, such as the proton, arises not from the masses of their constituent quarks, but from the quarks' kinetic energy and the energy stored in the gluon field, through processes involving the breakdown of "gauge symmetries". For instance, in the Nambu–Jona Lasinio model of nucleons, quarks are subject to contact forces, and their condensate becomes responsible for the generation of the nucleon mass M: the solution of an equation similar to (10.19) yields the nucleon (relativistic) energies $E_p = (p^2 + M^2 c^4)^{1/2}$, having the same form as in (10.18).

Problems

Problem 1. Consider two fermions moving in a j-shell:

1. Calculate the size of the Hamiltonian matrix if we assume two-particle states of the form

$$\phi_{mm'} = \frac{1}{\sqrt{2}} \left[\varphi_{jm}(1)\varphi_{jm'}(2) - \varphi_{jm}(2)\varphi_{jm'}(1) \right] ;$$

2. Approximate the matrix elements of the Hamiltonian by the expression $\langle mm'|H|m''m'''\rangle = -g\, \delta_{m(-m')}\delta_{m''(-m''')}$. Calculate the size of the matrix to be diagonalized;

3. Find the eigenvectors and eigenvalues. Hint: Try a solution of the form $\Psi = \sum_m c_m \phi_{m(-m)}$: (a) with amplitudes $c_m = $ constant, (b) with amplitudes such that $\sum_m c_m = 0$.

The particles in the resulting extra-bound state $[E_0 = -g(j + \frac{1}{2})]$ are said to form a Cooper pair. This extra binding is the basis for the explanation of the phenomenon of superconductivity.

Problem 2. Let us consider A_π pairs of particles which are allowed to move in degenerate, Ω pairs of time-reversed states. The particles are coupled by the pairing interaction (10.10). Calculate:

1. The exact ground state energy for $A_\pi = \Omega/2$. Hint: verify that the operators $\hbar \hat{P}^+$, $\hbar \hat{P}$ and $\hbar(\frac{1}{2}\Omega - \hat{N}_\pi)$ satisfy the same commutation relations as the three components of the angular momentum operator. Find the maximum value of J.

2. The moment of inertia $\mathcal{I}$ of the "rotational" band associated with the ground states of even systems. Hint: $\hat{H}_{rot} = \hbar^2(\frac{1}{2}\Omega - \hat{N}_\pi)^2/2\mathcal{I}$.

3. The lowest excitation energy for $A_\pi = \frac{1}{2}\Omega$. Hint: Use $J' = J - 1$ for the excited state.

Problem 3. Solve the BCS equations for the system considered in the previous problem

1. Write E_p, V_p^2, Δ, μ.

2. Calculate the three results obtained in Problem 2 within the BCS approximation.
3. Compare the results of the previous item with the exact results obtained in Problem 2, and explain the origin of the discrepancies.

Problem 4. Write the operator $\hat{P} - \frac{\Delta}{g}$ in terms of quasi-particles.

Problem 5. Consider a symmetric system of levels around the Fermi surface:

1. Verify that there is always one boson root at zero energy.
2. Calculate the energy of the first excited root.

Problem 6. Verify all terms in (10.50).

Problem 7. Show that all four terms in $\hat{H}_{unph}^{(2)}$ yield a positive contribution if applied to the ground state eigenvector φ_0.

Problem 8. 1. Obtain an expression for the operator $\hat{L}^{(0)}$ in terms of the boson degrees of freedom Γ_1^+, Γ_0^+.
2. Calculate the matrix element $\langle n_1 = n_0 = 1|L^{(0)}|0\rangle$.

Chapter 11
Eigenvectors of the Position Operator
Path Integral Formulation

In the first place, we enlarge the Hilbert space[1] by broadening the normalization procedure through the introduction of the Dirac delta function.[2] Subsequently, the notion of propagator as a probability amplitude is introduced. This concept allows us to present the formulation of quantum mechanics in terms of path integrals. This formalism, due to Feynman [72], provides a most powerful link between classical and quantum mechanics. It is widely applied in field theory, statistical mechanics, cosmology, financial mathematics, etc.

11.1[†]   Eigenvectors of the Position Operator and the Delta Function

It is convenient to include the eigenvectors φ_x of the position operator $\hat{x}$ in the quantum formalism.

$$\hat{x}\,\varphi_x = x\,\varphi_x \;. \tag{11.1}$$

We must give a value to the scalar product between continuum eigenstates $\langle x|x'\rangle$. By analogy with (2.58), we write the unit operator as

$$I = \int \mathrm{d}x\,|x\rangle\langle x| \;. \tag{11.2}$$

Thus, either discrete or continuous states φ_n may be expressed as

$$\varphi_n = \int \mathrm{d}x'|x'\rangle\langle x'|n\rangle \;. \tag{11.3}$$

---

[1] Another enlargement was accomplished in Sect. 10.2.4[†].

[2] Since the mathematical level of the present chapter is somewhat higher than in the other ones, it is only reccommended for a second lecture or to physics students oriented towards mathematical formalizations.

Let us apply the bra $\langle x|$ to both sides of this equation

$$\langle x|n\rangle = \int dx'\, \delta(x - x')\langle x'|n\rangle$$

$$\langle x|x'\rangle \equiv \delta(x - x'), \tag{11.4}$$

where the scalar product between position eigenstates is given by the Dirac delta function, a generalization of the Kronecker delta to the continuum case.[3] Since $\delta(x - x')$ vanishes for $x \neq x'$ and equals ∞ if $x = x'$, the limits of integration in (11.4) can be arbitrary, provided that the point x is enclosed within the interval of integration.

There exists a continuous formalism quite parallel to the discrete one used so far in this book. In fact, the wave functions $\varphi_n(x)$ introduced in connection with the Schrödinger representation may be interpreted as the probability amplitude of the system described by the state vector φ_n to be at the position x.

$$\varphi_n(x) = \langle x|n\rangle . \tag{11.5}$$

Upon a measurement of the position performed with a precision Δx, the state collapses into a wave packet of dimension Δx with probability $|\varphi_n(x)|^2 \, \Delta x$.

There are several mathematical representations of the delta function, such as

$$\delta(x) = \frac{1}{2\pi} \int_{-\infty}^{\infty} dk\, \exp(ikx)$$

$$= \lim_{\eta \to 0} \frac{1}{\eta\sqrt{\pi}} \exp(-x^2/\eta^2) . \tag{11.6}$$

The delta-normalization is not only applicable to the position eigenstates (as in (11.4)). In particular, the eigenfunctions (4.32) of the momentum operator can be written as

$$\varphi_k(x) = \frac{1}{\sqrt{2\pi}} \exp(ikx)$$

$$\langle k|k'\rangle = \delta(k - k') , \tag{11.7}$$

where (11.6) has been applied.

It is also possible to define the momentum probability amplitudes

$$\varphi_n(p) = \langle p|n\rangle = \int dx\, \langle p|x\rangle\langle x|n\rangle = \frac{1}{(2\pi\hbar)^{1/2}} \int dx\, \exp(-ipx/\hbar)\, \langle x|n\rangle . \tag{11.8}$$

The probability amplitudes $\langle x|n\rangle$ and $\langle p|n\rangle$ are the Fourier transforms of each other.

---

[3]The delta function is not a proper function, but a distribution. It is only defined within integrals such as in (11.4).

11.2† The Propagator

The propagator (or Green function) is the probability amplitude for the transition from (x_1, t_1) to (x_2, t_2).

$$\langle x_2, t_2; |x_1, t_1 \rangle = \langle x_2 | \mathcal{U}(t_2 - t_1) | x_1 \rangle , \qquad (11.9)$$

where we have assumed that $t_2 \geq t_1$. The propagator summarizes the quantum mechanics of the system.

- Using (9.2) and (11.4) one obtains

$$\lim_{t_2 \to t_1} \langle x_2, t_2 | x_1, t_1 \rangle = \langle x_2 | x_1 \rangle = \delta(x_2 - x_1) . \qquad (11.10)$$

- The time evolution of a state $\varphi_n(x, t)$ is given by the space integral

$$\varphi_n(x_2, t_2) = \int dx_1 \, \langle x_2, t_2 | x_1, t_1 \rangle \, \varphi_n(x_1, t_1) . \qquad (11.11)$$

- The propagator is also related to more familiar concepts, as energy levels and wave functions. We can write (11.9) as

$$\langle x_2, t | x_1, 0 \rangle = \sum_n \langle x_2 | n \rangle \exp(-iE_n t/\hbar) \langle n | x_1 \rangle$$

$$= \sum_n \varphi_n(x_2) \exp(-iE_n t/\hbar) \varphi_n^*(x_1)$$

$$\int dx \, \langle x, t | x, 0 \rangle = \sum_n \exp(-iE_n t/\hbar) , \qquad (11.12)$$

where $t = t_2 - t_1$. A Fourier transform is performed on both sides of (11.12)

$$\langle x_2, z | x_1, 0 \rangle = \sum_n \int_0^\infty dt \, \varphi_n(x_2) \exp[i(z - E_n)t/\hbar)] \varphi_n^*(x_1)$$

$$= i\hbar \sum_n \frac{\varphi_n(x_2) \, \varphi_n^*(x_1)}{z - E_n} , \qquad (11.13)$$

where $\text{Im}(z) > 0$ has been assumed. Singularities arise at $\text{Im}(z) > 0$. The poles of the energy propagator yield the energy of the states, while wave functions are given by the residues, in the case of a discrete spectrum. The propagator displays a cut for a continuous spectrum.

- An alternative interpretation of the propagator regarded as a function of x_2 is that it represents the wave function at time t_2 of a particle that was localized before at

(x_1, t_1). Thus, the propagator satisfies the time-dependent Schrödinger equation in the variables (x_2, t_2).

- The composition property of quantum mechanics allows us to divide the time interval $t_2 - t_1$ into two segments

$$\langle x_2, t_2 | x_1, t_1 \rangle = \int dx'' \langle x_2, t_2 | x'', t'' \rangle \langle x'', t'' | x_1, t_1 \rangle \,, \tag{11.14}$$

since the unit operator may be expressed as

$$I = \int dx' | x'', t'' \rangle \langle x', t'' | = \exp[-i\hat{H}t''/\hbar] \int dx' | x' \rangle \langle x'' | \exp(i\hat{H}t''/\hbar) \,. \tag{11.15}$$

Here $\hat{H}$ is assumed to be time independent and (11.2) has been used.

The amplitude for the transition from (x_1, t_1) to (x_2, t_2) may be expressed as the result of transition from (x_1, t_1) to all available intermediate points x'' followed by transitions from (x'', t'') to (x_2, t_2). In a two-slit experiment, the total probability amplitude for the particle being detected at the point x_2 on the screen is the sum of the amplitudes for the particle starting at the point x_1 and passing through either of the two holes. Interference plays here a fundamental role, since the probability of finding the particle at x_2 results from a double-path interference process.

- The interval $t_2 - t_1$ may also be further subdivided into n segments

$$\langle x_{2,2} | x_1, t_1 \rangle = \oint [dx] \prod_{\nu=1}^{n} \langle x^{(\nu)}, t^{(\nu)} | x^{(\nu-1)}, t^{(\nu-1)} \rangle$$

$$\oint \equiv \int \int \dots \int \,, \qquad [dx] \equiv \prod_{\nu=1}^{n-1} dx^{(\nu)} \,. \tag{11.16}$$

Here $t_2 - t_1 = \sum_{\nu=1}^{n} (t^{(\nu)} - t^{(\nu-1)})$ and $x^{(n)} = x_2, t^{(n)} = t_2, x^{(0)} = x_1, t^{(0)} = t_1$. These last two positions are fixed points, not variables of integration.

11.2.1† The Free Particle Propagator

We calculate now the propagator of a free particle. In this case, a continuous quantum number k labels the eigenstates of the momentum (11.7)

$$\langle x | k \rangle = \frac{1}{\sqrt{2\pi}} \exp(ikx) \,, \qquad E_k = \frac{\hbar^2 k^2}{2M} \,. \tag{11.17}$$

We obtain a Gaussian integral by introducing these expressions in (11.12)

$$\langle x_2, t_2 | x_1, t_1 \rangle_{\text{free}} = \frac{1}{2\pi} \int_{-\infty}^{\infty} dk \, \exp\left[-ik(x_2 - x_1) - ik^2 \hbar(t_2 - t_1)/2M\right] .$$

(11.18)

Completing squares yields the exponential function

$$\exp\left(-i\frac{\hbar(t_2 - t_1)}{2M}\left[(k + \alpha)^2 - \alpha^2\right]\right) .$$

(11.19)

Therefore,

$$\langle x_2, t_2 | x_1, t_1 \rangle_{\text{free}} = \frac{1}{2\pi} \exp\left[\frac{iM(x_2 - x_1)^2}{2\hbar(t_2 - t_1)}\right] \int_{-\infty}^{\infty} dk' \exp[-\beta^2 k'^2]$$

$$= \sqrt{\frac{M}{i2\pi\hbar(t_2 - t_1)}} \exp\left[\frac{iM(x_2 - x_1)^2}{2\hbar(t_2 - t_1)}\right] ,$$

(11.20)

where

$$\alpha = \frac{(x_2 - x_1)M}{(t_2 - t_1)\hbar} , \qquad \beta^2 = \frac{i\hbar(t_2 - t_1)}{2M} , \qquad k' = k + \alpha .$$

(11.21)

The free particle propagator (11.20) displays a central role in the next section.

11.3† Path Integral Formulation of Quantum Mechanics

Consider the case of a particle moving in a one-dimensional potential $V(x)$. The particle starts at the position (x_1, t_1) and ends at (x_2, t_2). The time $t_2 - t_1$ is divided into n equal intervals of duration τ. The propagator between the positions $x^{(\nu-1)}$ and $x^{(\nu)}$ during this time interval is[4]

$$\left\langle x^{(\nu)} \left| \exp\left[-\frac{i\tau}{\hbar}(T + V)\right] \right| x^{(\nu-1)} \right\rangle$$

(11.22)

$$= \left\langle x^{(\nu)} \left| \exp\left(-\frac{i\tau}{\hbar}T\right) \exp\left(-\frac{i\tau}{\hbar}V\right) \exp\left(-\frac{\tau^2}{2\hbar^2}[T, V]\right) \right| x^{(\nu-1)} \right\rangle ,$$

where T is the kinetic energy. In the limit $\tau \to 0$, the term proportional to the commutator $[T, V]$ can be neglected, since it is of higher order in $\tau/\hbar$.

---

[4]Use is made of the mathematical identity $\exp(A + B) = \exp(A) \exp(B) \exp(-\frac{1}{2}[A, B])$ (times exponential terms involving two or more commutators).

$$\lim_{\tau \to 0} \left\langle x^{(\nu)} \left| \exp\left[-\frac{i\tau}{\hbar}(T + V) \right] \right| x^{(\nu-1)} \right\rangle$$

$$= \lim_{\tau \to 0} \langle x^{(\nu)}, t^{(\nu)} | x^{(\nu-1)}, t^{(\nu-1)} \rangle_{\text{free}} \, \exp\left[-\frac{i\tau}{\hbar} V(x^{(\nu-1)}) \right]$$

$$= \lim_{\tau \to 0} \left(\frac{M}{i2\pi\hbar\tau} \right)^{1/2} \exp\left[\frac{i\tau}{\hbar} \left(T(\dot{x}^{(\nu)}) - V(x^{\nu}) \right) \right]$$

$$= \lim_{\tau \to 0} \left(\frac{M}{i2\pi\hbar\tau} \right)^{1/2} \exp\left[\frac{i\tau}{\hbar} \mathcal{L}(\dot{x}^{(\nu)}, x^{(\nu)}) \right] , \tag{11.23}$$

where $\mathcal{L}$ is the classical Lagrangian. The potential term has been factored out during each interval $\tau \to 0$ because it stays constant within such interval. The result (11.20) for the kinetic energy part of the Hamiltonian has been used.

The particle travels from x_1 to x_2 through a series of intermediate steps $x^{(1)}, x^{(2)}, ...$, which define a "path." The total amplitude for the particle to begin at x_1 and end up at x_2 is given by the sum over all possible paths. The number of integrations become infinite as the time interval τ tends to zero. In this limit, the propagator for the total time interval $t_2 - t_1$ may be written as a path integral
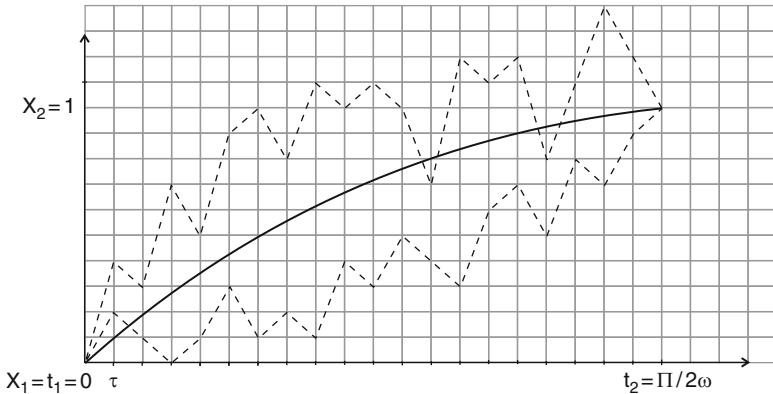
$$\lim_{\tau \to 0, n \to \infty} \langle x_2, t_2 | x_1, t_1 \rangle = \lim_{\tau \to 0, n \to \infty} \left(\frac{M}{i2\pi\hbar\tau} \right)^{n/2} \oint [dx] \exp\left[\frac{i}{\hbar} \mathcal{S}(x_2, t_2 | x_1, t_1) \right] , \tag{11.24}$$

where

$$\mathcal{S}(x_2, t_2 | x_1, t_1) = \sum_{\nu=1}^{n} \tau \langle x^{(\nu)}, t^{(\nu)} | x^{(\nu-1)}, t^{(\nu-1)} \rangle = \int_{t_1}^{t_2} dt \, \mathcal{L}(t) . \tag{11.25}$$

The action S has the same dimension as $\hbar$. The symbols $\oint$ and $[dx]$ have been defined in (11.16).

- All the paths contribute equally in magnitude, but the phase of their contribution is different. The phase is given by the classical action (in units of $\hbar$).
- Expression (11.24) has been derived from laws of quantum mechanics to which the reader has become familiar by now. One of them is the superposition principle, used in summing the contributions of alternative paths. The other is the composition property of the transition amplitude, which allows us to divide the total time interval into segments of vanishing duration τ. Feynman's original approach was to adopt (11.24) as an hypothesis and, subsequently, derive the time-dependent Schrödinger equation.
- The path integral relates certain quantum probability amplitudes to the classical action. Therefore, it provides a deep link between classical and quantum physics which is explained in [72] as follows: the classical approximation corresponds to the case of large $\mathcal{S}$ in relation to $\hbar$. A small change in the path induces a change

Fig. 11.1 Trajectory of a particle moving in a harmonic oscillator potential: minimum action trajectory (*full line*) and two other possible trajectories (*dashed lines*)

in $\mathcal{S}$ that is small in the scale of $\mathcal{S}$ but not negligible in the scale of $\hbar$. Thus, small changes in the path produce finite changes in the phase, and the contributions of the different trajectories mutually cancel because they do not add coherently in phase with one another. However, there is the special path for which $\mathcal{S}$ is an extreme (Fig. 11.1). In this case, there is no change in $\mathcal{S}$, at least to first order. In this way the classical laws of motion arise from the quantum laws. From the extreme condition one derives the Euler's equations of motion

$$\frac{\mathrm{d}}{\mathrm{d}t}\left(\frac{\partial \mathcal{L}}{\partial \dot{x}}\right) - \frac{\partial \mathcal{L}}{\partial x} = 0 . \tag{11.26}$$

Classical physics takes into account only the trajectory $x_{\mathrm{cl}}(t)$ satisfying (11.26).
- In the quantum case, $\mathcal{S}$ may be comparable with $\hbar$, and all the trajectories must be added in detail.
- Path integrals whose exponents are quadratic in x and $\dot{x}$ may be calculated exactly. Thus, it is useful to find first the classical path x_{cl} using (11.26) and, subsequently, to replace $x, \dot{x}$ by $y = x - x_{\mathrm{cl}}$, $\dot{y} = \dot{x} - \dot{x}_{\mathrm{cl}}$ in the Lagrangian. Exact quantum expressions for the quadratic fluctuations around the classical path can be obtained (see the example in Sect. 11.3.1[†]). Higher than quadratic terms in the potential may be calculated by means of perturbation expansions.
- "Since its inception in Richard Feynman's 1942 doctoral thesis, the path integral has been a physicist's dream and a mathematician's nightmare. To a physicist, the path integral provides a powerful and intuitive way to understand quantum mechanics, building on the simple idea that quantum physics is fundamentally a theory of superposition and interference of probability amplitudes... To a mathematician, the path integral is at best an ill-defined formal expression. It is some sort of vaguely integral-like object involving a sum over badly specified collection of functions, having an undefined measure, and whose value

is apparently determined by a group of unclear and perhaps incompatible limits that may or may not yield finite answers"[5] [74].

- Feynman's path integral is not a too convenient tool for solving problems in non-relativistic quantum mechanics, such as those tackled in this text. On the contrary, methods based on path integrals are very powerful in other branches of modern physics, such as quantum field theory and statistical mechanics. The Lagrange formulation of problems involving quantum chromodynamics (QCD), the theory of strong interactions, is amenable to quantification via path integrals and to subsequent perturbation expansion. Expressions are obtained in a Lorentz-covariant form. The relation with statistical mechanics stems from the third line in (11.12), which resembles the "sum over states" associated with the partition function

$$\mathcal{Z} = \sum_n \exp(-\beta E_n) \ . \tag{11.27}$$

In fact, one obtains the partition function from (11.12) by analytical continuation of t into the purely imaginary axis, with $\beta = it/\hbar$, real and positive.

11.3.1[†]   *The Harmonic Oscillator Re-revisited. The Path Integral Calculation*

Let us exemplify once more with the harmonic oscillator. The Lagrangian reads

$$\mathcal{L} = \frac{M}{2} \left(\dot{x}^2 - \omega^2 x^2 \right) \ . \tag{11.28}$$

Therefore, the classical equation of motion (11.26) yields the equation $\ddot{x} + \omega^2 x = 0$. The solution is

$$x_{\text{cl}} = A \sin \omega t + B \cos \omega t$$

$$A = \frac{x_2 \cos \omega t_1 - x_1 \cos \omega t_2}{\sin \omega (t_2 - t_1)} \ , \quad B = \frac{x_1 \sin \omega t_2 - x_2 \sin \omega t_1}{\sin \omega (t_2 - t_1)} \ . \tag{11.29}$$

We make now a transformation of variables

$$y = x - x_{\text{cl}} \ , \tag{11.30}$$

and thus, the action reads

$$\mathcal{S} = \mathcal{S}_{\text{cl}} + \frac{M}{2} (\dot{y}^2 - \omega^2 y^2) \ , \quad y(t_1) = y(t_2) = 0 \ . \tag{11.31}$$

---

[5] An up-to-date attempt to put path integral methods on a sound mathematical footing can be found in [73].

This expression is exact, since in this case there are no higher order terms in y. Therefore, the path integral has been factorized into

$$\langle x_2, t_2 | x_1, t_1 \rangle = \langle 0, t_2 | 0, t_1 \rangle \exp(\mathrm{i} \mathcal{S}_{\mathrm{cl}}) \, . \tag{11.32}$$

The two factors are calculated in Sect. 11.3.2*. The results are

$$\langle 0, t_2 | 0, t_1 \rangle = \sqrt{\frac{M\omega}{\mathrm{i} 2\pi\hbar \sin\omega(t_2 - t_1)}} \tag{11.33}$$

$$\mathcal{S}_{\mathrm{cl}} = \frac{M\omega}{2\sin\omega(t_2 - t_1)}[(x_1^2 + x_2^2)\cos\omega(t_2 - t_1) - 2x_1 x_2] \, .$$

The dependence on the spatial coordinates x_1 and x_2 is determined only by the classical action.

Let us obtain once more the energy levels of the harmonic oscillator. We use the trace of the propagator (11.32)

$$\int \mathrm{d}x \, \langle x, t | x, 0 \rangle = \left(\frac{M\omega}{\mathrm{i} 2\pi\hbar \sin\omega t}\right)^{1/2} \int \mathrm{d}x \exp\left(-\frac{\mathrm{i} 2 M\omega \sin^2(\omega t/2)}{\hbar \sin\omega t} x^2\right)$$

$$= \frac{1}{\mathrm{i} 2 \sin\omega t/2}$$

$$= \exp\left(-\mathrm{i}\frac{1}{2}\omega t\right) \sum_{n=0}^{\infty} \exp(-\mathrm{i} n\omega t) \, . \tag{11.34}$$

The sought energies are obtained by comparing the last line of (11.34) and of (11.12).

11.3.2*   The Classical Action and the Quantum Correction to the Harmonic Oscillator

In the first place we compute the classical action

$$\mathcal{S}_{\mathrm{cl}} = \frac{M}{2} \int_{t_1}^{t_2} \mathrm{d}t \, (\dot{x}_{\mathrm{cl}}^2 - \omega^2 x_{\mathrm{cl}}^2)$$

$$= \frac{M\omega}{4} \left[(A^2 - B^2)\cos 2\omega t - 2AB \sin 2\omega t\right]_{t_1}^{t_2} \, , \tag{11.35}$$

which yields (11.34), upon replacement of the values A, B given in (11.29).

Let us now evaluate the propagator $\langle 0, t_2 | 0, t_1 \rangle$ for the harmonic oscillator.[6] According to (11.23)

$$\langle 0, t_2 | 0, t_1 \rangle$$

$$= \lim_{n \to \infty} \left(\frac{M}{\mathrm{i}2\pi\hbar\tau} \right)^{n/2} \oint [\mathrm{d}y] \exp \left\{ \frac{\mathrm{i}M}{2\hbar} \sum_{\nu=0}^{n-1} \left[\frac{(y_{\nu+1} - y_\nu)^2}{\tau} - \tau\omega^2 y_\nu^2 \right] \right\}$$

$$= \lim_{n \to \infty} \left(\frac{M}{\mathrm{i}2\pi\hbar\tau} \right)^{n/2} \oint [\mathrm{d}\eta] \exp \left(-\frac{M}{\mathrm{i}2\tau\hbar} \eta^T \sigma \eta \right) , \tag{11.36}$$

with

$$y_0 = y_n = 0 ; \quad \tau = (t_2 - t_1)/n ; \quad [\mathrm{d}y] = \prod_{\nu=1}^{n-1} \mathrm{d}y_\nu . \tag{11.37}$$

In the second line of (11.36) we have used a vector (η_ν) and a matrix $(\langle \nu | \sigma | \omega \rangle)$ which are defined as

$$(\eta_\nu) = \begin{pmatrix} y_1 \\ y_2 \\ y_3 \\ \vdots \\ y_{n-1} \end{pmatrix} , \quad (\langle \nu | \sigma | \omega \rangle) = \begin{pmatrix} 2 - \tau^2\omega^2 & -1 & 0 & \dots & 0 \\ -1 & 2 - \tau^2\omega^2 & -1 & \dots & 0 \\ 0 & -1 & 2 - \tau^2\omega^2 & \dots & 0 \\ \vdots & \vdots & \vdots & \vdots & \vdots \\ 0 & 0 & 0 & \dots & 2 - \tau^2\omega^2 \end{pmatrix} .$$

$$\tag{11.38}$$

Diagonalization of the matrix σ yields the matrix ϵ with eigenvalues ϵ_a ($1 \leq a \leq n - 1$)

$$\sigma = \mathcal{U}^+ \epsilon \mathcal{U} , \quad \zeta = \mathcal{U} \eta \tag{11.39}$$

Here $\mathcal{U}$ is unitary and real. The vector ζ is also real and constitutes a $(n - 1)$ dimensional vector space. The Jacobian going from $[\mathrm{d}\eta]$ to $[\mathrm{d}\zeta]$ is also 1, since $|\det(\mathcal{U})| = 1$. Therefore, the integral in the second line of (11.36) has the value

$$\oint [\mathrm{d}\eta] \exp \left(-\frac{M}{\mathrm{i}2\tau\hbar} \eta^T \sigma \eta \right) = \oint [\mathrm{d}\zeta] \exp \left(-\frac{M}{\mathrm{i}2\tau\hbar} \zeta^T \epsilon \zeta \right) \tag{11.40}$$

$$= \prod_{a=1}^{n-1} \left(\frac{\mathrm{i}2\pi\tau\hbar}{M\epsilon_a} \right)^{1/2} = \left(\frac{\mathrm{i}2\pi\tau\hbar}{M} \right)^{(n-1)/2} \frac{1}{\sqrt{\det(\sigma)}} .$$

The determinant $\det(\sigma)$ is derived as follows: if s_j denotes the value of the determinant of the truncated matrix consisting of the first j rows and columns of (11.38), the value of s_{j+1} is given by means of an expansion in minors

---

[6]We follow the procedure used in [75].

$$s_{j+1} = (2 - \tau^2\omega^2)s_j - s_{j-1} , \tag{11.41}$$

with $s_1 = 2 - \tau^2\omega^2$, and s_0 is defined as 1. Equation (11.41) may be rewritten in the form

$$\frac{s_{j+1} - 2s_j + s_{j-1}}{\tau^2} = -\omega^2 s_j . \tag{11.42}$$

In the limit $\tau \to 0$ this relation yields a differential equation for the function $s(t)$ of the time variable $t = t_1 + j\tau$. This equation applies as well to the function $r(t) = \tau s(t)$, which has simpler initial conditions

$$r_{t=t_1} = 0 ; \quad \left.\frac{\mathrm{d}r}{\mathrm{d}t}\right|_{t=t_1} = \tau\left(\frac{s_1 - s_0}{\tau}\right) = 2 - \omega^2\tau^2 - 1 = 1. \tag{11.43}$$

The solution of the equation $\frac{\mathrm{d}^2 r(t)}{\mathrm{d}t^2} = -\omega^2 r(t)$ is

$$r(t) = \frac{\sin\omega(t - t_1)}{\omega}$$

$$\det(\sigma) = \frac{r(t_2)}{\tau} = \frac{\sin\omega(t_2 - t_1)}{\omega\tau} . \tag{11.44}$$

Replacement of (11.40) and (11.44) in (11.36) yields the value of the propagator $\langle 0, t_2|0, t_1\rangle$ appearing in (11.33).

Chapter 12
Entanglement and Experimental Tests of Quantum Mechanics

Equations (7.3)–(7.6) display two possible features appearing in the description of bipartite systems: in the first two equations, each subsystem possesses its own quantum state φ_p, which constitutes a complete description of the physical state of the subsystem (a familiar situation from classical physics). This feature of separability does not hold for the last two equations. Schrödinger was the first to emphasize the non-classical features of "entangled" states and coined this term in [76].

Alain Aspect describes the difference between classical and quantum correlations in bipartite systems as follows: "If we have a pair of identical twins we do not know what their blood type is before testing them, but if we determine the type of one, we know for sure that the other is the same type. We explain this by the fact that they were born with, and still carry along, the same specific chromosomes that determine their blood type. Two entangled photons are not two distinct systems carrying identical copies of the same parameter. A pair of entangled photons must instead be considered as a single, inseparable system, described by a global wave function that cannot be factorized into single photon states." [77].

The concept of entanglement is a direct consequence of the superposition principle applied to composite systems. It has become a fundamental tool in the solution of many quantum problems during the second half of the last century:

- In the discussions on the validity of quantum mechanics [Sect. 12.3, including the clarification of the EPR paradox (Sect. 12.3.2)].
- In the field of quantum information (Chap. 13).
- In the description of the emergence of the classical world from the quantum substrate and, as a consequence, in a consistent quantum explanation of the collapse postulate (Sect. 14.3[†]).

We also discuss in the present chapter some recent experiments confirming the validity of quantum mechanics (Sect. 12.3), all of which make use of the concept of entanglement.

Entanglement constitutes the central tool in the forthcoming chapters. In all presentations we make use of two-dimensional Hilbert spaces. Therefore the considerations on these spaces given in Sects. 3.2 and 5.2.2 are assumed here. In

particular, a set of basis states for a single qubit is given by the two-component column vector representation

$$
\varphi_0 = \begin{pmatrix} 1 \\ 0 \end{pmatrix} ; \qquad \varphi_1 = \begin{pmatrix} 0 \\ 1 \end{pmatrix} . \tag{12.1}
$$

Qubits are realized either by means of particles with spin $s = \frac{1}{2}$, two isolated levels, the two states of photon polarization (Sect. 9.8.2[†]), etc. It is yet unclear which is better for computational purposes, although photons are preferred in the case of communication.

The quantum formalism to be used from here on is rather different from the one that we have employed so far. For instance, the matrix density formulation of quantum mechanics (Sect. 14.4) is a convenient tool to deal with entangled states, and to depart from the considerations of isolated microsystems.

12.1   Entanglement
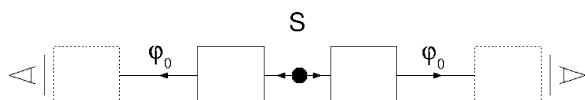
Let us perform some thought experiments with the same filters used in Sect. 2.5.1: two particles, 1 and 2, are emitted simultaneously from the same source, in opposite directions (Fig. 12.1). Each particle enters a filter aligned with the laboratory z-axis and may be detected by an observer provided with another filter. The same orientation β, relative to the laboratory frame, holds for both observers' filters. The down channel is blocked in all four filters. Thus $\cos^2(\beta/2)$ represents the probability that a particle is detected, and $\sin^2(\beta/2)$ the probability that it gets absorbed (5.25).

If two particles are emitted in the entangled state

$$
\frac{1}{\sqrt{2}} \left[\varphi_0(1)\varphi_0(2) + \varphi_1(1)\varphi_1(2) \right] , \tag{12.2}
$$

then:

- A measurement of particle 1 destroys the entangled state. Particle 2 assumes the same state as the one into which particle 1 was projected by the measurement.
- The correlation is 100%, regardless of the filter orientation β.

Fig. 12.1 Thought experiments illustrating the properties of entangled states. Both particles are filtered by the source filters into the state φ_0 through a first filter (*full line box*) and are detected by filters oriented at an angle β (*dashed box*). Trajectories inside the filters have not been drawn

- This result is also independent of the initial direction of the z-axis. Replacing φ_0, φ_1 by linear orthonormal combinations χ_0, χ_1 generated by rotations around the y-axis, yields the entangled state

$$\frac{1}{\sqrt{2}} \left[\chi_0(1)\chi_0(2) + \chi_1(1)\chi_1(2) \right] .$$

  A measurement of particle 1 would project particle 2 into the same state as particle 1.
- The comparison with the (non-entangled) product state $\varphi_0(1)\varphi_0(2)$ is illuminating: here the probability that the two particles get through is $\cos^4(\beta/2)$, while the probability that both are absorbed is $\sin^4(\beta/2)$. Therefore the probability that both observers find the same result is $1 - (1/2)\sin^2\beta$. If $\beta = \pi/2$, this last probability has the value 1/2, the same classical value as for two independent players tossing coins.
- The correlation implicit in (12.2) takes place regardless of the distance between the two particles: particle 2 (non-locally) becomes represented by a definite state as the result of the measurement of particle 1. Entanglement implies that nature is non-local, since the outcome of the local measurement on the second particle is determined by quantum correlations encoded in the total, entangled state of the bipartite system.
- Note that the outcome of the measurement on the first particle is completely random. This randomness implies that any useful information between the two partners has to be transmitted by conventional means. Therefore, although quantum mechanics is a non-relativistic theory, its probabilistic structure prevents any contradiction with relativity theory.

Entanglement constitutes a profound, non-classical correlation between two (or more) quantum entities. The constituent parts of entangled systems do not have their own individual quantum states. Only the total system is in a well-defined state. This is fundamentally unlike anything in classical physics.

12.2   The Bell States

A complete set of basis states for the two-spin system may be either constructed as products of the states (12.1), or represented by four component column vectors

$$\varphi_0^{(2)} = \varphi_0\varphi_0 = \begin{pmatrix} 1 \\ 0 \\ 0 \\ 0 \end{pmatrix} ; \quad \varphi_1^{(2)} = \varphi_0\varphi_1 = \begin{pmatrix} 0 \\ 1 \\ 0 \\ 0 \end{pmatrix} ,$$

$$\varphi_2^{(2)} = \varphi_1\varphi_0 = \begin{pmatrix} 0 \\ 0 \\ 1 \\ 0 \end{pmatrix} \ ; \quad \varphi_3^{(2)} = \varphi_1\varphi_1 = \begin{pmatrix} 0 \\ 0 \\ 0 \\ 1 \end{pmatrix}. \tag{12.3}$$

It is customary to think of the first qubit in the product representation as the control qubit, and the second as the target qubit.

A general state is written as the superposition

$$\Psi_c^{(2)} = \frac{1}{\sqrt{|c_{00}|^2 + |c_{01}|^2 + |c_{10}|^2 + |c_{11}|^2}} \begin{pmatrix} c_{00} \\ c_{01} \\ c_{10} \\ c_{11} \end{pmatrix}. \tag{12.4}$$

The Bell states constitute specific examples of entangled pairs

$$\varphi_{B_0} \equiv \frac{1}{\sqrt{2}} \begin{pmatrix} 1 \\ 0 \\ 0 \\ 1 \end{pmatrix}, \qquad \varphi_{B_1} \equiv \frac{1}{\sqrt{2}} \begin{pmatrix} 1 \\ 0 \\ 0 \\ -1 \end{pmatrix},$$

$$\varphi_{B_2} \equiv \frac{1}{\sqrt{2}} \begin{pmatrix} 0 \\ 1 \\ 1 \\ 0 \end{pmatrix}, \qquad \varphi_{B_3} \equiv \frac{1}{\sqrt{2}} \begin{pmatrix} 0 \\ 1 \\ -1 \\ 0 \end{pmatrix}. \tag{12.5}$$

- Since Bell states are orthonormal, any two-qubit state may be expressed as a linear combination of these states.
- The Bell states are eigenstates of the product operators $\hat{S}_z(1)\hat{S}_z(2)$ and $\hat{S}_x(1)\hat{S}_x(2)$ (see Problem 1). These product operators are included among the interactions in the controlling Hamiltonian (13.14), used to manipulate qubits.
- Successive introduction of these product interactions separates any two-qubit system into the four Bell channels, in a similar way as the interaction with the magnetic field splits the two channels associated with a single qubit (Sects. 2.5.1 and 5.2.1).
- The two spins in a product operator must be simultaneously measured, since detection of a single spin destroys the entanglement. On the contrary, unitary operations can be applied to any one spin or to both of them.

12.3   Experimental Tests of Quantum Mechanics

Thought experiments played a crucial role in the clarification of controversial aspects of quantum mechanics. The discussions between Bohr and Einstein are paradigmatic in this respect (Sect. 15.5.2). However, since the end of the twentieth

century, real experiments have replaced thought ones. Not only have earlier views been confirmed, but also more counterintuitive aspects of quantum mechanics have been brought into focus. In this presentation we restrict ourselves to the discussion of three types of experiments, in spite of other fascinating results that have been or are being obtained:

- Two-slit experiments which, according to Feynman constitute "a phenomenon which is impossible, *absolutely* impossible, to explain in any classical way." ([23], p. 1–1).
- Experiments that can decide between local realism or quantum mechanics as the proper tool for describing the physical world.
- Experiments with single quantum systems, which bear on the statistical framework of quantum mechanics.

Entanglement plays a central role in all these experiments. Present sources of entangled photons are based on the process of parametric down conversion: if a non-linear optical crystal is pumped by a laser beam, a photon may decay into two entangled photons (with a small probability, $10^{-12} - 10^{-10}$). The energy and momentum of the two photons add up to their value in the original one. The two photons may have the same or different polarizations.

12.3.1   Two-Slit Experiments Revisited

Two-slit experiments performed with a single qubit are described in Sect. 2.5.2.

The superposition (2.29) giving rise to interference phenomena requires that there is no way to know, even in principle, which path the particle took, a or a'. Interference is destroyed if this information exists, even if it is dispersed in the environment.

Two-slit experiments with two entangled particles have been used to verify even more spectacular and non-intuitive consequences of quantum mechanics.[1]
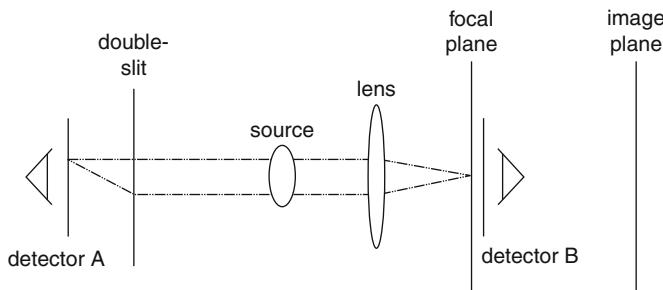
Consider two photons, A and B, emitted in opposite directions. Photon A is monitored by detector A after going through a double slit with holes at a and a'. Photon B gets across a lens and can be observed by detector B placed at different distances behind the lens (Fig. 12.2). Whenever photon A is found in a beam at a (a'), photon B is in the beam b (b'). The entangled quantum state is

$$\Psi = \frac{1}{\sqrt{2}} \left(\varphi_a(A)\varphi_b(B) + \varphi_{a'}(A)\varphi_{b'}(B) \right). \tag{12.6}$$

- If B is not registered, the distribution of A on a plane parallel to the double slit is incoherent. This is due to the fact that we can still obtain information about the path of A by measuring the state of B.

---

[1]Intensive use has been made of [78], [79].

Fig. 12.2 A double-slit diffraction pattern measured with entangled photons. The two photons are detected after the double slit and at the focal plane of the lens, respectively. Detector *B* may also be displaced towards the image plane

- If photon *B* is detected at the focal plane of the lens, information about its distance from the propagation axis before the lens is lost, and thus information about through which slit *A* proceeds is lost as well. The momentum of both photons is well defined and an interference pattern appears behind the two slit plane (wave feature). Photons are collected one by one, and the observed count rate implies that the average spatial distance between photons is at least of the order of 100,000 km.
- One can find through which slit *A* proceeds through, by detecting *B* at the image plane (particle feature), since there is a one-to-one relationship between positions on this plane and the double slit. No interference pattern appears in this case.
- Interference pattern and path information are mutually exclusive results. Therefore, Bohr's complementarity (Sect. 15.5.1) appears as a consequence that it is not possible to position detector *B* simultaneously at the focal and at the image plane. Intermediate situations are also possible, the visibility of the interference pattern being reduced by placing detector *B* between the focal and the image plane: the experiment displays a continuous complementarity.
- After detection of *A*, one can arbitrarily delay detection of *B*, either at the focal or at the image plane. Thus the possibility of detecting or not detecting a diffraction pattern is decided *after* the detection of the diffracted photon. According to this result, it has been claimed that the future can modify the past, in quantum mechanics. However, this interpretation is incorrect, since the prediction of the outcome requires a total specification of the experimental setup, including the position of all detectors (see Bohr's definition of "phenomenon," Sect. 2.4.1).
- Registration of A behind the double slit results in a Fraunhofer double slit pattern for *B* at the focal point, although *B* never proceeded through a double slit. This result has been interpreted as a consequence of the fact that the state incident on the double slit is a wave packet with appropriate momentum distribution such that the probability density has a peak at both slits. By virtue of the strong momentum entanglement at the source, *B* has a related momentum distribution (in fact, it

is the time reversal of the other wave packet) and the Fraunhofer observation conditions become realized after the lens [78].

12.3.2   EPR and Bell Inequalities

We consider a source emitting two particles in the Bell state

$$\varphi_{B_0} = \frac{1}{\sqrt{2}} \left[\varphi_0(1)\varphi_0(2) + \varphi_1(1)\varphi_1(2) \right]. \tag{12.7}$$

If each particle is detected by a Stern–Gerlach detector (Fig. 2.4c) and if the two detectors are oriented along the same direction, particle 2 will be detected in the same spin state as particle 1, independently of their mutual distance. Einstein, Podolsky and Rosen [16] admitted the validity of this quantum prediction, but concluded about the incompleteness of quantum mechanics using the following argument[2]:

- The state of particles exists independently of observation (the notion of physical reality stated in Sect. 2.1).
- A measurement of particle 1 cannot affect the state of particle 2 if they are at sufficient macroscopic distance (notion of locality).

Thus, particle 2 must have carried information about its spin state before detection of particle 1. Therefore, there must be an underlying mechanism – usually called hidden variable – completing quantum mechanics.
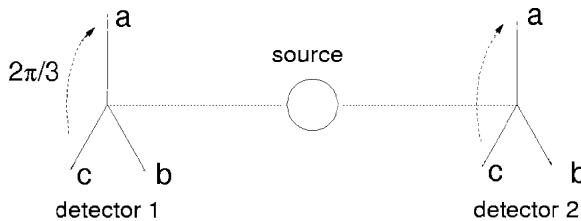
In 1964 John Bell realized that local realism, as understood by EPR, was incompatible with quantum mechanics [81]. He devised a thought experiment in which the two fundamental world views would yield different results. Thus physical facts, and not philosophical considerations, could decide between these points of view.

A double Stern–Gerlach apparatus is improved by allowing each of the two detectors to rotate around the beam axis (y-axis). They may be oriented along one of the three directions (Fig. 12.3): along the z-axis (orientation a); making an angle of $2\pi/3$ with it (orientation b); an angle of $4\pi/3$ (orientation c). In the following, the notation (α_1, α_2) labels the position of the detectors 1 and 2, respectively. For instance, (a, c) means that detector 1 points along the z-axis, and detector 2 is oriented at an angle $4\pi/3$ relative to this axis. It is assumed that the orientations of the two detectors are totally uncorrelated. Moreover, no connections between source and detectors or between detectors are allowed.

In the first place, we analyze the problem from the point of view of local realism.[3] The instructions carried by each particle are of the form $x_a x_b x_c$, meaning that if the

---

[2]The present argument is the spin version of the EPR original one. The adaptation is due to David Bohm [80].

[3]The Bell inequality described here is taken from [82].

Fig. 12.3 Sketch of an experiment testing the Bell inequality described in the text. At each detector position, the three axes a, b, c lie on the same plane perpendicular to the trajectories

detector is at the jth position ($j = a, b, c$), the result of the measurement is x_j ($x_j = 0, 1$).

There are eight possible sets of instructions, namely: 000, 001, 010, 011, 100, 101, 110, 111. It is unimportant which set is valid during a given run. It is important, however, that the two particles carry the same set, because it is an experimental fact that the same result is obtained for both particles if the two detectors display the same orientation (Bohm-EPR experiment).

Let us exclude for the moment the instruction sets 000 and 111. For any of the remaining six sets, the same results are obtained for both particles in five cases, and opposite results in four cases. For instance, if the instruction set is 011, the pairs $(aa),(bb),(bc),(cb),(cc)$ yield the same result, while opposite results are obtained from $(ab),(ac),(ba),(ca)$.

It is obvious that the two excluded sets of instructions can only increase the possibility that the two counters yield the same result. Therefore, the probability of obtaining the same result must always be $\geq 5/9$ (Bell inequality).

Let us now perform a quantum analysis of the experiment. According to (5.25), the expression of state $\varphi_0^{(a)} = \varphi_0$ in the basis corresponding to the orientations b, c is

$$\varphi_0^{(a)} = \frac{1}{2}\varphi_0^{(b)} + \frac{\sqrt{3}}{2}\varphi_1^{(b)} = -\frac{1}{2}\varphi_0^{(c)} + \frac{\sqrt{3}}{2}\varphi_1^{(c)}. \tag{12.8}$$

Since only the relative angle between the two detectors matters, we can assume without loss of generality that particle 1 has been detected in the state φ_0 with the apparatus in the orientation a. The probabilities of the different outcomes for particle 2 are given in Table 12.1. The sum of probabilities for each orientation divided by the number of orientations yields the same probability for obtaining equal or opposite results, at odds with the prediction of local realism. An identical argument applies if particle 1 was to be detected in the state $\varphi_1^{(a)}$.

At the time of Bell's publication it was not possible to perform an experimental test. In the first successful attempt, spin 1/2 particles were replaced by two photons emitted in a radiative $J = 0 \rightarrow J = 0$ cascade using Ca atoms as sources (1981). As expected for entangled photons, the same polarization state was verified for both of them. A Bell inequality somewhat different from the one explained above was

Table 12.1 Probabilities for the results of particle 2

Detector 2	a	b	c	Total probability (%)
Same result as for 1	1	1/4	1/4	50
Opposite result	0	3/4	3/4	50

used. The experiment contradicted the prediction of local realism and confirmed the existence of the quantum correlation [83].

The localization aspect was treated by increasing the distance between the two detectors as far as 13 m, so no signal from one to the other counter could be transmitted at subluminal velocities before detection.

However, two loopholes remained open.[4] One of them consisted of the possibility that the apparatus settings could be known by the detectors and/or by the source before registration of the photons. This loophole was closed by introducing the parametric down conversion (Sect. 12.3), by increasing distances to 355 m and by changing the measurement settings according to a random-number generator in a time scale much shorter than the photon time of flight (1/13). The importance of the last feature stresses the relevance of this experiment [84].

Another logical loophole consisted of the possibility that the detected photons were not faithful representatives of all photons emitted, most of which were lost. This possibility was ruled out by observing nearly all entangled pairs of ions in a cavity [87].

Today it is possible to violate Bell inequalities by many standard deviations in short times. Moreover, in case of Schrödinger cat states with three and four photons (see Sect. 14.2), situations exist in which predictions of quantum mechanics and local realism are exactly the opposite. Experiments have again confirmed the quantum prediction.
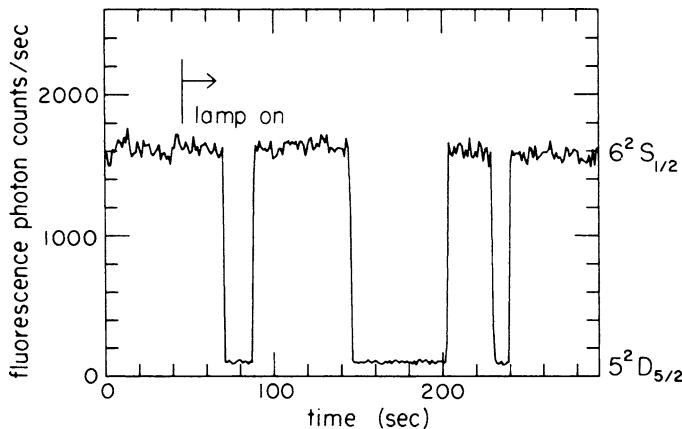
12.3.3   Single Quantum Systems

Starting in the 1970s, it became possible to manipulate and observe single quantum objects, such as a photon or an ion. Improvements in the knowledge of certain quantities, such as the gyromagnetic ratio of the electron (Sect. 5.2.2) were obtained through the trapping of an electron on a macroscopic time scale with electric and magnetic fields. It has also been possible to verify the indistinguishability between two electrons or two atoms of the same element, a key fact in quantum physics. Moreover, many thought and counterintuitive experiments became experimentally feasible.

A common feature of the ion and photon trap experiments is that the Jaynes–Cummings model can be applied if the bipartite interacting system (field plus atom) substitutes the quantum oscillator and the two-state system of Sect. 3.4. In this

---

[4]The two loopholes have not been closed yet in a single experiment.

Fig. 12.4 Quantum jumps of a single ion in a trap. (Reprinted with permission from Nagourney et al. [85], with authorization from the American Physical Society)

simple model there appears for the first time the entanglement of a microsystem with a macrosystem[5] (3.53). Note, however, that the unveiling of these direct quantum manifestations requires extremely sophisticated techniques, which we are unable to discuss here.

In one kind of experiment, an ion is confined to a region around equilibrium, the oscillations being reduced to zero-point fluctuations. Laser beams are used to manipulate the ion, to cool down its motion and to "see" it. The internal evolution can also be monitored, since the ion scatters laser light resonant with the distance between two levels. The light becomes invisible, however, if the ion "jumps" into a non-resonant third level. The scattered light suddenly reappears if the ion returns to one of the two levels resonating with the laser light. Figure 12.4 represents laser-induced fluorescence of a barium ion on the $\varphi_{6p} \rightarrow \varphi_{6s}$ transition versus time. Additional lamp irradiation interrupts the fluorescence by transitions from φ_{6s} to a metastable level.

Schrödinger believed in a statistical framework for quantum mechanics and thus, that sudden jumps of a single ion could not be observed: "We never experiment with just one electron or atom or (small) molecule. In thought-experiments we sometimes assume that we do; this invariably entails ridiculous consequences..." (quoted in [37]).

If many ions are present, the trap confining potential competes with the Coulomb repulsion and a quasi-crystalline order is observed.

In another type of experiment, the roles of matter and radiation are exchanged. Photons with wavelengths in the millimeter range are made to bounce between

---

[5]This type of entanglement constitutes the basis for understanding the emergence of classical macrosystems from the quantum substrate (Sect. 14.2[†]).

the walls of a cavity with highly reflecting superconducting walls. Rydberg atoms (Sect. 6.1.2) [interacting strongly with microwaves and having a long meanlife (Problem 14 in Chap. 9)], are sent one by one to interact with the photons.

Consider two consecutive states in the Rydberg atom, φ_e and φ_g. The radiation field is described by the eigenstates of the harmonic oscillator χ_n in the occupation number representation (Sects. 3.3.1 and 9.8.2[†]), with the resonant photon frequency ω_{ph}. The atom-field coupling Hamiltonian may be approximated by

$$\hat{H}_{coup} = -i\hbar \frac{\Omega_0}{2}(a\sigma_+ - a^+\sigma_-) \,, \tag{12.9}$$

where Ω_0 is proportional to the dipole moment of the Rydberg atom and to the mean square value of the electric field. The Jaynes–Cummings model applies (Sect. 3.4 and Problem 13 of Chap. 3). The resultant eigenenergies and eigenstates are

$$E_{n\pm} = \hbar\omega_{ph}\left(n + \frac{1}{2}\right) \pm \frac{\hbar\Omega_n}{2} \,; \qquad \Omega_n = \Omega_0\sqrt{\frac{n+1}{2}}$$

$$\Psi_{n\pm} = \frac{1}{\sqrt{2}}\left(\varphi_e\chi_n \pm i\varphi_g\chi_{n+1}\right). \tag{12.10}$$

Inversion of (12.10) yields

$$\varphi_e\chi_n = \frac{1}{\sqrt{2}}\left(\Psi_{n+} + \Psi_{n-}\right). \tag{12.11}$$
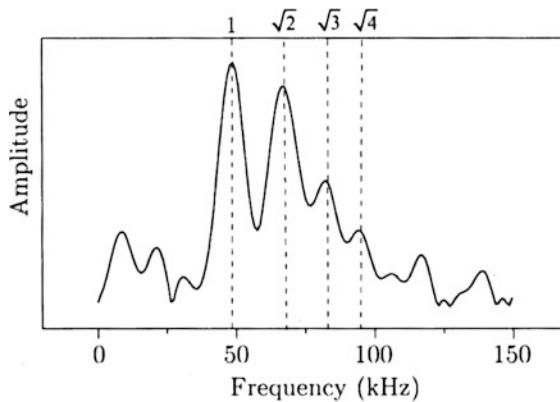
Up to an overall phase, the time-evolution of this state is given by

$$[\varphi_e\chi_n](t) = \frac{1}{\sqrt{2}}\left[\exp\left(-i\frac{\Omega_n t}{2}\right)\Psi_{n+} + \exp\left(i\frac{\Omega_n t}{2}\right)\Psi_{n-}\right]$$

$$= \cos\frac{\Omega_n t}{2}\varphi_e\chi_n + \sin\frac{\Omega_n t}{2}\varphi_g\chi_{n+1}. \tag{12.12}$$

If the atom is in an initial state φ_e in free space, it decays to the final state φ_g, while simultaneously emitting a photon that escapes (Sect. 9.8.4[†]). In the present case, the photon gets trapped by the cavity, and the atom-field coupling results in a reversible energy exchange.

Assume now that the atom, initially in the state φ_e, interchanges energy with a field that does not have a definite number of photons ($\chi = \sum_n c_n\chi_n$). Applying (12.12), one obtains

$$[\varphi_e\chi](t) = \sum_n c_n\left(\cos\frac{\Omega_n t}{2}\varphi_e\chi_n + \sin\frac{\Omega_n t}{2}\varphi_g\chi_{n+1}\right). \tag{12.13}$$

Fig. 12.5 Fourier transform of the time-dependent atomic signal detected after the interaction of a single Rydberg atom with a small field stored in a superconducting cavity. The average number of photons is $\bar{n} = 0.85 \pm 0.04$. The discrete peaks appear at frequencies which are proportional to the square root of the successive number of photons. (Reprinted with permission from Brune et al. [86], with authorization from the American Physical Society)

The probability of finding the atom in the state φ_e is

$$P_e(t) = \sum_n |c_n|^2 \frac{1 + \cos \Omega_n t}{2}. \tag{12.14}$$

Thus, the Fourier transform of the signal due to detection of the atoms leaving the cavity, displays peaks associated with transitions between states with a discrete number of photons (Fig. 12.5). The frequencies of the peaks are proportional to $\sqrt{n+1}$, as expected.

These cavity quantum electrodynamics (CQED) experiments show clear evidence of field "graininess," the fundamental hypothesis of Einstein in 1905 (Sect. 15.3.1). CQED experiments can also be considered to be modern versions of the photon box imagined by Einstein for the 1930 Solvay meeting (Fig. 15.3). Instead of weighing the box, information about the fields is imprinted on the exit ions, and photons are thus counted without being destroyed.

The cavity photons can also be prepared into a sort of Schrödinger cat state.

A thorough presentation of both ion and photon traps, covering both results and the experimental difficulties that have been overcome, can be found in [37].

12.3.4   A Quantum, Man-Made Mechanical Object

During 2010, quantum effects in the motion of a human-made object were experimentally observed for the first time [88]. A mechanical resonator – an oscillator –

displayed an isolated frequency such that $\hbar\omega = 2.6 \times 10^{-5}$ eV. It was cooled at 0.1 K using conventional cryogenic refrigeration, and thus $\hbar\omega/k_{\mathrm{B}}T \approx 3$. Quantum measurements of the resonator were made using a superconducting qubit as a measurement device. The coupled system can be described by the Jaynes–Cummings model (Sect. 3.4). The system has proved to be much more stable than the resonator plus a classical measuring device. The following features appeared experimentally:

- The mechanical resonator was cooled to its ground state. The estimated number of phonons was $\langle 0|n|0\rangle = 0.07$.
- An individual quantum excitation (phonon) could be created in the resonator and the exchange of this excitation between the resonator and the entangled qubit was observed.
- A superposition state was generated in the resonator, with a qubit response in good agreement with theory.

Therefore, quantum mechanics applies as well to a mechanical object large enough to be seen with the naked eye.

However, one may not conclude that present experimental successes have *proved* the validity of quantum mechanics. It is worthwhile to remember that experiments can only prove that a theory is not correct, if their results contradict predictions of the theory. In the future, we expect more and even more subtle tests on the validity of quantum mechanics.

Chapter 13
Quantum Information

13.1 Conceptual Framework

Assume for a moment that the Hilbert space is restricted to the pure basis states.[1]
For a single qubit, the only available states would thus be the two states (12.1). For
n qubits, there are 2^n orthogonal product vectors $\varphi_i^{(n)}$ in a space of 2^n dimensions.
Classical computation operates in this space. Linear combinations of vectors are
not allowed. Therefore, the only operations that can be performed are permutations
between the basis states (unless the size of the space is changed).

Quantum mechanics allows for superpositions $\Psi^{(n)}$ of the basis vectors $\varphi_i^{(n)}$
with complex amplitudes c_i (2.6). Quantum operations are only limited by the
requirement of unitarity, i.e. the norm of the state should be preserved. Therefore,
classical states and classical operations constitute sets of vanishingly small size
relative to those sets encompassing quantum states and quantum operations. Thus,
quantum information offers a wealth of new possibilities: all kinds of interference
effects may take place in the much larger space, much faster calculations can
be performed if all components of the state vector work in parallel, and so on.
Quite typically, the time for solving a problem may increase either exponentially
or polynomially with its complexity. By taking advantage of interference and
entanglement, a problem with an exponential increase in a classical computer may
be transformed into a problem with polynomial increase in the quantum case.

However, this promising picture is limited by the fact that it is very difficult to
extract anything from the state vector $\Psi^{(n)}$, despite the immense amount of informa-
tion that it carries. In fact, the only way is to perform a measurement, which relates
$\Psi^{(n)}$ to a single probability $|c_i|^2$. Therefore, the strategy consists in producing trans-
formations that lead to a state $(\Psi')^{(n)}$, in which very few amplitudes c_i' do not vanish.

A quantum process starts with the preparation of the system in some initial state
$\varphi_0^{(n)}$ (i.e. with a measurement) and ends with another measurement in the final

---

[1]See also Mermin's presentation [22].

state $\varphi_f^{(n)}$ (see Sects. 2.4 and 2.5). Measurements are a class of transformations that provide classical information but change the state irreversibly. Between any two measurement operations, quantum transformations are unitary operations that change the state of the system in a deterministic and reversible way. A quantum algorithm is a unitary operation that may be represented by successive unitary operations (9.7) – quantum gates (Sect. 13.5*).

A collection of n qubits is called a quantum register of size n. We assume that information is stored in the register in binary form. An n-register can store the numbers $J = 0, 1, \ldots, (2^n - 1)$. A quantum register of size 1 can store the numbers 0 and 1; of size 2, the numbers 0,1,2 and 3; etc.

We do not attempt to give a complete description of the recent developments on quantum information. Rather, we use the respectable knowledge of quantum mechanics which readers should now have to illustrate these new uses with pertinent examples: quantum cryptography (Sect. 13.2); teleportation (Sect. 13.3) and quantum computation (Sect. 13.4†).

A presentation of the most common gates used in quantum information processes is made in Sect. 13.5*.

13.2   Quantum Cryptography

Traditional strategies for keeping secrets in the distribution of cryptographic keys depend on human factors, so their safety is difficult to assess. As a consequence, they have been replaced to a large extent by cryptosystems. A cryptographic key is transmitted through a succession of numbers 0 and 1. Their present safety is due to the fact that, with classical computers, no fast algorithms can work out the decomposition of a large number in prime factors. However, this statement may no longer be true with the advent of quantum computation (see Sect. 13.4†). Hence the continuing interest in exploring safer systems for transmission of cryptographic keys. In this section, we show that the quantum key distributions are impossible to break, and that this impossibility arises from fundamental quantum laws.

A well-known protocol is called BB84 [89]: every actor involved is provided with a filter of the type discussed in Sect. 2.5.1. The encoder (usually named Alice) can send particles that are in an eigenstate of either $\hat{S}_z$ or $\hat{S}_x$. We label the corresponding states by φ_0, φ_1, χ_0, χ_1. The decoder (frequently called Bob) may orient his detection equipment along either the z- or the x-direction. For instance, if Alice has sent three qubits that are polarized according to $\uparrow z$, $\uparrow x$ and $\downarrow x$, and if Bob aligns his apparatus in the z-direction for the first qubit and the x-direction for the last two, he will detect intensities 1, 1 and 0 with certainty. These are the good qubits, i.e. those sent and measured with both pieces of apparatus along the same orientation. If Alice sends a qubit in the φ_0 state while Bob orients his equipment towards the x-direction, he may detect the intensities 1 or 0 with equal probability. Bad qubits are those in which the sender and receiver apparatus have different orientations.

For each qubit sent, Alice records the eigenvalue as well as the orientation of her filter. Bob selects his orientations at random and informs Alice of them. With this knowledge, Alice can tell Bob which ones are good qubits, the ones which are kept in order to codify the message. Both messages from Bob and Alice can even be made over an open phone, since they carry no information useful for a third party.

Let us assume that there is an eavesdropper, usually called Eve. Eve cannot be prevented from eavesdropping, but if she does, Alice and Bob will know: let us assume that Alice has sent a qubit in the φ_1 state, that Eve's apparatus is in orientation x, and Bob's in orientation z. Eve's measurement increases the probability that Bob will detect the particle from 0 to $1/4$ [$= |\langle\varphi_1|\chi_0\rangle\langle\chi_0|\varphi_0\rangle|^2$, see (3.21)]. Bob chooses a random subset of the good qubits that he has retained, and communicates them to Alice, also publicly. Alice may find discrepancies between her notes and Bob's message. If she does not, all good qubits constitute a perfect secret between Alice and Bob.

Quantum cryptography applies the rule that quantum states are perturbed by the act of measurement, unless the observer knows in advance what observables can be measured without being perturbed (Sect. 2.4). Eve cannot succeed without knowing the basis common to both Alice and Bob.

Commercial equipment for bank transfers by means of quantum cryptography is available, within city boundaries.

13.3 Teleportation
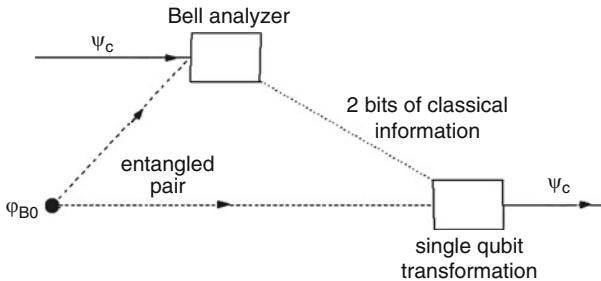
Alice and Bob are at a macroscopic distance from each other. Alice's particle is initially in the Ψ_c state

$$\Psi_c = c_0\varphi_0 + c_1\varphi_1 . \tag{13.1}$$

The objective is to put Bob's particle in the same state, but without transporting the particle or sending any classical information about it.

Alice and Bob start by each taking one of the two qubits which have been prepared, for instance in the Bell state φ_{B_0} (12.5). Alice now has two qubits, one in the state Ψ_c and the other in the Bell state (see Fig. 13.1). The three-qubit state can be written as

$$\Psi^{(3)} = \Psi_c\varphi_{B_0}$$

$$= \frac{1}{\sqrt{2}} (c_0\varphi_0\varphi_0\varphi_0 + c_0\varphi_0\varphi_1\varphi_1 + c_1\varphi_1\varphi_0\varphi_0 + c_1\varphi_1\varphi_1\varphi_1) \tag{13.2}$$

$$= \frac{1}{2}\left[\varphi_{B_0}\begin{pmatrix} c_0 \\ c_1 \end{pmatrix} + \varphi_{B_1}\begin{pmatrix} c_0 \\ -c_1 \end{pmatrix} + \varphi_{B_2}\begin{pmatrix} c_1 \\ c_0 \end{pmatrix} + \varphi_{B_3}\begin{pmatrix} -c_1 \\ c_0 \end{pmatrix}\right],$$

Fig. 13.1 Scheme illustrating the process of teleportation. *Dashed lines* represent entangled qubits in the state φ_{B_0}, while the *dotted line* indicates that classical information is transmitted

where the qubit taken by Bob from the Bell state has been explicitly separated and the two qubits in Alice's posesion have been expressed in terms of Bell states.

Alice now filters her two qubits into a well-defined Bell state (Problem 10). Simultaneously, Bob's qubit is also projected into a well-defined state, but Bob ignores the relation between this state and the initial state Ψ_c. Bob needs to know in which Bell state the system has collapsed to reconstruct the original qubit. This information must be provided by Alice by conventional means, i.e. at a speed less than or equal to the velocity of light.

Suppose, for instance, that instead of going through the previous procedure, Alice constructs the state Ψ_c by filtering the spin, and sends the information about the alignment axis to Bob, who can thus filter the particle in the same direction. Are there still advantages in teleportation? The answer is affirmative, for the following reasons:

- The teleported state Ψ_c might not be known by Alice. If she attempts to measure it, the state of the qubit could be changed.
- Bob receives complete information about Alice's qubit at the expense of that qubit: in quantum teleportation the original qubit is destroyed. This is a manifestation of the no-cloning theorem (Sect. 2.6.2).
- The qubit Ψ_c is determined by the amplitudes c_0, c_1, for which the transmission time increases with the required precision. Now the results of the quantum experiments are discrete numbers. In quantum teleportation, discrete information about the Bell state is transformed into continuous information about the state of the qubit.

Quantum teleportation was discovered in 1993 [90]. It was observed for the first time in 1997 with entangled photons [91].

13.4[†]   Quantum Computation

We describe the factorization procedure as one of the few "best typical" examples of the still unharnessed power of quantum computers.[2] Note that the security of widely used encryption codes rests on the present practical impossibility of breaking a large number N in its prime factors, using classical computers.

13.4.1[†]   *Factorization*

Factorization of a number in its prime components makes use of the following property: Let a be coprime with N (no common factors) and define the function

$$f_{aN}(J) \equiv a^J, \bmod N. \tag{13.3}$$

This function has at least two important properties:

- It is periodic. For instance, if $a = 2$, $N = 15$, the successive values of the function f are $1, 2, 4, 8, 1, 2$ and so on. Thus, the period $P = 4$.
- Provided that P is even, the greatest common divisors of the pairs $(a^{P/2} + 1, \bmod N)$ and $(a^{P/2} - 1, \bmod N)$ are factors of N. In the present example, they are 5 and 3, respectively.

The level of complexity in the calculation of the period using a classical computer is as large as any other factorization algorithm. By contrast, there exists the following quantum algorithm due to Schor [93]:

1. The operation makes use of a control register (left) and a target register (right). Start the operation with both registers in the state with $J = 0$ [all qubits in the φ_0 state (13.25)]

$$\Psi_1^{(n)} = \varphi_0^{(n)} \varphi_0^{(n)}. \tag{13.4}$$

2. Load the control register with the integer series (13.26)

$$\Psi_2^{(n)} = 2^{-n/2} \sum_{J=0}^{J=2^n-1} \varphi_J^{(n)} \varphi_0^{(n)}. \tag{13.5}$$

3. Select a value for a (coprime to N) and place the remainder $f_{aN}(J)$ in the target register, as in (13.27)

$$\Psi_3^{(n)} = 2^{-n/2} \sum_{J=0}^{J=2^n-1} \varphi_J^{(n)} \varphi_{f_{aN}(J)}^{(n)}. \tag{13.6}$$

---

[2]The contents of this section have been mainly extracted from [92].

For $n = 4$ and the previous example, $\Psi_3^{(n)}$ takes the value

$$\frac{1}{4}\left(\varphi_0^{(4)} + \varphi_4^{(4)} + \varphi_8^{(4)} + \varphi_{12}^{(4)}\right)\varphi_1^{(4)} + \frac{1}{4}\left(\varphi_1^{(4)} + \varphi_5^{(4)} + \varphi_9^{(4)} + \varphi_{13}^{(4)}\right)\varphi_2^{(4)}$$

$$+ \frac{1}{4}\left(\varphi_2^{(4)} + \varphi_6^{(4)} + \varphi_{10}^{(4)} + \varphi_{14}^{(4)}\right)\varphi_4^{(4)} + \frac{1}{4}\left(\varphi_3^{(4)} + \varphi_7^{(4)} + \varphi_{11}^{(4)} + \varphi_{15}^{(4)}\right)\varphi_8^{(4)}.$$

$$(13.7)$$

Thus, the period $P = 4$ is encoded in each of the superposition states representing the control register.

4. Measure the target register. This information yields one value $\chi = f_{aN}(J)$ and destroys the information about the others. According to (2.18) we retain only the terms $\varphi_J^{(n)}$ in the control register that are multiplied by $\varphi_\chi^{(n)}$

$$\Psi_4^{(n)} = \frac{1}{\sqrt{2^n/P}}\left(\sum_{r=0}^{r=2^n/P-1} \varphi_{J=rP+q}^{(n)}\right)\varphi_\chi^{(n)},\tag{13.8}$$

where we have assumed that $2^n/P$ is an integer,[3] as in (13.7).

5. The residue q must be eliminated in order to find the period. To do so we perform a Fourier transform on the control register

$$\Psi_5^{(n)} = \mathcal{U}_{FT}^{(ctrl)}\,\Psi_4^{(n)}$$

$$= \frac{\sqrt{P}}{2^n}\left(\sum_{K=0}^{K=2^n-1}\sum_{r=0}^{r<2^n/P} \exp[iK(rP+q)\pi/2^{(n-1)}]\varphi_K^{(n)}\right)\varphi_\chi^{(n)}$$

$$= \left(\sum_{r=0}^{r<2^n/P} c_{\chi,rP}\,\varphi_{rP}^{(n)}\right)\varphi_\chi^{(n)}.\tag{13.9}$$

The last step relies on the vanishing of the factor

$$\sum_{r=0}^{r<2^n/P} \exp[iK(rP)\pi/2^{(n-1)}],\tag{13.10}$$

unless K is zero or an integer multiple of $2^n/P$, if P is an integer divisor of 2^n. Accordingly, the Fourier transform of (13.7) yields

$$\left(c_{i0}\varphi_0^{(4)} + c_{i4}\varphi_4^{(4)} + c_{i8}\varphi_8^{(4)} + c_{i12}\varphi_{12}^{(4)}\right)\varphi_\chi^{(4)},\tag{13.11}$$

where all subindexes in the control register are multiples of the period.

---

[3]The procedure can be extended if this is not the case.

6. Measure the control system.
7. Repeat the operation until the period becomes established.

The number ν of bit operations required to factor the number N with a classical computer is expected to increase with N no less rapidly than

$$\nu(N) = \exp\left[1.32\, L^{1/3}\, (\log_2 L)^{2/3}\right], \tag{13.12}$$

where $L = \log_2 N$ is essentially the number of bits required to represent N. The number ν_q of universal quantum gates needed to implement Schor's algorithm has been estimated to be

$$\nu_q(N) = L^2\, (\log_2 L)\, (\log_2 \log_2 L). \tag{13.13}$$

Thus, the factorization is transformed from a problem in which time increases exponentially, to a problem in which it increases only polynomially. It has been estimated that the factorization time of a 400-digit number can be reduced from the age of the universe to a few years [77].

A variety of two-level quantum systems has been considered. Modern experimental techniques allow us to orient their spins (or equivalent observables) and to implement the gates. However, the situation becomes drastically more complicated when operating a large scale computer, combining many gates. The greatest problems lie in alteration of states due to decoherence, i.e. the unavoidable coupling with a surrounding medium (Sect. 14.2†). Up to now, the successes of quantum computation have been limited to the decomposition of small numbers into their prime factors [94]. The number of operational qubits can still be expressed with one digit, while many thousand qubits would be neeeded for the envisaged applications.

It is true that we cannot ignore the example of the path traveled "from the Pascal machine to the Pentium processor." There exist new strategies for partially controlling the effects of decoherence. For instance, by redundancy. The fact that this problem is linked to defence and financial activities has undoubtedly contributed to intense endeavors on the subject. But we should bear in mind that the interest in quantum computing is not limited to those applications: the physics involved in experiments with entangled particles is helping us to obtain a better understanding of the most fundamental aspects of quantum mechanics.

13.5*   Quantum Gates

A quantum gate is a device that performs a unitary transformation on selected qubits at a certain time. A quantum network is a device consisting of quantum gates that are synchronized in time.

It can be proved that any unitary operation in a system of qubits may be reproduced by a sequence of one- and two-qubit operations, which constitutes a practical advantage from the engineering point of view. Manipulations of a single qubit may be performed by controlling a magnetic field at its site (Sect. 9.2). Simultaneous manipulations of two qubits require an interaction between them. Therefore we use a controlling Hamiltonian

$$\hat{H}_{\text{ctr}} = -\mu_s \sum_i^N \boldsymbol{B}^{(i)}(t) \cdot \hat{\boldsymbol{S}}^{(i)} + \sum_{\substack{a,b \\ i \neq j}} J_{ab}^{(i,j)}(t) \hat{S}_a^{(i)} \hat{S}_b^{(j)} , \qquad (13.14)$$

where summation over space indices $a, b = x, y, z$ is understood (see Problem 9 in Chap. 6 and Problem 7 in Chap. 9). This Hamiltonian satisfies the requirements for controlling a quantum computer. In fact, it even exceeds them. The Hadamard gate, all the phase gates and the controlled-NOT gate constitute a universal set of gates, although this set is not unique. Any transformation between the n-states of a register may be constructed from them.

Interactions with the measurement device and with the environment should also be taken into account.

13.5.1*   One-Qubit Systems

The Hadamard gate $\mathcal{U}_H$ and the phase gate $\mathcal{U}_\phi(\beta)$ transform the one-qubit states through the operations[4]

$$\mathcal{U}_H \varphi_J = \frac{1}{\sqrt{2}} \sum_{K=0}^{K=1} \exp(\mathrm{i}JK\pi)\varphi_K , \qquad J = 0, 1,$$

$$\mathcal{U}_H \varphi_0 = \frac{1}{\sqrt{2}}(\varphi_0 + \varphi_1) , \qquad \mathcal{U}_H \varphi_1 = \frac{1}{\sqrt{2}}(\varphi_0 - \varphi_1) . \qquad (13.15)$$

The phase gate adds a phase to the state φ_1.

$$\mathcal{U}_\phi(\beta) \varphi_J = \exp(\mathrm{i}J\beta)\varphi_J . \qquad (13.16)$$

These two operations are sufficient to construct any unitary operation on a single qubit, since

---

[4]We keep the quantum mechanical notation previously used in this text. In computation texts, the Hadamard gate is denoted by H, successive transformations are read from left to right, and so on. Overall phases are frequently disregarded.

$$\mathcal{U}_\phi(\eta + \pi/2)\, \mathcal{U}_H \mathcal{U}_\phi(\beta)\, \mathcal{U}_H \varphi_0 = \varphi_0 \cos\frac{\beta}{2} + \varphi_1 \exp(i\eta) \sin\frac{\beta}{2}\,, \qquad (13.17)$$

up to a phase. This expression is the most general form for a qubit.

A qubit is manipulated by acting with the first term in (13.14). Switching on the z- or x-component of the magnetic field during a time τ introduces the transformations $\mathcal{U}_z(\beta/2)$ and $\mathcal{U}_x(\beta/2)$. They are given by (9.14) and (9.17), respectively, with $\beta = \omega_L \tau$.

The Hadamard gate and the phase gate can be constructed by means of the following operations:

$$\mathcal{U}_H = \mathcal{U}_z(\pi/2)\, \mathcal{U}_x(\pi/2)\, \mathcal{U}_z(\pi/2) = \frac{1}{\sqrt{2}}\begin{pmatrix} 1 & 1 \\ 1 & -1 \end{pmatrix}, \qquad (13.18)$$

$$\mathcal{U}_\phi(\beta) = \mathcal{U}_z(-\beta) = \begin{pmatrix} 1 & 0 \\ 0 & \exp(i\beta) \end{pmatrix}. \qquad (13.19)$$

We obtain expressions (13.15) upon application of matrices (13.18) and (13.19) to column states (12.1).

13.5.2*   Two-Qubit Systems

The two-qubit states can be represented as products of single qubits $\varphi_J(1)\varphi_K(2)$ or in the computational basis $\varphi_J^{(2)}$, with $J = 0, 1, 2, 3$. Any effect upon them of the Pauli principle is ignored, since they are separated in space and thus distinguishable.

Successive application of the Hadamard gate on the state $\varphi_0^{(2)}$ yields

$$\mathcal{U}_H(2)\, \mathcal{U}_H(1)\, \varphi_0^{(2)} = \mathcal{U}_H(2)\frac{1}{\sqrt{2}}\left(\varphi_0^{(2)} + \varphi_1^{(2)} \right) = \frac{1}{2}\sum_{J=0}^{J=3} \varphi_J^{(2)}. \qquad (13.20)$$

Useful gates acting on two-qubit systems are the controlled-NOT gate $\mathcal{U}_{CNOT}$ and the controlled-phase gate $\mathcal{U}_{CB}(\phi)$

$$\mathcal{U}_{CNOT}\, \varphi_J\, \varphi_K = \varphi_J\, \varphi_{J \oplus K},$$
$$\mathcal{U}_{CB}(\phi)\, \varphi_J\, \varphi_K = \exp[iJK\phi]\, \varphi_J\, \varphi_K\,, \qquad (13.21)$$

where the symbol $\oplus$ denotes the summation $(J + K)$ modulo 2. These two gates apply a single-qubit transformation to the target qubit if the control qubit is in the state φ_1, and do nothing if the control qubit is in the state φ_0. The control bit remains unchanged, but its states determine the evolution of the target.

The controlled-NOT and the controlled-phase gates are expressed, in matrix form

$$
\mathcal{U}_{\text{CNOT}} =
\begin{pmatrix}
1 & 0 & 0 & 0 \\
0 & 1 & 0 & 0 \\
0 & 0 & 0 & 1 \\
0 & 0 & 1 & 0
\end{pmatrix} ; \quad
\mathcal{U}_{\text{CB}}(\phi) =
\begin{pmatrix}
1 & 0 & 0 & 0 \\
0 & 1 & 0 & 0 \\
0 & 0 & 1 & 0 \\
0 & 0 & 0 & \exp(i\phi)
\end{pmatrix} . \quad (13.22)
$$

The construction of the controlled-NOT and controlled-phase gates starting from the Hamiltonian (13.14) has been omitted from this presentation.

Combining these operations yields the discrete Fourier transformation

$$
\mathcal{U}_{\text{FT}} \, \varphi_J^{(2)} = \frac{1}{2} \sum_{K=0}^{K=3} \exp[i J K \pi/2] \, \varphi_K^{(2)},
$$

$$
\mathcal{U}_{\text{FT}} = \mathcal{U}_{\text{SWAP}} \left(\frac{\pi}{2} \right) \mathcal{U}_{\text{H}}^{(\text{targ})} \mathcal{U}_{\text{CB}} \left(\frac{\pi}{2} \right) \mathcal{U}_{\text{H}}^{(\text{ctrl})}
$$

$$
= \frac{1}{2}
\begin{pmatrix}
1 & 1 & 1 & 1 \\
1 & i & -1 & -i \\
1 & -1 & 1 & -1 \\
1 & -i & -1 & I
\end{pmatrix} , \quad (13.23)
$$

where the SWAP transformation interchanges the values of the control and target bits

$$
\mathcal{U}_{\text{SWAP}} \, \varphi_J(1) \, \varphi_K(2) = \varphi_K(1) \, \varphi_J(2)
$$

$$
\mathcal{U}_{\text{SWAP}} = \mathcal{U}_{\text{CNOT}} \mathcal{U}_{\text{H}}^{\text{ctr}} \mathcal{U}_{\text{H}}^{\text{tag}} \sqcap_{\text{CNOT}} \mathcal{U}_{\text{H}}^{\text{tag}} \mathcal{U}_{\text{H}}^{\text{ctr}} \mathcal{U}_{\text{CNOT}}
$$

$$
=
\begin{pmatrix}
1 & 0 & 0 & 0 \\
0 & 0 & 1 & 0 \\
0 & 1 & 0 & 0 \\
0 & 0 & 0 & 1
\end{pmatrix} . \quad (13.24)
$$

13.5.3*   *n*-Qubit Systems

As for the one- and two-qubit cases, we may use either the product or the column representation. In most applications the initial state is

$$
\varphi_0^{(n)} = \prod_{k=1}^{k=n} \varphi_0(k). \quad (13.25)
$$

The transformations (13.20), (13.21) and (13.24) may be generalized to the case of n-qubits

$$\Pi_{k=1}^{k=n} \mathcal{U}_H(k)\, \varphi_0^{(n)} = \frac{1}{\sqrt{2^n}} \sum_{J=0}^{J=2^n-1} \varphi_J^{(n)}. \tag{13.26}$$

If the control and target are n-registers, operation (13.21) becomes

$$\mathcal{U}\varphi_J^{(n)}\varphi_K^{(n)} = \varphi_J^{(n)}\varphi_{K\oplus J}^{(n)}\,, \qquad \mathcal{U}_f\varphi_J^{(n)}\varphi_K^{(n)} = \varphi_J^{(n)}\varphi_{K\oplus f(J)}^{(n)}\,, \tag{13.27}$$

where the symbol $\oplus$ in the first equation (13.21) denotes summation modulo 2^n and a function $f(J)$ is defined mapping the number J into another number that may be stored by an n-register.

The discrete Fourier transformation (13.23) is generalized as

$$\mathcal{U}_{\mathrm{FT}}\varphi_J^{(n)} = 2^{-n/2} \sum_{K=0}^{K=2^n-1} \exp[\mathrm{i}JK\pi/2^{(n-1)}]\varphi_K^{(n)}\,. \tag{13.28}$$

All components of the state vector work in parallel using the gates described above.

Problems

Problem 1. Find the eigenvalues of the product operators $\hat{S}_z(1)\,\hat{S}_z(2)$ and $\hat{S}_x(1)\,\hat{S}_x(2)$ for each Bell state.

Problem 2. Alice and Bob share a good qubit (Sect. 13.2). Assume that Alice sends the qubit in the state φ_0. Determine the probability that Bob detects the intensity 1 if:

1. There is no eavesdropper and Bob's detector is aligned with the z-axis.
2. There is no eavesdropper and Bob's detector is antialigned with the z-axis.
3. There is no eavesdropper and Bob's detector is oriented at random.
4. Eve is active and Bob's detector is aligned with the z-axis.
5. Eve is active and Bob's detector is antialigned with the z-axis.
6. Eve is active and Bob's detector is oriented at random.

Problem 3. Find the generators of rotations that Bob has to perform in order to obtain the original qubit for each Bell state that Alice may have detected (Sect. 13.3).

Problem 4. Express the Fourier transform of a single qubit in terms of universal gates.

Problem 5. Show that $\mathcal{U}_x(\pi)\,\mathcal{U}_z(\beta)\,\mathcal{U}_x(-\pi) = \mathcal{U}_z(-\beta)$.

Problem 6. Show that $\dfrac{\hbar}{2}\mathcal{U}_{\text{CNOT}}\,\hat{S}_x^{(\text{ctrl})}\,\mathcal{U}_{\text{CNOT}} = \hat{S}_x^{(\text{ctrl})}\,\hat{S}_x^{(\text{targ})}$.

Problem 7. Verify (13.26) for the case $n = 3$.

Problem 8. Alice and Bob share two particles in a given Bell state. Alice performs a unitary transformation on her qubit using either the unit matrix $\mathcal{I}$ or one of the Pauli matrices. Subsequently, she sends her qubit to Bob.

1. Can Bob find which transformation Alice has performed?
2. Can Eve find which transformation Alice has performed?

The information that Bob receives (one of the four numbers) can be encoded in two bits of classical information, in spite of the fact that he receives a single qubit (from which a single bit is expected to be extracted). This quantum result is called superdense coding.

Problem 9. Find the value of the amplitudes c_{ir} in the Fourier transform (13.11).

Problem 10. Construct the algorithm for a Bell analyzer

1. Apply the controlled-NOT gate to each Bell state
2. Apply the Hadamard gate to the control qubit
3. Show that the resultant states are products of classical bits (12.1).

Chapter 14
Interpretations of Measurements.
Decoherence. Density Matrix

> *The problem of getting the interpretation proved to be rather*
> *more difficult than just working out the equations* [95].

Problems associated with the interpretation of the measurement processes are revisited in the present chapter. A brief survey of the orthodox line of thought is outlined in Sect. 14.1. Huge amounts of ink and paper have been devoted to the presentation of improved interpretations, without any of them having generated a general consensus.[1] However, a novel explanation of the coexistence between quantum and classical descriptions, based on the notion of *decoherence*, has been developed since the 1980s. The emergence of classicality from the quantum substrate interacting with the environment, outlined in Sect. 14.2[†], appears to be a consistent approach. Its application to the measurement process is described in Sect. 14.3[†].

In the present chapter, use is made of the density matrix, another formulation of quantum mechanics. It is appropriate for treating two entangled systems of which we have access to only one of them. The associated formalism is presented in Sect. 14.4.

14.1   Orthodox Interpretations

So far, predictions of quantum mechanics for isolated microsystems have never failed. However, the macroworld cannot be altogether forgotten even in the extreme Copenhagen interpretation, since it plays at least an essential role in the measurement process connecting quantum and classical systems.

If the quantum state of a system is denoted by $\Psi(t_0)$ at $t = t_0$, the system evolves swiftly and deterministically to the state $\Psi(t_1)$ at $t = t_1$, in accordance with the time-dependent Schrödinger equation. However, if a measurement takes place, it changes suddenly and impredictably.

---

[1]A critical discussion on alternative interpretations can be found, for instance, in [97].

None of the difficulties with the collapse principle has been so caricatured as the one due to Schrödinger [96]. He imagined an unstable nucleus inside a box. Its decay product, an α-particle, may free some poison that would also kill a cat staying inside the box.[2] Let $\mathcal{S}_0$, $\mathcal{S}_1$ represent the two states of the system (not-decayed-atom and decayed-atom) and $\mathcal{C}_0$, $\mathcal{C}_1$ those of the cat (alive and dead). The quantum evolution implies

$$\mathcal{S}_0\,\mathcal{C} \rightarrow \mathcal{S}_0\,\mathcal{C}_0,$$
$$\mathcal{S}_1\,\mathcal{C} \rightarrow \mathcal{S}_1\,\mathcal{C}_1, \tag{14.1}$$

where $\mathcal{C}$ is an initial, ready state for the cat. If the atom is in a quantum superposition, the linear evolution requires[3]

$$(c_0\mathcal{S}_0 \,+\, c_1\mathcal{S}_1)\,\mathcal{C} \rightarrow c_0\mathcal{S}_0\mathcal{C}_0 \,+\, c_1\mathcal{S}_1\mathcal{C}_1. \tag{14.2}$$

The collapse principle that we have been applying so far tells us that the cat will be either dead or alive after the measurement. Note that the composite system + cat is in an entangled state at the beginning of the measurement. Thus neither the atom nor the cat are in a definite state. But a superposition of an alive and a dead cat has never been seen![4]

Two orthodox interpretations are outlined in the following sections:

14.1.1   The Standard Interpretation

The standard interpretation is not much more than an enunciation of the basic Principle 3. Therefore, its main contents are:

- Every measurement performed on a quantum system induces a breakdown of the continuous evolution associated with the Schrödinger evolution, as a consequence of the collapse of the state Ψ into an eigenstate φ_n of the measured observable Q.
- The probability of a particular outcome q_n is given by $|\langle\Psi|\varphi_n\rangle|^2$.
- It is the observer who chooses the observable to be measured.

According to Zeilinger, "If we accept that the quantum state is no more than a representation of the information we have, then the spontaneous change of the state upon observation, the so-called collapse or reduction of the wave packet, is just a

---

[2]The link between the nuclear microsystem and the meter (the animal cat) goes through a chain of amplifying stages with intermediate systems (detector, poison, etc.) also getting correlated. In the text, we use the word "cat" to represent all of these items plus the animal.

[3]A similar operation may be accomplished by the controlled-NOT gate (13.21).

[4]Entangled states representing N spins pointing together in opposite directions $\Psi = \frac{1}{\sqrt{2}}[\varphi_0(1)\varphi_0(2)...\varphi_0(N) \,+\, \varphi_1(1)\varphi_1(2)...\varphi_1(N)]$ are called Schrödinger cat states or GHZ states.

very natural consequence of the fact that, upon observation, our information changes and therefore we have to change our representation of the information, that is, the quantum state." [78].

14.1.2   The Copenhagen Interpretation

Although the standard interpretation has often been confused with the Copenhagen interpretation, this last one includes the classical world in the process of measurement.

Intermediate classical apparatuses are necessary to convey to our classical minds the results of measurements on the quantum level. When particles are detected, the atoms of the detector become ionized, producing first a few electrons, and then a cascade of electrons. The state vector should take these macroscopic effects into account. Because of the linearity of the Schrödinger evolution, there is no mechanism to stop the evolution and yield a single result for the measurement.

Ultimately the evolution may involve the observer's brain, since the disappearance of macroscopic superpositions is attributed to the existence of the observer. Some extreme advocates of this interpretation have even argued that this mechanism may be linked to the property of consciousness in the human brain. Thus, it has been argued that quantum mechanics has an anthropocentric foundation, a concept which had disappeared from science after the Middle Ages.

However, the frontier between the quantum and the classical domains remained an ill-defined concept. This division was never accepted by Bell and other thinkers. In fact, there exist mesoscopic and even macroscopic quantum systems that are described with a global quantum wave function [Bose–Einstein condensates (Sect. 7.5†), superconductors (Sect. 10.1), neutron stars, etc.].

14.2†   The Emergence of Classicality from the Quantum Substrate. Decoherence

In this section we present a derivation of Newtonian mechanics as a limiting case of quantum mechanics.[5] Zurek was the first to emphasize the relevance of the interaction of systems with the environment [99], which in this case is represented by the initial state ε and the two states ε_0 and ε_1 that are obtained through the linear evolution

$$\begin{aligned} \varphi_0\, \varepsilon &\rightarrow \varphi_0\, \varepsilon_0, \\ \varphi_1\, \varepsilon &\rightarrow \varphi_1\, \varepsilon_1. \end{aligned} \tag{14.3}$$

---

[5]We mostly follow Chap. 2 of [98] throughout this section.

The system–environment interaction frequently manifests through a scattering process of surrounding particles interacting with the system (photons, air molecules, etc.).

If the initial state is a quantum superposition $\varphi_{\pm} = \frac{1}{\sqrt{2}}(\varphi_0 \pm \varphi_1)$, the evolution yields entangled states

$$\varphi_{\pm}\,\varepsilon \rightarrow \frac{1}{\sqrt{2}}(\varphi_0\,\varepsilon_0 \pm \varphi_1\varepsilon_1). \tag{14.4}$$

The reduced density matrix[6] operator for the system may be written[7]

$$\hat{\rho}_{\mathcal{S}} = \frac{1}{2}(|\varphi_0\rangle\langle\varphi_0| + |\varphi_1\rangle\langle\varphi_1| \pm |\varphi_0\rangle\langle\varphi_1|\langle\varepsilon_1|\varepsilon_0\rangle \pm |\varphi_1\rangle\langle\varphi_0|\langle\varepsilon_0|\varepsilon_1\rangle)$$

$$\approx \frac{1}{2}(|\varphi_0\rangle\langle\varphi_0| + |\varphi_1\rangle\langle\varphi_1|). \tag{14.5}$$

In deriving the last line we have assumed that the environment states are almost orthogonal to each other. This assumption is based on the complexity of the environment: if, for instance, we consider a beam of light quanta impinging over the system, the overlap between states before and after the collision may not be very much smaller than one for each individual photon, but the overlap of N photons may be close to vanishing in the limit of large N. If this is the case, the density matrix becomes similar to the one associated with an uncorrelated admixture of two separate states and thus, it is not able to display interference phenomena. Moreover, the larger the system, the more likely that the environment states become mutually orthogonal.

Therefore, classical macroscopic systems emerge as a consequence of being monitored by the rest of the universe. The environment acts as a device yielding information about which path in the two slit experiment (Fig. 2.5), which destroys the interference pattern.

Equation (14.5) does not imply that the system is in a mixture of states φ_0 and φ_1. Since these two states are simultaneously present in (14.4), the composite system + environment displays superposition and associated interferences. However, (14.5) says that such quantum manifestations will not appear as long as experiments are performed only on the system $\mathcal{S}$. Thus, there has been a leakage of coherence from the system to the composite entity. Since we are not able to control this entity, the decoherence has been completed to all practical purposes.

For many system–environment models the overlaps

$$\langle\varepsilon_i(t)|\varepsilon_j(t)\rangle \propto \exp(-t/\tau_d) \tag{14.6}$$

---

[6]The density matrix formalism is outlined in Sect. 14.4.

[7]An expansion of the environmental states in terms of an orthonormal set, $\varepsilon_i = \sum_l c_l^i \phi_l$, yields: trace$(|\varepsilon_i\rangle\langle\varepsilon_j|) = \sum_l c_l^i c_l^{j*} = \langle\varepsilon_j|\varepsilon_i\rangle$.

display an extremely fast exponential decay for $i \neq j$. Calculations for simplified cases yield decay times between $\mathcal{O}\left(10^{-14}\right)$ s and much less. In particular, the estimated decoherence times for neural superpositions $(10^{-19}$–$10^{-20})$ s is much smaller than typical times for cognitive processes $(10^{-2}$–$1)$ s [98].

In contrast with the states $\varphi_{\pm}$ of the system, the states φ_0 and φ_1 do not become entangled with the environment, according to (14.3). We thus conclude that there are states less prone to decoherence than others. They are called *pointer* states and make up the pointer subspace of the Hilbert space of the system. They play two essential roles:

- Sets of pointer states are made up from states most immune to decoherence. The composite pointer state + environment remains in a product state at all subsequent times. The selection of these states is determined through the structure of the system–environment Hamiltonian using methods developed in [99].
- Pointer states are also the states for which information is redundantly stored in a large number of fragments of the environment, in such a way that multiple observers can retrieve this information without disturbing the state of the system (as, for instance, through visual registration of photons that have been scattered from the system).

Since these are characteristic features of classical systems, classical reality has emerged from the quantum substrate.

Decoherence therefore explains why we do not see quantum superpositions in our everyday world: macroscopic objects are more difficult to keep isolated than microscopic objects. It also explains why spin up and down states are more easily preserved than their linear combinations through their interaction with the environment. This promising result is presently the subject of many studies.

14.2.1[†]   *A Mathematical Model of Decoherence*

Consider a qubit (the system) coupled to other $N - 1$ qubits representing the environment.[8] Let the Hamiltonian be

$$\hat{H} = -\frac{4}{\hbar} \, \hat{S}_z^{(1)} \sum_{k=2}^{k=N} j_k \, \hat{S}_z^{(k)}, \tag{14.7}$$

where any interaction between the qubits of the environment is disregarded. Assume an initial state of the form

$$\Phi(0) = \Psi(0) \prod_{k=2}^{k=N} \Psi^{(k)}(0)$$

---

[8]See [100], Sect. 2.5.

$$\Psi(0) = c_0\varphi_0 + c_1\varphi_1, \qquad \Psi^{(k)}(0) = c_0^{(k)}\varphi_0^{(k)} + c_1^{(k)}\varphi_1^{(k)}. \qquad (14.8)$$

The evolution of the system yields

$$\Phi(t) = \exp\left(-i\hat{H}t/\hbar\right)\Phi(0)$$

$$= c_0\varphi_0 \prod_{k=2}^{k=N}\left[c_0^{(k)}\exp\left(ij_kt\right)\varphi_0^{(k)} + c_1^{(k)}\exp\left(-ij_kt\right)\varphi_1^{(k)}\right]$$

$$+ c_1\varphi_1 \prod_{k=2}^{k=N}\left[c_0^{(k)}\exp\left(-ij_kt\right)\varphi_0^{(k)} + c_1^{(k)}\exp\left(ij_kt\right)\varphi_1^{(k)}\right]. \qquad (14.9)$$

The density operator is

$$\hat{\rho}(t) = |\Phi(t)\rangle\langle\Phi(t)|. \qquad (14.10)$$

Since we are interested in the system consisting of the first qubit, we trace out the remaining ones

$$\hat{\rho}^{(1)} = |c_0|^2|0\rangle\langle 0| + |c_1|^2|1\rangle\langle 1| + z(t)c_0c_1^*|0\rangle\langle 1| + z^*(t)c_0^*c_1|1\rangle\langle 0|,$$

$$z(t) = \prod_{k=2}^{k=N}\left[|c_0^{(k)}|^2\exp\left(ij_kt\right) + |c_1^{(k)}|^2\exp\left(-ij_kt\right)\right]. \qquad (14.11)$$

The time-dependence $z(t)$ included in the non-diagonal terms encompasses the relevant information concerning the coherence of the system. If $|z(t)| \to 0$, we are in the presence of a non-unitary process with an irreversible loss of information. This simple model is not quite up to this task, since there is a recurrence time τ_r for the function z to reassume the value 1. Nevertheless, there is an effective loss of coherence, since

$$\langle z(t)\rangle = \lim_{T\to\infty}\frac{1}{T}\int_0^T dt'z(t') = 0,$$

$$\langle|z(t)|^2\rangle = \frac{1}{2^{N-1}}\prod_{k=2}^{k=N}\left[1 + \left(\left|c_0^{(k)}\right|^2 - \left|c_1^{(k)}\right|^2\right)^2\right], \qquad (14.12)$$

which tell us that the fluctuations of $z(t)$ around the mean value 0 are inversely proportional to a function which increases exponentially with of the dimensions of the Hilbert space. Therefore, for a sufficiently large interval, and if the spins of the environment are initially oriented on the xy plane, the loss of information becomes

irreversible.[9] The φ_0 and φ_1 are the pointer states of the simplified model and there is decoherence.

14.2.2[†]   An Experiment with Decoherence

Since 1996, many experiments have demonstrated the dynamics of decoherence, by showing how superposition states become unobservable due to decoherence. In the following, we present one of such experiments.

As mentioned in Sect. 2.5.2, two-slit experiments were carried out even with relatively large objects such as fullerenes. The "matter" category of these objects appears evident from the fact that a molecule C_{70} has more than 10^3 particle components (electrons and nucleons). It is also possible to assign to them a temperature, and thermal radiation has also been observed.

A variation of the two-slit experiment consists of an application of the Talbot–Lau effect: if a wave impinges perpendicularly on a grating composed of parallel slits, as a consequence of interference the pattern of the grating will be reproduced at multiples of the distance $L_\lambda = d^2/\lambda$. Here d is the spacing between adjacent slits and λ, the wavelength.

Experiments clearly display the oscillatory fluctuations in the density of the C_{70} molecule along an axis perpendicular both to the incident direction and to the grating, at the distance L_λ. The confirmation of the existence of interference effects due to the Talbot–Lau effect was obtained by varying the velocity of the particles and thus the wavelength according to the de Broglie prescription.

Decoherence is produced by collisions between C_{70} molecules and molecules in the background gas. The amount of decoherence can be tuned by changing the density of the gas. Let us define the visibility factor as the ratio
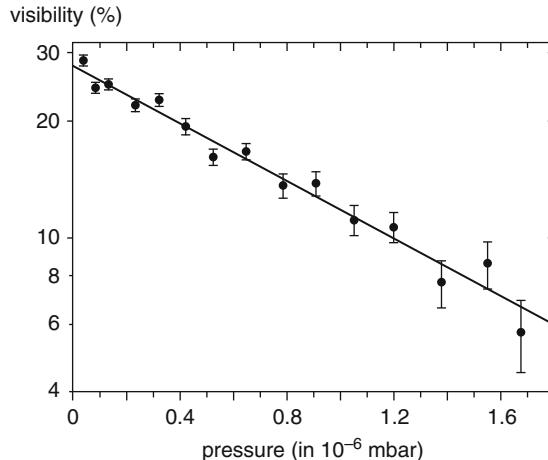
$$V = \frac{I_{\max} - I_{\min}}{I_{\max} + I_{\min}}, \tag{14.13}$$

where $I_{\max}$ and $I_{\min}$ are the maximum and minimum amplitudes in the interference pattern, respectively. The visibility decays exponentially with the increase in the density, as shown in Fig. 14.1.

"Thus these experiments provide impressive direct evidence for how the interaction with the environment gradually delocalizes the quantum coherence required for the interference effects to be observed... So we can smoothly navigate and explore the quantum-classical boundary, and we find our observations to be in excellent agreement with theoretical predictions." (M. Schlosshauer [98], p. 265).

Decoherence is currently the subject of a great deal of research. Many questions have been clarified to a large extent in recent years. These include the rate of

---

[9]This is due to the fact that (14.11) is a sum of periodic terms. However, for macroscopic environments of realistic size, Zurek has pointed out that τ_r can exceed the life of the universe.

Fig. 14.1 Dependence of the visibility (14.13) of the interference pattern on the pressure of the background gas [102] (reproduced with permission from the authors and from Springer Science and Business Media)

decoherence, the dynamical selection of the pointer states, the dissipation of energy into the environment, and many others.
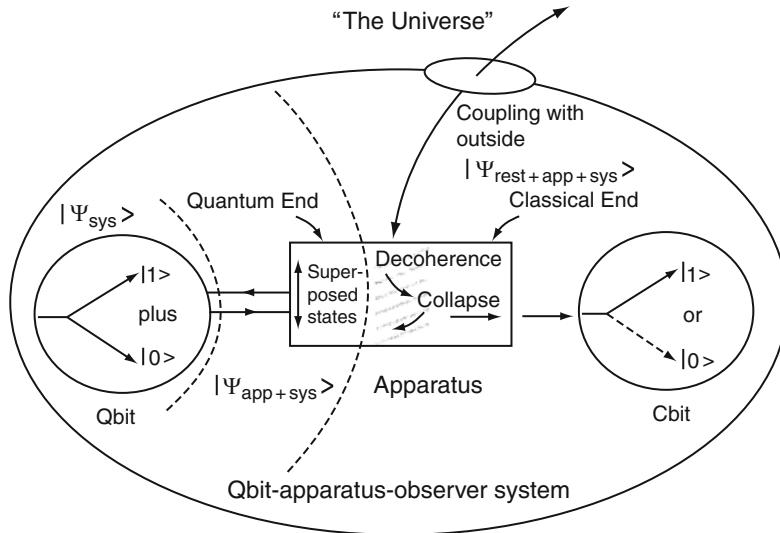
14.3[†] Quantum Measurements

A quantum measurement is an experiment coupling a microscopic system to a macroscopic meter. This last piece of the experiment is coupled to the environment. Decoherence ensures the classical description of the meter.

The von Neumann scheme for measurements assumes that all states are quantum mechanical, including the much smaller set of classical states. This is a different starting point than the one upon which the Copenhagen interpretation is based. Even though the possible superpositions in Hilbert space are potentially expanded with the Schrödinger equation, we have seen in Sect. 14.2[†] that the process of decoherence, i.e. the interaction between systems and environment, leads to the elimination of quantum superposition effects within the observed system, and to the selection of a small subset of classical, pointer states [100].

In the following, we sketch how this may be applied for the measurement of a two-state system (Fig. 14.2). Consider, for instance Schrödinger's thought experiment. At the quantum end (left side of the figure) the microsystem is represented by the two nuclear states, with an α-particle inside or outside the nucleus

$$\Psi^{\mathcal{S}}(0) = c_0\varphi_0 + c_1\varphi_1. \tag{14.14}$$

Fig. 14.2 Sketch of the measurement of a qubit. "Rest" is called "environment" in the text. Initially, there is a superposition of the two nuclear states. One of the two alternatives for the Schrödinger cat occurs at the classical end. (Reproduced from J. Roederer [20], with permission from Springer-Verlag)

We consider a quantum apparatus $\mathcal{Z}$ (cat et al.) with a Hilbert space spanned by the two states χ_1, χ_0. One can assume that the initial state of the binary microsystem-apparatus is

$$\Psi^{\mathcal{S},\mathcal{Z}}(0) = (c_0\varphi_0 + c_1\varphi_1)\chi_1. \tag{14.15}$$

The entanglement of the composite system may be produced by means of the interaction represented by a controlled-NOT gate [see (13.22)]. It is represented by the two arrows linking the qubit with the apparatus. Thus,

$$\Psi^{\mathcal{S},\mathcal{Z}}_t = c_0\varphi_0\chi_1 + c_1\varphi_1\chi_0. \tag{14.16}$$

If the detector is in the state χ_1, the microsystem is guaranteed to be found in the state φ_0, and vice versa. However, there is an ambiguity in a correlated state of the form (14.16), since we may rotate both the system and the apparatus without changing $\Psi^{\mathcal{S},\mathcal{Z}}_t$ (see p. 221). The ambiguity may be superseded by introducing another system, the environment $\mathcal{E}$, which is also represented by two quantum states $\varepsilon_1, \varepsilon_0$. From now on we apply the decoherence process to the composite system + apparatus

$$\Psi^{\mathcal{S},\mathcal{Z},\mathcal{E}}(0) = \Psi^{\mathcal{S},\mathcal{Z}}_t\varepsilon_1 \longrightarrow \Psi^{\mathcal{S},\mathcal{Z},\mathcal{E}}_t = c_0\varphi_0\chi_1\varepsilon_1 + c_1\varphi_1\chi_0\varepsilon_0. \tag{14.17}$$

Since we cannot control the environment, we are limited to evaluate expectation values of observables belonging to the $(\mathcal{S}, \mathcal{Z})$ subsystems. In the state (14.17), any such expectation value is

$$
\begin{aligned}
\langle Q \rangle = {} & |c_0|^2 \langle \varphi_0 \chi_1 | Q | \varphi_0 \chi_1 \rangle + |c_1|^2 \langle \varphi_1 \chi_0 | Q | \varphi_1 \chi_0 \rangle \\
& + 2\mathrm{Re} \left(c_0 c_1^* \langle \varphi_1 \chi_0 | Q | \varphi_0 \chi_1 \rangle \, \langle \varepsilon_0 | \varepsilon_1 \rangle \right).
\end{aligned} \tag{14.18}
$$

The third term in this equation is responsible for introducing interference. Interaction with the environment has the effect of modulating this interference term, whose magnitude is reduced by a factor determined by the absolute value of the overlap $\langle \varepsilon_0 | \varepsilon_1 \rangle$. When this overlap is sufficiently small, quantum interference effects become dynamically suppressed. The two (curved) arrows inside the box represent the correlation between the state of the system and the cat after decoherence has taken place.

The classical end appears at the extreme right of the figure, the word "Cbit" labels the cat, *either* dead *or* alive (and the observer looking at it).

As pointed out by M. Schlosshauer [98], p. 50, there are three issues in the measurement problem:

1. The problem of non-observability of interference. Through the interaction with the environment, decoherence explains why patterns of interference between macroscopic objects dissapear and only one of the possible outcomes is observed. An observer would only see the Schrödinger cat *either* dead *or* alive, because the duration of the weird state (14.2) will be incredibly short in a system with so many components. "Decoherence produces an effect that looks and smells like a collapse." [125].
2. The problem of the preferred basis. The preferred states of the system–apparatus are those that become least entangled with the environment in the course of the evolution and are thus most immune to decoherence. If the interaction between the (microscopic) system and the environment is neglected, the different pointer positions of the apparatus are the robust preferred states "superallowed" by the environment.
3. The question about why a particular outcome appears to the observer, rather than another possible one, is outside the domain of decoherence. It belongs to the philosophical aspects of the relation between quantum mechanics and reality.

14.4   The Density Matrix

The density matrix operator corresponding to a state Ψ is defined as the projector

$$
\hat{\rho} = |\Psi\rangle \langle \Psi|. \tag{14.19}
$$

In particular, $\hat{\rho}_i = |i\rangle\langle i|$ is used in (2.57). The expectation value of an operator $\hat{Q}$ in the state φ_i is given by

$$\text{trace}(\rho_i \, Q) = \sum_{i'} \langle i'|i\rangle\langle i|Q|i'\rangle = \langle i|Q|i\rangle. \qquad (14.20)$$

If our system is in a state Ψ, the descriptions in terms of Ψ and in terms of the density matrix (14.19) are completely equivalent.

14.4.1 Mixed Density Matrix

In a mixed state we do not know in which state φ_i the system is. Therefore, only probabilities π_i can be ascribed to each state

$$0 \le \pi_i \le 1, \qquad \sum_i \pi_i = 1, \qquad (14.21)$$

which can be interpreted as a classical probability distribution of quantum states. The projection operator can be generalized in terms of the density matrix

$$\hat{\rho} = \sum_i \pi_i \, |i\rangle\langle i| \, . \qquad (14.22)$$

Thus, the present formalism is especially useful when we have less than complete information on the system. For instance, the silver atoms leaving the furnace in a Stern–Gerlach experiment are randomly oriented in space (as in Fig. 2.4). In this case, $\pi_+ = \pi_- = 1/2$, the probabilities of the spin being up or down being the same. We say that the system is in a *mixed state* and the density matrix is given by

$$\hat{\rho} = \frac{1}{2} \left(|0\rangle\langle 0| + |1\rangle\langle 1| \right). \qquad (14.23)$$

If $\pi_{i'} = \delta_{i'i}$, we say that the system is in a *pure state*, like all those that we have studied so far in the present text. In this case the density matrix reduces to the projection $|i\rangle\langle i|$.

Some consequences of the definition (14.22) are:

- The expectation value of an operator $\hat{Q}$ acting within the complete set of states φ_i, is given by

$$\langle |Q| \rangle = \text{trace}(\rho \, Q) = \sum_{i'i} \pi_i \, \langle i'|i\rangle\langle i|Q|i'\rangle$$

$$= \sum_i \pi_i \, \langle i|Q|i\rangle, \qquad (14.24)$$

where the expectation values $\langle i|Q|i\rangle$ are weighted for each of the possible states φ_i by their respective classical probability.

- The matrix elements of the density matrix are given by

$$\langle i|\rho|j\rangle = \sum_k \pi_k \langle i|k\rangle\langle k|j\rangle \tag{14.25}$$

and therefore,

$$\mathrm{trace}(\rho) = \prod_{ik} \pi_k \, |\langle i|k\rangle|^2 = \sum_k \pi_k = 1, \tag{14.26}$$

where $\mathrm{trace}(\rho^2) < 1$, unless we are dealing with a pure state.

The matrix elements $\langle i|\rho|i\rangle$ represent the probability of finding the system in the state φ_i. The non-diagonal matrix elements $\langle i|\rho|j\rangle$ may vanish, even if none of their terms do.

- Let us rotate the spin axis by means of the transformation (5.26). In such a case (14.23) is transformed to

$$\hat{\rho} = \frac{1}{2} \left(|0^{(\beta,\phi)}\rangle\langle 0^{(\beta,\phi)}| + |1^{(\beta,\phi)}\rangle\langle 1^{(\beta,\phi)}| \right). \tag{14.27}$$

Thus, the mixed density matrix does not provide information about the particular axis in which the state has been prepared.

- A mixed state *is not* a superposition of pure states $\Psi = \sum_i \sqrt{\pi_i}\, \varphi_i$, which correspond to a density matrix with off diagonal terms

$$\hat{\rho} = \sum_i \pi_i |i\rangle\langle i| + \sum_{i \neq j} \sqrt{\pi_i \pi_j} \, |i\rangle\langle j|. \tag{14.28}$$

- The (useless) overall phase multiplying the state vector disappears from the formalism.
- As time changes,

$$\hat{\rho}(t) = \sum_i \pi_i \, |i(t)\rangle\langle i(t)|,$$

$$\langle i|\rho(t)|j\rangle = \sum_k \pi_k \langle i|k(t)\rangle\langle k(t)|j\rangle. \tag{14.29}$$

Therefore, according to the time principle (9.4),

$$\dot{\hat{\rho}} = -\mathrm{i}[\hat{H}, \hat{\rho}]. \tag{14.30}$$

14.4.2   Reduced Density Matrix

The reduced density matrix is the appropriate tool for the treatment of two (or more) entangled systems A, B, if we have access only to system A.

$$\hat{\rho}^{(A)} = \text{trace}_B\left(\hat{\rho}^{(AB)}\right), \tag{14.31}$$

where the operator $\hat{\rho}^{(A)}$ is obtained by performing a partial trace over the subsystem B. If we denote by $\Psi^{(AB)}$ a pure eigenstate of the whole system

$$\Psi^{(AB)} = \sum_{i,\nu} c_{i\nu}\, \varphi_i^{(A)}\, \chi_\nu^{(B)} \tag{14.32}$$

and $\hat{Q}$ is an operator acting only within the (complete) subspace $\varphi_i^{(A)}$, its expectation value can be written

$$\langle\Psi^{(AB)}|Q|\Psi^{(AB)}\rangle = \sum_{i,j,\nu}\langle i^{(A)}|Q|j^{(A)}\rangle = \text{trace}(\hat{\rho}^{(A)}Q). \tag{14.33}$$

The reduced density matrix can be written as

$$\hat{\rho}^{(A)} = \sum_{i,j,\nu} c_{i\nu}^* c_{j\nu}\, |i^{(A)}\rangle\langle j^{(A)}|,$$

$$\text{trace}(\rho^{(A)}) = 1 \qquad \langle k^{(A)}|\hat{\rho}^{(A)}|k^{(A)}\rangle \ge 0, \tag{14.34}$$

which are conditions equivalent to (14.21). Therefore, $\hat{\rho}^{(A)}$ satisfies the definition of a density matrix, upon the diagonalization within the subspace A.

As an example, consider the case of two qubits, A and B, in the Bell state Ψ_{B_0} (Sect. 12.2). The density matrix operator is written

$$\hat{\rho}_{B_0}^{(AB)} = \frac{1}{2}\left(|0^{(A)}0^{(B)}\rangle + |1^{(A)}1^{(B)}\rangle\right)\left(\langle 0^{(A)}0^{(B)}| + |\langle 1^{(A)}1^{(B)}|\right). \tag{14.35}$$

Since this is a pure state, $\text{trace}(\rho^2) = 1$. Let us assume that we do not have access to qubit B. We obtain the reduced density matrix for qubit A by tracing out qubit B

$$\hat{\rho}^{(A)} = \frac{1}{2}\left(|0^A\rangle\langle 0^{(A)}| + |1^{(A)}\rangle\langle 1^{(A)}|\right) = \frac{1}{2}\begin{pmatrix} 1 & 0 \\ 0 & 1 \end{pmatrix}, \tag{14.36}$$

which behaves as a mixed state, since $\text{trace}\left[(\rho^{(A)})^2\right] = 1/2$. In a Bell state we have incomplete information on the properties of each qubit. Moreover, the information encoded in (14.36) is the same for any of the Bell states.

The expectation value of the spin of qubit A along the x-direction vanishes

$$\langle |S_x| \rangle = \frac{\hbar}{2} \, \text{trace} \left(\sigma_x \rho^{(A)} \right) = 0. \tag{14.37}$$

The reduced density matrix is used in Sect. 14.2[†] to formalize the concept of decoherence. In such case, the universe is divided into two parts: A, the system upon which we are interested, and B, the rest of the universe.

Problems

Problem 1. A C_{70} molecule moves with a velocity of about 100 m/s. Calculate the Talbot–Law distance if the separation between two consecutive slits is $1\,\mu$m.

Problem 2. Show that the mean value of the density matrix is always positive.

Problem 3. Show that the density operator is Hermitian.

Problem 4. Consider the pure spin state $\varphi_\uparrow^{\beta\phi}$ (5.25).

1. Construct the density operator.
2. Obtain the averages $\langle S_x \rangle, \langle S_y \rangle, \langle S_z \rangle$.

Problem 5. Consider the unpolarized mixed spin state $(\pi_{\beta\phi} \rightarrow d\Omega/4\pi)$.

1. Construct the density operator and compare the result with (14.36).
2. Obtain the averages $\langle S_x \rangle, \langle S_y \rangle, \langle S_z \rangle$.
3. Interpret the difference between these averages and those obtained in Problem 4.

Problem 6. Calculate the value of Δx for a particle moving in a harmonic oscillator potential at temperature T. Assume a Maxwell–Boltzmann distribution $[\pi_n = \exp(-\hbar\omega\, n/k_B T)]$ and use $\int_0^\infty \exp(-x)\, x^n \mathrm{d}x = \Gamma(n)$.

Chapter 15
A Brief History of Quantum Mechanics

15.1 Social Context in Central Europe During the 1920s

To continue the building analogy of Chap. 1, the theoretical foundations of physics were shaken at the beginning of the twentieth century. These tremors preceded those of the society as a whole. The historian Eric Hobsbawm has written [103]:

> The decades from the outbreak of the First World War to the aftermath of the second, were an Age of Catastrophe for this society [...] shaken by two world wars, followed by two waves of global rebellion and revolution [...]. The huge colonial empires, built up before and during the Age of the Empire, were shaken, and crumbled to dust. A world economic crisis of unprecedented depth brought even the strongest capitalistic economies to their knees and seemed to reverse the creation of a single universal world economy, which had been so remarkable an achievement of nineteenth-century liberal capitalism. Even the USA, safe from war and revolution, seemed close to collapse. While the economy tottered, the institutions of liberal democracy virtually disappeared between 1917 and 1942 from all but a fringe of Europe and parts of North America and Australasia, as Fascism and its satellite authoritarian movements and regimes advanced.

Since quantum mechanics was developed for the most part in Northern and Central Europe (see Table 15.1), we will devote most of our attention here to the conditions prevailing at that time in Germany and Denmark.

Hobsbawm's description applies particularly well to the case of Germany: while the Anglo-Saxon world and the wartime neutrals more or less succeeded in stabilizing their economies between 1922 and 1926, Germany was overwhelmed in 1923 with economic, political and spiritual crises. Hunger riots erupted everywhere, as the value of the mark plunged to 10^{-12} of its pre-1913 value. Additional difficulties arose from a repressed military putsch in North Germany, a separatist movement in the Rhineland, problems with France on the Rhur, and radical leftist tendencies in Saxony and Thuringia. In the East, Soviet Russia did not fare better.

A cultural movement against dogmatic rationalism gained ground in German society after the war. A widely read book opposed causality to life, and assimilated physics into causality [104]. Moreover, a profound division along political, scientific and geographic lines started to grow in the German physics community. Right wing

physicists were in general chauvinistic, ultraconservative, provincial, anti-Weimar and anti-Semitic. They were interested in the results of experiments and dissociated themselves from quantum and relativity theory. On the opposite side, the Berlin physicists were labeled as liberal and theoretical. Note, however, that the German physicists of that time, with the possible exception of Einstein and Born, could only be labeled as liberal or progressive in comparison with Johannes Stark and Philipp Lenard. The adjective "theoretical" (appearing also in the name of Bohr's Institute in Copenhagen) would be translated today as "fundamental." Although the main theoretical center was in Berlin, strong theoretical schools also flourished in Göttingen and Munich. The start of Nazi persecutions in the 1930s and the exclusion of Jews from the first group had consequences on the world distribution of physicists devoted to the most fundamental aspects of physics.

After the First World War (1918) German physicists had been excluded from international collaborations, and the lack of foreign currency made it almost impossible to purchase foreign journals and equipment. However, a new national organization, the Notgemeinschaft der Deutschen Wissenschaft, created in 1920 under the direction of Max von Laue and Max Planck, was instrumental in the provision of funds for scientific research. Atomic theorists in Berlin, Göttingen and Munich received sufficient funds to support the work of physicists like Heisenberg and Born. The foreign boycott was not observed by Scandinavia and the Netherlands: Bohr kept friendly relations with his German colleagues (see p.).

Denmark had been on the decline at least since 1864, when it was defeated by Prussia and Austria with the resultant loss of about one-third of its territory. The years after the war represented a period of unprecedented turmoil in Denmark as well. For the first time in 400 years, this country teetered on the brink of revolution, although of a kind that was different from those experienced in neighboring countries, disputes over the shift of the border with Germany, social struggles between town and country and fights for extensive reforms in employment conditions. All these difficulties added to the loss of wartime markets, and to trade deficits and inflation. In spite of such hardships, Bohr's new institute was inaugurated in 1921.

The scientific and the social crisis during the first part of the twentieth century were both very profound. However, the first one was over by the end of the 1920s. The second one continued *in crescendo* until the aftermath of the Second World War (1945).

15.2 Pre-history of Quantum Physics ($1860 \leq t \leq 1900$)

Gustav Kirchhoff is at the origin of both radiation and matter branches of quantum physics.[1] In 1860 he showed that the emissive power of a black-body $E(\nu)$ depends only on the frequency ν and on the temperature T and challenged both the experimentalists and theoreticians to find such dependence [108]. This search

---

[1]The sources [105–107] have been used extensively for this chapter.

proved to be full of difficulties. Only in 1893 Wilhelm Wien demonstrated his displacement law and in 1896 he proposed the exponential dependence for the function $f(v/T)$ in (15.1) [109]. In 1900 Planck modified this dependence with an extremely successful guess (15.2), that still holds today

$$E(v) = v^3 f(v/T) \qquad f(v/T) = \alpha \exp[-\beta v/T] \tag{15.1}$$

$$\rightarrow \frac{hv^3}{c^2} \frac{1}{\exp[hv/kT] - 1}, \tag{15.2}$$

where the Planck constant h was introduced [2].

Analytical spectroscopy was also started by Kirchhoff in 1860, in collaboration with Robert Bunsen [110]. The Balmer formula fitting the frequencies of the discrete hydrogen spectrum dates from 1885

$$v_n = c R_{\mathrm{H}} \left(\frac{1}{4} - \frac{1}{n^2} \right), \qquad n = 3, 4, \dots, \tag{15.3}$$

where R_{H} is the Rydberg constant [7]. No significant progress was made in understanding Balmer's formula for 28 years.

15.3   Old Quantum Theory (1900 ≤ t ≤ 1925)

15.3.1   Radiation

Planck justified his law by means of an unorthodox way of counting partitions plus the quantum hypothesis: the (fictitious) oscillators of a black-body have energy [2]

$$\epsilon = hv . \tag{15.4}$$

In 1905 Einstein showed that the expression for the increase of entropy with volume of a gas composed of non-interacting molecules becomes identical to the same quantity for monochromatic radiation obeying Wien exponential law (15.1), if in such expression the number of molecules n is replaced by E/hv, where E is the total energy. Thus, from purely thermodynamic arguments, Einstein concluded that "... it seems reasonable to investigate whether the laws governing the emission and transformation of light are also constructed as if light consisted of ... energy quanta" [3]. This proposal constituted a revolution, in view of the so far wholly accepted Maxwell's wave theory of light. Moreover, Einstein endowed Planck's oscillators with physical reality.

On the basis of (15.4), Einstein interpreted the photoelectric effect as the total transfer of the photon[2] energy to the electron, whose energy E is given by

---

[2]The term "photon" was only coined during the 1920s.

$$E = h\nu - W \ , \tag{15.5}$$

where W is the work function of the metal. This relation was only confirmed experimentally in 1914 by Robert Millikan [111], although even then Millikan did not conclude in favor of Einstein's "bold, not to say reckless hypothesis." In fact, from 1905 to 1923 Einstein was the only physicist seriously considering the existence of light quanta.

From 1906 to 1911, quantum theory was Einstein's main concern (even more than the theory of relativity). He contributed to the specific heat of solids and to energy fluctuations of black-body radiation. In 1909, he foretold: "It is my opinion that the next phase of theoretical physics will bring us a theory of light which can be interpreted as a kind of fusion of the wave and the emission theory."

Between 1916 and 1917 Einstein made fundamental contributions to the theory of radiation [64]. Combining classical thermodynamics and electromagnetism with Bohr's first two quantum postulates (Sect. 15.3.2), and assuming thermal equilibrium between atoms and radiation field, he derived:

- The concepts of spontaneous and induced emission and absorption, from which he could obtain Planck radiation law (15.2) (see Sect. 9.8.4[†]).
- The momentum of the light particle $h\nu/c$ which, together with the energy (1905), completes the properties of a quantum particle.
- The need of a probabilistic description, inherent to the concept of spontaneous emission

Einstein's 1917 paper carried the seeds of many developments in physics. However, he did not work by himself two rather immediate consequences:

1. The scattering of an atom and a light particle. Such experiments made by Arthur Compton verified both the energy and the momentum conservation in these processes and thus confirmed the validity of the light quantum hypothesis[3](1923, [4]).
2. Satyendra Bose's derivation of Planck's law using symmetric states was translated and submitted for publication by Einstein in 1924 [55]. The same year Einstein applied Bose's ideas to an ideal gas of particles [46] (see Sect. 7.5[†] on Bose–Einstein condensation).

However, a last storm over the light quanta was on the way (Sect. 15.5.2).

---

[3]However, explanations based on classical electromagnetic fields and quantized processes of emission and absorption could only be completely ruled out after experimental evidence that there is no lower limit on the accumulation time of light energy in the photoelectric effect [112] or on the non-existence of correlations of a photon with itself [113].

15.3.2   Matter

In 1911, the work of Rutherford's young colleagues Hans Geiger and Ernest Mardsen showed conclusively that a hydrogen atom consists of one electron outside the positively charged nucleus, where almost all the mass is concentrated [6]. At that time, electrons were supposed to be just particles. (Electron wave behavior was experimentally verified in [5].)

Like Einstein in 1905, Bohr was aware that the postulates of his 1913 model [8] were in conflict with classical physics:

- An atom displays stationary states of energy E_n that do not radiate.
- Transitions between stationary states are accompanied by monochromatic radiation of frequency ν satisfying the Balmer series

$$h\nu = E_n - E_m \,. \tag{15.6}$$

   This assumption implied a renunciation of causality because of the absence of any directive for the transition.
- For large values of n, the quantum frequency ν should agree with the classical frequency of light irradiated by the rotating electron. This correspondence principle constituted the main link between classical and quantum theory. (See Fig. 4.2 as an illustration of the survival of the correspondence principle in quantum mechanics.)

The derivation of the Rydberg constant as a function of the mass and the charge of an electron and of Planck's constant, and the correct helium ion/hydrogen ratio to five significant figures, commanded the attention of the physics community.

By means of his precise determination of X-ray energies, Henry Moseley gave further support to the Bohr model both through the assignment of a Z value to all known elements and the prediction of the still missing elements [114]. James Frank and Heinrich Hertz further confirmed the model by using the impact of electrons on atoms to excite their atomic spectrum [115]. The Bohr model appeared to work, in spite of its assumptions. To joke about the situation with the old quantum theory, Bohr used to tell the story of a visitor to his country home who noticed a horseshoe hanging over the entrance door. Puzzled, he asked Bohr if he really believed that this brought luck. The answer was: "Of course not, but I am told it works even if you don't believe in it." [107].

Bohr developed his model during a post-doctoral stay at Rutherford's laboratory (Manchester, UK). He was appointed professor of physics at the University of Copenhagen in 1916 and the Universitetets Institut for Teoretisk Fysik (today, Niels Bohr Institutet) was inaugurated in 1921. Unlike Einstein and Dirac, Bohr seldom worked alone. His first collaborator was Hendrik Kramers (Netherlands), followed by Oscar Klein (Sweden). During the 1920s, there were 63 visitors to the Institute who stayed more than one month, including 10 Nobel Laureates. The flow of foreign

visitors lasted throughout Bohr's life: he became both an inspiration and a father figure.

Arnold Sommerfeld established an important school in Munich. In 1914, it was found that every line predicted by the Balmer formula is a narrowly split set of lines. By taking into account the influence of relativity theory, Sommerfeld showed that the orbits of the electrons are approximate ellipses displaying a parhelion precession [116]. Sommerfeld's work was also one of the first attempts to unite the quantum and relativity theories, a synthesis still not completely achieved.

In Göttingen, Born did not turn his attention to atomic theory until around 1921. Heisenberg and Jordan were his assistants.

In 1924 Pauli had published 15 papers on topics ranging from relativity to the old quantum theory, the first one before entering the University of Munich. In 1922, he went for a year to Copenhagen. Later he held a position at Hamburg. He made the assumption of two-valuedness for electrons and stated the exclusion principle [42] (Sect. 7.1) so important for understanding the properties of atoms, metals, nuclei, baryons, etc.

The crucial experimental results of Stern and Gerlach were known in 1921 [17]. A proposal concerning spin was made[4] by two Dutch students from the University of Leiden, Uhlenbeck and Goudsmit, who also suggested the existence of $m_s = \pm 1/2$ as a fourth quantum number [35] (Sect. 5.2.2). They explained the anomalous Zeeman effect by including the factor of two appearing in (5.22), which was accounted for in [117]. After receiving objections from Henrik Lorentz, Uhlenbeck and Goudsmit considered withdrawing their paper, but it was too late. (Their advisor, Paul Ehrenfest, also argued that the authors were young enough to be able to afford some stupidity.) The two-component spin formalism (5.20) was introduced by Pauli in 1927 [36].

Dirac, and independently Enrico Fermi, developed quantum statistics for anti-symmetric wave functions [56, 57].

However, until 1925, there were almost as many setbacks as successes in the application of the model. For instance, the spectrum of He proved to be intractable, in spite of heroic efforts by Kramers, Heisenberg and others. The final blow was the negative result of the BKS proposal (Sect 15.5.2).

---

[4]The combination of the Pauli principle and of spinning electrons prompted Ralph Kronig to propose the idea of half-integer spin. However, he was dissuaded from publishing it by Pauli and others, on the grounds that models for electrons carrying an intrinsic angular momentum $\hbar/2$ either required the periphery of the electron to rotate with a velocity much larger than the velocity of light c, or the electron radius to be much larger than the classical value.

15.4   Quantum Mechanics (1925 ≤ t ≤ 1928)

Periodically, Bohr used to gather his former assistants together at the Institute in Copenhagen (Fig. 15.1). In 1925, the ongoing crisis in quantum mechanics was examined by Bohr, Kramers, Heisenberg and Pauli. A few months later, back at Göttingen, Heisenberg found a way out of the impasse [9]. He succeeded in formulating the theory in terms of observable quantities, doing away with the concepts of orbits and trajectories (see Sect. 2.1). Heisenberg found a correspondence between the coordinate $x(t)$ and the double array x_{nm} (n, m labeling quantum states). $x_{nm}(t)$ was interpreted as a sort of transition coordinate, and hence an allowed observable. To represent $x^2(t)$, he made the crucial assumption that $(x^2)_{nm} = \sum_p x_{np} x_{pm}$. Heisenberg solved the simple but non-trivial problem of the harmonic oscillator by showing that the Hamiltonian is given by $H_{mn} = E_n \delta_{nm}$, where the E_n reproduce the correct eigenvalues (Sect. 3.3).

Born and Jordan realized that the arrays (x_{nm}) were matrices and arrived at the fundamental commutation relation (2.15) in its matrix form (3.45) [118]. Born, Heisenberg and Jordan wrote a comprehensive text on quantum mechanics, which included unitary transformations, perturbation theory, the treatment of degenerate systems and commutation relations for the angular momentum operators [10].

Many of these results were also obtained by Dirac [11], who introduced the idea that physical quantities are represented by operators (of which Heisenberg's matrices are just one representation), the description of physical states by vectors in abstract Hilbert spaces, and the connection between the commutator of two operators with the classical Poisson bracket.

In 1926, Pauli and Dirac independently reproduced the results for the hydrogen atom of old quantum theory using the new matrix mechanics [39].

Fig. 15.1 The 1930 Copenhagen Conference. In the *front row*: Klein, Bohr, Heisenberg, Pauli, Gamow, Landau and Kramers. (Reproduced with permission from the Niels Bohr Archive, Copenhagen)

Zurich-based Schrödinger did not belong to the Copenhagen–Göttingen–Munich tradition. In 1925 he came across de Broglie's suggestion [32] that the wave–corpuscle duality should also be extended to material particles, satisfying the momentum–frequency relation (4.34). This relation is reproduced if the momentum and the energy are replaced by the differential operators (4.4) and (9.5) and if such operators act on the plane wave solutions (4.32) and (9.10). Upon making the same substitution in a general Hamiltonian, Schrödinger derived the time-independent and the time-dependent equations that bear his name [12]. Quantization was obtained through the requirement that the wave function should be single-valued (as in (5.32)). Schrödinger presented his derivation as a step towards a continuous theory, the integers (quantum numbers) originating in the same way as the number of nodes in a classical vibrating string. Schrödinger's formulation gained rapid acceptance, both because of the answers that it produced and because it was built from mathematical tools that were familiar to the theoretical physicists of the time. Schrödinger hoped that quantum mechanics would become another branch of classical physics: waves would be the only reality, particles being produced by means of wave packets. This expectation turned out to be wrong.

In 1926, Schrödinger also proved that the matrix and the differential formulation are equivalent. Since physicists understood how to transcribe the language of wave mechanics into matrix mechanics, both of them were referred to as quantum mechanics.

The probability interpretation of $|\Psi(x,t)|^2$ is usually considered part of the Copenhagen interpretation. However, Born was the first to write it explicitly [31]. In his paper on collision theory, he also stated that $|c_i|^2$ (2.6) was the probability of finding the system in the state i. He emphasized that quantum mechanics does not answer the question: what is the state after a collision? Rather it tells us how probable a given effect of the collision is. Determinism in the atomic world was thereby explicitly abandoned.

In 1926 Heisenberg was able to account for the He problem using the Schrödinger equation plus the Pauli principle plus spin (Sect. 8.3) [119].

The relativistic generalization of the Schrödinger time-dependent, two-component spin formalism encountered some difficulties. In 1928, Dirac produced an equation, linear in both the coordinates and time derivatives, with the properties that:

- It is Lorentz invariant
- It satisfies a continuity equation (4.17) with positive density ρ (which previous attempts at relativistic generalization had failed to do)
- It encompasses spin from the start
- It reproduces the results of the Sommerfeld model for the H atom, which were more accurate than the predictions of (new) quantum mechanics [120]

The price that Dirac had to pay for this most beautiful product of twentieth century mathematical physics was that it turned out to be a four-component rather than a two-component theory. Its interpretation including the additional two components is beyond the scope of this exposition.

Table 15.1 Publications in quantum mechanics. July 1925–March 1927 [105]

Country	Papers written	Country	Papers written
Germany	54	France	12
USA	26	USSR	11
Switzerland	21	Netherlands	5
Britain	18	Sweden	5
Denmark	17	Others	7

A few comments are in order:

- Quantum mechanics and its traditional interpretation were developed over only a few years (1925–1928). The rate of publication in this period was such that many physicists complained about the impossibility of keeping up to date. Moreover, communication delays certainly hampered the ability of non-European physicists to contribute.
- Quantum mechanics was developed under a very unfavorable social context (see Sect. 15.1).
- Unlike previous scientific cornerstones, quantum mechanics was the result of the coherent effort of a group of people, mostly in Northern and Central Europe. Table 15.1 shows the number of papers written in each country during the period of major activity in the creation of quantum mechanics. It reflects both the predominance of Germany and the number of visitors, especially in the case of Denmark. It also reminds us that the scientific center of gravity was only transferred to the other side of the Atlantic after the Second World War (1939–1945).
- The Bohr Festspiele took place at Göttingen in 1922. After Bohr's speech, the 20 year old Heisenberg stood up and raised objections to Bohr's calculations. During a walk in the mountains that same afternoon, Bohr invited Heisenberg to become his assistant in Copenhagen. This anecdote points out the extreme youth (and self-confidence) of most of the contributors to quantum mechanics. In 1925 Dirac was 23 years old, Heisenberg was 24, Jordan 22, and Pauli 25. The "elders" were Bohr (40), Born (43), and Schrödinger (38). Feynman (24) produced the path integral formulation of quantum mechanics being a graduate student at Priceton (Sect. 11.3[†]).

15.5 Philosophical Aspects

15.5.1 Complementarity Principle

Neither the Heisenberg nor the Schrödinger formulations improved the contemporary understanding of wave-particle duality. In 1927, Heisenberg answered the question: can quantum mechanics represent the fact that an electron finds itself

approximately in a given place and that it moves approximately with a given velocity and can we make these approximations so close that they do not cause mathematical difficulties? [26]. The answer was given in terms of the uncertainty relations (2.37) and (9.35) (see the last paragraph of Sect. 2.6.1). Heisenberg's paper was the beginning of the discussion of the measurement problem in quantum mechanics (Chap. 14), about which so many volumes have been written.

As most theoretical physicists would have done, Heisenberg derived his uncertainty principle from the (matrix) formalism (Sect. 2.6.1). Bohr had the opposite attitude. While being duly impressed by the existence of at least two formulations predicting correct quantum results, he insisted on first understanding the conceptual implications, rather than the formalisms. His main tools consisted of words, which he struggled continually to define precisely. Bohr pointed out that theories – even quantum theories – were checked by readings from classical instruments. Therefore, all the evidence has to be expressed within classical language, in which the mutually exclusive terms "particle" and "wave" are well defined. Either picture may be applied in experimental situations, but the other is then inapplicable. The idea of complementarity is that a full understanding of this microscopic world comes only from the possibility of applying both pictures; neither is complete in itself. Both must be present, but when one is applied, the other is excluded.

The complementary principle is not an independent principle of quantum physics but a series of conceptual statements interpreting the mathematical formalism. Bohr's ideas were stated at the Como Conference, September 1927. Bohr continued to reformulate the presentation of complementarity throughout the rest of his life [21].

15.5.2   Discussions Between Bohr and Einstein

Many histories of science display a sequence of continuous successes, thus ignoring the many frustrations accompanying creative processes. The discussions between Bohr and Einstein about problems of principle illustrate the difficulties inherent to changes in the description of the physical world, even in the case of our greatest forefathers.

The first meeting between Bohr and Einstein took place in 1920, on the occasion of Bohr's visit to Berlin. Verification of general relativity through the bending of light had taken place shortly before. Thus Einstein was on the zenith, while Bohr was only a rising star. Although they interchanged affectionate compliments, the subject of their Berlin conversations remains unclear. Like many other physicists, at that time Bohr did not believe in light quanta, and this disbelief continued even after Compton's experiment (1923). In 1924 there appeared a paper signed by Bohr, Kramers and the American physicist John Slater with the following contents [121]:

• Since the simultaneous validity of the (continuous) wave theory of light, and the description of matter processes involving (discrete) energy transitions is

incompatible with conservation of energy in individual events, this principle is given up, as well as the conservation of momentum. They hold only statistically.

- Statistical independence of the processes of emission and absorption in distant atoms is also assumed.
- The mediation of virtual fields produced by virtual oscillators is proposed. However the paper describes neither formal mechanisms governing the behavior of these entities, nor their interaction with real fields. In fact, (15.6) is the only mathematical expression included in the paper.

Born, Klein and Schrödinger reacted positively. Einstein and Pauli were against. However, two experiments on Compton scattering ended the BKS speculation during the following year. They concerned the time-interval between the electron recoil and the scattered photon, and momentum conservation in individual processes. The BKS proposal marked the end of old quantum mechanics.

Einstein's initial appraisal of Heisenberg's and Schrödinger quantum mechanics appears to have been positive. However, the approval was withdrawn after Born's probabilistic interpretation. Einstein never accepted limitations to our knowledge arising from first principles of the theory.
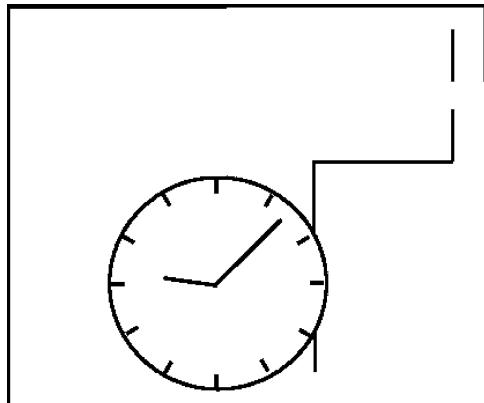
Quantum mechanics was discussed at the V Solvay Conference (1927) in Brussels, attended by all founders. Einstein expressed his concern over the extent to which the causal account in space and time had been abandoned in quantum mechanics. The discussions centered on whether a fuller description of phenomena could be obtained through the detailed balance of energy and momentum in individual processes. For instance, in the case of a beam of particles passing through a slit in a diaphragm, Einstein would suggest that the indetermination principle could be invalidated by measuring the momentum of the recoiling slit. During the evenings Bohr would explain how the inherent uncertainty in the location of the slit due to its recoil restored Heisenberg's principle. Bohr systematically emphasized the need to fully specify the measuring apparatus in any experiment. It was on this occasion that Einstein asked whether God had recourse to playing dice, to which Bohr replied by calling for great caution in ascribing attributes to Providence in everyday language.

At the next Solvay meeting in 1930 (Fig. 15.2), Einstein claimed that a control of energy and time could be achieved using relativity theory. He proposed the device represented in Fig. 15.3, consisting of a box with a hole on a wall and a clock inside, such that a single photon might be released at a known moment. Moreover, it would be possible to measure the energy of the photon with any prescribed accuracy by weighing the box before and after the event, and make use of the relativity equation $E = mc^2$. Bewilderment among quantum physicists lasted until the next day, when Bohr came up with an answer based on general relativity: since the rate of the clock depends on its position in a gravitational field, the lack of precision in the box displacement generates an uncertainty Δt in the determination of time, while the indeterminacy in the energy ΔE is obtained through the position–momentum relation (2.37). The product $\Delta t \, \Delta E$ satisfies the Heisenberg time–energy uncertainty relation.

Fig. 15.2 Einstein and Bohr
leaving the Solvay meeting of
1930. (Reproduced with
permission from the Niels
Bohr Archive, Copenhagen)

Fig. 15.3 Sketch of the
thought experiment proposed
by Einstein to reject the
time–energy uncertainty
relation. (Reproduced with
permission from the Niels
Bohr Archive, Copenhagen)

In 1935 Einstein, Podolsky and Rosen presented a profound argument pointing
to the incompleteness of quantum mechanics [16]. They considered a system
consisting of two entangled and spatially separated particles, which required the
existence of a hidden mechanism to reproduce the quantum results (Sect. 12.3.2).
An adaptation of their argument to the case of spin entanglement was produced by
David Bohm [80].

Bohr's reply was based on his concept of "phenomenon": the two (mutually
exclusive) experimental setups were not specified in the EPR definition of reality
[122].

Probably the best description of Einstein's and Bohr's respective positions is stated in Bohr's presentation on the occasion of Einstein's 70th birthday [124] and in Einstein's answer in the same volume [123].

15.6   Recent Quantum Mechanics

Rather than dwell on philosophical interpretations of equations, most physicists proceeded to carry out many exciting applications of quantum mechanics [125]:

> This approach proved stunningly successful. Quantum mechanics was instrumental in predicting antimatter, understanding radioactivity (leading to nuclear power), accounting for the behavior of materials such as semiconductors, explaining superconductivity, and describing interactions such as those between light and matter (leading to the invention of the laser) and of radio waves and nuclei (leading to magnetic resonance imaging). Many successes of quantum mechanics involve its extension, quantum field theory, which forms the foundations of elementary particle physics . . . .

On the other hand, the controversy over the EPR experiment did not die down. Einstein believed that, although quantum predictions were correct, indeterminacies appeared because some parameters characterizing the systems were unmeasurable. Therefore, an ensemble of identically prepared systems, all of them represented by the same quantum state Ψ, would not represent a collection of identical systems. Quantum mechanics would only appear probabilistic because we cannot measure the values of the "hidden variables." A more fundamental theory restoring determinism should bear to quantum mechanics a relation similar to the one existing between classical and statistical mechanics.

There were also attempts to prove that no hidden variable theory could reproduce the statistical properties of quantum theory. In particular, von Neumann's classic book [101] contains a mathematical proof that quantum theory is incompatible with the existence of "dispersion free ensembles" (such that $\langle |Q^2| \rangle = \langle |Q| \rangle^2$, for any observable Q). This precision would entail the existence of hidden variables.

In 1964, Bell wrote two seminal papers. In the first one, he showed that there was a questionable assumption in von Neumann's proof. In fact, he explicitly constructed a deterministic non-local model, generating results whose averages were identical to the predictions of quantum theory [126]. The second paper was not about quantum mechanics, but develops the consequences of both the existence of hidden variables and of Einstein's locality [81]. He found that such systems[5] would induce correlations that could be measured. He also showed that quantum predictions violated such restrictions. Thus quantum theory and Einstein's locality could not both be right. From there on, the emphasis was shifted from hidden variables to locality. Non-locality became an important feature of this world.

---

[5]One such systems is presented in Sect. 12.3.2.

Note that hidden variables are not ruled out, provided they are non-local. However, they have become a less attractive concept, since they were initially invoked to preserve locality.

The quantum-classical boundary persisted for decades as an ill-defined concept, although it was essential for the Copenhagen interpretation of measurements. Moreover, quantum effects were observed beyond the microscopic domain [fullerenes (Sect. 2.5.2), Bose–Einstein condensation (Sect. 7.5[†]), superconductivity (Sect. 10.1)].
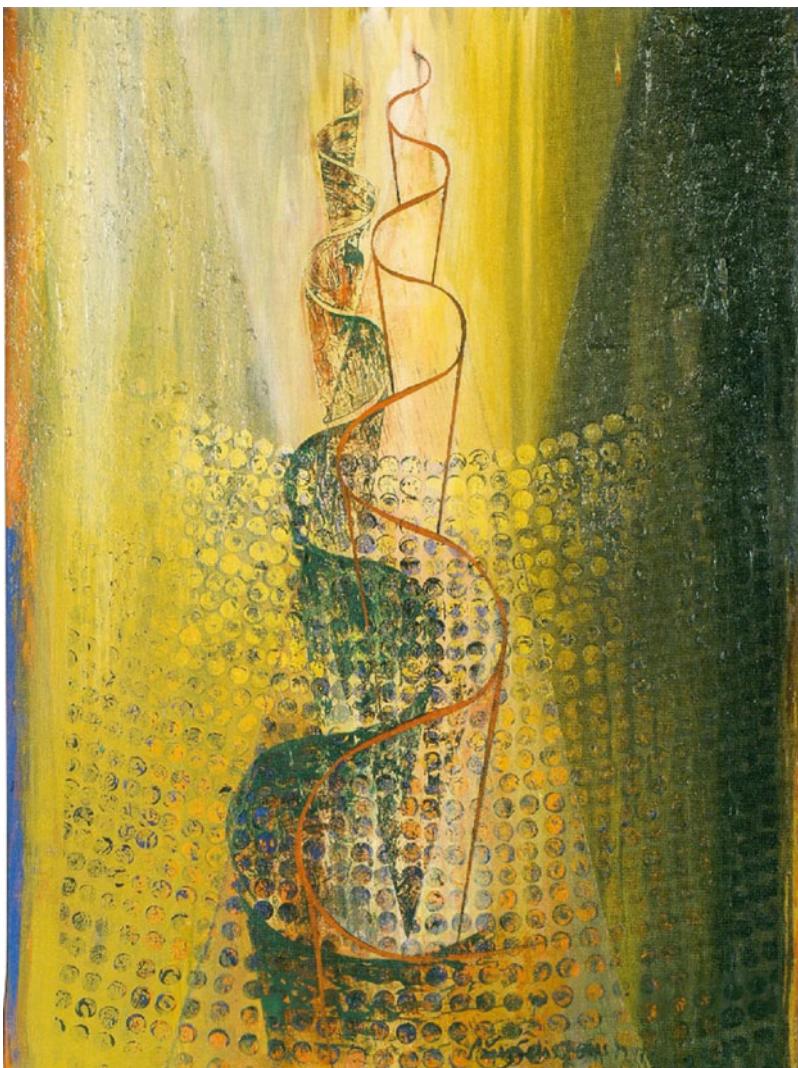
The notion of isolated systems, which originated in classical physics, was adopted in quantum mechanics without further scrutiny. Only recently was it realized that the openness of quantum systems (i.e. their interaction with the environment) is essential to explain how a quantum system becomes effectively classical. In Sect. 14.2[†] it is described how the coupling to the environment defines the observable physical properties of the system. Quantum coherences are delocalized into the entangled system–environment system, which effectively removes them from our observation. This process is very fast and irreversible in practice. Thus, classical systems appear to emerge from the quantum substrate [98]. Ironically, the locality of classical systems had been responsible for the idealization of the isolated-system concept.

The first paper on what was later called "decoherence" was written in 1970 by H. Dieter Zeh [127], who observed that realistic macroscopic quantum systems are typically found in states that are correlated with the environment, inhibiting the description of the dynamics of the system itself by means of the quantum formalism.

In 1981, Zurek developed the concept of environment-induced superselection [128]. He also showed how environment-induced superselection determines the "pointer" preferred states, and how it explains the fact that position is observed to be the usually preferred quantity in the everyday world. In 1984, Zurek derived a quite general expression from which typical decoherence timescales could be evaluated [129].

Erich Joos and Zeh presented in 1985 a detailed model for decoherence induced by the scattering of environmental particles, including numerical timescales for objects of various sizes and immersed in different environments [130].

Will quantum computing eventually become an accomplished instrument? As objects become larger and larger, they become more sensitive to external perturbations, which can destroy quantum superpositions. Nobody knows whether there is a hypothetical limit beyond which decoherence would be inevitable, or whether we always can, at least in principle, take sufficient precautions to protect the system against perturbations, no matter how large they are. Laboratory incident light is not even needed to produce decoherence. Thermal radiation, cosmic background radiation, gravity waves, etc., may be sufficient.

An Evanescent Particle (1997). Pérez Celis, Argentine painter (1939–2008). Starting from the *bottom*, this beautiful picture conveys the image of the linear combination (2.29), representing a particle exiting from the intermediate screen in a two-slit experiment (Fig. 2.5). Both *green* and *brown* components display a definite wave length, as befits a plane wave. Environment effects become effective after traveling some distance, resulting in a classical, decohered, single component. This picture belongs to the collection of Banco de la Nación Argentina, and is reproduced with authorization from this institution and from Pérez Celis' family

Appendix A
Solutions to Problems and Physical Constants

Solutions to Problems

Chapter 2

Problem 1. (1) $\Psi = \dfrac{c_1}{\sqrt{|c_1|^2 + |c_2|^2}}\Psi_1 + \dfrac{c_2}{\sqrt{|c_1|^2 + |c_2|^2}}\Psi_2$.

(2) $\dfrac{|c_1|^2}{|c_1|^2 + |c_2|^2}$.

Problem 2. (1) $\Psi_3 = -\dfrac{c}{\sqrt{1 - |c|^2}}\Psi_1 + \dfrac{1}{\sqrt{1 - |c|^2}}\Psi_2$.

(2) $\Psi = \dfrac{(c_1 + cc_2)\Psi_1 + c_2\sqrt{1 - |c|^2}\,\Psi_3}{\sqrt{|c_1|^2 + |c_2|^2 + c_1 c^* c_2^* + c_1^* c c_2}}$.

Problem 5. $-\mathrm{i}\dfrac{\hbar\hat{p}}{M}$.

Problem 6. (1) $-\mathrm{i}\hbar n\,\hat{p}^{n-1}$. (2) $-\mathrm{i}\hbar\dfrac{\mathrm{d}f}{\mathrm{d}\hat{p}}$.

Problem 8. (1) $\hat{R}\Psi = \Psi$. (2) $\hat{R}\Psi = 0$.

Problem 9. $\dfrac{\langle i|p|j\rangle}{\langle i|x|j\rangle} = \dfrac{\mathrm{i}M(E_i - E_j)}{\hbar}$.

Problem 10.

result	probability	result	probability
g_1, f_1	16/25	g_1, f_2	4/25
g_2, f_1	1/25	g_2, f_2	4/25

Problem 11.   (1) $P(4K_p) = \dfrac{1}{6}$ $P(K_p) = \dfrac{5}{6}$.   (2) $\langle |K|\rangle = \dfrac{3}{2}K_p$ $\Delta K = \dfrac{\sqrt{5}}{2}K_p$.
(3) $\dfrac{1}{\sqrt{5}}\varphi_2 + \dfrac{2}{\sqrt{5}}\varphi_3$.

Problem 12. $\Delta x \approx 10^{-19}\,\text{m},\ \Delta v \approx 10^{-19}\ \text{m}\,s^{-1}$.

Problem 13.   (1) $\Delta E_{\text{H}}/\Delta E = O(10^{-25})$.   (2) $x = O(10^{10})\,\text{m}$.

Chapter 3

Problem 1.   (1) $0,\ \pm\sqrt{2}$.   (2) $\varphi_{\pm\sqrt{2}} = \dfrac{1}{2}\begin{pmatrix}1\\0\\0\end{pmatrix} \pm \dfrac{1}{\sqrt{2}}\begin{pmatrix}0\\1\\0\end{pmatrix} + \dfrac{1}{2}\begin{pmatrix}0\\0\\1\end{pmatrix}$,

$$\varphi_0 = \dfrac{1}{\sqrt{2}}\begin{pmatrix}1\\0\\0\end{pmatrix} - \dfrac{1}{\sqrt{2}}\begin{pmatrix}0\\0\\1\end{pmatrix}\ ,\qquad \mathcal{U} = \dfrac{1}{2}\begin{pmatrix}1 & \sqrt{2} & 1\\ \sqrt{2} & 0 & -\sqrt{2}\\ 1 & -\sqrt{2} & 1\end{pmatrix}\ .$$

Problem 2.   (1) $\Delta_\pm = \pm\sqrt{a^2 + c^2}$.   (2) $\Delta_\pm = \pm|a|\left(1 + \dfrac{c^2}{2a^2} + \cdots\right)$.
(3) $\Delta_\pm = \pm|c|\left(1 + \dfrac{a^2}{2c^2} + \cdots\right)$.

Problem 3. $\langle 1|2\rangle = \langle 1|3\rangle = \langle 2|4\rangle = \langle 3|4\rangle = 0$.

Problem 4.   (1) $\Delta_Q = (0.5, 0.5, -1)$, $\Delta_R = (0.5, -0.5, 1)$.
(2) $[\hat{Q}, \hat{R}] = 0$.   (3) $\begin{pmatrix}1/\sqrt{2}\\1/\sqrt{2}\\0\end{pmatrix}$, $\begin{pmatrix}1/\sqrt{2}\\-1/\sqrt{2}\\0\end{pmatrix}$, $\begin{pmatrix}0\\0\\1\end{pmatrix}$.

Problem 5.   (1) $\pm\dfrac{\hbar}{2}$.   (3) $\varphi_{\beta\uparrow} = \cos\dfrac{\beta}{2}\begin{pmatrix}1\\0\end{pmatrix} + \sin\dfrac{\beta}{2}\begin{pmatrix}0\\1\end{pmatrix}$,
$\varphi_{\beta\downarrow} = -\sin\dfrac{\beta}{2}\begin{pmatrix}1\\0\end{pmatrix} + \cos\dfrac{\beta}{2}\begin{pmatrix}0\\1\end{pmatrix}$.

Problem 7.   (1) $E = V_0 + \dfrac{7\hbar}{2}\sqrt{\dfrac{c}{M}}$.   (2) $E = -\dfrac{b^2}{2c} + \hbar\sqrt{\dfrac{c}{M}}\left(n + \dfrac{1}{2}\right)$.

Problem 8.   (1) $x_{\text{c}} = \sqrt{\hbar}/(Mc)^{1/4}$.   (2) $3\hbar\omega$.

Problem 9.   (1) $\dfrac{2M\omega}{\hbar}\langle n+2|x^2|n\rangle = -\dfrac{2}{\hbar M\omega}\langle n+2|p^2|n\rangle =$

$\sqrt{(n+1)(n+2)}$, and 0 otherwise.   (3) $\dfrac{\langle n|K|n\rangle}{\langle n|V|n\rangle} = -\dfrac{\langle n\pm 2|K|n\rangle}{\langle n\pm 2|V|n\rangle} = 1$.

Problem 10.   Zero.

Problem 11.   (1) $\Psi = \dfrac{1}{\sqrt{2}}\varphi_0 + \dfrac{1}{\sqrt{2}}\varphi_1$.   (2) $\langle\Psi|x|\Psi\rangle = \dfrac{1}{\sqrt{2}}x_c$, $\langle\Psi|p|\Psi\rangle = \langle\Psi|\Pi|\Psi\rangle = 0$.

Problem 13. $c_{an}^{\pm} = \mp i c_{b(n+1)}^{\pm} = \dfrac{1}{\sqrt{2}}$.

Chapter 4

Problem 2.   (1) $\varphi_n = \sqrt{\dfrac{2}{a}}\sin(k_n x)$ $(0 \le x \le a)$ and $\varphi_n = 0$ otherwise. $k_n = n\pi/a$, $E_n = \hbar^2 k_n^2/2M$.   (3) No.

Problem 3. $E \approx (\hbar\Delta p)^2/2M \ge \hbar^2/8Ma^2$.

Problem 4. $i\kappa\coth\dfrac{\kappa a}{2} = k\cot\dfrac{ka}{2}$, $\kappa = \sqrt{2M(V_0 - E)}/\hbar$, $k = \sqrt{2ME}/\hbar$.

Problem 5. $\displaystyle\sum_k E_k - \dfrac{a}{2\pi}\int E_k \, dk \approx E_{k_{\max}} = \hbar^2 k_{\max}^2/2M$.

Problem 6.   (1) $\rho(E) = \dfrac{a}{\pi\hbar}\sqrt{\dfrac{M}{2E}}$.   (2) $0.81\ 10^7$ eV.

Problem 7.   (1) $-\cot\dfrac{ka}{2} = \dfrac{\kappa}{k}$.

Problem 8.   1 eps, 1 eps + 1 ops, 2 eps + 1 ops, 2 eps + 2 ops.

Problem 9. $R = 0.030$, $T = 0.97$.

Problem 10.   (1) $x_d \approx 1/\kappa = 1.13$ Å.   (2) $T = 1.7 \times 10^{-15}$.

Problem 11. $\displaystyle\lim_{\kappa a \ll 1} T = \dfrac{2E/V_0}{2E/V_0 + MV_0 a^2/\hbar^2}$,

$\displaystyle\lim_{\kappa a \gg 1} T = \dfrac{16E}{V_0}\left(1 - \dfrac{E}{V_0}\right)\exp\left[-\dfrac{2a}{\hbar}\sqrt{2M(V_0 - E)}\right]$.

Problem 12. $3\ 10^{-3}$ Å.

Problem 13.   (2) The lattice exerts forces on the electron.
(3) $\langle k|p|k\rangle = \hbar k\displaystyle\int |u_k|^2 dx - i\hbar\int u_k^*\dfrac{du_k}{dx}dx$.

Problem 14. $\dfrac{1}{M_{eff}} = \dfrac{1}{M} \mp \dfrac{d^2}{\hbar^2(\mathrm{d}f/\mathrm{d}E)_{E=E_0}}$, where $f(E_0) = \pm 1$.

Problem 15. (1) $\eta = \left(\dfrac{2\hbar\sqrt{2\pi}}{a\alpha}\right)^{1/2}$. (2) $|\Psi|^2 = \dfrac{\alpha}{\hbar\sqrt{2\pi}}\exp[-x^2\alpha^2/2\hbar^2]$

(3) $0, \hbar^2/\alpha^2$. (4) $0, \alpha^2/4$.

Chapter 5

Problem 1. $O\left(10^{31}\right)$.

Problem 2. $\dfrac{\hbar}{\sqrt{2}}\begin{pmatrix} 0 & 1 & 0 \\ 1 & 0 & 1 \\ 0 & 1 & 0 \end{pmatrix} \longrightarrow \hbar\begin{pmatrix} 1 & 0 & 0 \\ 0 & 0 & 0 \\ 0 & 0 & -1 \end{pmatrix}$.

Problem 4. $\mathrm{i}\hbar\,J$.

Problem 5. (1) $\langle 00|Y_{20}|00\rangle = \langle 11|Y_{21}|21\rangle = \langle 00|Y_{11}|11\rangle = \langle 00|\Pi|10\rangle = 0$.
(2) $\langle 10|Y_{20}|10\rangle = 0.25$, $\langle 00|Y_{11}|1(-1)\rangle = -0.28$, $\langle 00|\Pi|00\rangle = -\langle 11|\Pi|11\rangle = 1$.

Problem 7. (1) $\varphi_{s_x=\pm\frac{1}{2}} = \dfrac{1}{\sqrt{2}}\begin{pmatrix} 1 \\ \pm 1 \end{pmatrix}$, $\varphi_{s_y=\pm\frac{1}{2}} = \dfrac{1}{\sqrt{2}}\begin{pmatrix} 1 \\ \pm \mathrm{i} \end{pmatrix}$.

(2) $\pm\dfrac{\hbar}{2}$, $\dfrac{1}{2}$. (3) $\hat{S}_x = \dfrac{\hbar}{2}\begin{pmatrix} 0 & \mathrm{i} \\ -\mathrm{i} & 0 \end{pmatrix}$.

(4) $\varphi_{s_x=\pm\frac{1}{2}} = \dfrac{1\pm\mathrm{i}}{2}\varphi_{s_y=\frac{1}{2}} + \dfrac{1\mp\mathrm{i}}{2}\varphi_{s_y=-\frac{1}{2}}$.

Problem 8. (1) $\dfrac{1}{2}(a+b)^2$. (2) $\dfrac{1}{2}(a^2+b^2)$. (3) a^2.

Problem 9. (1) $\dfrac{\hbar}{2}$, $\cos^2\dfrac{\beta}{2}$, $-\dfrac{\hbar}{2}$, $\sin^2\dfrac{\beta}{2}$. (2) $\dfrac{\hbar}{2}\cos\beta$.

Problem 10. (1) $\varphi_{\frac{3}{2}\frac{1}{2}} = -\sqrt{\dfrac{2}{5}}Y_{20}\begin{pmatrix} 1 \\ 0 \end{pmatrix} + \sqrt{\dfrac{3}{5}}Y_{21}\begin{pmatrix} 0 \\ 1 \end{pmatrix}$,

$\varphi_{\frac{5}{2}\frac{1}{2}} = \sqrt{\dfrac{3}{5}}Y_{20}\begin{pmatrix} 1 \\ 0 \end{pmatrix} + \sqrt{\dfrac{2}{5}}Y_{21}\begin{pmatrix} 0 \\ 1 \end{pmatrix}$. (3) $Y_{ll}\begin{pmatrix} 1 \\ 0 \end{pmatrix}$, 1.

Problem 11. Equation (7.12).

Problem 12. $\sum_{m_1 m_2} c(j_1 m_1, j_2 m_2, jm) c(j_1 m_1, j_2 m_2, j'm') = \delta_{jj'} \delta_{mm'}$,
$\sum_{jm} c(j_1 m_1, j_2 m_2, jm) c(j_1 m'_1, j_2 m'_2, jm) = \delta_{m_1 m'_1} \delta_{m_2 m'_2}$.

Problem 13. $\varphi_{\frac{1}{2} l j m} = (-1)^{\frac{1}{2} + l - j} \varphi_{l \frac{1}{2} j m}$.

Chapter 6

Problem 1. 2.5×10^{-3} eV.

Problem 2.   (1) $1s_{\frac{1}{2}}$, $2s_{\frac{1}{2}}$, $2p_{\frac{1}{2}}$, $2p_{\frac{3}{2}}$, $3s_{\frac{1}{2}}$, $3p_{\frac{1}{2}}$, $3p_{\frac{3}{2}}$, $3d_{\frac{3}{2}}$, $3d_{\frac{5}{2}}$.
(2) $0s_{\frac{1}{2}}$, $1p_{\frac{1}{2}}$, $1p_{\frac{3}{2}}$, $2s_{\frac{1}{2}}$, $2d_{\frac{3}{2}}$, $2d_{\frac{5}{2}}$, $3p_{\frac{1}{2}}$, $3p_{\frac{3}{2}}$, $3f_{\frac{5}{2}}$, $3f_{\frac{7}{2}}$.

Problem 3.   (1) $(N + 1)(N + 2)$.   (2) $\dfrac{\hbar^2}{2} N(N + 3)$.

(3) $E_{Nlj} = \hbar\omega \left(\dfrac{\alpha_{Nlj}}{16} + \dfrac{3}{2} \right)$, where $\alpha_{Nlj} = 0(0s_{\frac{1}{2}})$, $10(1p_{\frac{3}{2}})$, $20(1p_{\frac{1}{2}})$,

$27(2d_{\frac{5}{2}})$, $37(2d_{\frac{3}{2}})$, $37(2s_{\frac{1}{2}})$, $39(3f_{\frac{7}{2}})$, $53(3f_{\frac{5}{2}})$, $53(3p_{\frac{3}{2}})$, $59(3f_{\frac{1}{2}})$.

(4) $l = N$, $j = N + \dfrac{1}{2}$.

Problem 4. $\varphi_n = \dfrac{1}{\sqrt{2\pi a}} \dfrac{1}{r} \sin \dfrac{n\pi r}{a}$, $E_n = \dfrac{1}{2M} \left(\dfrac{\hbar n \pi}{a} \right)^2$.

Problem 5. $r_{\max}^{(n_r = 1, l = 0)} = 5.2a_0$, $\langle 200|r|200 \rangle = 6a_0$, $r_{\max}^{(n_r = 0, l = 1)} = 4a_0$,
$\langle 21 m_l | r | 21 m_l \rangle = 5a_0$.

Problem 7.   (1) $\dfrac{R}{\langle 100|r|100 \rangle} = 1.5 \times 10^{-5}$ (H) ,

$\dfrac{R}{\langle 100|r|100 \rangle} = 7.3 \times 10^{-3}$ (Pb) .   (2) $\dfrac{R}{\langle 100|r|100 \rangle} = 3.1 \times 10^{-3}$ (H) ,

$\dfrac{R}{\langle 100|r|100 \rangle} = 1.5$ (Pb) .

Problem 8. $r^2 \to s$, $\varphi(r^2) \to s^{1/4} \phi(s)$, $l(l + 1) \to \dfrac{1}{4} l(l + 1) - \dfrac{3}{16}$,
$\dfrac{1}{4} E \to e^2 / 4\pi\epsilon_0$, $\dfrac{1}{8} M\omega^2 \to -E$.

Problem 9. $E_{s=0} = -\dfrac{3}{4} a\hbar^2$, $E_{s=1} = \dfrac{1}{4} a\hbar^2$.

Problem 10.   (1) $\mu_B B_z$.   (2) $\dfrac{3}{2} v_{so} \hbar^2$.   (3) $\dfrac{1}{2} v_{so} \hbar^2 (9 + 2q + q^2)^{1/2}$.

Problem 11. $j_r = |A|^2 \hbar k / r^2 M$,   flux$(d\Omega) = |A|^2 \hbar k d\Omega / M$.

Problem 12.   (1) $\beta_- = -1 + ak_- \cot ak_-$; $k_- = \frac{1}{\hbar} \sqrt{2MV_0}$.
(2) $\beta_+ = \sin \delta_0 / (ak \cos \delta_0 + \sin \delta_0)$; $k = \frac{1}{\hbar} \sqrt{2ME}$.
(3) $\tan \delta_0 = ka\ (1 - \tan ak_-/ak_-)$.   (4) $\sigma(\theta) = a^2\ (1 - \tan ak_-/ak_-)^2$.
(5) $\sigma = 4\pi\, a^2\ (1 - \tan ak_-/ak_-)^2$.

Problem 13.   (1) $V = V(\rho)$, $\rho \equiv \sqrt{x^2 + y^2}$, $\phi \equiv \tan^{-1}(y/x)$.

(2) $\dfrac{1}{2M} \left(\hat{p}_x^2 + \hat{p}_y^2 \right) = -\dfrac{\hbar^2}{2M} \left(\dfrac{\partial^2}{\partial \rho^2} + \dfrac{1}{\rho} \dfrac{\partial}{\partial \rho} + \dfrac{1}{\rho^2} \dfrac{\partial^2}{\partial \phi^2} \right)$, $E_{m_l} = E_{-m_l}$.

(3) $E_n = \hbar\omega(n + 1)$, $n + 1$, $n = 0, 1, 2, \ldots$.

Problem 14.   (1) $\omega_{\text{ph}} = \omega_{\text{cl}} = \hbar / M a_0^2 n^3$.
(2) Bohr correspondence principle (Sect. 15.3.2).

Chapter 7

Problem 1.   (1) $\dfrac{1}{2x_c \sqrt{2\pi}} \exp\left(-\dfrac{x^2}{2x_c^2} \right) \left(1 + \dfrac{x^2}{x_c^2} \right)$, $x_c \sqrt{2}$, 0.10 .

(2) $\dfrac{1}{x_c \sqrt{2\pi}} \exp\left(-\dfrac{x^2}{2x_c^2} \right)$, x_c , 0.16 .

(3) $\dfrac{1}{x_c^3 \sqrt{2\pi}} \exp\left(-\dfrac{x^2}{2x_c^2} \right) x^2$, $x_c \sqrt{3}$, 0.0021 .

Problem 2.   (1) $\varphi_+ = \dfrac{1}{\sqrt{2}} \left[\varphi_{100}(1)\varphi_{21m_l}(2) + \varphi_{100}(2)\varphi_{21m_l}(1) \right] \chi_{s=0}$,

$\varphi_- = \dfrac{1}{\sqrt{2}} \left[\varphi_{100}(1)\varphi_{21m_l}(2) - \varphi_{100}(2)\varphi_{21m_l}(1) \right] \chi_{s=1,m_s}$.   (2) $E_+ > E_-$.

Problem 3. $J = 0, 2, 4$.

Problem 4.   (1) s. (2) a. (3) s. (4) a. (5) s.

Problem 5. J even.

Problem 6.   (1) $3/2, 1/2$.   (2) $1/2$.

Problem 8. $\dfrac{1}{2}+$, $\dfrac{3}{2}-$, $\dfrac{1}{2}-$, $\dfrac{5}{2}+$, $\dfrac{7}{2}-$, $\dfrac{1}{2}-$.

Problem 9.   (1) $3.8/-0.26/4.8\ (\mu_{\text{p}})$.   (2) $-1.9/0.64/-1.9\ (\mu_{\text{p}})$.

Problem 10.   (1) $1\ 10^{-3}$.   (2) $2\ 10^{-1}$.   (3) $4\ 10^{-3}$.

Problem 11. $n(\epsilon) = \dfrac{M\epsilon}{\pi\hbar^2}$, $C_V = 2n_F k_B \dfrac{T}{T_F}$.

Problem 12.   1/3; 1/2; 3/5.

Problem 13.   (1) 5.9×10^3 Å.   (2) Red.

Problem 14.   (1) $-\frac{\pi^2}{12}\left(k_B T\right)^2 / \epsilon_F$.   (2) -1.7×10^{-4} eV.

Problem 15.   Constant.

Problem 16. $q_{aa} + q_{bb}$, $-q_{ac}$, q_{bc} .

Chapter 8

Problem 1.   (1) Equation (8.10).

(2) $c^{(2)}_{p\neq n} = \dfrac{1}{E^{(0)}_n - E^{(0)}_p}\left[\sum_{q\neq n} c^{(1)}_q \langle \varphi^{(0)}_p | V | \varphi^{(0)}_q \rangle - E^{(1)}_n c^{(1)}_p\right]$,

$c^{(2)}_n = -\dfrac{1}{2}\sum_{p\neq n} |c^{(1)}_p|^2$.

Problem 2.   (1) $E^{(1)}_1 = E^{(1)}_2 = 0$, $E^{(1)}_3 = 2c$.

(2) $E^{(2)}_1 = -E^{(2)}_2 = \dfrac{|c|^2}{3}$, $E^{(2)}_3 = 0$.

(3) $\varphi^{(1)}_1 = \dfrac{c}{3}\varphi^{(0)}_2$, $\varphi^{(1)}_2 = -\dfrac{c}{3}\varphi^{(0)}_1$, $\varphi^{(1)}_3 = 0$.

(4) $\varphi^{(2)}_1 = -\dfrac{|c|^2}{18}\varphi^{(0)}_1$, $\varphi^{(2)}_2 = -\dfrac{|c|^2}{18}\varphi^{(0)}_2$, $\varphi^{(2)}_3 = 0$.

(5) $E_\pm = \dfrac{7}{2} \pm \dfrac{3}{2}\sqrt{1 + \dfrac{4|c|^2}{9}} \approx \dfrac{7}{2} \pm \dfrac{|c|^2}{3}$, $E_3 = -1 + 2c$.

Problem 3.   (1) $E^{(1)}_0 = 0$, $E^{(2)}_0 = -\dfrac{k^2}{2M\omega^2}$.

(2) $E^{(1)}_0 = \dfrac{bx^2_c}{4}$, $E^{(2)}_0 = -\dfrac{b^2 x^2_c}{16M\omega^2}$.

Problem 4.   (1) $E^{(1)}_0 = -\dfrac{3}{32M}\left(\dfrac{\hbar\omega}{c}\right)^2$.   (2) 10^{-8} .

Problem 5. $\Psi_n = \left[1 - \dfrac{1}{2} \displaystyle\sum_{p \neq n} \dfrac{|\langle \varphi_p^{(0)} | V | \varphi_n^{(0)} \rangle|^2}{(E_n^{(0)} - E_p^{(0)})^2} \right] \varphi_n^{(0)}$

$+ \displaystyle\sum_{p \neq n} \dfrac{\langle \varphi_p^{(0)} | V | \varphi_n^{(0)} \rangle}{E_n^{(0)} + \langle \varphi_n^{(0)} | V | \varphi_n^{(0)} \rangle - E_p^{(0)}} \varphi_p^{(0)} + \displaystyle\sum_{p,q(\neq n)} \dfrac{\langle \varphi_p^{(0)} | V | \varphi_q^{(0)} \rangle \langle \varphi_q^0 | V | \varphi_n^{(0)} \rangle}{(E_n^{(0)} - E_p^{(0)})(E_n^{(0)} - E_q^{(0)})} \varphi_p^{(0)}$.

Problem 7.

(1) $\langle H \rangle = \dfrac{\hbar \omega}{4} \left[\dfrac{M}{M^*} + \dfrac{M^*}{M} - \dfrac{3}{8} \dfrac{\hbar \omega}{Mc^2} \left(\dfrac{M^*}{M} \right)^2 + \dfrac{15}{32} \left(\dfrac{\hbar \omega}{Mc^2} \right)^2 \left(\dfrac{M^*}{M} \right)^3 + \cdots \right]$.

(2) $1 = \left(\dfrac{M^*}{M} \right)^2 - \dfrac{3}{4} \dfrac{\hbar \omega}{Mc^2} \left(\dfrac{M^*}{M} \right)^3 + \dfrac{45}{32} \left(\dfrac{\hbar \omega}{Mc^2} \right)^2 \left(\dfrac{M^*}{M} \right)^4 + \cdots$.

(3) $\dfrac{M^*}{M} = 1 + \dfrac{3}{8} \dfrac{\hbar \omega}{Mc^2} - \dfrac{45}{128} \left(\dfrac{\hbar \omega}{Mc^2} \right)^2 + \cdots$.

(4) $\langle H \rangle = \dfrac{\hbar \omega}{2} \left[1 - \dfrac{3}{16} \dfrac{\hbar \omega}{Mc^2} + \dfrac{3}{16} \left(\dfrac{\hbar \omega}{Mc^2} \right)^2 + \cdots \right]$.

Problem 8. $\left\langle 1s2p \pm \left| \dfrac{e^2}{4\pi\epsilon_0 r} \right| 1s2p\pm \right\rangle = -(0.98 \pm 0.08) E_H$.

Problem 9.

	$\langle H \rangle_Z$	Z^*	$\langle H \rangle_{Z^*}$	exp
He	5.50	1.69	5.69	5.81
Li$^+$	14.25	2.69	14.44	14.49
Be^{++}	27.00	3.69	27.19	27.21

Problem 10. $\Delta E = \dfrac{3\hbar\omega}{4} \left(\dfrac{x_c}{R_0} \right)^4 l(l+1) - \dfrac{\hbar\omega}{2} \left(\dfrac{x_c}{R_0} \right)^6 l^2(l+1)^2$.

Problem 11.   (1) $\epsilon_0 = -8.75 \ 10^{-4} \,\text{eV}$; $R_0 = 2.87 \ \text{Å}$.

(2) $\hbar\omega = 4.0 \ 10^{-3} \,\text{eV}$.   (3) $\dfrac{\hbar^2}{2\mu R_0^2} = 1.29 \ 10^{-4} \,\text{eV}$.

Problem 12. $E_\pm(m=0) = E_{n=2}^{(0)} \pm 3eE_z a_0$, $E(m=\pm 1) = E_{n=2}^{(0)}$.

Problem 13.   (1) $H = \dfrac{1}{2M} \displaystyle\sum_{\mu\eta} \langle \mu | p^2 | \eta \rangle a_\mu^+ a_\eta$

$+ \dfrac{g}{2} \displaystyle\sum_{\mu\eta} \langle \mu | x^2 | \eta \rangle \sum_v a_\mu^+ a_v^+ a_v a_\eta - \dfrac{g}{2} \displaystyle\sum_{\mu v \eta \zeta} \langle \mu | x | \eta \rangle \langle v | x | \zeta \rangle a_\mu^+ a_v^+ a_\zeta a_\eta$.

(2) $H_H = \hbar\omega_H \displaystyle\sum_\mu \left(a_\mu^+ a_\mu + \dfrac{1}{2} \right)$; $V' = -\dfrac{g}{2} \left(\displaystyle\sum_{\mu\eta} \langle \mu | x | \eta \rangle a_\mu^+ a_\eta \right)^2$;

$$\omega_H = \sqrt{\frac{Ng}{M}}. \quad \text{(3)} \ H_{RPA} = \hbar\omega_H \gamma^+\gamma - \frac{g}{2}\langle N+1|x|N\rangle^2 (\gamma^+ + \gamma)^2 ;$$

$$\gamma^+ = a^+_{N+1}a_N ; \quad \omega_{RPA} = 0. \quad \text{(4) Translational invariance.}$$

Chapter 9

Problem 1. $0.50 - 0.40 \sin(3\pi^2 \hbar t / 2Ma^2)$.

Problem 2. $\dfrac{d\langle\Psi|p|\Psi\rangle}{dt} = -\left\langle \Psi \left| \dfrac{dV}{dx} \right| \Psi \right\rangle$.

Problem 3. $c_{y\uparrow} = \dfrac{1-i}{\sqrt{2}} \cos\left(\dfrac{1}{2}\omega_L t + \dfrac{\pi}{4}\right)$.

Problem 4. $\mathcal{U}_{\mathbf{n}}(t,0) = \cos\dfrac{\omega_L t}{2} \mathcal{I} + i\sin\dfrac{\omega_L t}{2} \mathbf{n}\cdot\boldsymbol{\sigma}$.

Problem 5. $0.36, 0.50, 0.13$.

Problem 6. $P^{(1)}_{\uparrow\to\downarrow} = \dfrac{\omega'^2}{(\omega-\omega_L)^2} \sin^2\left[\dfrac{1}{2}t(\omega-\omega_L)\right]$.

Problem 7.

$$\text{(1)} \ c_{0\to1} = -\frac{ivV_0}{\hbar x_c}\sqrt{\frac{2}{\pi}}\exp\left(-\frac{\hbar\omega}{4Mv^2}\right)\int_{t_1}^{t_2} t\exp\left[-\frac{v^2}{x_c^2}\left(t - i\frac{\hbar\omega}{2Mv^2}\right)^2\right]dt .$$

$$\text{(2)} \ |c_{0\to1}|^2 = \frac{V_0}{2Mv^4}\exp\left(-\frac{\hbar\omega}{2Mv^2}\right).$$

Problem 8.

$$\text{(1)} \ \Psi(t) = \cos\theta_0\exp\left[-\frac{iV_0\sin(\omega t)}{4\hbar\omega}\right]\chi_0^1 + \sin\theta_0\exp\left[\frac{i3V_0\sin(\omega t)}{4\hbar\omega}\right]\chi_0^0 .$$

$$\text{(2)} \ \Psi(t) = \exp\left[-\frac{iV_0\sin(\omega t)}{4\hbar\omega}\right]\varphi_{B_0} .$$

Problem 9. $P_{0\to1} = 2\left(\dfrac{Kx_c}{\hbar\omega}\right)^2 \sin^2\dfrac{\omega t}{2}$.

Problem 10.

$$\text{(1)} \ c_k^{(2)} = \frac{1}{\hbar^2}\sum_j \langle k|V|j\rangle\langle j|V|i\rangle\left[\frac{1}{\omega_{ki}\omega_{kj}} + \frac{\exp(i\omega_{ki}t)}{\omega_{ki}\omega_{ji}} + \frac{\exp(i\omega_{kj}t)}{\omega_{kj}\omega_{ij}}\right] .$$

$$\text{(2)} \ P_{0\to2} = 2\left(\frac{Kx_c}{\hbar\omega}\right)^4 \sin^4\frac{\omega t}{2} .$$

Problem 11.   (1) 0.5 and 0.5×10^{-7}.   (2) 2×10^{-2}.

Problem 12. $\left| \dfrac{\langle 210|\boldsymbol{r}|100\rangle}{\langle 310|\boldsymbol{r}|100\rangle} \right|^2 = 6.3$, $\dfrac{P(100 \to 210)}{P(100 \to 310)} = 3.8$.

Problem 13.   (1) $\dfrac{P(310 \to 200)}{P(310 \to 100)} = 0.13$.   (2) 1.1×10^{-8} s.   (3) 4×10^{-7} eV.

Problem 14.   (1) $\langle n, n-1 || Q_1 || n-1, n-2 \rangle = -a_0 \, n^3/\sqrt{2}$.

(2) $\tau(n, n-1 \to n-1, n-2) = 6n^4 \hbar / \alpha^5 M c^2$.

(3) $\dfrac{\tau(n, n-1 \to n-1, n-2)}{\tau(2, 1 \to 1, 0)} = 7n^4$.

Chapter 10

Problem 1.   (1) $j(2j+1) \times j(2j+1)$.   (2) $\left(j + \dfrac{1}{2} \right) \times \left(j + \dfrac{1}{2} \right)$.

(3) $E_a = -g \left(j + \dfrac{1}{2} \right)$, $E_b = 0$.

Problem 2.   (1) $\langle 0 | H_{tb} | 0 \rangle_{A_\pi = \frac{\Omega}{2}} = -g \dfrac{\Omega^2}{4} \left(1 + \dfrac{2}{\Omega} \right)$.   (2) $\mathcal{I} = \dfrac{h^2}{2g}$.

(3) $\Delta E_{A_\pi = \frac{\Omega}{2}} = g \, \Omega$.

Problem 3.   (1) $E_p = \dfrac{g\Omega}{2}$; $V_p^2 = \dfrac{A_\pi}{\Omega}$; $\Delta = g \sqrt{A_\pi(\Omega - A_\pi)}$;

$\mu = g \left(A_\pi - \dfrac{\Omega}{2} \right)$.

(2) $\langle 0 | H_{tb} | 0 \rangle_{A_\pi = \frac{\Omega}{2}} = -g \dfrac{\Omega^2}{4}$; $\mathcal{I} = \dfrac{h^2}{2g}$; $\Delta E_{A_\pi = \frac{\Omega}{2}} = g \, \Omega$.

(3) The BCS approximation is only correct to leading order in Ω^{-1}.

Problem 4. $P^+ = \sum_{p>0} \left[U_p V_p (1 - \alpha_p \alpha_{-p}) + U_p^2 \alpha_p^+ \alpha_{-p}^+ - V_p^2 \alpha_{-p} \alpha_p \right]$.

Problem 5. 2Δ.

Problem 8.   (1) $\hat{L}^{(0)} = \sqrt{\dfrac{\mathcal{I}}{2}} \left(\Gamma_1^+ + \Gamma_0^+ + \Gamma_1 + \Gamma_0 \right)$.   (2) 0.

Chapter 13

Problem 1.

	φ_{B_0}	φ_{B_1}	φ_{B_2}	φ_{B_3}
$\hat{S}_z(1)\,\hat{S}_z(2)$	1	1	-1	-1
$\hat{S}_x(1)\,\hat{S}_x(2)$	1	-1	1	-1

Problem 2. $1,\ 0,\ \dfrac{1}{2},\ \dfrac{3}{8},\ \dfrac{1}{8},\ \dfrac{1}{4}.$

Problem 3. $\hat{S}_z\left(\varphi_{B_1}\right),\quad \hat{S}_x\left(\varphi_{B_2}\right),\quad \hat{S}_y\left(\varphi_{B_3}\right).$

Problem 4. $\mathcal{U}_{\mathrm{H}}.$

Problem 8.   Alice's transformations yield a unique Bell state.

Problem 9.

f_i	c_{i0}	c_{i4}	c_{i8}	c_{i12}
1	1	1	1	1
2	1	i	-1	$-i$
4	1	-1	1	-1
8	1	$-i$	-1	i

Chapter 14

Problem 1. $L_\lambda = 0.2$ m.

Problem 4.

(1) $\hat{\rho} = \dfrac{1}{2}\begin{pmatrix} 1+\cos\beta & \exp[-i\phi]\,\sin\beta \\ \exp[i\phi]\,\sin\beta & 1-\cos\beta \end{pmatrix}$

(2) $\langle S_x\rangle = \dfrac{\hbar}{2}\sin\beta\,\cos\phi;\quad \langle S_y\rangle = \dfrac{\hbar}{2}\sin\beta\,\sin\phi;\quad \langle S_z\rangle = \dfrac{\hbar}{2}\cos\beta.$

Problem 5.

(1) $\hat{\rho} = \dfrac{1}{2}\begin{pmatrix} 1 & 0 \\ 0 & 1 \end{pmatrix}$

(2) $\langle S_x\rangle = \langle S_y\rangle = \langle S_z\rangle = 0.$

Problem 6. $\Delta x = \sqrt{\dfrac{\hbar}{M\omega}\left(\dfrac{1}{2}+\dfrac{k_{\mathrm{B}}T}{\hbar\omega}\right)}.$

Physical Units and Constants

Table A.1 Equivalence between physical units and the value of constants used in the text [131]

Quantity	Symbol	Units (m.k.s.)	Atomic scale	Nuclear scale
		1 m	10^{10} Å	10^{15} F
		1 J	0.625×10^{19} eV	0.625×10^{13} MeV
		1 kg	0.56×10^{36} eV c^{-2}	0.56×10^{30} MeV c^{-2}
Bohr magneton	μ_B	0.93×10^{-23} J T^{-1}	0.58×10^{-4} eV T^{-1}	0.58×10^{-10} MeV T^{-1}
Bohr radius	a_0	0.53×10^{-10} m	0.53 Å	0.53×10^5 F
Boltzmann constant	k_B	1.38×10^{-23} J K^{-1}	0.86×10^{-4} eV K^{-1}	0.86×10^{-10} MeV K^{-1}
Constant in Coulomb law	$e^2/4\pi\epsilon_0$	2.34×10^{-28} J m	14.4 eV Å	1.44 MeV F
Electron charge	e	-1.60×10^{-19} C		
Electron mass	M, M_e	0.91×10^{-30} kg	0.51×10^6 eV c^{-2}	0.51 MeV c^{-2}
Fine structure constant	$\alpha = e^2/4\pi\epsilon_0\hbar c$	$1/137$		
Hydrogen atom ground state	E_H	-2.18×10^{-18} J	-13.6 eV	-1.36×10^{-5} MeV
Deuteron nucleus ground state	E_D	-3.57×10^{-13} J	-2.23×10^6 eV	-2.23 MeV
Nuclear magneton	μ_p	0.51×10^{-26} J T^{-1}	0.32×10^{-7} eV T^{-1}	0.32×10^{-13} MeV T^{-1}
Planck constant/2π	$\hbar$	1.05×10^{-34} J s	0.66×10^{-15} eV s	0.66×10^{-21} MeV s
Proton mass	M_p	1.67×10^{-27} kg	0.94×10^9 eV c^{-2}	0.94×10^3 MeV c^{-2}
Rydberg constant	R_H	1.10×10^7 m^{-1}	1.10×10^{-3} Å^{-1}	1.10×10^{-8} F^{-1}
Speed of light in vacuum	c	3.00×10^8 m s^{-1}	3.00×10^{18} Å s^{-1}	3.00×10^{23} F s^{-1}

References

1. B.C. Olschak: *Buthan. Land of Hidden Treasures*. Photography by U. and A. Gansser (Stein & Day, New York 1971).
2. M. Planck: Verh. Deutsch. Phys. Ges. **2**, 207, 237 (1900).
3. A. Einstein: Ann. der Phys. **17**, 132 (1905).
4. A.H. Compton: Phys. Rev. **21**, 483 (1923).
5. C.L. Davisson and L.H. Germer: Nature **119**, 528 (1927); G.P. Thomson: Proc. Roy. Soc. A **117**, 600 (1928).
6. H. Geiger and E. Mardsen: Proc. Roy. Soc. A **82**, 495 (1909); E. Rutherford: Phil. Mag. **21**, 669 (1911).
7. J. Balmer: Verh. Naturf. Ges. Basel **7**, 548, 750 (1885); Ann. der Phys. und Chem. **25**, 80 (1885).
8. N. Bohr: Phil. Mag. **25**, 10 (1913); **26**, 1 (1913); Nature **92**, 231 (1913).
9. W. Heisenberg: Zeitschr. Phys. **33**, 879 (1925).
10. M. Born, W. Heisenberg and P. Jordan: Zeitschr. Phys. **35**, 557 (1926).
11. P.A.M. Dirac: Proc. Roy. Soc. A **109**, 642 (1925).
12. E. Schrödinger: Ann. der Phys. **79**, 361, 489 (1926); **80**, 437 (1926); **81**, 109 (1926).
13. D.F. Styer et al.: Am J. Phys. **70**, 288 (2002).
14. J. Schwinger: *Quantum Mechanics. Symbolism of Atomic Measurements*, ed. by B.G Englert (Springer-Verlag, Berlin, Heidelberg, New York 2001) Chap. 1.
15. P.A.M. Dirac: *The Principles of Quantum Mechanics* (Oxford University Press, Amen House, London 1930).
16. A. Einstein, B. Podolsky and N. Rosen: Phys. Rev. **47**, 777 (1935).
17. O. Stern and W. Gerlach: Zeitschr. Phys. **8**, 110 (1921); **9**, 349 (1922).
18. G. Kaiser: J. Math. Phys. **22**, 705 (1981).
19. D.F. Styer: Am. J. Phys. **64**, 31 (1996).
20. J. Roederer: *Information and its Role in Nature* (Springer-Verlag, Berlin, Heidelberg, New York 2005).
21. N. Bohr: *The Philosophical Writings of Niels Bohr* (Ox Bow Press, Woodbridge, Connecticut 1987).
22. N.D. Mermin: Am. J. Phys. **71**, 23 (2003).
23. R.F. Feynman, R.B. Leighton and M. Sands: *The Feynman Lectures on Physics. Quantum Mechanics* [Addison-Wesley, Reading (Massachusetts), London, New York, Dallas, Atlanta, Barrington (Illinois) 1965] Chap. 5.
24. A. Zeilinger, R. Gähler, C.G. Shull, W. Treimer and W. Hampe: Rev. Mod. Phys. **60**, 1067 (1988).
25. O. Nairz, M. Arndt and A. Zeilinger: Am. J. Phys. **71**, 319 (2003).
26. W. Heisenberg: Zeitschr. Phys. **43**, 172 (1927).

27. B. Cougnet, J. Roederer and P. Waloshek: Z. für Naturforschung A **7**, 201 (1952).
28. W. Wootters and W. Zurek: Nature **299**, 802 (1982); Phys. Today, 76 (Feb. 2009).
29. R.S. Mulliken: Nature **114**, 350 (1924).
30. E.T. Jaynes and F.W. Cummings: Proc. I.E.E.E. **51**, 81 (1963).
31. M. Born: Zeitschr. Phys. **37**, 863 (1926); **38**, 499 (1926).
32. L. de Broglie: C. R. Acad. Sci. Paris **177**, 507, 548 (1923).
33. G. Binning and H. Rohrer: Rev. Mod. Phys. **71**, S324 (1999) and references contained therein.
34. F. Bloch: Zeitschr. Phys. **52**, 555 (1928).
35. G.E. Uhlenbeck and S.A. Goudsmit: Nature **113**, 953 (1925); **117**, 264 (1926).
36. W. Pauli: Zeitschr. Phys. **43**, 601 (1927).
37. S. Haroche and J.M. Raimond: *Exploring the Quantum. Atoms, Cavities and Photons* (Oxford University Press, Oxford (2010).
38. Å. Bohr and B. Mottelson: *Nuclear Structure* (W.A. Benjamin, New York, Amsterdam 1969)
39. R.P. Martinez–y–Romero, H.N. Nuñez–Yepez and A.L. Salas–Brito: Am. J. Phys. **75**, 629 (2007).
40. A.K. Grant and J.L. Rosner: Am. J. Phys. **62**, 310 (1994).
41. D.A. McQuarrie: *Quantum Chemistry* (University Science Books, Herndon, Virginia 1983) Fig. 6-12.
42. W. Pauli: Zeitschr. Phys. **31**, 625 (1925).
43. K.L. Jones et al.: Nature 465, 454 (2010).
44. M. Kastner: Physics Today **46**, 24 (1993).
45. R. Fitzgerald: Physics Today **57**, 22 (2004) and references contained therein.
46. A. Einstein: Sitz. Ber. Preuss. Ak. Wiss. **2**, 261 (1924); **3** (1925).
47. D. Kleppner: Physics Today **49**, 11 (1996); F. Dalfovo, S. Giorgini, L.P. Pitaevckii and S. Stringari: Rev. Mod. Phys. **71**, 463 (1999).
48. M.H. Anderson, J.R. Enscher, M.R. Matthews, C.E. Wieman and E.A. Cornell: Science **269**, 198 (1995); J.R. Enscher, D.S. Jin, M.R. Matthews, C.E. Wieman and E.A. Cornell: Phys. Rev. Lett. **77**, 4984 (1996).
49. K. von Klitzing, G. Dorda and M. Pepper: Phys. Rev. Lett. **45**, 494 (1980).
50. D.C. Tsui, H.L. Störmer and A.C. Gossard: Phys. Rev. Lett. **48**, 1559 (1982); Phys. Rev. B **25**, 1405 (1982).
51. R.E. Prange: Introduction to *The Quantum Hall Effect*, ed. by R.E. Prange and S.M. Girvin (Springer-Verlag, New York, Berlin, Heidelberg 1987) Fig. 1.2.
52. B.L. Halperin: Scientific American **254**, Vol. 4, 52 (1986).
53. J.D. Jackson: *Classical Electrodynamics* (John Wiley & Sons, New York, Chichester, Brisbane, Toronto 1975) p. 574.
54. R.B. Laughlin: Phys. Rev. Lett. **50**, 1395 (1983).
55. S.N. Bose: Zeitschr. Phys. **26**, 178 (1924).
56. P.A.M. Dirac: Proc. Roy. Soc. A **112**, 661 (1926).
57. E. Fermi: Zeitschr. Phys. **36**, 902 (1926).
58. R. Eisberg and R. Resnick: *Quantum Physics of Atoms, Molecules, Solids, Nuclei and Particles* (John Wiley & Sons, New York (1975).
59. R.P. Feynman: Phys. Rev. **76**, 769 (1949).
60. C. Itzykson and J.B. Zuber: *Quantum Field Theory* (McGraw-Hill, New York, St. Louis, San Francisco, London 1980).
61. B.H. Brandow: Rev. Mod. Phys. **39**, 771 (1967); E.M. Krenciglowa and T.T.S. Kuo: Nucl. Phys. A **240**, 195 (1975).
62. C. Bloch and J. Horowitz: Nucl. Phys. **8**, 91 (1958).
63. J.J. Sakurai: *Modern Quantum Mechanics*. Addison–Wesley Pub. Co., Reading, Massachusetts (1994).
64. A. Einstein: Verh. Deutsch. Phys. Ges. **18**, 318 (1916); Mitt. Phys. Ges. Zürich **16**, 47 (1916); Phys. Zeitschr. **18**, 121 (1917).
65. T.H. Maiman: Nature **187**, 493 (1960).
66. J. Bardeen, L.N. Cooper and J.R. Schrieffer: Phys. Rev. **106**, 162 (1957).

67. C. Becchi, A. Rouet and R. Stora: Phys. Lett. B **52**, 344 (1974).
68. M. Henneaux and C. Teitelboim: *Quantization of Gauge Systems* (Princeton University Press, Princeton, New Jersey 1992).
69. D.R. Bes and J. Kurchan: *The Treatment of Collective Coordinates in Many-Body Systems. An Application of the BRST Invariance* (World Scientific Lecture Notes in Physics, Vol. 34, Singapore, New Jersey, London, Hong Kong 1990); D.R. Bes and O. Civitarese: Am. J. Phys. **70**, 548 (2002).
70. H. Kammerlingh Onnes, Comm. Phys. Lab. Univ. Leiden, Nos. 122 and 124 (1911).
71. B.D. Josephson, Phys. Lett. **1**, 251 (1962).
72. R. Feynman and A. Hibbs: *Quantum Mechanics and Path Integrals* (Mc Graw–Hill Book Co., New York 1965).
73. P. Cartier and C. DeWitt–Morette: *Functional Integration* (Cambridge U. Press, New York 2007).
74. S. Carlip: Phys. Today **61**, 61 (2008).
75. L.S. Schulman: *Techniques and Applications of Path Integrals* (John Wiley & Sons, New York 1981).
76. E. Schrödinger: Naturwissenschaften **23**, 807, 823, 845 (1935)
77. A. Aspect: *Introduction: John Bell and the Second Quantum Revolution*, in J.S. Bell, "Speakable and Unspeakable in Quantum Mechanics", Cambridge University Press (2008).
78. A. Zeilinger: Rev. Mod. Phys. **71**, S288 (1999) and references contained therein
79. A. Zeilinger, G. Weihs, T. Jennewein and M. Aspelmeyer: Nature **433**, 230 (2005).
80. D. Bohm: *Quantum Theory*. Prentice Hall, New Jersey (1951); Phys. Rev. **85**, 166, 180 (1952).
81. J.S. Bell: Physics **1**, 195 (1964).
82. N.D. Mermin: Physics Today, 38 (1985).
83. A. Aspect, P. Grangier and G. Roger: Phys. Rev. Lett. **47**, 460 (1981); **49**, 91 (1982).
84. G. Weihs, T. Jennewein, C. Simon, H. Weinfurter and A. Zeilinger: Phys. Rev. Lett. **81**, 5039 (1998).
85. W. Nagourney, J. Sandberg and H. Dehmet, Phys. Rev. Lett. **56**, 2797 (1986).
86. M. Brune et al.: Phys. Rev. Lett. **76**, 1800 (1996).
87. M.A. Rowe et al.: Nature **409**, 791 (2001).
88. A.D. O'Connell et al.: Nature **464**, 697 (2010).
89. C.H. Bennet and G. Brassard: Proc. I.E.E.E. Int. Conf. on Computers, Systems and Signal Processing (IEEE Press, Los Alamos, California 1984) p. 175.
90. C.H. Bennett, G. Brassard, C. Crépeau, R. Jozsa, A. Peres and W. Wooters: Phys. Rev. Lett. **70**, 1895 (1993).
91. D. Bouwmeester, J.W. Pan, K. Mattle, M. Eibl, H. Weinfurter and A. Zeilinger: Nature **390**, 575 (1997).
92. E. Gerjuoy: Am. J. Phys. **73**, 521 (2005).
93. P.W. Schor: Proc. 34th Annual Symp. Found. Comp. Scien. (FOCS), ed. by S. Goldwasser (IEEE Press, Los Alamitos, California 1994) p. 124.
94. I.L. Chuang, L.M.K. Vandersypen, X.L. Zhou, D.W. Leung and S. Lloyd: Nature **393**, 143 (1998).
95. P.A.M. Dirac: Hungarian Ac. of Sc. Rep. KFK-62 (1977).
96. E. Schrödinger: Naturwissenschaftern. **23**, 807, 823, 844 (1935).
97. R. Penrose: *The Road to Reality* (Alfred A. Knopf, New York, 2005, Chapter 29).
98. M. Schlosshauer: *Decoherence and the Quantum–to–Classical Transition* (Springer–Verlag, Berlin, Heidelberg 2007).
99. W.H. Zurek: Revs. Mod. Phys. **75**, 715 (2003) and references contained therein; Phys. Today **49**, 36 (1991).
100. J.P. Paz and W.H. Zurek: Environment-Induced Decoherence and the Transition from Classical to Quantum. In: *Coherent Atomic Matter Waves*, Les Houches Session LXXXII, ed. by R. Kaiser, C. Westbrook and F. Davids (Springer-Verlag, Berlin, Heidelberg, New York 2001) p. 533.
101. J. von Neumann: *Mathematische Grundlagen der Quantenmechanik* (Springer, Berlin 1932).

102. L. Hackermüller, K. Hornberger, B. Brezger, A. Zeilinger, M. Arndt: Appl. Phys. B **77**, 781 (2003)

103. E. Hobsbawn: *The Age of Extremes. A History of the World, 1914–1991* (Vintage Books, New York 1996) p. 7.

104. O. Spengler: *Der Untergang des Abendlandes. Umrisse einer Morphologie der Welt-geschichte*, Vol. 1: *Gestalt und Wirklichkeit* (Munich, 1918). First English translation: *The Decline of the West*, Vol. 1: *Form and Actuality* (Knof, New York 1926).

105. H. Kragh: *Quantum Generations. A History of Physics in the Twentieth Century* (Princeton University Press, Princeton, New Jersey 1999).

106. A. Pais: *'Subtle is the Lord ...' The Science and the Life of Albert Einstein* (Oxford University Press, Oxford, New York, Toronto 1982). *Inward Bound* (Oxford University Press, Oxford, New York, Toronto 1986); *Niels Bohr's Times. In Physics, Philosophy and Politics* (Clarendon Press, Oxford 1991).

107. P. Robertson: *The Early Years. The Niels Bohr Institute 1921–1930* (Akademisk Forlag. Universitetsforlaget i København, Denmark 1979).

108. G. Kirchhoff: Ann. Phys. Chem. **109**, 275 (1860).

109. W. Wien: Sitz. Ber. Preuss. Ak. Wiss. 55 (1893); Ann. Physik **58**, 662 (1896).

110. G. Kirchhoff and R. Bunsen: Ann. Phys. Chem. **110**, 160 (1860).

111. R. Millikan: Phys. Rev. **4**, 73 (1914); **6**, 55 (1915).

112. E. Lawrence and J. Beams: Phys. Rev. **32**, 478 (1928); A. Forrester, R. Gudmundsen and P. Johnson: Phys. Rev. **90**, 1691 (1955).

113. J. Clauser: Phys. Rev. D **9**, 853 (1974).

114. H.G.J. Moseley: Nature **92**, 554 (1913); Phil. Mag. **26**, 1024 (1913); **27**, 703 (1914).

115. J. Frank and H. Hertz: Verh. Deutsch. Phys. Ges. **16**, 457 (1914).

116. A. Sommerfeld: Sitz. Ber. Bayer. Akad. Wiss. 459 (1915).

117. L.H. Thomas: Nature **117**, 514 (1926); Phil. Mag. **3**, 1 (1927).

118. M. Born and P. Jordan: Zeitschr. Phys. **34**, 858 (1925).

119. W. Heisenberg: Zeitschr. Phys. **38**, 499 (1926).

120. P.A.M. Dirac: Proc. Roy. Soc. A **117**, 610 (1928); A **118**, 351 (1928).

121. N. Bohr, H.A. Kramers and J.C. Slater: Phil. Mag. [6] **47**, 785 (1924); Zeitschr. Phys. **24**, 69 (1924).

122. N. Bohr: Nature **136**, 65 (1935); Phys. Rev. **48**, 696 (1935).

123. A. Einstein: Reply to Criticisms. In: *Albert Einstein. Philosopher-Scientist*, ed. by P.A Schilpp (Open Court Publishing, Peru, Illinois 2000) p. 663.

124. N. Bohr: Discussions with Einstein on Epistemological Problems in Atomic Physics. In *Albert Einstein. Philosopher-Scientist*, ed. by P.A Schilpp (Open Court Publishing, Peru, Illinois 2000) p. 199.

125. M. Tegmark and J.A. Wheeler: Scientific American **284**, Vol. 2, 54 (2001).

126. J. Bell, Rev. Mod. Phys. **38**, 447 (1966).

127. H.D. Zeh: Found. Phys. **1**, 69 (1970).

128. W.H. Zurek: Phys. Rev. D **24**, 1516 (1981); **26**, 1862 (1982).

129. W.H. Zurek: *Reduction of the Wavepacket: How Long does it take?*. In: *Frontiers in Nonequilibrium Statistical Mechanics*, G.T. Moore and M.O. Scully, eds. (Plenum Press, New York, 1986) p.145

130. E. Joos and H.D. Zeh: Z. Phys. B: Condens. Matter **59**, 223 (1985).

131. The NIST Reference on Constants, Units, and Uncertainty: Appendix 3. http:/physics.nist. gov/cuu/Units/units.html.

132. R.W. Richardson: Phys. Lett. **3**, 277 (1963); J. Dukelsky, H.S. Lerma, L. Robledo, R. Rodriguez-Guzman and S.M. Rombouts: Phys. Rev. C **84**, 061301 (2011).

Index

Abelian symmetry, 203
Abelian transformation, 200
Absorption processes, 177
Action, 212, 215
Adjoint vector, 33
Ag atom, 78
Alkali atoms, 96
Allowed transitions, 179
Alpha particle, 111
Angular momentum
    addition, 81, 89
    commutation relations, 73, 74
    matrix treatment, 74, 85, 87
    orbital, 74–77, 87, 88
Angular subspace, 73
Anthropocentric foundation of quantum
        mechanics, 247
Anticommutation relation, 138, 199
Antisymmetric states, 110
Antiunitary transformation, 172
Anyons, 111, 134
Apparatus, 12, 13, 16, 253
Artificial atoms, 125
Atomic periodic table, 115
Average, 30

Balmer series, 261, 263, 264
Band structure of crystals, 68, 120, 152
Bardeen, J., 122, 183, 184
Basic principles, 9–11, 111, 162
Basis states, 7
BCS, 184, 187, 188, 190
Be atom, 158
Becchi, C., 184
Bell inequality, 225–227

Bell states, 221, 222, 225, 235, 236
Bell, J., 225, 271
Bessel functions, 100, 105, 106
Binnig, G., 66
Black-body radiation, 1, 260
Bloch theorem, 68
Bloch–Horowitz diagonalization procedure,
        151
Bohm, D., 225, 226
Bohr
    correspondence principle, 108
    Festspiele, 267
    frequency, 168
    magneton, 78–80, 286
    model, 1, 97, 263, 264
    radius, 95, 97, 102, 103, 286
Bohr, Å, xv
Bohr, N., xv, 1, 2, 54, 79, 224, 260, 263–265,
        267–271
Boltzmann constant, 119, 286
Boltzmann, L., 1
Born, M., 1, 260, 264–267, 269
Born–Oppenheimer approximation, 122,
        145
Bose, S., 262
Bose–Einstein
    condensation, 112, 127–129, 262
    distribution, 135, 262
Boson, 111, 139
    occupation number, 111, 112, 137
Boundary conditions, 52, 53, 57, 61, 62, 99,
        100, 149
Bra, 9
Brattain, W., 122
Brillouin–Wigner perturbation theory, 143,
        151, 158
Broken symmetry, 183, 187